RTO-MP-24
AC/323(AVT)TP/12

RTO-MP-24

NORTH ATLANTIC TREATY ORGANIZATION

RESEARCH AND TECHNOLOGY ORGANIZATION

BP 25, 7 RUE ANCELLE, F-92201 NEUILLY-SUR-SEINE CEDEX, FRANCE

RTO MEETING PROCEEDINGS 24

Application of Damage Tolerance Principles for Improved Airworthiness of Rotorcraft

(l'Application des principes de la tolérance à l'endommagement pour une meilleure aptitude au vol des aéronefs à voilure tournante)

Papers presented at the Specialists' Meeting of the RTO Applied Vehicle Technology Panel (AVT) held in Corfu, Greece, 21-22 April 1999.

Published February 2000

Distribution and Availability on Back Cover

RTO-MP-24
AC/323(AVT)TP/12

NORTH ATLANTIC TREATY ORGANIZATION

RESEARCH AND TECHNOLOGY ORGANIZATION

BP 25, 7 RUE ANCELLE, F-92201 NEUILLY-SUR-SEINE CEDEX, FRANCE

RTO MEETING PROCEEDINGS 24

Application of Damage Tolerance Principles for Improved Airworthiness of Rotorcraft

(l'Application des principes de la tolérance à l'endommagement pour une meilleure aptitude au vol des aéronefs à voilure tournante)

Papers presented at the Specialists' Meeting of the RTO Applied Vehicle Technology Panel (AVT) held in Corfu, Greece, 21-22 April 1999.

The Research and Technology Organization (RTO) of NATO

RTO is the single focus in NATO for Defence Research and Technology activities. Its mission is to conduct and promote cooperative research and information exchange. The objective is to support the development and effective use of national defence research and technology and to meet the military needs of the Alliance, to maintain a technological lead, and to provide advice to NATO and national decision makers. The RTO performs its mission with the support of an extensive network of national experts. It also ensures effective coordination with other NATO bodies involved in R&T activities.

RTO reports both to the Military Committee of NATO and to the Conference of National Armament Directors. It comprises a Research and Technology Board (RTB) as the highest level of national representation and the Research and Technology Agency (RTA), a dedicated staff with its headquarters in Neuilly, near Paris, France. In order to facilitate contacts with the military users and other NATO activities, a small part of the RTA staff is located in NATO Headquarters in Brussels. The Brussels staff also coordinates RTO's cooperation with nations in Middle and Eastern Europe, to which RTO attaches particular importance especially as working together in the field of research is one of the more promising areas of initial cooperation.

The total spectrum of R&T activities is covered by 7 Panels, dealing with:

- SAS Studies, Analysis and Simulation
- SCI Systems Concepts and Integration
- SET Sensors and Electronics Technology
- IST Information Systems Technology
- AVT Applied Vehicle Technology
- HFM Human Factors and Medicine
- MSG Modelling and Simulation

These Panels are made up of national representatives as well as generally recognised 'world class' scientists. The Panels also provide a communication link to military users and other NATO bodies. RTO's scientific and technological work is carried out by Technical Teams, created for specific activities and with a specific duration. Such Technical Teams can organise workshops, symposia, field trials, lecture series and training courses. An important function of these Technical Teams is to ensure the continuity of the expert networks.

RTO builds upon earlier cooperation in defence research and technology as set-up under the Advisory Group for Aerospace Research and Development (AGARD) and the Defence Research Group (DRG). AGARD and the DRG share common roots in that they were both established at the initiative of Dr Theodore von Kármán, a leading aerospace scientist, who early on recognised the importance of scientific support for the Allied Armed Forces. RTO is capitalising on these common roots in order to provide the Alliance and the NATO nations with a strong scientific and technological basis that will guarantee a solid base for the future.

Printed on recycled paper

Published February 2000

ISBN 92-837-1024-X

Printed by Canada Communication Group Inc.
(A St. Joseph Corporation Company)
45 Sacré-Cœur Blvd., Hull (Québec), Canada K1A 0S7

Application of Damage Tolerance Principles for Improved Airworthiness of Rotorcraft

(RTO MP-24)

Executive Summary

Rotorcraft are essential to carry out critical military missions in various military scenarios. Their structure in general has been traditionally designed to safe-life principles with damage tolerance and fail-safe aspects for ballistic damage only. Today the variety of mission requirements inherent to the multipurpose military usage leads to extremely complicated flight and load envelopes. Fatigue design of structures and dynamic components is becoming a challenging task. Recent design approaches and regulatory efforts include alternative concepts based on damage tolerance principles, explicitly allowing for manufacturing or service induced flaws and defects. This is analog to fixed wing concept design principles and aims at benefits regarding operational safety, readiness and reduced life cycle costs. An examination of the present status of fatigue substantiation of rotorcraft components based on damage tolerant requirements revealed the need for further research, owing to specific load environment, usage cycles and structural design of rotorcraft.

The goal of the Specialists' Meeting was to offer a forum to present and discuss the applicability of this new design approach to major rotorcraft components such as the dynamic system, primary load carrying structures and flight control systems. Prerequisites and areas of further development were identified for the introduction of this alternative design concept. Furthermore the aim was to bring together operators, agencies and manufacturers in Europe and North America to address the specific needs and requirements of the military customers.

The meeting covered both metal and composite structures including special material related topics such as crack growth models and impact delamination modeling.

Due to a high number of withdrawals the disciplines involved in this task were not complete, and in particular there was an absence of experts from certification agencies and large fleet military operators which meant that this objective could not be fully met.

Certain presentations clearly showed that further progress on topics such as specific crack growth models, material allowables and thresholds together with load spectrum analysis and inspection technologies are vital to the successful application of damage tolerance principles, especially in the high load cycle regime of dynamic systems. Most of the major manufacturers concluded that at present the flaw tolerant "enhanced safe-life" methodology is more viable for these parts. However one paper presented experience using the slow crack growth method for both, dynamic system and structure.

The consensus was that operating loads or structural health monitoring systems could be used to establish usage spectrum data and support inspection intervals, if a "true" damage tolerant design for metallic structures were to be used in the future.

Besides the various pros and cons of the two design principles, discussions revealed additional topics such as the need to adapt material selections to the chosen design principle. Additional design efforts may lead to safe-life parts with damage tolerance features. There was also the requirement to reduce initial crack sizes compared with fixed wing structures. It was considered that steps should be made towards improved inspection techniques for cracks and flaws to enable the operation of rotorcraft without additional economic burden.

The overall subject of new design and certification requirements for rotorcraft will remain with manufacturers, users and certification and research agencies. It will certainly require continuous work and discussions throughout the community to further improve life management of rotorcraft in civil and military fleets. A common design and certification methodology for rotorcraft components would be one important step towards this goal.

L'application des principes de la tolérance à l'endommagement pour une meilleure aptitude au vol des aéronefs à voilure tournante

(RTO MP-24)

Synthèse

Les aéronefs à voilure tournante sont indispensables à l'exécution de certaines missions militaires décisives dans différents scénarios militaires. Traditionnellement, leur structure est conçue en conformité avec les principes de la sécurité par l'estimation de la vie, les mesures relatives à la tolérance à l'endommagement et à la sûreté intégrée ne s'appliquant qu'aux dommages balistiques. Aujourd'hui, le large éventail de missions assignées du fait d'une grande polyvalence dans leur utilisation militaire implique des domaines de vol et des configurations d'emport très compliqués. La conception des structures et des composants dynamiques en vue de leur résistance à la fatigue devient une tâche de plus en plus ardue. Les dernières approches conceptuelles et les derniers efforts réglementaires mettent en oeuvre des concepts alternatifs fondés sur les principes de la tolérance à l'endommagement, ce qui autorise, de façon explicite, des imperfections et des défauts au niveau de la fabrication ou du fait de l'emploi du matériel. Cette approche est analogue aux principes de conception des aéronefs à voilure fixe et vise à procurer des avantages en termes de sécurité opérationnelle, de disponibilité, ainsi qu'au niveau de la réduction du coût global de possession. Un examen de l'état actuel des connaissances dans le domaine de l'amélioration de la résistance contre la fatigue des composants des aéronefs à voilure tournante, fondé sur les exigences en matière de la tolérance à l'endommagement souligne le besoin d'entreprendre des travaux de recherche plus approfondis en raison des conditions d'emports, des cycles d'exploitation et de la construction spécifiques des aéronefs à voilure tournante.

La réunion de spécialistes a eu pour objectif de servir de forum pour la présentation et la discussion des possibilités d'application de cette nouvelle approche en matière de design conceptuelle aux principaux organes des aéronefs à voilure tournante tels que le système dynamique, les principales structures porteuses et les systèmes de commandes de vol. Les conditions préalables à l'adoption de cette variante de conception ont été identifiées, ainsi que des domaines de développement ultérieur. La réunion a eu également pour objectif de rassembler des exploitants, des agences et des fabricants européens et nord-américains pour examiner les besoins et exigences spécifiques des clients militaires.

La réunion a traité des structures métalliques et composites, y compris des sujets spécifiques relatifs aux matériaux, comme les modèles de propagation des fissures et la modélisation du délaminage à l'impact.

En raison du nombre élevé de personnes qui se sont désistées, l'ensemble des disciplines impliquées par cette étude n'ont pu être traitées, ainsi l'absence des spécialistes des agences de certification et des exploitants de grandes flottes d'avions militaires en particulier n'a pas permis d'atteindre tous les objectifs visés.

Certaines présentations ont montré très clairement qu'il est indispensable de faire avancer les connaissances dans certains domaines tels que la modélisation de la propagation des fissures, les domaines et les seuils de résistance des matériaux, l'analyse des spectres de charge et les technologies d'inspection afin d'assurer une mise en oeuvre réussie des principes de tolérance à l'endommagement, en particulier dans le cas d'une fréquence élevée des changements de configuration des systèmes dynamiques. La majorité des grands fabricants a conclu que pour le moment la méthodologie améliorée de sécurité par l'estimation de la vie, basée sur la tolérance des défauts demeure la méthodologie la plus viable pour ces éléments. Cependant, une communication a présenté l'expérience acquise en matière de mise en oeuvre de la méthode de propagation lente des fissures, tant pour le système dynamique que pour la structure.

De l'avis de tous, si une « véritable » conception en vue de la tolérance à l'endommagement était adoptée à l'avenir pour les structures métalliques, des charges d'exploitation et des systèmes d'inspection de l'état des structures pourraient être utilisés pour établir des données sur les domaines d'utilisation et les intervalles entre les visites d'inspection.

En dehors des différents avantages et inconvénients des deux principes de conception, les discussions qui ont eu lieu ont mis en lumière d'autres sujets tels que le besoin d'adapter les choix de matériaux au principe de conception retenu. Des travaux de recherche supplémentaires en matière de conception pourraient déboucher sur des structures conçues en conformité avec les principes de la sécurité par l'estimation de la vie, ayant des caractéristiques de tolérance à l'endommagement. Il y a lieu également de réduire les dimensions des fissures initiales par rapport aux structures des aéronefs à voilure fixe. Des mesures doivent être prises pour améliorer les techniques d'inspection en ce qui concerne les fissures et les imperfections afin de permettre l'exploitation d'aéronefs à voilure tournante sans coûts additionnels.

La question des nouvelles exigences en matière de conception et de certification des aéronefs à voilure tournante va rester un sujet de préoccupation pour les avionneurs, les exploitants et les agences de certification et de recherche. Il est clair que l'amélioration de la gestion du cycle de vie des aéronefs à voilure tournante des flottes militaires et civiles ne pourra être obtenue qu'au travers de discussions et d'efforts soutenus de la part de l'ensemble des acteurs impliqués. La définition d'une méthodologie de conception et de certification commune pour les composants des aéronefs à voilure tournante représenterait une étape décisive dans la réalisation de cet objectif.

Contents

* This paper was not presented at the meeting.

* This paper was not presented at the meeting.

Theme

Rotorcraft are essential for carrying out critical military missions, following extremely demanding flight envelopes. Determining manoeuvre and vibration loads, establishing usage spectra and designing structural and system components with respect to fatigue requirements is highly complex. Recent design approaches and regulatory efforts permit more general application of damage tolerance principles, which explicitly allows for manufacturing or service induced flaws and defects. This concept has been demonstrated for fixed wing A/C in the past and can bring about considerable benefits with regard to operational safety and readiness and life cycle cost. The review of the present status indicated a need for considerable further work on loads and spectrum generation, determination of material data i.e. crack growth data for small cracks and in the near threshold regime, stress intensity solutions for typical design geometry, determination of suitable inspection methods and intervals, implementation of HUMS (Helicopter Usage Monitoring Systems) and its link to lifing algorithms and certification aspects.

The meeting will offer a forum to the NATO nations to discuss the applicability and further development of this design approach especially for rotorcraft. Components from the dynamic system, the primary load-carrying structure, transmission and flight control systems and more will be addressed. Prerequisites, databases and suitable analytical tools and areas of further development will be addressed and progress necessary for application will be identified. The RTO provides a unique forum, bringing together all major manufacturers, operators, agencies and research institutes in Europe and North America to address the specific needs and requirements of the military customers. Arriving at a common design and certification methodology for rotorcraft components is the longer term goal of this activity.

Thème

Pour l'exécution de missions militaires délicates dans des domaines de vol très exigeants les aéronefs à voilure tournante sont indispensables. Mais il est très difficile de déterminer les charges de manoeuvre et de vibration, d'établir l'éventail des utilisations possibles et de concevoir les composants de systèmes et de structures en fonction des critères de résistance à la fatigue.

Grâce aux approches conceptuelles récentes et aux efforts entrepris dans le domaine des règlements, les principes de tolérance à l'endommagement sont appliqués de façon plus générale en tenant compte, de façon explicite, des imperfections et des défauts de fabrication ou de service. Dans le passé, ce concept a été démontré pour les aéronefs à voilure fixe. Il peut entraîner des améliorations considérables dans les domaines de la sécurité, de la disponibilité opérationnelle, et du coût global de possession.

L'examen de la situation actuelle a fait ressortir un besoin urgent pour des travaux sur l'origine des charges, sur l'éventail des utilisations, sur le recueil des données sur les matériaux c'est à dire sur la propagation des fissures pour les petites criques et en régime proche du seuil critique, sur des solutions concernant l'intensité des contraintes pour des configurations géométriques caractéristiques, sur la détermination de méthodes avec des intervalles d'inspection appropriées, sur la mise en oeuvre du HUMS (Systèmes de contrôle du vieillissement des hélicoptères) et ses liens avec les algorithmes de gestion du cycle de vie, ainsi que sur les aspects liés à la certification.

La réunion servira de forum aux membres des pays de l'OTAN pour aborder les problèmes liés l'applicabilité et au développement ultérieur de cette approche de la conception, en particulier pour les aéronefs à voilure tournante. Ces éléments du système dynamique, de la structure porteuse principale, des systèmes de transmission et des systèmes de commande de vol. Les conditions préalables, les bases de données, les outils analytiques adaptés et les domaines de développement futurs seront traités, ainsi que les progrès à réaliser pour procéder aux applications.

En permettant le rassemblement de tous les grands fabricants, exploitants, agences et instituts de recherche de l'Europe et de l'Amérique du Nord, pour examiner les besoins spécifiques des utilisateurs militaires, la RTO fournit un forum unique. L'objectif à long terme est de pouvoir définir une méthodologie commune de conception et de certification pour les composants des aéronefs à voilure tournante.

Specialists' Meeting Programme Committee

Technical Evaluation Report On 1999 Specialists' Meeting On Application of Damage Tolerance Principles for Improved Airworthiness of Rotorcraft

Held on 21-22 April 1999 in Corfu, Greece

R. A. Everett, Jr.
Army Research Laboratory, VTD
NASA Langley Research Center
MS 188E
Hampton, VA 23681 USA

SUMMARY

Rotorcraft are essential for carrying out critical military missions, often following extremely demanding flight envelopes. The very nature of the rotorcraft, rotating wing, results in a high vibratory load environment where fatigue is a prime consideration in the design of rotorcraft components. Up until the late 1980's rotorcraft had been designed primarily using the safe-life methodology. During the 1980's it became more and more obvious that fatigue problems found after the helicopter was in service were evaluated and sometimes solved using damage tolerance considerations. As attention turned more and more towards a damage tolerance life management system, many issues arose that appeared to make the classic slow crack growth damage tolerance methodology difficult to apply to rotorcraft. Hence, this Specialists' meeting was designed to bring together all major manufacturers, operators, certifying agencies, and research institutes in Europe and North America to address the issues needed to make damage tolerance a viable design philosophy for rotorcraft. Arriving at a common design and certification methodology for rotorcraft components is the longer term goal of this activity.

This Specialists' meeting was chaired by Dipl.-Ing G. Gunther of DiamlerChrysler Aerospace (Germany) and offered a forum to the NATO nations to discuss the applicability and further development of the damage tolerance methodology to rotorcraft. This meeting covered both metallic and composite materials and brought together major manufacturers from Europe and North America along with researchers, civilian certifying agencies, military experts in structural life management, and University professors. Among the topics covered were the evaluation of crack growth models, material allowables, the flaw tolerant enhanced safe-life methodology, a civil agency view of fatigue and damage tolerance, and the application of damage tolerance to increase safety of helicopters in service. Most of the major manufacturers' presentations concluded that at present the flaw tolerant enhanced safe-life methodology was more viable for rotorcraft dynamic components. One manufacturer did present their successful experience with applying the slow crack growth damage tolerance methodology to three dynamic components and one area of the airframe. In this report, summaries of the 16 papers submitted to this meeting are given followed by the roundtable discussion at the end of the meeting and some conclusions from the recorder.

INTRODUCTION

Up until the late 1980's rotorcraft components were almost exclusively designed using the "safe-life" methodology. However, during the 1980's it became more and more obvious that damage tolerance principles were used to evaluate and solve fatigue problems that occurred because of manufacturing errors or in-service damage. During this time frame the United States Air Force and several NATO nations were using damage tolerance design philosophies in fixed-wing aircraft to improve safety and reliability. The latter consideration translates into life-cycle costs. Over the past decade an ever increasing emphasis has been placed on the operational safety, readiness, and life cycle cost of rotorcraft. In the 1980's the U.S. Army sought to handle some of these concerns by requiring a reliability of six nines on future rotorcraft. In another attempt to increase safety, the FAA (United States) added in the late 1980's an additional requirement to the federal air regulations (FAR's) requiring a flaw tolerant safe-life evaluation for the larger transport category rotorcraft.

This new methodology is a mixture of safe-life and a "type" of damage tolerance design philosophy and is known by several names. Among them are the "flaw tolerant safe-life" and "enhanced safe-life". Sometimes it is even called damage tolerance, although classic damage tolerance as started by the U.S. Air Force in the early 1970's assumes that a pre-existing fatigue crack exists in the structure while the flaw tolerant method assumes a flaw(not a sharp fatigue crack) pre-exists in the structure. The flaw tolerant method still uses the Palmgren/Miner rule to establish retirement lives with the applied stress versus life cycle to crack initiation curves, S/N curves, coming from tests on structures that have pre-existing flaws such as nicks, dents, scratches, and corrosion (to name but a few of these flaw types). Because of the success that the rotorcraft community has shown with the safe-life method, the flaw tolerance method was thought to be an acceptable method to handle the fatigue problems that occur from such things as manufacturing and in-service defects. However, much controversy currently exists with this method to the point where the Technical Oversight Group for Aging Aircraft, TOGAA, in its review of civil rotorcraft fatigue substantiation practices, is recommending that the flaw tolerance method be removed from FAR 29.571 (Fatigue evaluation of structures for rotorcraft over 7,000 pounds). Currently, no rotorcraft has been fully certified using flaw tolerance and until this meeting very little data existed in the literature to show the success of the flaw tolerant method.

Paper presented at the RTO AVT Specialists' Meeting on "Application of Damage Tolerance Principles for Improved Airworthiness of Rotorcraft", held in Corfu, Greece, 21-22 April 1999, and published in RTO MP-24.

Over the past thirty years or so , the U.S. Air Force has successfully used the classic crack-growth damage tolerance method in fixed-wing aircraft. One of the principle attributes of the damage tolerance philosophy in the fatigue life management of aircraft structures is that a flaw (fatigue crack) is assumed to exist in the structure at the beginning of the service life of the aircraft and inspection intervals are calculated using fracture mechanics. Compared to this design methodology, the safe life design method calculates a retirement life using the Palmgren-Miner rule which assumes the structure is free of any defects. It has often been stated that the mean life of a dynamic component determined by the Palmgren-Miner rule could be 200,000 flight hours while the replacement time is only 2,000 hours. It has also been stated that potentially many good parts are retired without any existing damage. One of the principal advantages of the crack growth damage tolerance method is that it models the actual physical damage that causes fatigue failure, namely a crack. However, as pointed out by several presentations in this meeting, there are several obstacles that must be overcome before crack growth damage tolerance can be used on all dynamic components. Some even state that this can never be done on all dynamic components. In this meeting many of the obstacles such as the high cycle content of the rotorcraft load spectrum and the small crack sizes that must be reliably detected by nondestructive inspections were addressed. A part of the intent of this meeting was to discuss these obstacles and other technical issues that need to be clarified before the benefits of a fracture mechanics approach for designing rotorcraft components can be fully realized by NATO nations.

SUMMARIES OF PAPERS

1. "The Significance of Small Cracks in Fatigue Design Concepts as Related to Rotorcraft Metallic Dynamic Components"
   R.A. Everett, U.S. Army, ARL, VTD, USA

In this presentation the significance of the "small" crack effect as defined in fracture mechanics was presented as it related to life managing rotorcraft dynamic components using the conventional safe-life, the flaw tolerant safe-life, and the damage tolerance design philosophies. The "small" crack effect was defined in fracture mechanics terms where it has been observed that cracks on the order of 300 microns or less in length will propagate at higher growth rates than long cracks and also will grow at ΔK values below the long crack ΔK threshold. The small-crack effect is illustrated herein as resulting from a lack of crack-closure and is explained based on continuum mechanics principles using crack-closure concepts in fracture mechanics.

In the conventional safe-life design methodology the presenter noted that one of the major concerns with the safe-life methodology is the sensitivity of safe-life designed parts to manufacturing and in-service flaws. This stems from a selection of the wrong materials from a damage tolerance perspective as the safe-life approach gives very little understanding of the physics of the fatigue and fracture process somewhat because of the use of the Palmgrem/Miner rule. In this presentation a computer code developed at NASA Langley based on a fracture mechanics crack-closure model using small-crack growth characteristics was shown to predict total fatigue life (safe-life, S/N curve fatigue lives) of several different metallic materials. However, in order to calculate total fatigue life from a crack growth analysis a very small initial crack size (0.001mm to 0.050mm) was assumed to exist in the structure.

The small-crack total fatigue life analysis was shown to predict the total fatigue life of test coupons made of 4340 steel under constant amplitude loading and the standardized helicopter spectra called Felix/28 with reasonable accuracy. It was also shown to predict the fatigue lives of a laboratory type specimen of 4340 steel with a machine-like scratch with a depth of 0.05 mm. Hence, small-crack fatigue life analysis may be an analytical tool that could used in flaw tolerant safe-life evaluations.

It was stated that it did not appear that small-crack theory would need to be considered in the crack growth damage tolerance design concept since the small-crack effect appears to only occur when cracks are of micro-flaw sizes (1- to -10 μm). The damage tolerance inspectable flaw size currently being suggested for rotorcraft is about 0.38 mm. However, one area where small-crack considerations could be of benefit would be that of determining the crack-growth threshold, ΔK_{th} . It was illustrated that one aspect of small-crack growth is that they grow at ΔK values below the long crack ΔK threshold. If this situation is real and the "small" crack growth effect is ignored, unconservative predictions of crack growth times to failure might occur since cracks will be growing below the long crack ΔK threshold. Hence, considerations of small-crack growth may help define a more realistic crack-growth threshold.

2. "The Development of a Robust Crack Growth Model for Rotorcraft Metallic Structures"
   Presenter: D. Matthew, GKN Westland Helicopters, UK

This presentation focused on evaluating the ability of existing crack growth models to predict crack growth behavior in two different materials using different specimen configurations and different loading sequences. It was noted that this work was motivated by a change in the airworthiness directions from the safe-life methodology used in the past to the current regulations which require using flaw growth methods. This work was done under a collaborative program involving GKN Westland Helicopters, DERA, Cranfield University and nCode International. While six topics that affect a crack growth analysis were investigated (i.e., stress intensity solution, fitting of crack growth data, etc.), the main focus was the evaluation of the several crack growth models considered. Both plastic zone correction models (like Wheeler and Willenborg) and models which are based on strip-yield considerations (like Stripy and FASTRAN) were evaluated. A model was also evaluated that is a more sophisticated version of the plastic zone models which also includes

crack closure considerations. The evaluation used a procedure that used increasingly complex loading sequences (constant amplitude to helicopter representative sequences) and increasingly complex specimen configurations (compact tension to structural elements).

Some of the conclusions drawn from this study were: (1) the method used to fit the raw crack growth rate data affected the model predictions of crack growth life by up to a factor of three, (2) using different equations to represent the fitted crack growth data for computer model use (like a Paris, Walker of Foreman equation), resulted in predicted differences up to a factor of five, (3) tabular input of the data is the most appropriate method to describe the crack growth rate data, (4) calibrated models (like adjustments to better fit near threshold data) gave improvements in more complex loading predictions , (5) predictions of the representative helicopter loading sequences (Asterix and Rotorix) are very sensitive to small changes in near crack growth threshold data, (6) and all models other than Kragen gave unconservative predictions when comparing to test data.

Other observations made from this study include the following. Some evaluations gave better predictions for titanium (comparing data fit methods) while others gave better predictions for aluminum-lithium (simple variable amplitude loading tests for calibrated models). When loading spectra contain compressive loading, it is important to use constant amplitude crack growth behavior from negative stress ratio test and not just data from tensile stress ratio tests. The importance of this increases with more compressive loading content in the spectra. Evaluations of the same experimental data by different evaluators can give noticeably different results. When calculating the delay cycles from a simple variable amplitude loading sequence, one participant showed predictions that were as large as 4.66 different than the test data. For this same comparison, another participant showed much better agreement (both participants used the Kragen program which generally gave conservative predictions compared to tests where all other models were usually unconservative). One general conclusion of this study states that even though predictions were improved after the models were calibrated, these predictions did not always give acceptable results. Further work is needed to improve such areas as accounting for the effects of underloads and a fully understanding crack growth behavior near the threshold region.

4. "Material Allowables for High Cycle Fatigue in Gas Turbine Engines"
   Paper not presented at the meeting.
   T. Nicholas, U.S.A.F. Research Lab. WPAFB, USA

This paper focuses on the materials allowable data and how it relates to a damage tolerance (DT) design approach in managing high cycle (HCF) fatigue in gas turbine engines. HCF as defined in the USAF engine structural integrity program is fatigue that occurs in the 10^9 cycle range for non-ferrous metals. The USAF is moving away from setting design allowables using an alternating stress versus mean stress diagram (Haigh diagram), to a damage tolerance approach which uses crack growth considerations. It is noted that a DT approach to relate remaining life based on predictions of crack growth to an inspectable flaw size (airframe DT approach) is not appropriate for engines because the required inspection sizes would be well below the current non-destructive inspection capabilities. Most HCF problems are caused either by the existence of vibratory stresses from unexpected drivers or the result of damage caused by production errors or service usage. The current use of the Haigh diagram in managing HCF employs the concept of a threshold below which HCF will not occur. A threshold concept (crack growth can be neglected during the expected life of a material) will also be the probable approach used in a DT management system.

Establishing material allowables for HCF whether in fatigue or DT is very time consuming (10^7 cycles or beyond). It is suggested that this testing time could be reduced by either using recently developed high frequency test machines (up to 2 KHz and ultrasonic resonant machines) or using a rapid test technique involving step loading as proposed by Maxwell and Nicholas. This paper also highlights several areas where more research is needed in order to develop a reliable HCF methodology. Among these are HCF and low cycle fatigue interactions. Does low cycle fatigue affect the damage that occurs in the HCF portion of fatigue life? How do load interactions affect "small" crack growth where it is very difficult to monitor crack growth because of the very small size of the fatigue crack? How do residual stresses from foreign object damage affect the determination of inspection intervals? Is fretting fatigue due completely to the relative motion that develops in a fretting environment or is it due to the complex stress states that develop in the contact regions?

5. "Damage Tolerance Characteristics of Composite Sandwich Structures"
   L. Lazzeri, Univ. of Pizza, Italy

This presentation focused on the effects of impact damage and delaminations on the residual strength and fatigue life of composite sandwich structures. Both static and fatigue tests were conducted on test coupons which simulated the EH-101 helicopters tail unit not only to assess the effect of damage on strength, but to evaluate and help develop reliable analytical tools to predict this type of damage. Barely visible impact damage, BVID, was assumed to be impact damage visible from a distance of 1 meter and was place in the panel using a drop weight procedure with a hemispherical impactor. Cleary visible impact damage, CVID, was put into the panels using the same device as for the BVID, but increasing the energy by 50 % and by using a pyramidal impactor, simulating a toll box using the same energy level as for the BVID. A teflon insert was used to simulate delamination damage which was thought to be important since many manufacturing defects (porosity, foreign object inclusion, etc.) can be considered to be equivalent to a simple delamination. Three types of specimen configurations were used all having the same core material, but with differences in core thickness and the

lay-ups of the skins. Anti-buckling guides were used since the panels were unsymmetrical and bending resulted during compression.

From the results presented, panels with the thinner skins showed a larger fatigue strength reduction for the CVID tests compared to the BVID tests. The thicker skin panel fatigue test results for the CVID panels were within the scatter of BVID tests. In the static tests the severity of the damage had a larger affect on static strength giving an indication of the well-known notch sensitivity of composites. In the fatigue tests with the teflon inserts delaminations grew to a much greater extent than in static tests and the influence of buckling was noted where without buckling delamination growth was negligible.

A delamination analysis was used to help explain a rather odd test result where test results from the teflon strip specimens showed delamination growth rate decreasing while the delamination dimension was increasing. This behavior is opposite to that usually reported in the literature. A finite element analysis was performed using MSC/NASTRAN to evaluate the strain energy release rate, G, which is the parameter many are using to describe interlaminar fracture behavior. Using a global/local modeling approach and noting the importance to describe accurately the out-of-plane displacements to represent the sublaminate bucking behavior, a rapid decrease in G_I , mode I, was shown to occur for these test panels with an increase in delamination length (G_{II} increased). This explained why the delamination growth shown in these panel tests decreased with increasing length and showed why the total G is not necessarily an important parameter, while the contribution of the different fracture modes, G_I and G_{II}, can be of particular importance.

The presentation concluded by noting that impact damage is the most severe damage to composite damage tolerance and that the extensive test programs currently used to evaluate this type of damage is very time consuming and expensive. A better understanding of the fracture behavior of composite is needed to help reduce this intensive evaluation while not affecting the desired level of safety.

6. "Damage Tolerance of Low Velocity Impact on Laminated Composites."
   G.A.O. Davies, Imperial College, London, UK

This presentation illustrated an approach for predicting the threshold delamination independent of the shape of the laminated structure. The presenter noted that past research has shown a significant reduction in the compression strength after impact, CAI (up to 70% for a thermoset resin) for laminated composites. It was noted that while coupon tests are useful for evaluating delamination damage after impact for comparing different materials, they are not adequate for evaluating delamination in real structures where such factors as the structures mass, geometry, and stiffness affect the internal stress field that develops from the impact. For low velocity impact, which is the focus of this presentation, the resulting damage is virtually invisible to the observer. Low velocity impact is defined as impact events that occur at velocities less than 20 m/sec such as from tool drops where impact velocities are up to 9 m/sec from a height of 4 meters. The main concern from this type of impact and its affect on CAI is the internal delamination that results in separation of the laminae which may cause local buckling and propagation of a local blister.

From a very large number of coupon tests which included a few stiffened panel tests, a map of damage against incident energy showed a very chaotic behavior which the presenter states illustrates why coupon tests can not be used to explain all aspects of impact damage. A clearer relationship was shown when the maximum impact force is plotted against the impact damage with only a dependence on plate thickness allowing the evaluation to be made from just one set of coupon tests. Fracture mechanics considerations were used to predict a critical threshold force corresponding to sudden unstable propagation independent of the radius of the delamination. An equation based on the assumption of axisymmetric strains was presented that shows threshold force as a function of the elastic constants, plate thickness and G_{IIC}.

To find the force history and the threshold for delamination in the laminate, a shell element-based finite element analysis was recommended. The analysis employs a ply discount approach to delete the contributions from individual plies once a ply strain failure criteria is exceeded. The predicted gradual decrease in stiffness shows much closer agreement with a variety of test results than otherwise similar analyses that do not employ the ply discount methodology. To predict the extent of damage, the authors used another shell element-based method where two layers of elements were layered on either side of an assumed initial delamination. The elements were joined with a system of links which were individually removed as the interlaminar forces reached a critical value based either on the interlaminar shear strength or the peel strength of the resin.

Compression after impact (CAI) response of a structure with known damage was also determined using a finite element-based approach. Examination of the strain energy release rates indicated that the delamination would propagate at right angles to the applied load direction. The authors indicated that the European Union is currently sponsoring a task to address the issue of computational efficiency of this type of modeling while accurately tracking the delamination front. An alternative idea was proposed that involves modeling the damage with a clean circular hole in conjunction with a kink-band failure analysis. In their combined analyses, the authors note that Mode II is the dominant mode of failure during impact, while mode I is the dominant mode during compression after impact.

7. "Application of Damage Tolerance to Increase Safety of Helicopters in Service"
   Bogdan R. Krasnowski, Bell Helicopter Textron, US

This presentation illustrated how several in-service problems that resulted in fatigue cracks were evaluated and

how an acceptable level of reliability was obtained using a damage tolerance assessment. It is noted that even though most rotorcraft currently in service were designed to safe-life requirements, damage tolerance is often used to insure the reliability of the components when they are redesigned because of in-service problems. The paper also stated that while the safe-life design method could evaluate why a shorter fatigue life resulted from such things as more severe usage, higher loads, or lower component fatigue strength than intended in design (due to corrosion, manufacturing defects, etc.) that it could not account for variabilities often shown to result (shorter and longer fatigue lives) when using Miner's rule. It is further noted that since a fatigue crack caused the service problem, that a crack growth analysis (obtained in a damage tolerance assessment) would model the actual damage mechanism (a growing crack). This allows for evaluating different scenarios that include initial crack sizes, load spectrums, and part geometry to address options available to solve the problem such as structural modifications and setting crack inspection intervals.

The problems evaluated were cracking in the skin of a tailboom, tail rotor blade doublers, main rotor pitch link, and corrosion in a main rotor grip. The crack in the tailboom was caused by high vibratory loads which were reduced in a modified design using "dynamic fixes." To extend the inspection interval the thickness of the critical section was increased. Flight load spectrum tests on field-returned tailbooms confirmed the conservatism of crack growth analysis and allowed an extension on the inspection interval. In the tail rotor blade doubler excessive sanding caused cracking of the skin which through a redesign using spar reinforcement substantially increased the inspection interval. In the main rotor grip the material was changed to a more corrosive resistance material for which the crack growth analysis established an inspection interval to increase the components reliability. For the main rotor pitch link the material was changed from aluminum to steel and even though both parts had an infinite safe life, a crack growth analysis was used to show that the steel pitch link had a higher reliability. One of the conclusions of the paper is that the level of safety can be measured by reliability and that a damage tolerance design approach can give a higher level of reliability than a safe-life approach.

8. "AGUSTA Experience on Damage Tolerance Evaluation of Helicopter Components"
   U. Mariani and L. Candiani, AGUSTA, Italy

This presentation reviewed Agusta's program on the fatigue evaluation of the EH-101 helicopter using the flaw tolerance requirement which was instituted into the Italian, British, and United States civil air regulations in 1989. The presenter expressed that one of the main benefits of the flaw tolerance approach when combined with the traditional safe-life evaluation is an expected improvement in maintenance and repair actions. Because of the high frequency content of the rotor induced loads on dynamic components, damage growth from inspectable flaw sizes would require very short inspection intervals. Therefore, a "no damage growth" approach was used. Many of the components in the EH-101 are a combination of metallic and composite materials. The main rotor hub is made of a titanium core with carbon fiber loop windings enclosed by a glass/epoxy box. The metal parts were mostly safe-life evaluated with some additional flaw tolerance tests being done on such parts as the main rotor hub titanium core, the damper hub attachment, the support cones, and the tension link titanium frames. The composite parts were concerned with such damage as barely and clearing visible impact damage, BVID and CVID, respectively.

For the main rotor hub, no damage growth in a service life test was observed for the composite parts from either BVID or CVID. The BVID was simulated with a spherical inpactor at an energy level of 50 joules, while for CVID a sharp tool was used made from a 90 degree pyramid. Some damage growth occurred in a Navy spectrum tests where the glass wrapping had scratches and delaminations. The loads were amplified with damage growth occurring during the start-stop cycles of the spectrum. Still a target of 10,000 hours was achieved, which results in an inspection interval of 2,500 hours using a factor of safety of four. This was also an amplified load test. Test on the titanium core showed damage tolerance features in a test where 10% of the hubs teeth and the solid lubricant were removed. Fail-safe capabilities were also shown in a test where 4 out of 15 bolts were removed from the upper and lower aluminum plates in the splined area. For other components where composite parts were used such as the main rotor inboard and outboard tension links, tail rotor hub and blade, parts of the tail unit structure, adequate retirement lives were shown when evaluated for BVID.

A typical flaw tolerance test in a metal part was illustrated on the main rotor support cone which is connected to the hub with two special bolts and four stud bolts. Flaws were put in the lugs of the special bolts to simulate assembling and maintenance induced flaws. These flaws were simulated by "V" grooves of 0.35 and rogue flaws of 0.50 mm deep. To illustrate the concern of the designer in putting excessive compressive residual stresses in the material from the simulated flaws, a sharp tool was used to minimize plastic deformation at the flaw tip.

9. "Application of Damage Tolerance to the EH101 Airframe"
   D. Matthew, GKN Westland Helicopters, UK

This presentation outlined the test and analysis program used in the damage tolerance evaluation of the EH101 airframe. The EH101 is a medium/large three engine helicopter which has just entered service with the Royal Navy and will shortly enter service with the RAF. A civil version is also in production. In this study, a comprehensive test program used compact tension specimens to develop the crack growth behavior of aluminum lithium forgings which are used as part of the lift frames. Tensile tests at stress ratios of 0.1 through 0.9 were conducted to generate da/dN versus ΔK, ΔK_{th}, and fracture toughness data. Progressively more detailed structural element tests were conducted composed of six structural elements representing the geometry of the roof

frames in the region of a lightening hole. Full size component test were also conducted on a production roof frame and side frame with flaws at four locations. A full scale complete airframe test which is the final stage of testing (in progress at the time of this presentation) will investigate load distribution from crack growth in the multiple mode loading of a complete airframe. Tests were also conducted to establish the flaw tolerant characteristics of the material.

A commercially available crack growth code called KRAGEN was used which allows input of a complex load spectrum, user defined stress intensity solutions, and has crack growth retardation and acceleration modeling capabilities. The maximum vibratory load was conservatively assumed to apply for the whole manuever. Because previous analyses using KRAGEN has shown very little load history effects on crack growth under helicopter load spectra, the sequencing of the load spectra was ignored. One of the conclusions from this program was that because of "disappointingly short inspection intervals", a fail safe, enhanced safe life (flaw tolerant) approach was more suited for the EH101 main load path on the airframe. Future work is focusing on stress intensity solutions, a better understanding of crack growth thresholds, and how the behavior of short cracks might affect the crack growth thresholds. It was also noted the KRAGEN can give very conservative crack growth behavior at high stress ratios and that crack growth models need to accurately predict growth rates over a wide range of stress ratios, R.

10. "Treatment of High-Cycle Vibratory Stress in Rotorcraft Damage Tolerance Design"
J. Lincoln, WPAFB, US

This presentation showed some of the results of the US Air Force damage tolerance assessment, DTA, performed by Sikorsky on the HH-53 helicopter as well as an example problem which addressed several issues that have been stated to be potential problem areas for using a slow crack growth DTA for helicopters. Recommendations were also made for areas that need improving for DTA to be successful in helicopter design. With the success of the DTA in fixed wing aircraft being noted, the USAF expected it could be applied to engine structures. As it proved also to be successful on engines used in such aircraft as the F-100 and the F-15 and 16 it appeared reasonable that it might also apply to helicopter. The DTA on engines again highlighted that the proper choice of materials is necessary such as using materials with a good fracture toughness.

Some of the findings in the HH-53 DTA were the need for detailed stress analysis (usually not done in a safe life design), an accurate stress spectrum, a careful evaluation to identify the areas that are critical for inspections, and the proper choice of the initial flaw size to use in the calculation of the inspection interval. It was noted that a reasonable goal for inspections is a flaw size of 0.254 mm. In the HH-53 DTA some parts were found to be damage tolerant, while others had unacceptable inspection intervals even for an initial flaw of 0.127 mm. It was stated that these locations would be candidates for modification. In some cases the recommended component replacement time was less than the crack growth time from a 0.127 mm flaw.

In the example problem using Ti-6Al-4V as the material, it was noted that the ΔK threshold can have an significant effect on the damage tolerance life, but with guidance from "small-crack" understandings increased confidence can be obtained in calculations that involve crack growth in the ΔK threshold region. Also shot peening can significantly extend the inspection intervals. It was stated that the omission of the effects of shot peening in the HH-53 DTA probably led to some of the components being unmanageable using damage tolerance.

Some conclusions drawn were that stresses used for damage tolerance design may need to be reduced from those required in safe life designs. It was noted that for the prototype of the V-22 aircraft that the weight impact was not significant. The need for usage tracking was expressed.

11. "Fatigue Substantiation and Damage Tolerance Evaluation of Fiber Composite Helicopter Components."
H. Bansemir and S. Emmerling, Eurocopter Deutschland GmbH, Munchen, Germany

This presentation described the fatigue and damage tolerance methodology used by Eurocopter Deutschland for composite structures on a new multi-mission helicopter, the EC135. The presentation covered the critical areas related to quality assurance and flaw detection, certification requirements, establishment of fatigue and damage tolerance criteria, overall structural behavior, and dynamic strength and limit load capacity.

Computed tomography (CT) that can detect flaw sizes (damage, debonds, waviness, etc.) as small as 0.2 mm in length is used by Eurocopter for quality assurance of helicopter rotor blades. The authors show the results of CT taken for early prototypes of the EC135 main rotor blade with manufacturing defects. The EC135 was certified according to the Joint Aviation Requirement JAR27 "Small Rotorcraft," the fatigue evaluation of Transport Category Rotorcraft Structures FAR29.571, and the German airworthiness authority regulations on "Primary structures designed with composite material." The Flaw Tolerant Safe Life Method was used to substantiate the rotor blade. Requirements also include: no interlaminar failure at limit load, no fiber failure at ultimate load, and certain considerations related to environmental factors.

Rather than dynamically test the complete rotor blade, several sections were tested according to their critical load and mode of failure. A standard Transverse Crack Tension (TCT) specimen was used to determine the static and dynamic delamination behavior of the laminated flexbeam under mode II loading, while a modified TCT specimen was proposed to determine delamination behavior under mixed mode I and mode II loading. Relationships for delamination onset and stable delamination growth were

derived from test results. The addition of a layer of adhesive at critical interfaces was shown to more than double G_{IIC}. The last of the sequence of tests for the flexbeam involved testing a representative section 50 cm in length by applying an axial force of 150 kN and a torque producing a twist of 100° over the length of the beam with no apparent failure.

12. "Rotorcraft Damage Tolerance Evaluated by Computational Simulation"
Presenter: F. Minnetyan, NASA Glenn Research Center, Cleveland, OH

This presentation discussed a methodology for predicting damage initiation and propagation in unstiffened and integrally stiffened laminated composite panels and shells. The computational methodology is composed of three modules: (1) composite mechanics, (2) finite element analysis, and (3) damage progression tracking. A modified distortion energy criterion is proposed for failure where the applied stress and the longitudinal and transverse allowable stresses are considered. Fiber and matrix modes are delineated by examination of the dominant terms in the expression for failure.

Two AS4/3501-6 laminated composite panels and two AS4/3501-6 laminated composite shells were considered in the analyses. The first panel had integrated ±45° intermittent lattice stiffeners, while on the second panel, the stiffeners were replaced with additional skin thickness such that the material volume of the two plates was the same. Examination of the undamaged structural response of the two panels revealed that the buckling load of the stiffened panel was 5.2 times the buckling load of the unstiffened panel. Additionally, the bending stiffness of the stiffened panel was 7.2 times the bending stiffness of the unstiffened panel. In contrast, the damage initiation load in tension of the integrally stiffened panel was approximately one-third of the damage initiation load of the unstiffened panel. In compression, the damage initiation load of the integrally stiffened panel was only one-fifth of the damage initiation load of the unstiffened panel. An analysis for similar integrally stiffened and unstiffened composite shells was also performed. The ultimate strength of the stiffened shell in tension was approximately 60 percent of the ultimate strength of the unstiffened shell. Under pressure loading, the ultimate pressure for the stiffened shell was approximately 75 percent of the ultimate pressure for the unstiffened shell.

13. "The US Navy's Helicopter Integrated Diagnostics System (HIDS) Program: Power Drivetrain Crack Detection Diagnostics and Prognostics, Life Usage Monitoring, and Damage Tolerance; Techniques, Methodologies, and Experiences"
Paper not presented at the meeting.
A. Hess , NAWC AD, et al, US

This paper described the U.S. Navy's Helicopter Integrated Diagnostic System (HIDS) to illustrate some of its capabilities and accomplishments. Also discussed are a drive train crack detection diagnostic technique, component life usage monitoring philosophies, and damage tolerance methodologies. HIDS is designed to evaluate the health of propulsion and power, rotor, and structural systems. It also records cockpit instruments and control positions during an entire flight for usage monitoring and flight analysis. The system is designed with an industry-standard open architecture concept to allow for modularity and insertion of new hardware and software. It is divided into two avionic units. One unit is a commercial off-the-self aircraft parameter-usage monitor and the other is a vibration acquisition, analysis and rotor track and balance system. One of the major challenges of this system was in acquiring and managing large amounts of data. The system was designed to exceed the requirements for a total onboard health and usage monitoring system in order to provide the rationale to specify the minimum system requirements needed to achieve low false alarms and all functional goals. Evaluation of the system has been performed using a test cell (iron bird test stand) and SH-60B/F helicopters.

The paper summarizes a subset of 14 objectives used in the evaluation of the HIDS. Among these were to evaluate the ability of the diagnostic system to identify localized faults in an entire drive system, evaluated sensor placement to minimize the total number of sensors, and to demonstrate the ability of the diagnostics to reduce component "false removals" and trial and error maintenance practices. In evaluating HIDS for identifying localized faults in a drive system, HIDS was used to detect these faults in the H-60 engine high speed shaft/input module interface which contains the difficult to inspect Thomas Coupling disc pack. A high speed shaft was removed from a H-60 and evaluated in the test cell by comparing its vibration signal to a good drive shaft. The HIDS system not only correctly identified the cracked Thomas Coupling, but also isolated it to the starboard side. In evaluating sensor placement a starboard and port sensor were placed on the main module input pinion of bearing SB2205. At the start of the test the starboard main sensor was designated as the primary sensor. However, the test evaluation showed the port main sensor to be the primary sensor. One of the conclusions from this project is that diagnostic and life monitoring are invaluable tools for managing damage tolerance concerns on aging helicopter fleets, especially for engines, gearbox and drive trains, and rotor head assemblies.

14. "Flaw Tolerant Safe-Life Methodology"
D.O. Adams, Sikorsky Aircraft Corp., USA

This presentation described five examples of the successful application of the flaw tolerant safe-life fatigue substantiation method currently in FAR 29.571. Also presented was a brief explanation of some of the procedures that are a part of the flaw tolerant method. Early in this presentation it was noted that various sources have used different definitions for the terms commonly used in the language one employs in describing the various attributes of fatigue methodology. To keep things as clear as possible this presentation employed the definitions as proposed in the joint position paper of the AIA/AECMA helicopter companies also known as the "white paper" which was presented to TOGAA (Technical Oversight

Group for Aging Aircraft) in January 1999. The recorder has noted in his review of all the papers presented at this meeting that there was a tendency to use the words damage tolerance and flaw tolerance as if they described the same methodology. This presentation defined damage tolerance as "the evaluation of crack growth characteristics, including the conclusion of no growth of cracks" while flaw tolerance describes "the evaluation of crack initiation characteristics from flaws."

As presented the flaw tolerant method develops S/N curves which result from constant amplitude fatigue test specimens with the type of flaws that may be experienced in service or during manufacturing of the component. The types of flaws considered should include nicks, dents, scratches, inclusions, corrosion, fretting, wear, and loss of mechanical joint preload or bolt torque. To determine a component retirement time it is assumed that "barely detectable" flaws are present in the structure at all critical locations. Barely detectable flaws are defined as flaws that "conservatively represent the largest probable undetectable manufacturing or service-related flaws." Retirement times should also be determined on specimens with no flaws (as-manufactured specimens) with the time used to retire the part being defined as the lowest time determined from the barely detectable flawed or unflawed calculations. Inspection intervals for finding flaws use a similar procedure, but use a flaw type that is called a "clearly detectable flaw." The clearly detectable flaw is defined as "the largest probable manufacturing or service-related flaws that would not normally be detected in a routine visual inspection such as a pre-flight or weekly.

Two of the helicopter components where a flaw tolerant evaluation was successfully used were a CH -53A/D main rotor head horizontal hinge pin and a S-76 tail rotor pitch horn both subjected to corrosion. For the CH-53 evaluation an inspection interval was determined considering coupon testing with various degrees of corrosion with an inspection interval recommended being that at the scheduled overhaul every 1200 hours. For the S-76 full-scale corrosion tests were conducted from which a retirement time of 12,000 hours was chosen instead of the original convention safe-life of 22,000 hours. For four of the five components evaluated in this study, it was concluded that the classic slow crack-growth damage tolerance (DT) method would either produce too short inspection intervals or DT would be much more complex to apply compared to flaw tolerance. In the case of the S-92 main rotor hub it was concluded that DT approach would result in "excessive weight penalties and/or an inability to meet the rotor head geometry constraints.

15. "Damage Tolerance Applied on Metallic Components"
T. Marquet, Eurocopter, France

In this presentation it was noted that up until 1989 the safe-life concept has been used almost exclusively in the fatigue evaluation of rotorcraft, with parts being retired at specified times regardless of their condition. Safety was improved by visual inspections, preventive scheduled maintenance, maintenance actions as a result of problems found in the scheduled maintenance program, and the detection of abnormal rotorcraft operational behavior. In 1989 a new civil regulation established a damage tolerance requirement to enhance the safety level that could be reduced by manufacturing and in-service induced flaws. The presenter stated that up to this time no rotorcraft has been fully certified according to these damage tolerance requirements which can be met by a flaw tolerant safe life design and/or a fail safe design.

A Eurocopter accident survey was shown where 77 % of accidents (37 per million flight hours) were due to operational and environmental causes, 17 % from maintenance errors, and 0. 3 % from poor design. It was further stated that 20 of these could have be avoided by using a damage tolerance design approach. In complying with the new damage tolerance requirements, Eurocopter has established the following possible actions for a component at the time of the inspection interval: retired without inspection, returned to service if no flaw (or crack) found, or retired or repaired if a flaw (or crack) is detected. Some conclusions from a research program were presented that showed at least 10 areas of technology that were deficient if a slow crack growth approach was used for rotorcraft design. Among these were a lack of understanding of the region near the crack growth threshold and the effects of crack growth retardation and acceleration for a rotorcraft load spectrum. It was also noted that several difficulties exist in applying a slow crack growth method to rotorcraft which include the large number of load cycles per hour experienced by rotorcraft dynamic components and short crack growth times for inspection intervals due to the relatively large crack sizes that can be reliably detected.

Some results were also shown from Eurocopter's program to develop the data needed to support a flaw tolerant design approach. For steel parts a 0.15 mm deep scratch was shown to reduce the fatigue endurance limit of an unscratched bending coupon by 50 %. It was also noted in this presentation that the Technical Oversight Group For Aging Aircraft, TOGAA, (FAA appointed review group) wanted the flaw tolerant design concept removed from FAR 29 and replaced with the slow crack growth method. Several weak points in the flaw tolerant method as noted by TOGAA were addressed in this presentation with Eurocopter's approach to handling these weaknesses being shown. It is Eurocopter's position as well as other rotorcraft manufacturers to leave the flaw tolerant design method in the current rules.

17. "Strategies for Ensuring Rotorcraft Structural Integrity"
R. Eastin, FAA, USA

This paper examines the three primary strategies for assuring the structural integrity of rotorcraft under FAR 29.571 and discusses some of their weaknesses and strengths concluding with a recommended approach to achieving the objective of FAR 29.571. The author starts by defining two categories of fatigue that are a threat to

structural integrity. "Normal" fatigue which is predictable and steadily increasing with time in service. This type of fatigue results from operations above the endurance limit for structures designed and manufactured without errors and operated as expected. "Anomalous" fatigue results from unpredictable events such as underestimating loads and stresses, manufacturing errors, and unusual usage. The traditional safe-life and damage tolerance philosophies are said to be adequate for managing both normal and anomalous fatigue. Whereas, the relatively new flaw tolerance philosophy is "unduly pessimistic relative to normal fatigue threat and inadequate with respect to the anomalous fatigue threat."

While the paper states that the safe-life philosophy is adequate for dealing with the normal fatigue threat, the definition of safe-life as stated in FAR 29.571 is felt to be somewhat ambiguous in its use of the wording "without detectable cracks." This ambiguity arises since what can be detectable is a function of the inspection method and that improvement in inspection methods change with time. One of the potential weaknesses in the safe-life method as now practiced is the lack of quantification of the failure strength associated with the state of fatigue at the average life. For components where the fatigue state does not degrade the failure strength such that the component can withstand ultimate load, the retirement live based on the average life reduced by a factor of safety is probably adequate. When the opposite scenario occurs (failure strength below ultimate load), the retirement life still may be adequate depending on the value of the factor of safety used.

A damage tolerance approach similar to that used by the USAF is proposed for rotorcraft. One difference being regardless of how good or marginal the DT characteristics are for a component it can be found adequate provided the inspection requirements match its DT characteristics. The USAF approach requires a minimum acceptable level of inherent tolerance to damage.

One concern noted about the flaw tolerance approach is that it could determine retirement lives that are less than the traditional safe-life approach and thus make part retirement an even more economic burden than it is now. It is further stated that it would be difficult to "imagine that potential flaw sources can be anticipated, flaw types characterized and severity quantified to a degree that is sufficient to bound anomalous" fatigue threats. Another concern about flaw tolerance is that it does not produce inspections that have crack detection as their primary objective, while the damage tolerance approach has as one its strongest assets the setting of inspection intervals based on crack growth (for it is cracks, in the end, that cause failure).

ROUNDTABLE DISCUSSIONS

The roundtable discussions was chaired by Professor G.A.O. Davies. To start the discussions, Professor Davies made several comments on his perceptions of the presentations and discussions during the meeting. First, he expected more conflict between the proponents of the safe-life and damage tolerance design methodologies. It appeared that a safe-life or damage tolerance approach may be decided based on the material a designer was using. He further noted the success of using the damage tolerance approach on fixed wing aircraft. However, as a result of the meeting presentations and discussions, it was not apparent that the damage tolerance approach is yet viable for use on rotorcraft components. Professor Davies further noted that component and full-scale tests are getting very expensive and that good analysis techniques are needed to guide us in deciding which tests are the most critical to perform.

One short coming of the meeting was the absence of certifying agency personnel. Two comments were made by participants that stated their understanding of the United States FAA and the British CAA positions on the use of damage tolerance in rotorcraft design. The FAA appears to be encouraging a move towards the use of damage tolerance, but for the present if damage tolerance does not appear viable safe-life can be used. However, it was expressed fairly strongly that the CAA position is to move to damage tolerance immediately. Further comments on this possible confusion will be presented after this section on the round table discussions.

The remainder of the roundtable discussion can be summarized under three topics. First, reasons why damage tolerance is not practical for rotorcraft. Second, reasons for moving towards damage tolerance for rotorcraft. Third, general comments that embrace both damage tolerance and safe-life.

Reasons why damage tolerance is not practical for rotorcraft.

- Inspections are costly.
- Some parts can not be inspected in the field.
- Significant weight increase on large parts.
- Small weight increase on other parts.
- Low reliability of detecting small crack sizes (smaller than fixed wing inspectable cracks)
- High cycle load content of spectrums causes short inspection intervals.

Reasons for moving towards damage tolerance.

- Better method for solving field problems.
- Since test are getting more and more expensive, analysis will be used in the future to decide what tests to do. With fracture mechanics there is a sound mathematical approach to model the actual damage (crack growth).
- Potential cost savings over safe-life. Replace parts only when damaged (safe-life replaces them when retirement life is reached). Some good parts are probably thrown away.
- Weight increase only a few percent on many parts.

General comments.

- Design safe-life parts with damage tolerance features. Possible alternative to exclusively being either safe-life or damage tolerance.
- Material selection often dictated by whether safe-life or damage tolerance is being used for design. Parts with good crack initiation times often do not have good crack growth behavior.
- For good damage tolerance designs an accurate analysis is needed using the actual load spectrum and not top-of-scatter loads. A smaller initial cracks size than used by the U.S. Air Force (1.27 mm) is required on rotorcraft. More thought needs to be considered in design details to have good damage tolerance characteristics.
- In a single rotorcraft design, the mixing of components some designed by safe-life and some by damage tolerance is possible if a good plan is adopted.
- Inspections for cracks or flaws are here to stay.

After this meeting communications with Dr. John Bristow of the CAA clarified some of the certification confusions stated previously (see the second paragraph under round table discussions). According to Dr. Bristow, the FAA and the JAA (CAA is part of the JAA) have identical requirements for rotorcraft and even though the certifying agencies are mostly in agreement on how to interpret the regulations, various rotorcraft manufacturers have developed other interpretations to these regulations. As an example: under the flaw tolerant safe-life evaluation in the civil regulations, various manufacturers have interpreted the regulations to allow establishing inspection intervals using flaw tolerant considerations. However, Dr. Bristow stated that the "CAA does not believe that the SN approach is a reliable way to establish an inspection interval and furthermore (he) believes that the FAA shares this same view." Various technical positions were expressed during this meeting on the suitability of the flaw tolerance method as a viable certifying requirement for rotorcraft. Even though one influential group in the United States (TOGAA) wants the flaw tolerant method removed from the regulations, it will probably be some time before this happens. In the interim, suitable forums such as this meeting are needed to continue the debate and hopefully evolve to a more unified consensus by all involved in the manufacturing and certification of rotorcraft.

This report will conclude with a few comments that the recorder sees as some of the issues that need to be resolved before the slow crack growth damage tolerance method can possibly be used exclusively on rotorcraft.

1) Inspections for small cracks (0.5 mm and less) must be accomplished with high reliability.
2) Possible truncations of the high cycle load contents of rotorcraft fatigue load spectra needs further research.
3) Crack growth thresholds are critical for rotorcraft. Most, if not all of the stresses need to be below the crack growth threshold. Are the long crack thresholds currently in the literature too high ? Are "small" crack thresholds different than long crack thresholds ? More research is needed on the fundamental nature of crack growth threshold development.
4) Are "small" crack effects significant for rotorcraft ?
5) Usage spectrum varies widely because of rotorcraft multipurpose applications. HUMS needed.
6) Need to identify the analytical tools that can arrive at the stress intensity solutions for 3-D stress states that occur in rotorcraft because of complex loadings and 3 -D geometry (e.g., main rotor grip, mast).

This list is by no means all inclusive. Only as all aspects of life management of rotorcraft using a damage tolerance design philosophy are worked, will these issues be understood and resolved. But like all of our technologies, other problems will surface during rotorcraft operations and these problems will be addressed as the rotorcraft community moves toward an ever evolving life management of rotorcraft with damage tolerance.

AGING SYSTEMS IN AERONAUTICS AND SPACE DAMAGE TOLERANCE IN HELICOPTERS

Paolo Santini
Universita "La Sapienza"
Dipartimento Aerospaziale
Via Eudossiana 16
00185 Roma
Italy

1 INTRODUCTION

The aim of this keynote lecture should be that of introducing the main (or, at least,the common) features of the papers that will be presented during the Workshops that will take place in Corfou this week: Aging Aeronautical Systems, Life Extension for Helicopters,Propulsion and Gas Generators for aerospace vehicles.
A keynote lecture may be given in several ways. The most obvious form is probably an overview of the subjects that are to be discussed, trying to connect them together, so as to prepare the audience to a more detailed knowledge of them. However, in this way one runs the risk of saying something that will be repeated much better by the specific Authors, (and, often in a much poorer way than the Authors themselves), also because the time is in general very short.
Another way is to address and illustrate forthcoming needs and future trends in the area of interest: for this kind of presentation it would be necessary to be able to predict the future, because it happens very often that the future is not so smooth as everybody may imagine at the time of the lecture, and so, after a few years, or even a few months, needs and trends are completely different: a good example is the continuous series of war actions in the Balkans and in the Middle East, that may have a strong impact on the policy of the aeronautical production.
I have chosen another approach. When AGARD was established, I had the chance to take part in the first meeting in 1952, and I can well remember the great expectations resting on the new structure. I then followed AGARD throughout the decades, attending many meetings of the Structures and Materials Panel, until I became Panel Member in 1975 and, eventually, Panel Chairman during the period 1986-1988.

Paper presented at the RTO AVT Specialists' Meeting on "Application of Damage Tolerance Principles for Improved Airworthiness of Rotorcraft", held in Corfu, Greece, 21-22 April 1999, and published in RTO MP-24.

I think therefore that it might be of some interest to look to the past, in order to trace back the historical development that led from the early scope of AGARD to the current situation.

2 THE HISTORICAL ROLE OF THE TECHNOLOGY

In order to understand clearly the development of AGARD we must before all else try to recall some general circumstances, summarizing them in two axioms.

The first axiom is that HISTORY IS DRIVEN BY TECHNOLOGY. This stems from two historical facts.First of all, political supremacy is retained by the States and by the political entities having a technological superiority with respect to other groups.

There are several examples of this in history. The Hittites of Asia Minor were a very small nation, but they were subjugating and overwhelming some much greater political groups, since they were able to master iron metallurgy, so that their carts were definitely superior to those of other surrounding populations. According to some historians, the military superiority of the Spartans was in part due to the fact that the waters of their rivers were colder than those of other regions of Greece, so that their quenching gave better manufacts. The Romans had a very efficient technology, in particular in civil engineering; they were first-class bridges and roads constructors, so their transportation systems was exceptionally well organized and allowed them rapid strategic movements of great armies. More recently Germany had a great advantage over the Allied Forces at the beginning of the war, and when the technological supremacy passed on the other side, Germany lost the war. And from this we learn a lesson: technology is not only a matter of scientific advance, but also of capability of mass production and of organization.

However the effect of technology on history is not confined to military superiority only. Its effect upon the quality of life is even more evident. Again here we have several examples. The so-called neolithic revolution, producing a much improved technology of stone artifacts, caused better methods for the stone-age man to acquire food, to cook it, to have better shelters, whose consequence was a lengthening of the average life expectation. Some historians consider the replacement of the double rigid yoke by the single flexible yoke in the Middle Age as a very import technological advance: as a matter of fact, it caused an increase of agricultural efficiency by a factor of 3 to 5.

There is no need to emphasize the scientific and technological discoveries of the Renaissance, or the tremendous progresse that created a completely new world in the 19.th century in the wake of the Industrial Revolution. And what about present times where we have a continuous increase not only of technological progress but of its rate of growth. We live today in a way which is completely different from what it was fifty, forty, and even thirty years ago: long trips are possible almost for everybody, every

family has one or two cars, TV and radio keep us informed in real time of the most extraordinary events: ladies at the age of 50-60 years are still charming (due to the much reduced work at home caused by modern appliances), and so on.

The second axiom is : TECHNOLOGY IS NOT CULTURE. By no means do I mean that the level of Technology is lower, but simply that Technology and Culture are two different expressions of the human imagination, and must be treated and considered differently. Culture is a free expression of what the mankind feels, either by reaction to the external world, or through an internal elaboration: the best examples for the latter being music (whatever music) and mathematics. Neither stem from external stimuli.

By contrast, technology cannot be free; it stems from human needs although in many cases industry creates those needs and imposes them: fifty years ago, nobody missed TV broadcasting, today nobody could live without it.

Technology is not applied science, but an application of science, which is culture. That is the difference and there is a continuous transformation moving from science to technology: a vivid example is provided by the history of spaceflight, synthetized by this sequel: Tsiolkowsky, Oberth, Goddard, von Braun.

3 THE DEVELOPMENT OF AGARD

AGARD seems to have been well aware of, and to have applied, the two axioms above.

In 1949, in connection with the 'warmest' period of the 'cold' war, NATO was founded (called at that time the Atlantic Pact) with a declared feature of military deterrent as a reaction to the increasing armament of the Eastern Block. The first axiom was immediately clear to the top men of the Western World; and, of course, one of the main concerns was relevant to Aeronautics (Space at that time was almost unknown). For this reason, some of the top scientists of the NATO countries were asked to meet and to propose which kind of organization would have been most adequate to improve the level of research and of technology in the aeronautical field in western country.

There was a large meeting in Rome at the end of 1952, attended by a great number of scientists; among them probably the most outstanding one was Theodore von Karman, a man of great scientific prestige and great cultural level. A typical mitteleuropean gentleman, he was the Chairman of the Meeting. I am proud to say: I was there, and I took part, although unofficially, in the foundation of AGARD. During those days, I had the opportunity to talk several times with Karman; especially at lunchtime we often sat together with Professor Broglio, my mentor, and Karman illustrated us his ideas on what the new organization should have been like. In industry at that time there was very lit-

tle research, also because the requirements were not so stringent as today: and he thought that a field such as aeronautics, in order to be competitive, should have been fed by science, by culture. In thinking so, he applied the second Axiom.

Theodor von Karman was a volcano: every time we met he came out with new ideas. I saw him personally drawing on a blackboard the word AGARDograph: he drew up a first draft of the future organization; he also chose the men who should have been the leaders of AGARD, and most of them were scientists or University Professors. Let me remember just some of them: Frank Malina, Frank Wattendorff, Luigi Broglio. Antonio Ferri. Karman transferred the same imagination to the other bodies he created in subsequent years and which are still in existence and florishing: ICAS (International Council for Aeronautical Sciences), IAF (International Astronautical Federation), IAA (International Academy for Astronautics).

The following year AGARD was formally established and the first Panels were formed. I remember the early steps of SMP, in 1955 with Broglio as Chairman, and four members only; among them was Thurston, recently dead. A great number of Members of the Panels came from the Universities, and brought their University mental attitude into the activities which were being proposed.

Thus the birth of AGARD was, in agreement with Karman's ideas, almost an academic institution, where basic research had a very important role. The 50's and the 60's saw a terrific development of the basic sciences of Aeronautics, and the beginning of the attention for Space. I will give just some examples. In 1957 there was a famous Meeting of SMP in Copenhagen where the foundations of modern structural dynamics were laid down. In 1960 a Meeting of the same SMP in Rome was one of the first Meetings dealing with the effect of kinetic heating upon structures, with special attention to reentry: and it should be remembered that we were in the very era of space challenge between USA and URSS, with the latter well ahead of the former. And, again, a basic step in Fluidodynamics was the famous meeting of FDP in Scheveningen, Netherlands, with the first results and methodologies in hypersonics, again with an eye to Space; of particular interest were the discussions and the forecast for future high speed experimental facilities. And let me also remember the wonderful results in the field of Aeroelasticity, an activity that lasted for decades, and that became a kind of permanent institution in SMP: and the great cooperative effort in this area, with the contribution of all the Nations under the leadership of giants such as Ashley, Kussner, Mazet; the discussions among them became a kind of social event!

I was appointed an official Member of SMP in 1975, and since then I took an active role in proposing activities: I must say that AGARD was for me an invaluable vehicle of contacting outstanding personalities in the aeronautical world. Also, my Department and my University took advantage,at a large extent, from the exchange of ideas and of personnel through

the Support Program which I believe was very beneficial not only to the supported nations but to the supporting nations as well.

However I noticed that the twenty years elapsed since the establishment of AGARD had basically changed the objectives and the general frame. Most of the Panel Members came from industry or from Air Force, and the subjects of investigations had gradually shifted towards applications: or, if you wish, towards Technology or Engineering. I consider that a very positive circumstance, since people like me were put directly in contact with the realities of the world of production. At every Meeting I learned a lesson; and I hope that some of my colleagues of the Panel also learned something from me.

I proposed several activities in SMP, also gradually shifted from science to Technology. Not everything, of course, was quite satisfactory: one of my criticisms concerned the fact that an Aero- Space Panel had very minor Space Activities. This was true also of other Panels. I was invited once to chair a session in a meeting of FMP centered on Space Flight and I was surprised to discover that the subjects were not as up to-date as I would have thought.

As a Panel Deputy Chairman I was for two years the Chairman of the Program Committee, and thus I had the opportunity to have a clearcut idea on what the general trend was,with an increasing shift towards more and more applied technology. F.i., I was rather surprised when a subject like 'Painting Removal' was proposed. Now I am well convinced that Painting Removal is of prime importance in everyday aviation practice. This is an example of what I believe was the invaluable contribution of AGARD.

In today's world much progress has been made in the past to improve our products. Now we also have another need: preserve what we have acquired, avoiding wast. AGARD and, subsequently, RTA have followed such requirement; this is the reason for the present Meeting on aging aircraft.

4 AGING AIRCRAFT

The age of the current aeronautical fleet can best be appreciated by referring to statistical value. Most of them refer to US data, which are probably the most updated and complete.

In 1997, 46% of the commercial aircraft were over 17 years of age, 28% over 20 years: the average age for the major companies is reported in Tab.I (from Ref.1).

TAB:I

Airline	Average Aircraft Age (years)
Alaska	7.6
American	10.0
American West	11.0
Continental	14.4
Delta	12.2
Northwest	19.9
Southwest	8.8
TWA	17.0

United	10.8
US Airways	12.8

The expectations for the near future are of an increase of 70% in the next ten years, with a total of 12,000 new airliners to meet the demand in 2015, for a typical design life of 60,000 cycles. Probably already in 2001 2,500 US commercial airliners will be flying beyond the original life span.

The definition of 'aged' or 'aging' structure and/or system would need a clear definition, which, on the contrary, is rather vague.We report, (from Ref.2) two definitions as provided by ESA: Aged Structure - A structure which may have structural degradation or damage as the result of being exposed to the combined effects of the environment.

Aging - The process of the effect t on materials of exposure to an environment (elevated temperature, ultraviolet radiation, moisture or other hostile environment) for a period of time.

The problem of aging aircraft has attracted the attention of civil and military authorities since more than a decade. In general, the attention and the need for new studies are prompted by some spectacular accidents, which have a strong impact on the public opinion.

In 1988 a Boeing 737 of the Aloha Airlines, 19 ys.old, suffered from an accident caused by a fatigue failure in a panel of the fuselage: a flight attendant was killed, and 171 passengers were injured .This accident was almost immediately followed by an action from FAA who established the NAAR (National Aging Aircraft Research).

In 1996 another most famous accident occurred with the flight 800 TWA: the airplane was a Boing 747, 25 years old, 90000 flight hours, 18000 cycles, vs.the original design life of 60,000 hours, and 20,000 cycles (Ref.(1)). In this case the cause was attributed to an electrical malfunction followed by a spark in the fuel compartment. This was followed by a five year project to investigate and check nonstructural parts of the airplanes, such as wiring, hydraulics, avionics, etc. Especially wiring seems to need careful maintenance and inspections (almost zero until few years ago). Now in a commercial airplane there are miles and miles of wires and careful and systematic inspections may cost several million dollars to a Company. Yet they are necessary.

On the other hand, it must be recognized that maintaining old aircraft in service is a definitely positive factor from an economic viewpoint; f.i., the current cost of an Airbus 300 would be of the order of 100 million dollars, while refurbishing an old airplane of a comparable capacity could only cost 4 to 5 million dollars.

Very similar problems apply to military fleets also. F.i., the United States Air Force has many old (20 to 35 years) aircraft that are the backbone of the total operational force, some of which will be retired and replaced with new aircraft. However, for the most part, replacements are a number of years away: for many aircraft, no replacements are planned and many are expected to remain in service for another 25 years or more. Such aircraft have encountered or are considered likely to encounter aging problems,

such as fatigue cracking, stress corrosion cracking, corrosion and wear.

For these reasons, Committees and Working Groups were formed within the Air Force scientific framework, with the following objectives: (i) Identify and correct structural deterioration that could threaten aircraft safety; (ii) prevent and minimize structural deterioration that could become an excessive economic burden or could adversely affect force readiness, in terms of performances; (iii) predict. for the purpose of future force planning, when the maintenance burden will become so high or the aircraft availability so poor that it will no longer be viable to retain the aircraft in the inventory.

The Committee arrived at Near Term and Long - Term Research Recommendations, and produced a rather lengthy list of items to address the attention to. This list can be found in Ref.(3) (it would be too long to reproduce it here): looking at it, we can see that there is room not only for technology, but also for basic research, and for items that are prone to be completely re-invented.

It is very instructive to have a look at the items of the list. First of all we have the confirmation of the prime role of corrosion in defining the lifetime of an airplane.This well known to everybody, except perhaps for the 'size' of this role. As a matter of fact, corrosion is a social problem : it costs about 100 billions USD per year to United States, almost 300 dollars per citizen. And USAF is responsible for about 10% of this figure. Furthermore we see other fields to which, in my opinion, insufficient attention has hitherto been given by fatigue people, such as structural dynamics and dynamic response. But it must be a completely new structural dynamics, not based on the conventional analitycal methods, eigenfrequencies and modes, but rather on the need of predicting stress concentrations arising from dynamic effects and following cracks under dynamic conditions. I am sorry for not being able to illustrate other important suggestions that can be derived from the list for lack of space.

But the subject of aging aircraft is so important that there is a sure need in the future of specialized technical staff in this area. Appropriate courses of formation have been designed, with the aim of providing the attendees with the necessary knowledge: an example is given in Ref.(4-5). Specialists in aging airplanes will become in the future a new professional profile.

5 DAMAGE TOLERANCE ISSUES

The life of a structural component is limited by the effects of its usage history, which may consist of cyclic loads, fluctuations in temperature,etc. In the past, and also today , several design philosophies have been introduced into current practice, and among them damage tolerance has probably become one of the most prominent in aircraft industry (Ref.(6)).

I shall not dare to give a general overview on what damage tolerance concept is. I just will confine myself to recall - or try to imagine- why

there is a special need to treat damage tolerance as applied to helicopters in a very special way. As said, the life of a structural component depends on its usage, which varies from one type of flying machine to another. There is however a general agreement that critically loaded components such as engine rotors or landing gears can have shorter replacement intervals. In any case, the usage profile must describe the various flight conditions, and the amount of time spent at each gross weight, speed, and altitude, which define the load factor spectrum, and subsequently dictate the inspection intervals.

There is no need to illustrate how much the environmental spectra for an helicopter is different from that of an airplane. Considerable effort is needed on loads generation, and determination of material data. Also, this is a field where theoretical investigation must also be accompanied by experimental data.

Let me clarify this concept in some detail. In the past there has always been a dichotomy: theory vs. experiments, the former being looked at rather suspiciously. The two activities were almost independent of each other, and the optimum was reached when there was a satisfactory (not always well-defined) agreement between the two results. With the advent of computers, 'theory' has been replaced by 'mathematical model'and everybody is happy, but the dicotomy has not yet been fully overcome. It is my opinion that the two activities must be viewed not from the point of 'mutual check' but from that of 'mutual integration'. Experimental data for a specific problem or design must supplement mathematical models, providing information that no theory whatever can provide : theory must provide detailed information that no experiment can provide.Although the last statement is more difficult to accept, there are several examples validating it (e.g., in Fluid Dynamics).

And again, I must say, damage tolerance in helicopters is a good example on how increasing industrial needs stimulate basic research.

6 PROPULSION

I am not an expert in Propulsion: I am simply an admirer of it. I have already mentioned the names of the pioneers of Spaceflight, which is one of the top conquests of man : for all of them Spaceflight was identical with Propulsion. And, as a matter of fact, space activities only became possible when sufficient thrust was made available to scientists. This is very often, not to say too often, forgotten today.

Most recently, because of economic problems, as happens more and more frequently today, the subject of small rocket motors has become increasingly popular. In this Symposium attention is focused on the specific goals of NATO and on the relevant applications. All the main features of the problems are examined with respect to weapon systems. And here a further remark is appropriate: in the history of technological development, military applications have very often led the way to a more general use of the progress achieved.My hope and my message is that this will be the case also for this

Conference.

7 CONCLUSION

We have two main conclusions to draw. The first that we are at an era in which we rediscover a new feature of Technology: the Technology of restoring, refurbishing, reusing the system created by the human imagination in the recent past. Second, that such operations of re-whatever we must use Science and Culture again, although in a different (and probably more advanced) way than in the past.

Paolo Santini

8 references

1. *"Aging Aircraft In Our Skies"*, Internet Address airtravel.about.com., Jan-10-1998
2. AA.VV. *" Structural Materials and Space Engineering"*, ESA, PSS-03-121, issue 1
3. Committee on Aging of U.S Air Force Aircraft, National Materials Advisory Board *" Aging of U.S. Air Force Aircraft"*, National Academy Press, Washington D.C. 1997
4. UCLA University *"Structural Integrity of New and Aging Metallic Aircraft"*
5. Fatigue Concepts *"Aging Aircraft Course*, FAX: +1 (916) 933-3361 1 (800) 342-7225
6. M.P.Kaplan, T.A.Wolff *"Life Extension and Damage Tolerance of Aircraft*, ASM Handbook, Vol.19, Fatigue and Fracture, pp.557-565, 1996.

THE SIGNIFICANCE OF SMALL CRACKS IN FATIGUE DESIGN CONCEPTS AS RELATED TO ROTORCRAFT METALLIC DYNAMIC COMPONENTS

R.A. Everett, Jr. and W. Elber
U.S. Army Vehicle Technology Directorate
NASA Langley Research Center
2 West Reid Street
Hampton, VA 23681-2199, USA

1. SUMMARY

In this paper the significance of the "small" crack effect as defined in fracture mechanics will be discussed as it relates to life managing rotorcraft dynamic components using the conventional safe-life, the flaw tolerant safe-life, and the damage tolerance design philosophies. These topics will be introduced starting with an explanation of the small-crack theory, then showing how small-crack theory has been used to predict the total fatigue life of fatigue laboratory test coupons with and without flaws, and concluding with how small cracks can affect the crack-growth damage tolerance design philosophy. As stated in this paper the "small" crack effect is defined in fracture mechanics where it has been observed that cracks on the order of 300 microns or less in length will propagate at higher growth rates than long cracks and also will grow at ΔK values below the long crack ΔK threshold. The small-crack effect is illustrated herein as resulting from a lack of crack closure and is explained based on continuum mechanics principles using crack-closure concepts in fracture mechanics.

2. INTRODUCTION

Up to the 1990's rotorcraft fatigue design has combined constant amplitude tests of full-scale parts with flight loads and usage data in a conservative manner to provide "safe life" component replacement times. The replacement times are determined using the Palmgren/Miner nominal stress rule [Ref. 1,2] where the stress versus life curves, S/N curves, are determined from constant amplitude fatigue tests on actual parts that contain no defects or flaws. In contrast to the safe life approach, over the past twenty five years the United States Air Force (USAF) and several other NATO nations have used damage tolerance design philosophies for fixed wing aircraft to improve safety and reliability. The reliability of the safe life approach being used in rotorcraft started to be questioned shortly after presentations at an American Helicopter Society's specialist meeting in 1980 showed predicted fatigue lives for a hypothetical pitch-link problem to vary from a low of 9 hours to a high in excess of 2594 hours. This presented serious cost, weight, and reliability implications. Somewhat later in the 1980's, when the U.S. Army introduced its six nines reliability on fatigue life requirement, attention was starting to shift towards using a possible damage tolerance approach to the life management of rotorcraft dynamic components. In 1983, Sikorsky Aircraft started a damage tolerance assessment of selected HH-53 rotorcraft structure [Ref. 3] through a contract with the USAF. A "type" of damage tolerance requirement for rotorcraft certification [Ref. 4, 5] first appeared in the late 1980's when the Federal Aviation Administration, FAA, added an additional requirement to the federal air regulations (FAR's) requiring a flaw tolerant safe-life evaluation for the larger transport category rotorcraft.

The flaw tolerant safe-life evaluation was introduced in the FAR's to address some of the in-service problems that had begun to appear in rotorcraft that were a result of either manufacturing defects or in-service defects. This new methodology is known by several names. Among them are the "flaw tolerant safe-life" and "enhanced safe-life". Sometimes it is even called damage tolerance, although classic damage tolerance as started by the U.S. Air Force in the early 1970's [Ref.6] assumes that a pre-existing fatigue crack exists in the structure while the flaw tolerant method assumes a flaw (not a sharp fatigue crack) pre-exists in the structure. The flaw tolerant method still uses the Palmgren/Miner rule to establish retirement lives with the applied stress versus life-cycle to crack initiation curves, S/N curves, coming from tests on structures that have pre-existing flaws such as nicks, dents, scratches, and corrosion (to name but a few of these flaw types). The size of these flaws can range from very short measurements of 0.01 mm to as large as the classic USAF damage tolerance crack size of 1.27 mm.

As stated in the flaw tolerant safe-life evaluation as described in the U.S. FAR's [Ref. 4], "the structure, with flaws present, is able to withstand repeated loads

Paper presented at the RTO AVT Specialists' Meeting on "Application of Damage Tolerance Principles for Improved Airworthiness of Rotorcraft", held in Corfu, Greece, 21-22 April 1999, and published in RTO MP-24.

of variable magnitude without detectable flaw growth..." Since the Palmgren/Miner rule is used to establish the retirement lives in a flaw tolerant analysis, no type of flaw or crack growth analysis is involved. Since about the mid-1980's a trend has been developing to predict total fatigue life (from the first load cycle to failure) using only fatigue crack growth considerations (Newman and his colleagues, Ref. 7). In order for this to be accomplished, a very small initial crack size (1μm to 50μm) is assumed to exist in the structure. It has also been shown recently that total fatigue life can also be predicted on a high strength steel containing a 50 μm machine-like scratch using fracture mechanics concepts and small-crack theory.

In this paper the significance of the "small" crack theory as defined in fracture mechanics will be discussed as it relates to life managing rotorcraft dynamic components using the conventional safe-life, the flaw tolerant safe-life, and the damage tolerance design philosophies. These topics will be introduced starting with an explanation of the small-crack theory, then showing how small-crack theory has been used to predict the total fatigue life of fatigue laboratory test coupons with and without flaws, and concluding with how small cracks can affect the crack-growth damage tolerance design philosophy.

3. SMALL-CRACK THEORY

As stated previously, the crack and flaw sizes that are a part of the flaw tolerant safe-life and the damage tolerance design philosophies range from 0.01 mm to 1.27 mm. To place the size of the cracks considered in small crack theory into perspective with these two design concepts, the sketch as shown in Figure 1 depicts flaws (and cracks) in size from crack formation to failure and shows how they relate to different design philosophies. The size of the cracks in Figure 1 where small-crack theory is shown to apply are very small compared to the USAF damage tolerance crack size (1mm), whereas, for at least one study in a type of flaw tolerant evaluation a tool mark type of flaw was considered with a depth of 0.02 mm [Ref. 8]. Some studies have indicated that the so-called "small" crack effect could exist for cracks as large as 0.30 mm [Ref. 9]. As shown by numerous investigations (Ref. 10-14) these very small cracks have crack growth characteristics that are considerably different than large cracks (cracks longer than 2.0 mm). This "small" crack effect is illustrated in Figure 2 where large crack behavior is shown by the solid curve and small crack behavior by the dashed curves. As seen in Figure 2, these small cracks when described by linear-elastic fracture mechanics (LEFM), grow faster than long cracks at the same stress intensity factor range and grow at stress intensity factors below the long-crack threshold (ΔK_{th}).

The small-crack effect as illustrated in Figure 2 is based on a continuum mechanics explanation of crack growth where the lack of crack-closure, as shown by Newman[Ref. 15], is used to explain the rapid growth and deceleration of small cracks when compared to large-crack behavior. These small-cracks often initiate at inclusion particles, voids, or weak grains where no prior plastic deformation has had time to develop. At the beginning of fatigue crack development, the crack is fully open and thus the stress-intensity factor range is fully effective and the crack-growth rate is faster than in large cracks where crack-closure has developed and thus limited the effective stress-intensity factor range [Ref. 16]. The crack-closure concept as originally conceived by Elber [Ref. 17] concluded that a fatigue crack actually closes under many loading conditions before the minimum cyclic load is reached and that only that portion of the loading cycle where the fatigue crack is said to be "open" contributes to the crack-tip driving force that grows the cracks. Thus, the term the effective stress-intensity factor range has been defined as

$$\Delta K_{eff} = (S_{max} - S_o) (\pi a)^{1/2} F \qquad (1)$$

where S_O is the crack-opening stress, a is the crack length, and F is the boundary correction factor which accounts for the effects of structural configuration on the stress intensity factor. Crack-closure has been explained to exist because of residual plastic deformations that remain in the wake of the advancing crack due to yielding adjacent to the crack tip. Small-cracks as shown by the dash curves in Figure 2 are assumed to be fully open since no plastic wake has had a chance to develop, but as the small-crack grows the small crack starts developing a plastic wake and as shown in Figure 2 the dashed curves approach the large-crack results shown by the solid curve. Since the main objective of this paper is to illustrate how small-crack considerations are used in the design concepts previously mentioned (safe-life, etc.), the reader is referred to several references for more detailed explanations of the small-crack theory [Ref. 7 and 13-16].

4. SAFE-LIFE AND SMALL CRACKS

As stated previously the Palmgren/Miner linear cumulative damage rule is normally used in rotorcraft

fatigue design to determine safe-life component replacement times. Conservatism's on fatigue strength and flight loads are used to insure that safe-life replacement times are normally calculated [Ref. 18]. In spite of the reasonably good safety record for rotorcraft the safe-life methodology using the Palmgrem/Miner rule has been questioned as being the best method for fatigue design in light of the successful use of the damage tolerance methodology in the fixed-wing community [Ref. 19]. One of the major concerns with the safe-life methodology is the sensitivity of safe-life designed parts to manufacturing and in-service flaws. This stems from the fact that the safe life approach may lead to the selection of wrong materials from a damage tolerance perspective as it gives very little understanding of the physics of the fatigue and fracture process somewhat because of the use of the Palmgrem/Miner rule. Since in the damage tolerance design methodology the growth of fatigue cracks is a primary characteristic in the design procedure, it would be advantageous if a crack growth analysis could be used to help determine replacement times as defined in the safe-life methodology. As stated earlier in this paper, Newman and his colleagues have used a fracture mechanics crack-closure based model along with small-crack growth characteristics to predict total fatigue life of several different metallic materials [Ref. 7,16, and 20].

The main differences in the USAF damage tolerance methodology and the fracture mechanics small-crack total life analysis is the choice of the initial crack size. In the USAF damage tolerance methodology, an inspection interval is often determined for slow growth cracks by integrating a crack growth rate versus stress intensity factor relationship like

$$da/dN = C(\Delta K)^m \qquad (2)$$

where da/dN is the crack growth rate, ΔK is the stress intensity factor range, with C and m being curve fit parameters. In the USAF damage tolerance methodology a safe inspection interval is normally calculated using an initial crack size of 1.27 mm for corner cracks emanating from a hole [Ref. 6]. However, in order to calculate total fatigue life it has been shown that a very small initial crack size (0.001mm to 0.05mm) has to be assumed to exist in the structure in order to use fracture mechanics crack growth concepts to predict fatigue life (safe-life, S/N fatigue behavior).

In the small-crack total life fatigue analysis by Newman [Ref. 16], crack-closure concepts as explained previously, are used to define an effective ΔK and the initial crack length is determined from a small-crack study [Ref. 7,22, and 27]. The expression for ΔK_{eff} from equation (1) is used in equation (2) replacing ΔK with ΔK_{eff} with the crack growth rate as calculated from equation (2) now being expressed as

$$da/dN = C[(S_{max} - S_o) (\pi a)^{1/2} F]^m \qquad (3)$$

Total life is then calculated by numerically integrating equation (3) from the initial crack length to failure as

$$N = \sum_{a_i}^{a_f} \frac{\Delta a}{C\left[(S_{max} - S_o)(\pi a)^{1/2} F\right]^m} \qquad (4)$$

where a_i is the initial crack length as determined from the small crack studies and a_f is the final crack length at failure. Cycles are summed as the crack grows under the applied loading until $K_{max} = K_c$, where K_c is the fracture toughness of the material. When $K_{max} = K_c$, the summation of the load cycles, N, becomes the total fatigue life. A total fatigue life computer algorithm has been developed by Newman [Ref. 26] using the above general procedure which is based on crack-closure concepts in fracture mechanics and small-crack considerations.

This computer program was developed almost two decades ago and was originally conceived as a crack growth analysis tool based on fatigue crack-closure concepts in fracture mechanics and was shown to help explain load interaction effects (crack growth retardation and acceleration) in fatigue crack growth. This computer program was originally called FAST (Fatigue Crack Growth Analysis of Structures), [Ref. 21]. Later the use of "small-crack" concepts were incorporated into FASTRAN [Ref. 26] and this analysis was shown to be very effective in calculating total fatigue life based solely on crack growth data [Ref. 7].

4.1 Small-crack study.

As stated previously, a small crack study of the material is needed to determine the initial crack size to be used in the small-crack total fatigue life analysis. This will be illustrated herein, with the work done by Swain et al. [Ref. 22] where small- and large-crack growth rate data were generated on high strength 4340 steel. The small-crack data were obtained from a single-edge-notch specimen configuration, $K_T = 3.3$ (based on gross stress, not

net-section), using the plastic-replica method [Ref. 22]. In this study, small-crack data were measured on 35 fatigue cracks giving information on the distribution of crack-initiation site dimensions. The crack-initiation sites for this 4340 steel were observed to be either a spherical or a stringer particle. The most dominate of these two particles was the spherical (calcium-aluminate) particle which is shown in the scanning electric microscope, SEM, photograph in Figure 3.

To calculate the total fatigue life using the computer algorithm developed by Newman [Ref. 26], an initial crack size is chosen based on the small-crack distributions obtained from small-crack studies. In such a study, a cumulative distribution function of these small-crack defects is often plotted to aid in choosing the initial crack size. Such a distribution is shown in Figure 4 where the cumulative distribution function is plotted against an equivalent semi-circular defect radius based on the actual area of the defect (spherical-inclusion particle). For the high strength 4340 steel used in this study the mean defect was about 13-μm in radius with defects of 8- and 30-μm covering about 80 % of all the defects.

4.2 Fatigue life predictions

Fatigue life predictions using the total life small-crack analysis are shown in Figure 5 compared to constant amplitude test data (symbols) conducted on open-hole test specimens [Ref. 20] at a stress ratio of R = 0. The constant amplitude test data at a given stress level exhibits the typical scatter in fatigue lives. Hence, in order to bound the test data, initial crack sizes of 8- and 30-μm were used in the small-crack analysis. The crack configuration chosen for the stress intensity solution was a semi-circular surface crack located at the center of the hole in the specimen's thickness direction. The small-crack analysis is seen to bound the test data very well especially near the endurance limit. However, the analysis tend to predict slightly longer lives at the highest stress level. The reason for this over prediction is not known at this time.

Similar comparisons on high strength 4340 steel have been made with spectrum load fatigue tests [Ref. 20]. Figure 6 shows these comparisons with fatigue test data (symbols) conducted with the standardized helicopter load sequence called Felix/28 [Ref. 23]. The maximum stress in the spectrum is plotted against the cycles to failure. A similar procedure was used for the spectrum fatigue life predictions as was used for the constant amplitude fatigue life predictions. The small-crack analyses with the two initial defect sizes predicted the scatter in the Felix/28 spectrum fatigue tests very well.

5. FLAW TOLERANT SAFE-LIFE AND SMALL CRACKS

In the flaw tolerant safe-life methodology, component retirement times are established using the Palmgrem/Miner rule on structures that have pre-existing flaws such as nicks, dents, scratches, and corrosion. This was done to address some of the in-service problems that appear in rotorcraft that were a result of either manufacturing defects or in-service damage. Since rotorcraft components are often complex configurations as opposed to flat parts, it would not seem unlikely that inadvertent flaws could be put into these components during the fabrication process. This problem was addressed by the rotorcraft industry in the 1980's when the U.S. Rotorcraft Advisory Group (RAG) formed an ad-hoc committee on fatigue methodology to address such issues as abnormally low strength parts which may result from manufacturing process changes or errors, assembly errors, or service-induced damage [Ref. 8]. In the work, presented in reference 8, the affect on the S/N fatigue life of several types of manufacturing defects were evaluated on rotorcraft drive shafting. One of these involved longitudinal tool marks on the drive shaft tube bore which was stated to be "introduced during the extrusion process." A fatigue test was conducted to compare the original fatigue qualification test results to shafts having longitudinal tool marks up to 0.02 mm deep intersecting rivet holes. It was concluded that no significant change in strength resulted from the 0.02 mm deep tool mark. In fact, the fatigue crack origins were not at the tool marks, but at rivet holes not intersected by the tool mark [Ref. 8]. In this study 12 different "degrading" conditions were recommended as defects that should be evaluated in a degraded mode evaluation program. One of these were poor surface finishes and scratches.

The effect on the fatigue life of a machining-like scratch was the focus of a recent study. This study resulted from a structural review of a helicopter which experienced a crash, where one of the fatigue design curves appeared to have one of the data points that defined the design curve as coming from a test article which had a pre-existing flaw in the test article. During the design review this flaw was defined as a surface scratch which occurred during the machining process of the test article. Since the conventional safe-life fatigue design methodology assumes no flaws are present in the structure when a retirement life is calculated, it was felt that this test

data point should not have been included in defining the design curve. As a result of this seeming anomaly in the fatigue design curve, a study was initiated to explore the effects of a machine-like scratch on fatigue life.

In the study to assess the affect of machine-like scratches on fatigue life, constant amplitude fatigue tests were conducted at a stress ratio of R = -1 on the same material used in the helicopter where the machine-like scratch test data point appeared on the fatigue life design curve. The material used for this study was 4340 steel heat treated to an ultimate strength of 1448 MPa. The fatigue endurance limit for this heat of material was determined to be about 469 MPa at a stress ratio, R = -1. This agreed with the value given in the Military Handbook 5B [Ref. 24]. Specimens were machined to have a surface finish of 32 rms which is the same finish used on the helicopter parts that were under investigation. The nominal thickness of the test specimens was 8.9 mm. Specimens were machined to an hour glass shape producing an elastic stress concentration factor, K_T, of 1.03 as determined by a boundary force method [Ref. 25]. All fatigue test lives reported in this study were to specimen failure. The machine-like scratch was machined into the specimen surface using an end mill. The scratch was machined across the entire width of the specimen, but only on one side of the specimen. The depth of the scratches was nominally 0.05 mm with the width being about twice the depth. Each specimen scratch was measured to insure uniformity in geometry of the scratches for the test specimens tested in this study. Figure 7 shows the results of the fatigue tests on the specimens with machine-like scratches compared to the pristine specimens. As seen in this figure the endurance limit was reduced from 469 MPa for the pristine specimen to about 276 MPa for the specimen with a 0.05 mm deep scratch. This is a decrease of about 40 percent.

Because of the success shown by the small-crack fracture mechanics model in predicting the total fatigue life of test specimens without flaws, it was logical to try to employ these concepts to predict the fatigue life of the test specimens with the machine-like scratches. As a first step in the analysis of the machine-like scratch, it was decided to use the small-crack analysis to predict the fatigue life of the pristine test specimens (specimens without flaws) in order to check the basic material data input into the crack-growth computer code. The small-crack analysis used was the computer code known as FASTRAN [Ref. 26] which requires several parameters that are a function of the material being analyzed. As stated previously, perhaps the most important parameter is the initial crack size. The long and small crack characteristics of the 4340 steel used in this study were thoroughly investigated as part of an AGARD study done during the 1980's [Ref. 22]. In the study conducted by Swain et al, examination of 35 crack initiation sites described the distribution of initiation sites shown previously in Figure 4 with the dominate initiation site being a spherical (calcium-aluminate) particle as shown in Figure 3. The mean defect size was determined to be a radius of about 13 μm. Using the mean defect size of 13 μm and the surface crack configuration for the stress intensity solution of the defect, the small-crack analysis predicted the pristine test data as shown in Figure 8 quite well. This gave confidence that the basic material data needed for the computer crack-growth code was good. In order to predict the total fatigue life of the machine-like scratch test specimen two approaches were investigated. First, it was thought to model the scratch like a corner or surface crack and use the stress intensity solution for these crack geometries. The applied stress would be assumed to be the K_T of the scratch-like notch times the applied load. However, one of the weaknesses of this approach would be that the fatigue crack would be in the K_T stress field from initiation until failure. The other problem in this approach was to determine the proper K_T to be used. Even though this analysis did a reasonable job in predicting the machine-like scratch test data, the weaknesses of this assumption made this approach unsatisfactory. Finally, the scratch was modeled as a single-edge crack under a tensile loading. In this analysis the crack length was chosen as the average depth of the scratch, 0.051 mm (see Table 1) with the applied stress being the applied load divided by the cross-sectional area of the test specimen. The fatigue life predictions of the machine-like scratch using these input parameters are shown in Figure 8. Here, the agreement between the FASTRAN small-crack analysis and the test data is very good. The results of this study indicate that a fairly robust total fatigue life analysis based only on fatigue crack growth data is emerging as a possible analytical tool for fatigue life assessments using the flaw tolerant safe-life design methodology.

6. SMALL CRACKS AND DAMAGE TOLERANCE

As shown in Figure 1, it would not appear that small-crack theory would need to be considered in the damage tolerance design concept since the small-crack effect appears to affect only cracks of micro-flaw sizes (< 0.1 mm). However, as stated in section 3 on small-crack theory, the small-crack effect has been shown by some studies to be as large

as 0.3 mm [Ref. 9]. For rotorcraft design the damage tolerance inspectable flaw size currently being suggested for rotorcraft design is about 0.38 mm. This is only slightly larger than the 0.30 mm small-crack upper limit as determined from the studies reported in reference 9. The research done by Newman and his colleagues have only shown the small-crack effect to exist below 0.1 mm [Ref. 15]. Furthermore, their work has also shown that the small-crack effect is not significant in all materials.

This is illustrated in Figure 9 where small- and large-crack data on 4340 steel is shown at the constant amplitude loading condition of R = 0. In this figure the large-crack data is shown by the dashed-dot curve and the small-crack data by the symbols. Also shown in Figure 9 (solid curve) is a prediction of the small-crack growth behavior as determined by the computer code FASTRAN. For most of this data the small- and large-crack data agree very well. In work done by Swain et al [Ref. 22] at a stress ratio R = -1, some differences were noted between small- and large-crack data in 4340 steel, but the differences where not overly significant. In research on several materials [Ref. 22, 27] the small-crack effect did not appear to be very dominate at positive stress ratio conditions. The most significant small-crack effects appear to be at negative stress ratios, especially towards R = -1.

One area of concern in damage tolerance analysis that small-crack studies have revealed is the magnitude of the large-crack threshold values that are reported in the literature. As shown in Figure 10 where small- and large-crack data on aluminum alloy 2024-T3 data are presented, a large difference exists between the large-crack threshold and the small-crack behavior. Small cracks were shown to grow at ΔK values as low as 0.75 MPa$\sqrt{m}$ which is well below the large-crack ΔK threshold of about 3 MPa$\sqrt{m}$. This large difference between the small-crack growth behavior and the large-crack threshold has caused some researchers to speculate that the large-crack threshold values often reported in the literature are too high (for some materials) and are probably elevated due to the rise in the crack-opening loads as a result of the load-reduction procedure often used to determine the large-crack threshold [Ref. 15].

A series of analyses was recently done to see how a change in the crack-growth threshold, ΔK_{th} , would affect the crack inspection interval which is often a part of a damage tolerance design. The computer code FASTRAN was used for these analyses with the helicopter standardized fatigue load spectrum (Felix/28) being used to represent a typical loading experience. The inspection interval for this analysis was defined as one-half of the crack growth interval from an initial crack size of 0.38 mm (see the first paragraph of this section) to fracture. For this example problem, the material was 4340 steel (ultimate strength of 1448 MPa). A simple laboratory specimen configuration was assumed with a 6.35 mm diameter hole located in the center of a 25.4 mm wide specimen. Specimen thickness was 3.2 mm. To make the problem somewhat realistic the maximum applied stress in the spectrum was chosen to produce an inspection interval of about 500 flight hours (possibly a minimum inspection interval that would not unduly burden the operator). Using an effective ΔK_{th} of 3.2 MPa$\sqrt{m}$, a typical value for 4340 steel at an ultimate strength of 1448 MPa, the maximum stress in the Felix/28 loading spectrum that would give an inspection interval of about 500 flight hours was 150 MPa. Using an increase in the ΔK_{th} of about 40 % (Figure 9 shows small-cracks growing for 4340 steel at about ΔK values of 4.5 MPa$\sqrt{m}$) the inspection interval was only increased by about 15 % (497 hours to 571). Similar analysis were done on the aluminum alloy 7075-T6 and the titanium alloy Ti-6-4 with about the same results as for the 4340 steel. It is standard practice in most design scenarios to have to consider reducing design stresses if certification goals (short inspection intervals, etc.) are not met. Some studies conducted in the rotorcraft community have indicated that reasonable reduction in design stresses can be made in order to obtain practical inspection intervals for use in damage tolerance designs. Some of these studies have also indicated that when the design stresses are reduced the inspection intervals become more sensitive to changes in the crack growth threshold, ΔK_{th} .

7. CONCLUDING REMARKS

In this paper the significance of the "small" crack effect as defined in fracture mechanics was reviewed as it relates to life managing rotorcraft dynamic components using the conventional safe-life, the flaw tolerant safe-life, and the damage tolerance design philosophies. These topics were introduced starting with an explanation of the small-crack theory, then showing how small-crack theory has been used to predict the total fatigue life of fatigue laboratory test coupons with and without flaws, and concluding with how small cracks can affect the crack-growth damage tolerance design philosophy. As stated in this paper the "small" crack effect is defined in fracture mechanics where it has been observed that cracks on the order of 300 microns or less in length will propagate at higher growth rates than long cracks and

also will grow at ΔK values below the long crack ΔK threshold. The small-crack effect is illustrated herein as resulting from a lack of crack-closure and is explained based on continuum mechanics principles using crack-closure concepts in fracture mechanics.

A newly emerging analytical tool was illustrated in which a fracture mechanics crack-closure based model which uses small-crack characteristics can predict total fatigue life with reasonable accuracy. This was illustrated on 4340 steel under constant amplitude loading and the standardized helicopter spectra called Felix/28. References were made where this has been also done on aluminum and titanium alloys. This small-crack total fatigue life analysis was shown also to successfully predict the fatigue lives of a laboratory type specimen of 4340 steel with a machine-like scratch with a depth of 0.05 mm. Hence, small-crack fatigue life analysis may be an analytical tool that could used in flaw tolerant safe-life evaluations.

It was stated that it would not appear that small-crack theory would need to be considered in the damage tolerance design concept since the small-crack effect appears to affect only cracks of micro-flaw sizes (1- to -10 μm) where the damage tolerance inspectable flaw size currently being suggested for rotorcraft is about 0.38 mm. However, one area where small-crack considerations could be of benefit would be that of determining the crack-growth threshold, ΔK_{th}. It was illustrated that one aspect of small-crack growth is that they grow at ΔK values below the long crack ΔK threshold. If this situation is real and the "small" crack growth effect is ignored, unconservative predictions of crack growth times to failure might occur since cracks will be growing below the long crack ΔK threshold. Hence, considerations of small-crack growth may help define a more realistic crack-growth threshold.

8. REFERENCES

1. Palmgren, A., *Ball and Roller Bearing Engineering,* translated by A. Palmgren and B. Ruley, SKF Industries, Inc. Philadelphia, pp. 82-83, 1945.

2. Miner, M.A. "Cumulative Damage in Fatigue," *Journal of Applied Mechanics, ASME,* Vol. 12, Sept 1945.

3. Tritsch, D.E., Schneider, G.J., Chamberlain, G., and Lincoln, J.W., *Damage Tolerance Assessment of the HH-53 Helicopter,* Proceedings of the 46th Annual Forum of the American Helicopter Society, Wash. D.C., 1990.

4. Regulation - U.S. Federal Aviation Administration Airworthiness Standards : Transport Category Rotorcraft, Paragraph FAR 29.571 , "Fatigue Evaluation of Structure".

5. Adivisory Circular - U.S. Federal Aviation Administration Advisory Circular AC 29-2A, Appendix 1, "Fatigue Evaluation of Transport Category Rotorcraft Structure (Including Flaw Tolerance)."

6. Gallagher, J.P., Gewssler,F.J. and Berens,A.P., *USAF Damage Tolerance Design Handbook,* AFWAL - TR-82-3073, May 1984.

7. Newman,J.C., Jr., Swain, M.H. and Phillips, E.P.,"An Assessment of the Small-Crack Effect for 2024-T3 Aluminum Alloy", Small Fatigue Cracks , The Metallurgical Society, Inc., Warrendale, PA, pp. 427-452, 1986.

8. Adams, D.O., Albrecht, C., and Harris, W.D. "Methodology for Fatigue Substantiation of Alternate Sources And Degraded Modes on Helicopter Dynamic Components," Proceedings of the 44th Annual National ForumOf the American Helicopter Society, Washington, D.C., June, 1988.

9. Halliday, M.D., Poole, P., and Bowen, P., "In Situ SEM Measurements of Crack Closure for Small Fatigue Cracks in Aluminium 2024-T351," Fatigue Fract. Engng Mater. Struct. , Vol. 18, No. 6, pp 717-729, 1995.

10. Pearson, S., "Initiation of fatigue cracks in commercial aluminum alloys and the subsequent propagation of very short cracks", Engng. Fract. Mechs., Vol. 7, No. 2, pp 235-247, 1975.

11. Zocher, H., (ed.), "Behavior of Short Cracks in Airframe Components," AGARD CP- 328, 1983.

12. Miller, K.J. and de los Rios, E.R. (eds.) The Behavior of Short Fatigue Cracks , European Group on Fracture, Publication No. 1, 1986.

13. Newman, J.C., Jr., "A Nonlinear Fracture Mechanics Approach to the Growth of Small Cracks," AGARD CP-328, pp 6.1-6.26 , 1983.

14. Newman, J.C., Jr., "Fracture mechanics parameters for small fatigue cracks", Small

Crack Test Methods, ASTM STP 1149, J. Allison and J. Larsen (eds.) pp. 6-28, 1992.

15. Newman, J.C., Jr., "The Merging of Fatigue and Fracture Mechanics Concepts: A Historical Perspective,"Fatigue and Fracture Mechanics: 28th Volume, ASTM STP 1321, J.Underwood, B. Macdonald, and M.Mitchell, (eds.), pp. 3-51, 1997.

16. Newman, J.C., Jr., "A Review of Modelling Small-Crack Behavior and Fatigue-Life Predictions for Aluminum Alloys," Fatigue Fract. Engng Mater. Struct. Vol. 17, No. 4, pp 429-439, 1994.

17. Elber, W., Engineering Fracture Mechanics, Vol. 2, No. 1, pp 37-45, July 1970,

18. Everett, R.A., Jr., Bartlett, F.D., Jr., and Elber, W., "Probabilistic Fatigue Methodology for Safe Retirement Lives," Journal of the American Helicopter Society, Vol. 37, No. 2, pp. 41-53, April, 1992.

19. Everett, R.A., Jr. and Elber, W., "Damage Tolerance Issues as Related to Metallic Rotorcraft Dynamic Components," proceedings of the 54th Forum of the American Helicopter Society International , Washington, D.C., May 1998.

20. Everett, R.A., Jr., "A comparison of fatigue life prediction methodologies for rotorcraft," Journal of the American Helicopter Society, Vol. 37, No. 2, pp. 54-60, April 1992.

21. Newman, J.C., Jr., "A Crack-Closure Model for Predicting Fatigue Crack Growth Under Aircraft Spectrum Loading," Methods and Models For Predicting Fatigue Crack Growth Under Random Loading, J.B. Chang and C.M. Hudson, eds., ASTM STP 748, pp. 53-84, 1981.

22. Swain, M.H., Everett, R.A., Newman, J.C., Jr., and Phillips, E.P., "The growth of short cracks in 4340 steel and Al-Li 2090," pp. 7.1-7.30, AGARD Report 767, 1989.

23. Edwards, P.R. and Darts, J., "Standardized Fatigue Loading Sequences for Helicopter Rotors (Helix and Felix) Part I, Background and Fatigue Evaluation," Royal .Aeronautical Establishment, TR 84084, Aug 1884.

24. U.S. Military Standardization Handbook, MIL-HDBK-5B, August 1975.

25. Tan, P.W., Raju, I.S., and Newman, J.C., "Boundary Force Method for Analyzing Two-Dimensional Cracked Plates," ASTM STP 945, Feb 1988.

26. Newman, J.C., Jr., "FASTRAN-II - A Fatigue Crack Growth Structural Analysis Program", NASA TM 104159, 1992.

27. Newman, J.C., Jr., and Edwards, P.R., "Short-Crack Growth Behaviour in an Aluminum Alloy - an AGARD Cooperative Test Programme,", AGARD R-732, 1988.

28. Newman, J.C., Jr., Phillips, E.P., and Everett, R.A., Jr., "Fatigue Analyses under Constant and Variable Amplitude Loading Using Small-Crack Theory," NASA /TM-1999- April 1999.

Table 1. Scratch Depth Measurements

Specimen No.	Left Edge (mm)	Right Edge (mm)
92	0.0406	0.0406
93	0.0584	0.0559
94	0.0559	0.0533
95	0.0508	0.0559
96	0.0356	0.0381
100	0.0508	0.0406
107	0.0610	0.0737
108	0.0483	0.0533
112	0.0533	0.0635
113	0.0483	0.0660
117	0.0508	0.0457
118	0.0457	0.0406
120	0.0483	0.0559
Average:	0.050	0.052
Total:	0.051	

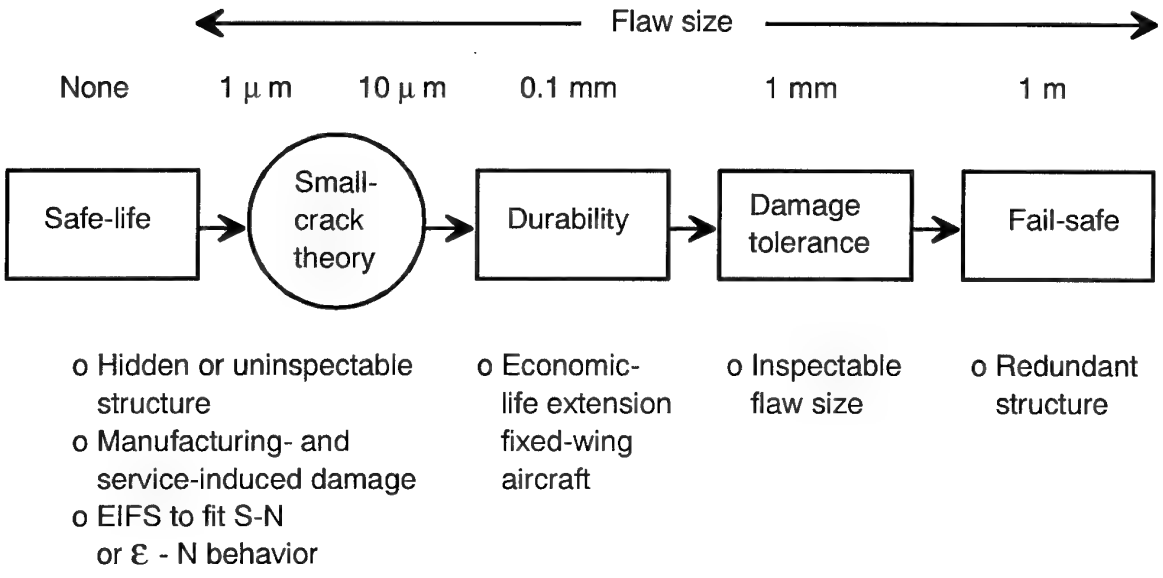

Figure 1. Design concept using small-crack theory (after Ref.15)

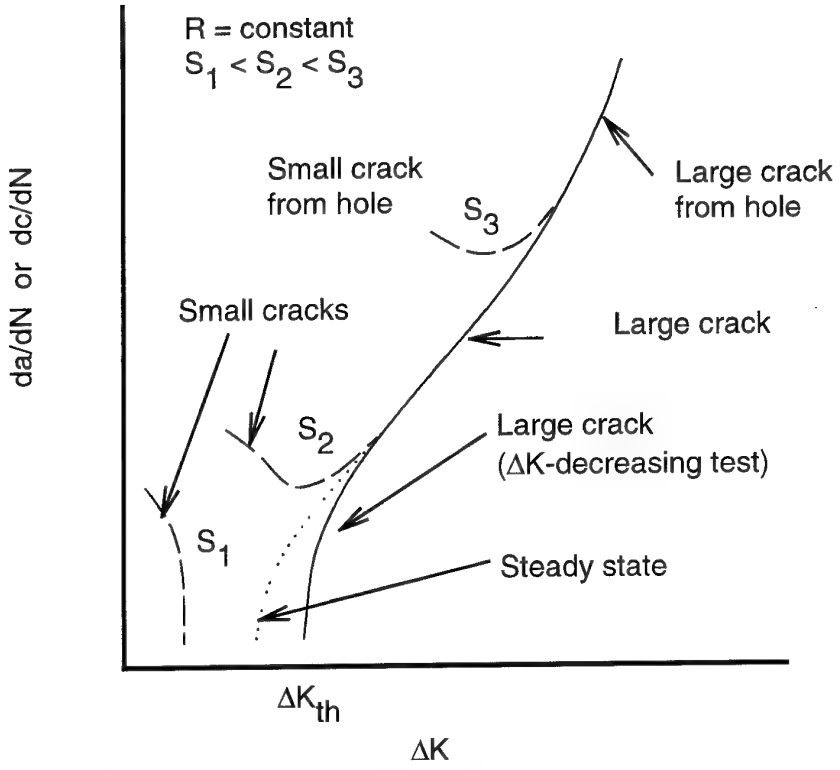

Figure 2. Typical fatigue-crack growth rate data for small and large cracks.

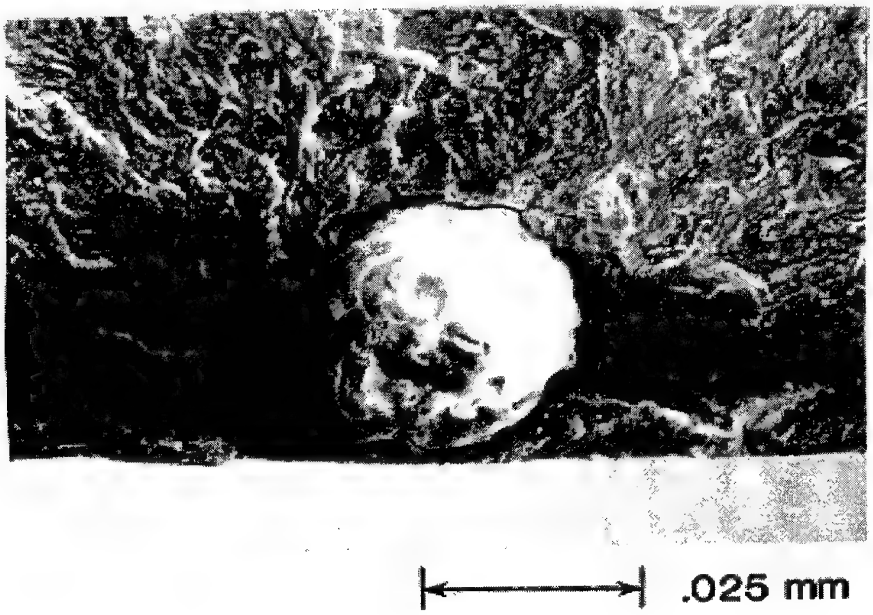

Figure 3. Crack initiation site at spherical-inclusion particle in 4340 steel.

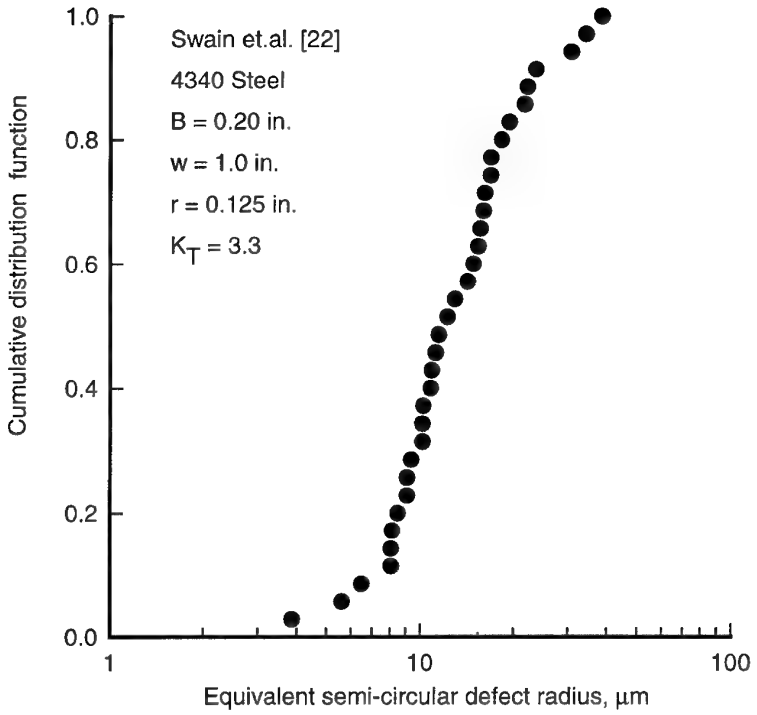

Figure 4. Cumulative distribution function for initiation sites in 4340 steel.

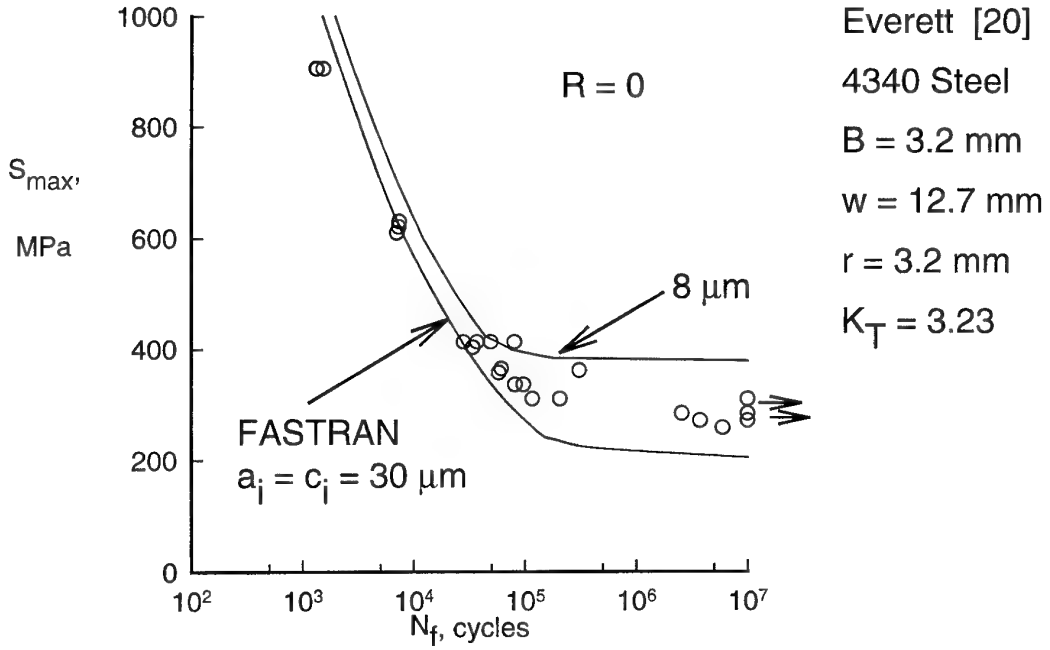

Figure 5. Measure and predicted fatigue live for 4340 steel under constant amplitude loading.

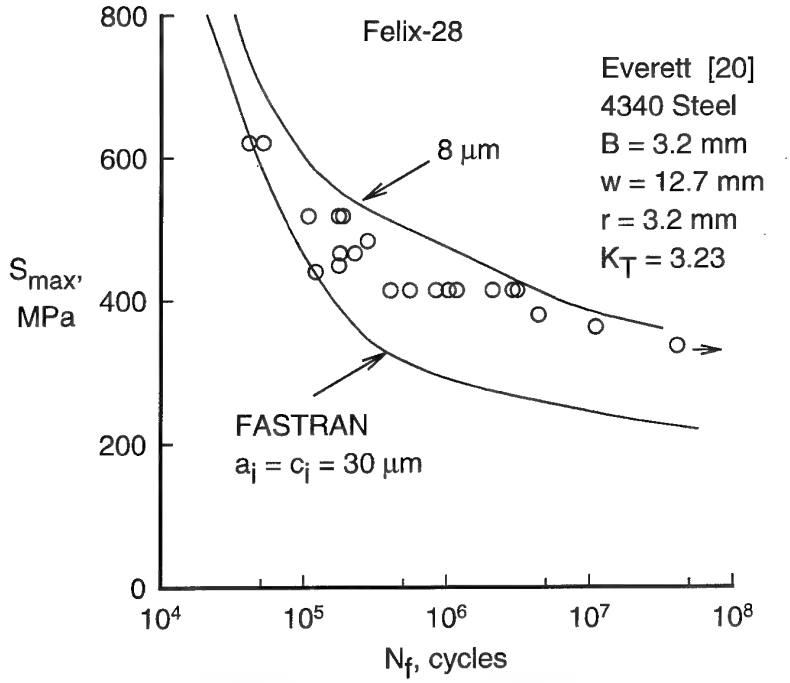

Figure 6. Measured and predicted fatigue lives for 4340 steel under Felix/28 spectrum loading.

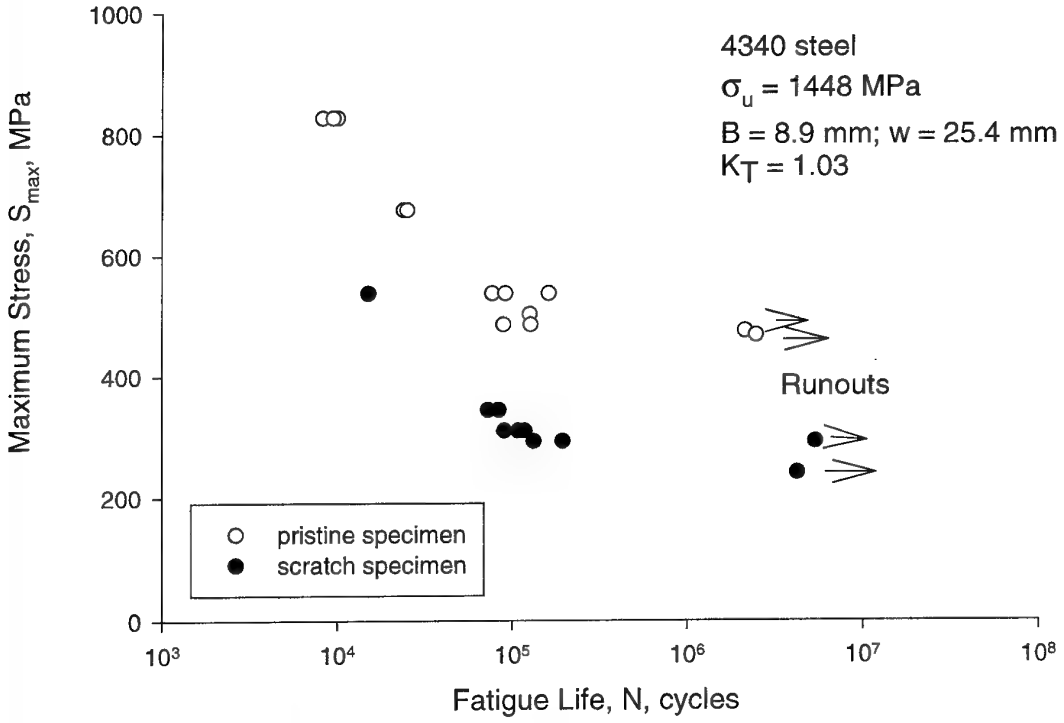

Figure 7. Fatigue life of pristine and scratch specimens under constant amplitude loading at R = -1 with scratch depth of 0.05 mm.

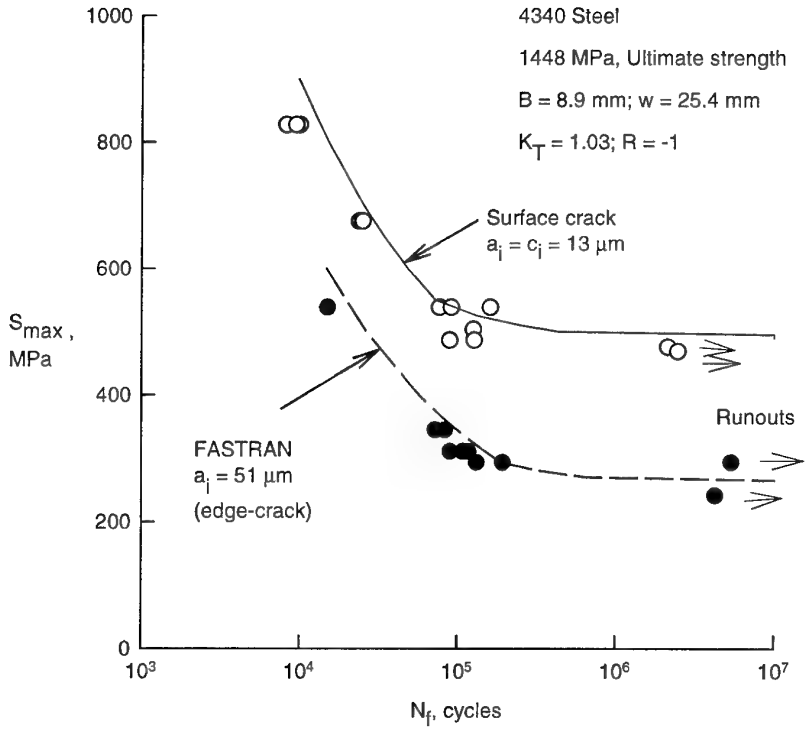

Figure 8. Measured and predicted fatigue lives for the pristine and scratched specimens.

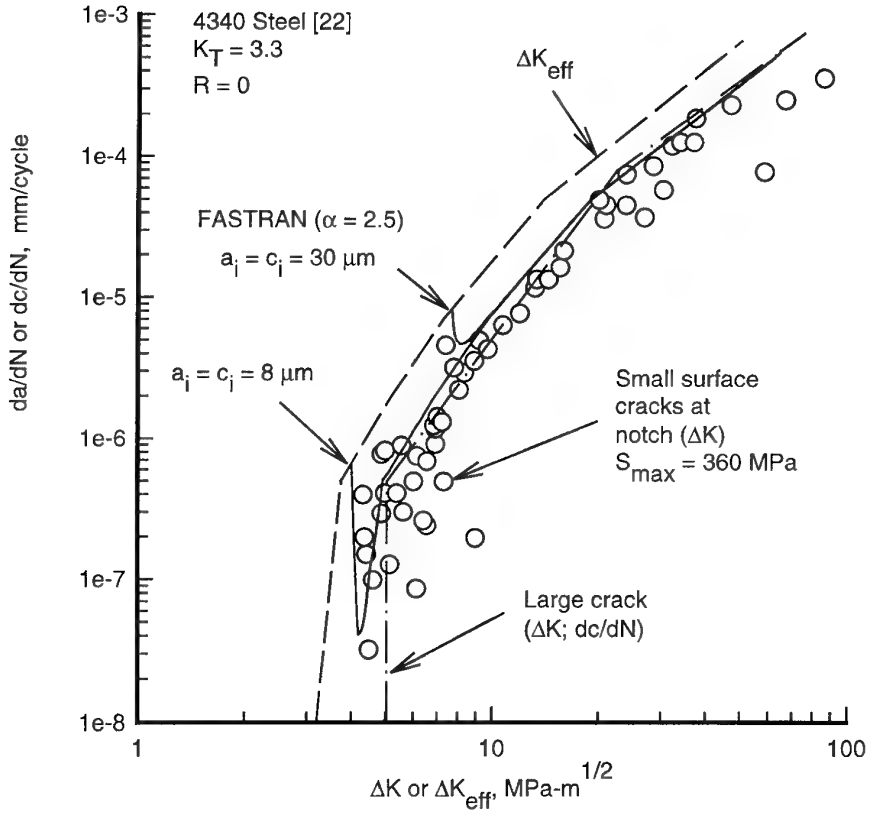

Figure 9. Measured and predicted small corner crack growth at a notch in 4340 steel(after Ref. 28).

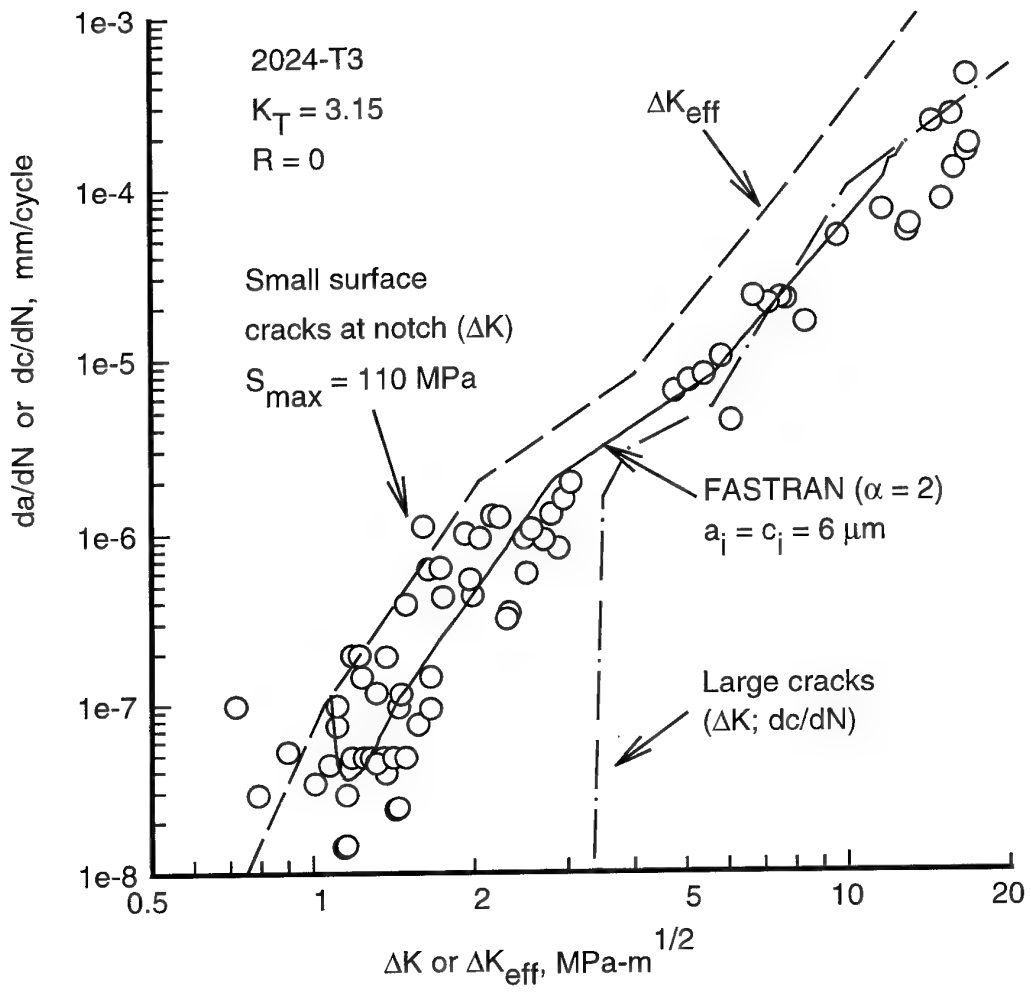

Figure 10. Measured and predicted small surface crack growth at a notch in 2024-T3 (after Ref. 28).

The Development of a Robust Crack Growth Model for Rotorcraft Metallic Structures.

R Cook (DERA, Room 2008, A7 Bldg., SMC,
Farnborough, Hants, GU14 0AQ, UK)
PC Wood, S Jenkins, D Matthew (GKN Westland Helicopters Ltd.)
P Irving (Cranfield University)
I Austen (nCode International Ltd.)
R Buller (GKN Westland Design Services Ltd.)

1 INTRODUCTION

In the United Kingdom, helicopters have traditionally been designed using safe life principles. However, proposed changes to the airworthiness regulations require that, in the future, structures are qualified using flaw growth methods. Therefore, a robust crack growth model is required. A collaborative project has been undertaken by GKN Westland Helicopters, DERA, Cranfield University and nCode International to develop such a model and define the methodologies required for its implementation. The work was funded by the Department of Trade and Industry and the Ministry of Defence whose support is gratefully acknowledged. This report describes work carried out in the collaborative project and the recommendations formulated.

The project consisted of six main areas of investigation namely the derivation of stress intensity factors, determination of typical flight load sequences, measurement of fracture mechanics material properties for use in models, measurement of crack growth data for model verification, evaluation and development of crack growth models, and definition of a helicopter damage tolerance methodology. The project considered two areas of helicopter design, these were 1) a dynamic rotating component found in a rotorhead and 2) a typical structural feature in the main load path lift frames. The two areas are fundamentally different and involve different materials and loading actions which may, therefore, require different damage tolerance approaches.

In this paper each of the six areas of investigation are described, with the main focus on the development and evaluation of crack growth models. The approach used for model development and evaluation was to increase gradually the complexity of the loaded structure. Initially, simple compact tension coupons subjected to constant amplitude loading were studied and models were evaluated against test measurements. The complexity of the loading was increased to include discrete loading events, compressive loading events, and finally two representative flight load sequences, Asterix and Rotorix, which were developed during the project. The complexity of the components was also increased, to include part through thickness cracks and finally structural elements representative of features in a rotorhead mast and an area of a main lift frame. At each of these stages, the models were evaluated against experimental measurements. From the results of the investigation, an overall methodology was developed for damage tolerance assessments, although a number of areas require further investigation. The applications and limitations of the approach are presented and recommendations for further work made.

2 OVERVIEW OF THE COLLABORATIVE PROGRAMME

Fracture mechanics based crack growth prediction programs require information on material properties, a description of constant amplitude crack growth rates in terms of Stress Intensity Factor range (SIF), and a description of SIF in terms of crack length. The first two sets of information were determined from experimental measurements made in this programme. Tensile properties and fracture toughness measurements were made on each of the two materials investigated; a Titanium and an Aluminium-Lithium forged alloy. Crack growth data were measured using compact tension (CT) specimens subjected to constant amplitude loading at four tensile stress ratios, R=0.1, R=0.4, R=0.7 and R=0.9. Crack growth rate data at negative stress ratios (R=-0.5 and R=-1.5) were generated using Single-Edge-Notched-Tensile (SENT) specimens. In addition crack growth rate data were generated in the near threshold SIF region at each of the tensile stress ratios.

In order to validate the models, further experimental crack growth rate data were required for comparison with predictions. The approach adopted was to increase the complexity of the test pieces and the loading independently to allow models to be calibrated prior to prediction of crack growth in representative structures subjected to helicopter loading spectra. The specimens selected were surface-crack-tension (SCT), to examine the growth of a part through thickness flaw, and two structural elements, one representing a feature in a rotorhead mast and one representing a feature in a lift frame. The first loading sequences selected were simple variable amplitude loading (SVAL) which consisted of constant amplitude loading interspersed with large tensile load excursions (overloads) and small tensile load excursions (underloads). The second loading series consisted of the two sequences derived from strain gauge measurements, as described below.

The two helicopter structural locations studied in this project (rotorhead and lift frame) experience dynamic flight loading primarily due to the action of the main and auxiliary rotors. The loading spectra are complex and no standard sequences exist to simulate these regions. The standard sequences Helix and Felix [1,2] represent loading on rotor blades, and the mix of helicopter missions and manoeuvres described by their load generation program, HIXFIX, was thought to be appropriate to the loading experienced by the two structural locations of interest in this project. Accordingly, HIXFIX was used in the project in combination with strain gauge data measured on a Westland/Agusta EH101 and a Westland Lynx helicopter in order to define two new sequences named Asterix[3]and Rotorix[4], relevant to a lift frame location and a rotorhead location respectively.

Paper presented at the RTO AVT Specialists' Meeting on "Application of Damage Tolerance Principles for Improved Airworthiness of Rotorcraft", held in Corfu, Greece, 21-22 April 1999, and published in RTO MP-24.

In order to conduct a crack propagation analysis, Stress Intensity information is required as a function of applied load, crack length, and geometry. For many simple components, these data exist and can easily be incorporated into the crack growth models. SIF solutions for the CT specimen were obtained from ASTM E647, and participants were free to select solutions for the SENT and SCT specimens. SENT SIF solutions were already coded into most of the crack growth models, though in fact all were different. Solutions for the SCT specimen need to account for growth in the surface and thickness directions and again partners were free to select their preferred solutions; this is discussed further in section 3.3. No standard solutions were available for the two structural elements so alternative methods were investigated. These included Finite Element (FE) and Boundary Element (BE) methods and compliance functions derived from tests. The test derivation involved measuring crack growth rates and determining SIF's at equivalent growth rates from data obtained on CT specimens. 2-D and 3-D FE approaches were tried and good agreement was found indicating that the simpler 2-D approach was adequate. Overall it was decided that the experimental compliance function was best suited to the prediction exercise, though clearly this would not be a generally acceptable solution for the wide range of helicopter components which would need to be assessed in a damage tolerant design.

3 ASSESSMENT OF CRACK GROWTH MODELS

3.1 Assessment procedures

Crack growth prediction programs usually calculate the incremental crack extension for individual applied load cycles and sum them over the entire load sequence until some critical value is reached and the component fails. This requires the calculation of effective stress intensity factors at incremental crack lengths from which crack growth rates can be inferred using a database of constant amplitude data. The calculation of effective stress intensity factor requires the use of a model which accounts for load interaction effects. These load interactions may increase (accelerate) or decrease (retard) the rate of crack growth, depending on the relative magnitudes and frequencies of the applied loading cycles. Models which describe these load interactions are generally considered to be the most important aspect of crack growth prediction programs. A range of load interaction models were evaluated in the project, but various other procedures within the crack growth prediction programs were also examined. These other procedures are frequently overlooked and may in fact cause greater differences in predictions than those resulting from the choice of load interaction model. The procedures considered are presented and discussed in section 3.2.

Load interaction models vary not only in their complexity but also in the underlying mechanisms which they aim to describe. The simplest models recognise the role that the plastic zone plays in retarding crack growth when a load cycle is preceded by one of a larger magnitude. Such models are termed plastic zone interaction models and calculate load interaction effects based on the dimensions of the plastic zones due to the current and preceding load excursions. Plastic zone interaction models examined in the project include those developed by Wheeler[5] and Willenborg[6]. There have been many proposed improvements to the Willenborg model and a number of these have also been examined. A more sophisticated version of Willenborg has been adopted by nCode International in their Kraken program [7], which also considers crack closure in its calculations. Crack closure is the notional position during a load cycle at which the crack faces come into contact. In practice, crack faces do not close uniformly along their length at a specific load, but an 'average' load at which crack closure occurs within a cycle is a useful concept in determining the effective stress intensity range experienced by a growing crack. The effective stress intensity factor range can be simply determined from the maximum applied stress during the cycle to the minimum or closure stress, whichever is the greater. This concept is also used in the Loseq model developed by Fuhring [8] which like Kraken also uses plastic zone correction methods. A further group of models are based on strip-yield considerations which follow the Dugdale and Barenbladt approach. The region ahead of a crack tip is considered to be a thin strip of material which comprises rigid-perfectly plastic elements within the yielded zone. As the crack develops these rigid elements are maintained and those behind the crack tip now describe the behaviour in the crack wake. The stress distribution ahead of the crack tip, and in its wake are used to derive the crack closure load for any loading sequence. Models utilising this approach have been developed by Newman[9] and by de Koning and ten Hoeve[10] which are entitled Fastran and Stripy respectively. All of the models described above were evaluated in the project.

The models were assessed against experimentally determined fatigue crack growth data which were selected from a database generated as part of the project. The models were first used to predict crack growth rates in constant load amplitude tests as described in section 3.3. These data were then used to optimise the models and blind predictions were made of crack growth rates in tests where discrete loading events (overloads and underloads) were introduced. The ability of the models to predict changes in crack growth rates associated with these periodic load excursions is assessed in section 3.4. The experimental data were then used to further optimise the models prior to blind prediction of the complex variable amplitude loading (CVAL) tests. The prediction of CVAL crack growth rates is described in section 3.5.

The accuracy of the different crack growth models was assessed at each stage of the project. Some models were found to be inappropriate for specific applications and were dropped at various stages of the project. The most important modelling parameters were also defined by examining their effect on the accuracy of crack growth predictions. A summary of these findings and recommendations on the most appropriate procedures to be used for crack growth modelling of rotorcraft structures is presented in section 4.

3.2 Data fitting procedures

3.2.1 Crack growth data fitting methods

Fitting appropriate curves through experimental data may appear a trivial step in the crack growth prediction process, however, its importance needs to be assessed. Participants were free to choose a data fitting method and those selected included visual best-fits and fits obtained from commercial software packages. Fits were made for each of the four stress ratios in each of the two materials used in the experimental programme. Fits in the linear (Paris) regime were similar for all three methods. However, interpretation of the raw data in the threshold and near failure regimes, where data were

sparse, showed some variation between the methods (see fig 1). Fits to the Aluminium-Lithium data were less consistent, due to the higher scatter, than for the Titanium data. Variations in the near threshold region, will have a significant impact on predicted fatigue lives under spectrum loading. This is because cracks spend a significant proportion of their lives at short crack lengths and because a significant percentage of loads in a helicopter loading sequence are of small magnitude. These two effects result in a large percentage of the life of a cracked helicopter structure being spent in the near threshold crack growth regime.

The fits achieved by the different participants were used as input data to the LOSEQ model with all other parameters remaining constant. Thus variations in predicted growth rates could only result from the different data fits used. The differences in predicted lives between the most and least damaging data fits for Titanium range from 7% to 30% of the least damaging life with an average of 19%. The differences in predicted lives between the most and least damaging data fits for Aluminium-Lithium range from 11% to 41% of the least damaging life with an average of 25%. It can be concluded that average errors of 20% to 25% of the predicted life under constant amplitude loading can arise simply from the choice of method adopted for determining the best fit to the raw data.

3.2.2 Crack growth data representation

Having obtained curves which describe the crack growth data sets to be used, it is necessary to describe them in a form which can be interpreted by the various computer models. The simplest form of this is digitisation of the crack growth curves at selected points (within the limits of the program). Other data input methods used by the partners included fitting Paris, Walker or Forman equations to the crack growth data. In order to assess the importance of the data input method, a series of predictions were made at each of the four stress ratios for the Titanium material with the inputs listed above; all other parameters were kept constant.

The results show major differences between the predictions for the various data representation methods. Differences in predicted lives between the most and least damaging data fits range from 25% to 86% of the least damaging life with an average of 61%. This means that differences in predictions by a factor of 2:1 are typical and up to 4:1 are possible as a result of the data representation method. The most appropriate method was a tabular input of crack growth rates to be used in conjunction with an interpolation and extrapolation routine. The least successful method was, not surprisingly, a single Paris representation, whilst the Forman equation, and to a lesser extent the Walker equation, over-predicted the effect of stress ratio on crack growth, resulting in consistently conservative predictions at high stress ratios. For the low stress ratios predictions were conservative at low delta K and unconservative at high delta K.

3.3 Constant amplitude loading (CAL)

The constant amplitude part of the programme was undertaken to validate the models for a range of specimen and crack geometries, and loading actions. The test programme focused on CT specimens, but included SENT and SCT specimens to examine compressive loading excursions and part-through-thickness cracks respectively. There were two parts to the prediction exercise for constant amplitude loading, the first involved a blind prediction and the second allowed model optimisation to minimise differences between predicted and experimental measurements. The final part of the constant amplitude programme was to perform predictions, using the optimised models, of crack growth in two structural elements, one representative of a feature in a rotorhead mast and the second of a feature in a main load frame.

Model calibration resulted in significant improvements in predictions; errors in predicted lives were within +/- 40% of the test life, and 60% were within +/- 10% of the test life for the Titanium CT tests (see for example fig 2). However, due to the higher scatter in the Aluminium Lithium data, errors were more than double those found for Titanium. The largest errors occurred at the low stress ratios (0.1 and 0.4), but predictions at the higher stress ratios (0.7 and 0.9) were generally quite good.

Cracks in the CT specimens were fairly uniform through the thickness of the material. In general, however, cracks are quarter or semi-elliptical in shape for a large percentage of the life of a component, particularly in materials of the thickness considered in this programme. SCT specimens were selected for use in this programme as cracks in this type of specimen remain semi-elliptical in shape for the majority of the fatigue life. Most of the models do not have the capability of predicting crack growth in both surface and through thickness directions, so some simplifications and modifications were required to the computer codes. Each participant was free to choose how crack growth would be represented but data predictions were required of crack growth on the specimen surface as a function of crack length. Various crack growth options were selected which included; constant aspect ratio, variable aspect ratio calculated from Newman and Raju[11], and compliance solutions from test measurements.

Methods which assume a constant crack aspect ratio equal to that of the initial flaw were conservative, as the cracked area was always greater in the predictions than in the test. The Newman and Raju approach gave reasonably accurate predictions, but as expected best accuracy was obtained by using the test compliance curve. Since this will not, in general, be available independent calculation of growth rates in the two directions using approximate methods such as Newman and Raju are recommended in preference to constant aspect ratio assumptions.

Analyses of measured loads at the selected structural locations showed that some minor compressive load excursions were present. A SENT specimen was selected to examine the effect of compressive loading excursions on crack growth and to facilitate evaluation of the prediction models with a compressive component of loading present. Crack growth tests were conducted on SENT specimens at stress ratios of R=-0.5 and R=-1.5. Significant discrepancies between predictions (using tensile stress ratio data only) and experimental measurements were found at R=-1.5, which were generally non-conservative (see for example fig 3). At a stress ratio of R=-0.5, predictions were still non-conservative but the results were much closer to the measured behaviour. It was concluded that predictions of crack growth under partial compressive loading could not be predicted accurately using any of the models if tensile constant amplitude crack growth data only were available. The predictions became less accurate, and more non-conservative, as the compressive

loading content was increased. For predictions in which compressive loading is to be applied, it is important to ensure that crack growth rate data for compressive constant amplitude loading are used as model inputs which cover the complete range of stress ratios for which predictions are required.

Predictions of growth rate in the two structural elements using a compliance function derived from experimental measurements and analysis predicted trends in the crack growth curves extremely well and the total lives were within 30% of the measured values.

3.4 Simple variable amplitude loading (SVAL)

Fatigue crack propagation tests were performed on CT and SCT specimens which were identical to those used in the constant amplitude part of the programme. Fatigue tests on CT specimens consisted of constant amplitude loading at stress ratios of 0.1, 0.4 or 0.7, with different load events applied at crack lengths of 16, 20 or 24mm. The events superimposed on the constant amplitude loading sequence consisted of single overloads (OL), double overloads (DOL) or a single overload followed by an underload (OL/UL). The magnitude of the overload ratios (peak load/peak constant amplitude load) were typically 1.47, 1.75 and 2 at crack lengths of 16, 20 and 24mm respectively. The underload ratio (minimum load/peak constant amplitude load) was 0.1. The double overloads were not applied on consecutive cycles but separated by 3000 load cycles such that the second overload was applied at a point where crack retardation was active as a result of the first overload. The underload in the OL/UL tests were applied immediately following the overload. Fatigue tests on SCT specimens were similar to those described above. Single overloads, double overloads and overloads followed by underloads were applied at crack lengths of 5, 7 or 9 mm. Overload ratios varied from 1.25 to 2 and were superimposed on constant amplitude loading with stress ratios of 0.1, 0.4 or 0.7.

In order to compare the accuracy with which the models predicted these events, two metrics were defined; a) the number of loading cycles, and b) the crack extension over which crack acceleration and retardation occurred. These parameters are relatively simple to determine from predictions, by setting appropriate flags in the computer programs. Determination from experimental data is rather subjective so a fixed procedure was defined to ensure a uniform approach. Detailed predictions were made of crack growth at cyclic intervals prior to and immediately following individual load events.

The Wheeler model predicted delay cycles typically between a factor of two too small or too large, though the average for all tests was close to unity. The predicted delay distance was always considerably smaller than observed in test, the average prediction being about 10% of that observed. The predictions using Loseq were generally better than those using the Wheeler model. The delay cycles were between 0.48 and 1.36 of those observed in test. The delay crack lengths were slightly better than for the Wheeler case but were still typically only 16% of those observed in tests. Crack arrest was predicted for all cases where arrest was observed in tests but also for three cases where arrest did not occur in tests. The Stripy model predicted delay cycles closest to those observed in test for a stress ratio of R=0.1, but predicted delay cycles for all other cases were less than 0.65 of those observed in tests and always less accurate than for both the Loseq and Wheeler models. In contrast, the delay crack lengths predicted by Stripy were more accurate than those predicted by Loseq or Wheeler.

Kraken was used by two participants, one showed a bigger variation in predicted delay cycles than any of the other models, ranging from 0.024 to 4.66; the results obtained by the other participant showed much less variation. Similarly, the delay lengths predicted by the first participant showed a much wider variation than predicted by the second participant. For Kraken the delay cycles and delay lengths were closely correlated, which indicates that the crack growth rates are being more accurately predicted than by the other models.

Having examined the errors between predicted and experimental delay lengths and cycles and also any differences in growth rate characteristics, the participants were faced with the task of optimising their models once again. The discrepancies in delay cycles were mainly related to crack growth in the near threshold region. Accordingly most of the effort to optimise the models was spent in adjusting the constant amplitude crack growth rate data in this regime. All CT-SVAL predictions were repeated using the optimised models, and significant improvements were found as can be seen for example in figure 4 which shows blind and optimised predictions for a range of models.

Having optimised the models to best represent the measured SVAL data on compact tension specimens, the 'optimised models' were used to predict crack growth rates in SCT specimens under SVAL loading conditions. Predictions of tests conducted on Titanium specimens were generally quite good, although, out of the 52 predictions made, 17 still predicted arrest when none occurred in the test. Predictions of tests conducted on specimens of Aluminium-Lithium material were better than those for the Titanium material and crack arrest was not predicted for any of the tests.

3.5 Complex variable amplitude loading (CVAL)

The aim of this phase of the programme was to determine whether accurate predictions could be made of crack growth in structural components, using the procedures developed in the programme. Predictions were made of crack growth in CT and SCT specimens, and structural elements subjected to the two sequences Asterix and Rotorix. Predictions of tests on CT specimens subjected to Asterix loading were rather disappointing in that predictions were in error by up to a factor of ten, and the greatest errors occurred for predictions which were non-conservative. The Willenborg model predicted lives within a factor of about 3 but was overall non-conservative. The generalised version of Willenborg predicted longer lives than the original version and as a result they were consistently non-conservative by a factor of up to 10. Wheeler predictions were very poor and were also consistently non-conservative by a factor up to 10. The Loseq model predictions were non-conservative and resulted in errors of up to a factor of 5. Kraken predictions were within a factor of two of the test life, and were consistently conservative. Esacrack, which is a linear summation model taking no account of load interactions, generally predicted results in close agreement with the experimental results.

Linear summations were made for each of the models to examine a) the magnitude of the predicted load interactions

and b) whether linear summations would yield consistently conservative predictions. Relatively small load interaction effects (see fig 5) were predicted by the two Willenborg models (less than 20% increase in life), very large load interaction effects are predicted by Wheeler (factor of ~4 increase in life) and moderate load interaction effects are predicted by Loseq (factor of ~2 increase in life). More importantly, all of the predictions were non-conservative.

Predictions of tests on CT specimens subjected to Rotorix loading were similar to those observed for Asterix loading. Kraken predicted consistently conservative lives, generally within a factor of two, whilst all of the other models gave unconservative predictions. Linear summations were again non-conservative for the Wheeler, Willenborg, Generalised Willenborg and Loseq models.

The fits used for the Loseq, Willenborg, modified Willenborg and Wheeler models were all selected to best fit the crack growth data supplied and also to best fit the CAL and SVAL test results. For these models, crack growth rate data are described independently for each of the stress ratios tested. In contrast, a best fit to all of the constant amplitude data is selected automatically within the Kraken program. The data fits for each model were found to be quite similar for R=0.1 and R=0.4, but these will have little effect on the CVAL predictions, since most of the load cycles in Rotorix are at much higher stress ratios, typically between 0.7 and 0.9. The fits used in the different models at these higher stress ratios were quite different (see fig 6). Notably, the fits used by Kraken give crack growth rates significantly greater than those of the other models for a given stress intensity factor over the entire stress intensity factor range at R=0.9 and at stress intensity factor ranges less than 10 MPa. $\sqrt{m}$ at R=0.7. The predicted crack growth rates and endurances under Rotorix loading will be dominated by growth rates in the low stress intensity factor region and consequently Kraken predictions will be much shorter than those of the other models if a linear summation routine is used.

To study the sensitivity of predicted growth rates to the selected data fits, predictions were performed using the linear Loseq model. The resultant predictions for a compact tension specimen using the Rotorix loading sequence with a maximum load of 10 kN are presented in figure 7. The effects of the assumed data fits are clearly demonstrated with Kraken predicting the shortest lives, as expected. A similar exercise was undertaken for the Aluminium-Lithium material using Asterix loading and similar results were found . Predictions of SCT crack growth rates for Asterix and Rotorix loading gave similar results to those for compact tension specimens i.e. predictions using Kraken were conservative and all other predictions were non-conservative.

Predicted crack growth in the Titanium structural element was completely different to that observed in CT and SCT specimens. All predictions with the exception of Wheeler and Loseq were conservative and in extremely good agreement with test results. Kraken predictions were consistent with those made for tests on CT and SCT specimens in that they were conservative and within about 20% of the measured test endurances. The differences in crack growth patterns from those observed in CT and SCT predictions are that the Loseq, Wheeler and Willenborg predictions were conservative for the structural element tests. Predictions for structural element tests in Aluminium-Lithium material, however, were similar to those reported for the CT and SCT tests under CVAL loading in that Kraken produced conservative results and all of the other models were non-conservative.

4 DISCUSSION

Factors which can affect the accuracy of crack growth predictions have been investigated and their importance assessed. The method chosen to fit a curve through the available raw data had a significant effect on the predicted crack growth; typically differences of 20 to 25% were found in the predicted lives. Of greater significance were the differences in predictions resulting from the method selected to represent the fitted raw data in the prediction programs. The differences between the four selected methods were typically 2:1 with peak values of around 5:1. A simple Paris equation was found to be unsuitable and the Forman and Walker equations were very conservative at the high stress ratios. It can be concluded that more complex equations (e.g. Newman) are required to represent the data. Alternatively a tabular input of fits to the raw data should be used in conjunction with an interpolation routine. The SENT prediction exercise demonstrated that constant amplitude crack growth rate data to be used in the models must cover the entire range of stress ratios that occur in the loading sequence for which predictions are required. Extrapolation of the data to stress ratios less than those included in the available data lead to significant errors in predictions.

The SCT prediction exercise examined various methods to describe stress intensity factors for part through thickness cracks. Various methods were used in the models and the simplest ones which assumed constant crack aspect ratio were found to be very conservative. The most appropriate method of those examined was the one in which crack growth along the surface and thickness directions was described using the Newman and Raju expressions. The structural element prediction exercise demonstrated that experimental determination of compliance is a good method for crack growth predictions. However, it should be noted that this is not a very practical solution for the number of complex geometries which will be encountered in helicopter structures and a robust analytical approach should be sought.

Evaluation of models against SVAL data was achieved by comparison of the crack extension (delay distance) and the cyclic interval (delay cycles) over which crack retardation occurred. Whilst the delay cycles were generally predicted to within a factor of 2 by all models, the delay distance was poorly represented and in 31 of the 35 predictions it was underestimated. The average delay distance ratios (predicted/measured) were very different in the models; 0.1 for Wheeler, 0.15 for Loseq, 0.37 for Stripy and 0.47 for Kraken. This gives an initial ranking of the models in their ability to predict the distance over which crack lengths will be affected by overload events. The predicted delay distance is closely related to the plastic zone size and the differences in predicted values were found to result primarily from the different expressions used in the models to calculate the plastic zone size.

However, it was significant that the delay distances following an overload were much greater than the plane strain overload plastic zone size (OLPZ). Typically the ratio of test delay distance to OLPZ size ranged form 3 to 22. This has been observed previously by Suresh[12] who invoked a crack closure argument to explain the prolonged delay distance. However, this does not offer a satisfactory mechanism

because the fractography results did not give any evidence of fracture surface damage consistent with roughness induced closure either before or after the overloads. The fracture surface appearance remained virtually unchanged so that it is unlikely that this mechanism gave prolonged delay distances.

Delay distances longer than the overload plastic zone size have also been observed by Shuter and Geary[13] who found that delay distances were shorter in plane strain specimens than in plane stress specimens. This observation provides a plausible explanation which is that different growth rates occur between the surface and interior of the specimen. Turner *et. al.*[14] suggest that delay responses are different through the thickness because of a variation in constraint from the plane stress surface to the plane strain interior. They found that the post-overload crack front had greater curvature than pre-overload due to crack 'tunnelling' in the plane strain interior.

The observations of Turner *et. al.* suggest that the surface plastic zone has a significant retarding effect on crack growth on the surface only, due to greater plasticity at the crack tip. This was not specifically observed in the tests, because the specimens were not broken open after each overload (they were used for subsequent overload tests). The DCPD method used in this investigation measures changes in cross-sectional area of the specimen so the crack length would be an average of the through-thickness crack front length. If retardation is minimal in the specimen interior and grows a significant distance before the surface region grows through the plane stress OLPZ then the DCPD system would measure a change in length greater than the OLPZ.

Delay cycles are more important than delay length in the prediction of crack growth life, and the success of efforts to improve predictions were measured using this parameter. The calibration exercise proved extremely successful and predictions of the SVAL data were improved significantly for all of the models. In particular it was possible to eliminate prediction of crack arrest following overloads in all cases where crack arrest was not observed in tests; this was not the case for blind prediction of the SVAL data. It can be concluded that calibration is an important part of the process in developing methods for crack growth prediction.

The accuracy of predictions under CVAL loading was rather disappointing. Predictions varied from a factor of two on the conservative side to a factor of five on the non-conservative side. The Kraken model predicted consistently conservative growth rates, whilst the other models (Loseq, Wheeler, Willenborg and generalised Willenborg) predicted non-conservative growth rates. The non-conservative predictions did not result from inaccurate modelling of load interaction effects as linear summations were also found to be non-conservative. Examination of the constant amplitude crack growth data used in the different models revealed that the Kraken description of crack growth rates at high stress ratios (R=0.7 and R=0.9) was considerably more damaging than the baseline constant amplitude data, whilst descriptions of constant amplitude crack growth data used by the other models were in good agreement with experimental data (see figure 8).

The sensitivity of predictions to the input data was further examined using the various constant amplitude data fits from the different models and performing linear summations with the Loseq model, thus eliminating any differences between the operation of the different models. This resulted in very similar observations to those described above for CVAL loading with Kraken data fits giving the shortest lives compared with those using data fits from the other models. The large differences in predicted fatigue crack growth and fatigue endurances can thus be attributed to the different constant amplitude crack growth rate data fits used in the models.

The sensitivity of data fits in the near threshold regime requires accurate data fitting. Experimental data will, in general, exhibit large scatter in this region which will preclude accurate data fitting. Further work needs to be carried out to define suitable data fitting methods. There is also growing evidence that crack growth in the threshold region is dependent on crack length. This has been accepted for the growth of short cracks for a number of years [15], and an investigation at a range of crack lengths is warranted. This may be an important addition to the models where short crack growth is not modelled explicitly.

It was also noted that the Kraken, Willenborg and generalised Willenborg predicted very little effect of load interaction, whereas the Loseq and Wheeler predicted a significant effect. This needs further study to establish the real load interaction effects and which models give the best representation. It is possible that the development of new models may be necessary to improve crack growth predictions for helicopter structures which describe the effects of underloads more accurately.

A further possible reason for the poor predictions of crack growth rates under the Asterix sequences is that the fracture surface morphology is very different to that observed in constant amplitude tests. The fracture surfaces of compact tension test pieces subjected to Asterix loading were quite smooth, as were those subjected to constant amplitude loading at low ΔK values. At high ΔK values, however, constant amplitude tests had rough surfaces resulting from transgranular cracking. The crack closure levels in the CA tests would, therefore, be higher due to this surface roughness. The predictions used the CA data to predict crack growth under Asterix loading, where the closure levels were lower. Thus the stress range experienced by the crack tip for any given crack length and stress ratio would be greater in the Asterix test than in the CA test. This is likely to result in non-conservative predictions as the assumed stress range experienced by the crack tip would be lower in the predictions (based on CA data) than in the Asterix tests. This also requires further investigation.

5 CONCLUSIONS

5.1 Predicted fatigue endurances varied by up to 1.3:1 dependent on the method chosen to fit the raw crack growth rate data.

5.2 Predicted fatigue endurances varied by up to 5:1 dependent on the equation chosen to describe crack growth rate data at different stress ratios.

5.3 A tabular input of crack growth rate data at individual stress ratios is recommended as the most appropriate method to describe crack growth rate data at different stress ratios.

5.4 In general, calibrated models produced reasonable predictions of the constant amplitude fatigue endurances, i.e. within a factor of 2 of the experimental data.

5.5 Experimentally measured delay lengths in SVAL tests were greater than predicted in 90% of tests.

5.6 Experimentally measured delay lengths in SVAL tests were greater than the calculated plastic zone sizes.

5.7 Crack growth predictions of Asterix and Rotorix are extremely sensitive to small changes in near threshold crack growth rates at high stress ratios.

5.8 All models, other than Kraken, generally predicted non-conservative fatigue endurances

5.9 Linear summations of crack growth rates generally resulted in non-conservative predictions.

6 RECOMMENDATIONS

This project examined a potential procedure for predicting crack growth, consisting of model calibrations for increasingly complex geometries and loading actions. Whilst it has been demonstrated that this procedure gives improved predictions, it does not always yield acceptable predictions. It is considered that the CAL optimisation is an important stage but the SVAL optimisation needs to be re-examined. The SVAL stage was highly demanding in terms of experimental effort and further work should be carried out to determine the most appropriate tests to be performed to ensure adequate model optimisation. In particular the emphasis of this work should be on the effects of underloads rather than overloads and thereby examine crack acceleration as well as crack retardation effects.

Comparison of model predictions with experimental data showed that the effects of periodic overloads were not described well by the models. In general, the cyclic interval during which crack retardation was effective could be adequately described by the models although optimisations were required to achieve this. However, the crack growth increment over which crack retardation occurred was poorly described by all of the models. Even after optimisation, all models underestimated the overload affected crack growth increment. Further work should be undertaken to examine whether the experimental procedures adopted are valid and whether parameters other than plastic zone size affect the crack growth increment during which crack retardation occurs.

Perhaps the most concerning outcome of this work was the non-conservative predictions from most models when a linear summation of crack growth rates was made for Asterix and Rotorix loading. It was shown that the predictions were particularly sensitive to crack growth rate data fits in the near threshold region at high stress ratios. However, given a wide range of data fits, all of which gave a reasonable representation of the constant amplitude data, non-conservative predictions still resulted. The only conservative predictions resulted from fits which had lower thresholds and considerably faster growth rates than the experimental constant amplitude data. A number of aspects need to be addressed in future programmes, particularly the definition of methods to describe crack growth data in near threshold regions and determination of the effect of crack length on near threshold crack growth behaviour.

7 REFERENCES

1 Edwards, P.R. and Darts, J. "*Standardised Fatigue Loading sequence for Helicopter Rotors (Helix and Felix) Part 1: Background and Fatigue Evaluation*" RAE Technical report TR84084.

2 Edwards, P.R. and Darts, J. "*Standardised Fatigue Loading sequence for Helicopter Rotors (Helix and Felix) Part 2: Final Definition of Helix and Felix*" RAE Technical report TR84085.

3 Wood, P.C. "*A standardised loading sequence for helicopter structures*", DTI-LINK RA/6/30/06, Final Report, GKN WHL Research Report RP1003, 1997.

4 Buller, R.G. "*A standardised fatigue loading sequence for helicopter main rotorhead structures (ROTORIX)*", DTI-LINK, CU/927N/2.7, August 1996.

5 Wheeler, O.E. "*Spectrum loading and crack growth*". Transaction of ASME, Journal of basic engineering, pp 181-186, 1972.

6 Willenborg, J.D., Engle, R.M. and Wood, H.A. "*A crack growth retardation model using an effective stress concept*". AFFDL-TM-FBR-71-1, 1971.

7 nCode. "*Kraken Users Manual*". nCode International Ltd, Sheffield, UK, 1996.

8 Fuhring, H. "*Model for non-linear crack growth prediction, taking load sequence (Loseq) effects into consideration*". Royal Aircraft Establishment Library Translation, LT2144, 1983.

9 Newman Jr., J.C. "*Fastran II - A fatigue crack growth structural analysis program*". NASA TM 104159, Langley Research Center, Virginia, 1992.

10 ten Hoeve, H.J. and de Koning, A.U. "Implementation of the improved Strip-yield model into the NASGRO software. Architecture and detailed design comments". NLR CR 953122.

11 Newman, Jr J.C. and Raju, I.S. "*Stress Intensity Factor equations for cracks in 3-D finite bodies*". Fracture mechanics 14th Symposium, Vol 1, Theory and analysis, ASTM STP 791, 1983.

12 Suresh, S. "*Micromechanisms of fatigue crack growth retardation following overloads*". Engineering Fracture Mechanics, Vol. 18, No. 3, pp. 577-593, 1983.

13 Shuter, D.M. and Geary, W. "*The influence of specimen thickness on fatigue crack growth retardation following an overload*". International Journal of Fatigue, Vol. 17, No. 2, pp. 111-119, 1995.

14 Turner, C.C., Carmen, C.D. and Hillberry, B.M. "Fatigue crack closure behaviour at high stress ratios". Mechanics of Fatigue Crack Closure, ASTM STP 982, J.C. Newman, Jr. and W. Elber, Eds. American Society for Testing and Materials, Philadelphia, pp. 528-535, 1998.

15 Newman, J.C. Jr. and Edwards, P.R. "*Short-Crack Growth Behaviour in an Aluminium Alloy - an AGARD Cooperative Test Programme*", AGARD-R-732.

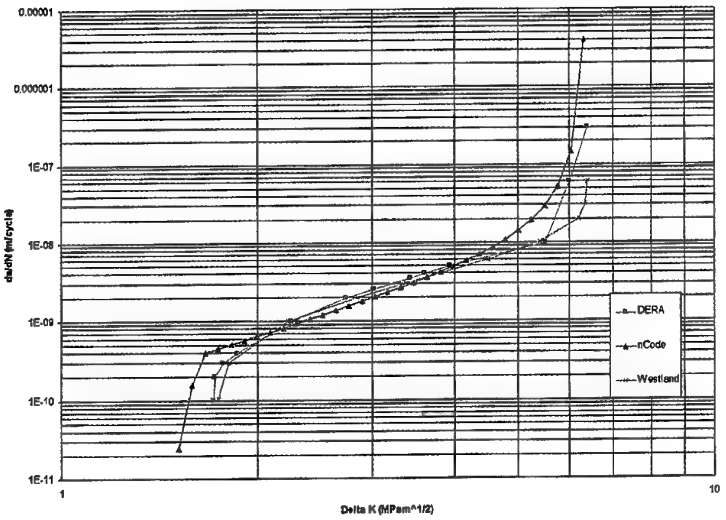

Figure 1 Fits to raw data – Titanium R = 0.9

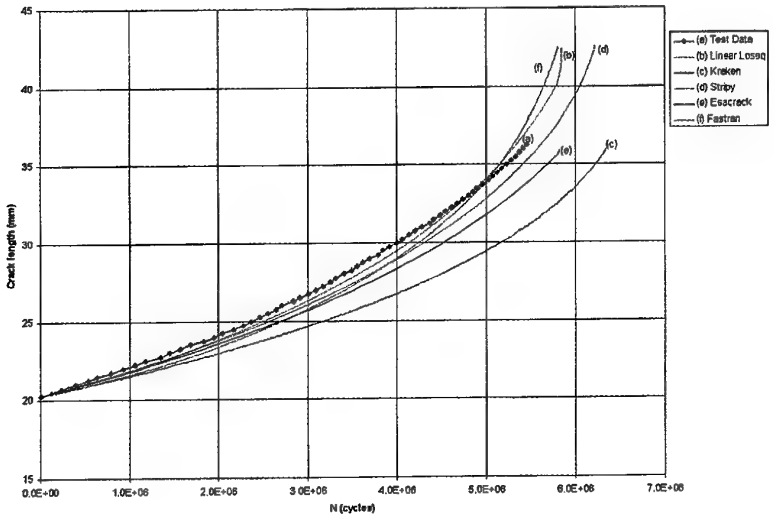

Figure 2 Predicted and experimental crack growth – CAL-Titanium R = 0.9

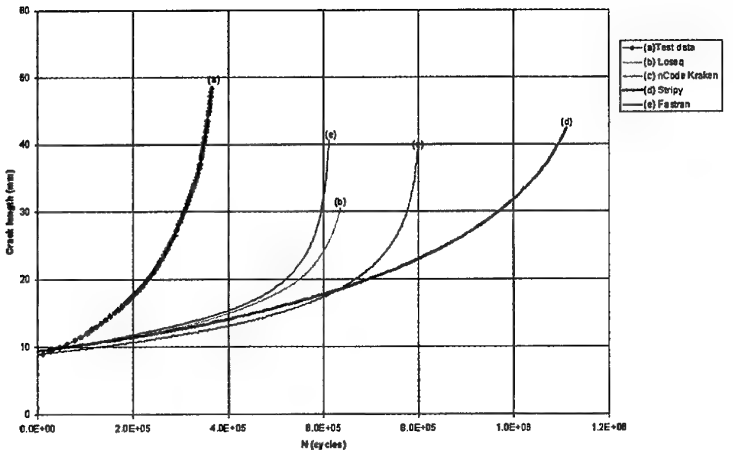

Figure 3 Predicted and experimental crack growth – CAL-Titanium R = -1.5

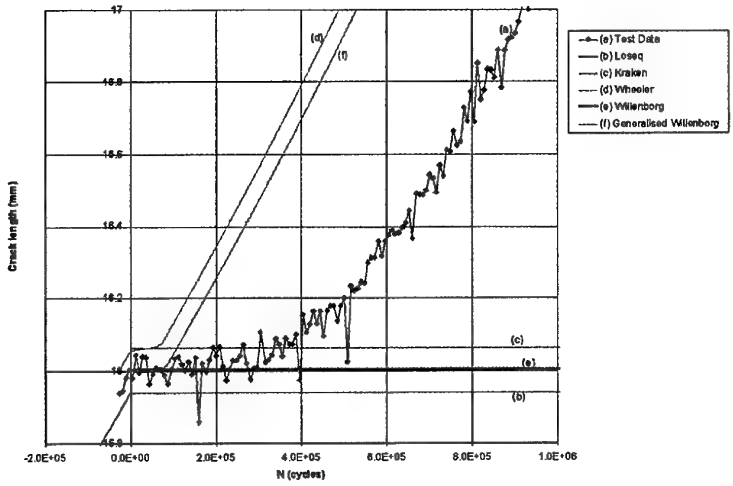

Figure 4a Effect of model optimisation – Blind SVAL Aluminium-Lithium

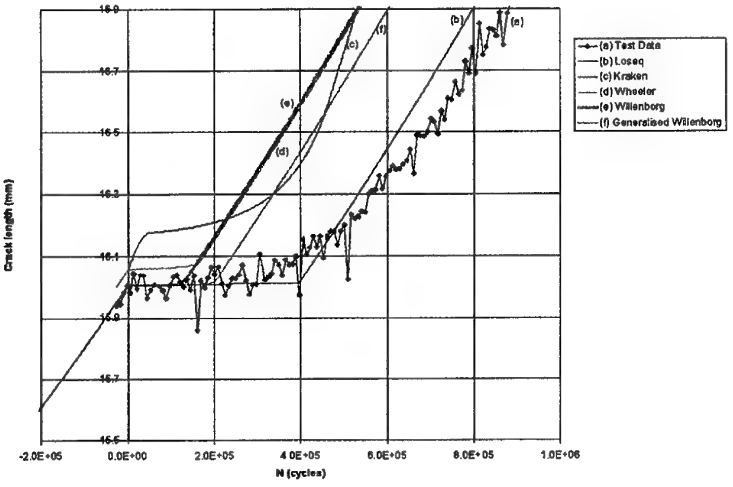

Figure 4b Effect of model optimisation – Optimised SVAL Aluminium-Lithium

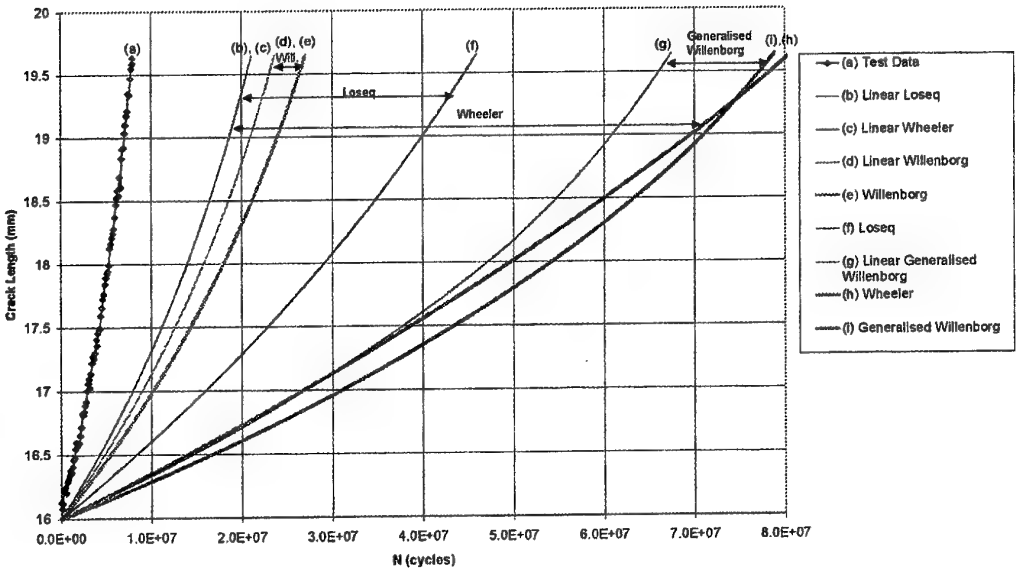

Figure 5 Load interactions predicted by the different models

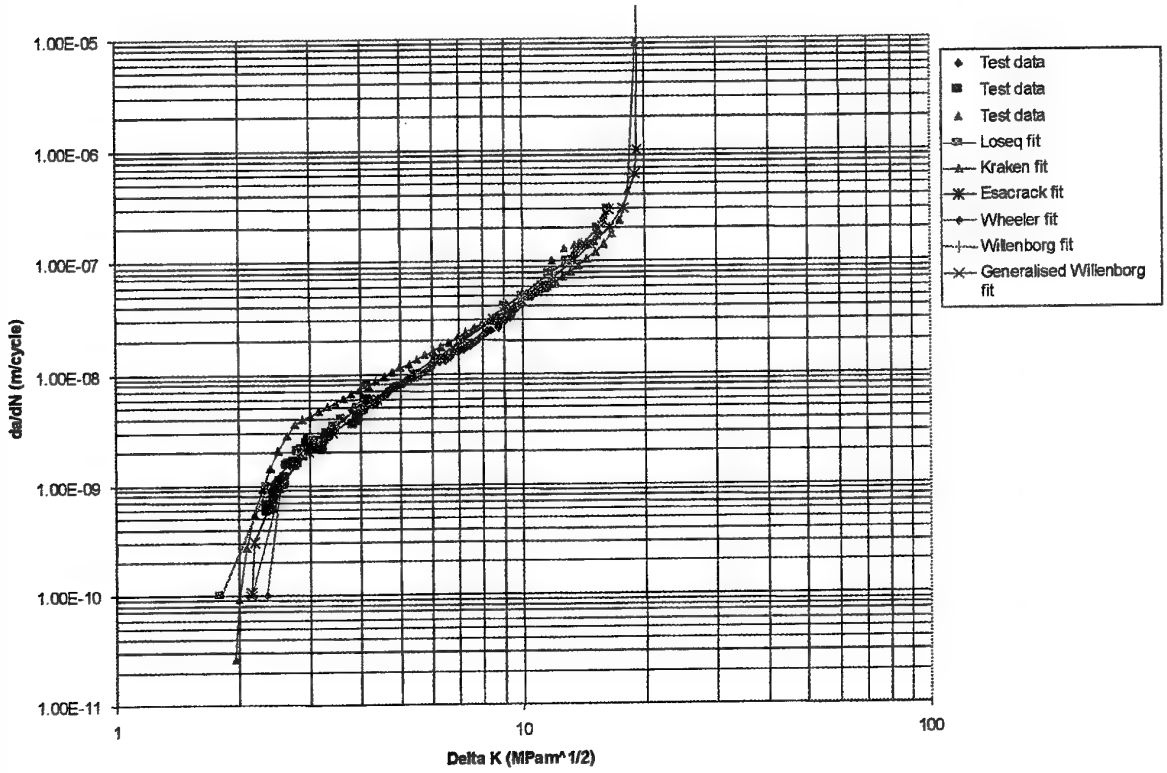

Figure 6 Crack growth data fits – Titanium R = 0.7

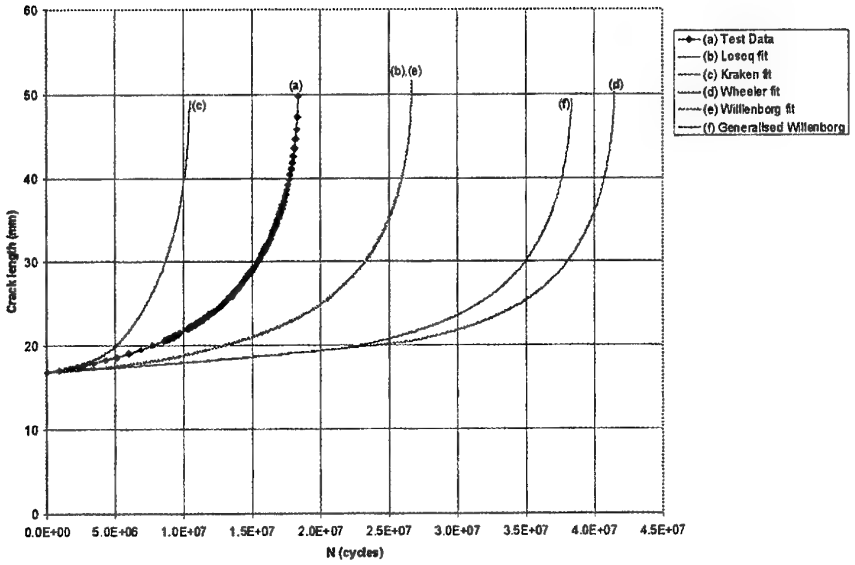

Figure 7 Effect of data fit selections on predicted crack growth for Rotorix 8

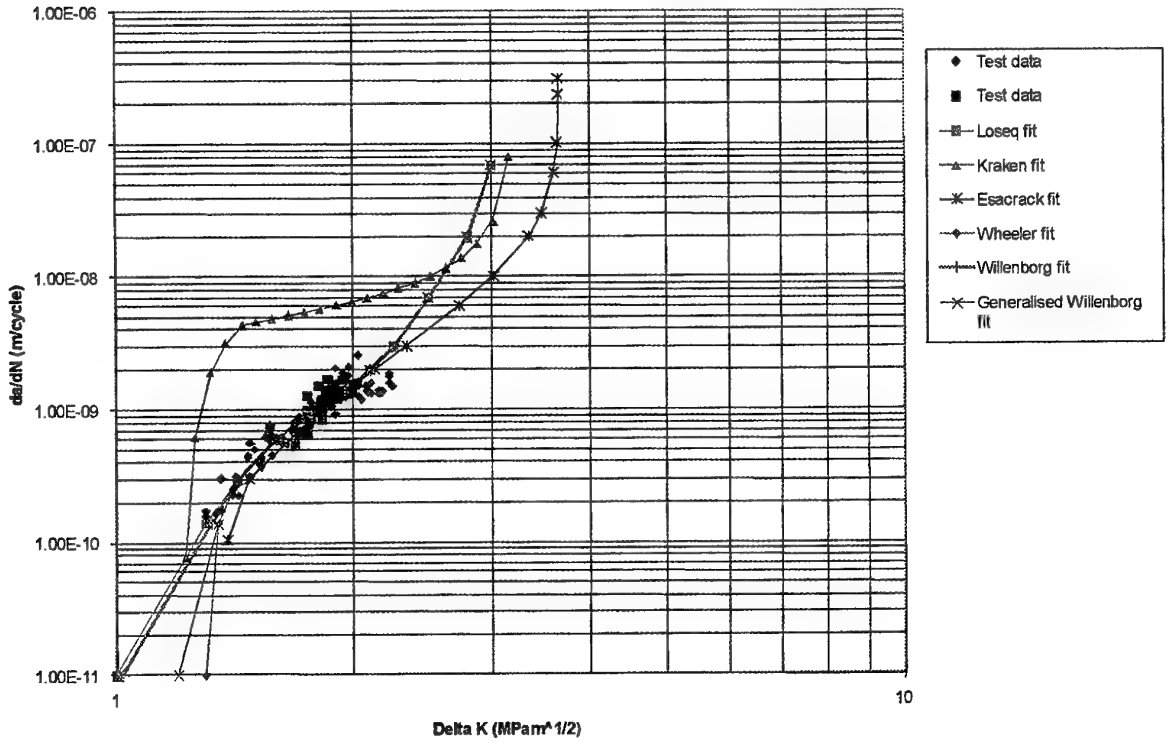

Figure 8 Crack growth data fits Aluminium-Lithium R = 0.9

MATERIAL ALLOWABLES FOR HIGH CYCLE FATIGUE IN GAS TURBINE ENGINES

T. Nicholas
U.S. Air Force Research Laboratory
Materials & Manufacturing Directorate
Wright-Patterson AFB, OH 45433-7817, USA

SUMMARY

HCF failures in materials used in both static and rotating components of gas turbine engines have often been found to be attributable to fatigue loading on materials which have sustained some type of damage. Damage can be present from initial material or manufacturing defects, or can develop during service operation. In-service damage, while not catastrophic by itself, can degrade the HCF resistance of the material below that for which it was designed. Three major sources of in-service damage which can alter the HCF capability individually or in conjunction with one another are low cycle fatigue (LCF), foreign object damage (FOD), and contact fatigue. Other types of damage include creep, corrosion and thermal fatigue. The present design methodology is highly empirical and relies heavily on service experience to establish material allowable knockdown factors for each type of damage. To reduce HCF failures, the U.S. Air Force is developing a damage tolerant approach which addresses these issues in a less empirical manner. The effects of damage on HCF capability and a discussion of the material allowables under HCF are presented.

1. INTRODUCTION

The high incidence of HCF related failures over the past several years in U.S. Air Force gas turbine engines, combined with the substantial maintenance costs and potential detrimental effects on operational readiness, have led the Air Force to re-evaluate the design and life management procedures for HCF. In attempting to assess the root cause of HCF failures and find methods for reducing the incidence of such failures, the relatively empirical nature of the procedures now in place becomes abundantly clear. Further, the lack of detailed information on vibratory loading and dynamic response of components as well as material capability under HCF, particularly in the presence of initial or in-service damage, makes anything but a highly empirical approach impractical at this time. To address these shortcomings, the U.S. Air Force initiated a National High Cycle Fatigue Program to develop a technology base for implementation of damage tolerance procedures for HCF in gas turbine engines. This paper focuses on the material capability aspects of the damage tolerant approach for design and life management of components subjected to HCF.

2. DAMAGE TOLERANCE

The natural tendency in the implementation of a "damage tolerant" approach to fatigue would be to relate remaining life based on predictions of crack propagation rate to inspectable flaw size. In LCF, this has been shown to work well, and such an approach was adapted by the U.S. Air Force in 1984 as part of the ENSIP Specification [1]. For HCF, direct application of such an approach cannot work for "pure" HCF because required inspection sizes are well below the state-of-the-art in non-destructive inspection (NDI) and the number of cycles in HCF is extremely large because of the high frequencies involved. Whereas LCF involves early crack initiation and a long propagation life as a fraction of total life, pure HCF damage is rarely observed in service or even in the laboratory and occurs only very late in life. It is therefore impractical to apply the damage tolerant approach as used for LCF to pure HCF. While considerable research is being conducted at the present time to identify and detect HCF damage in the early stages of total fatigue life, damage tolerance seems out of the question at present for HCF. However, the problems which arise in the field are generally not related to the lack of knowledge of material capability under pure HCF. Rather, the problems fall into two main categories. First, and foremost, is the existence of vibratory stresses from unexpected drivers and structural responses which exceed the material capability as determined from laboratory specimen and sub-component tests. Design allowables are normally obtained on material which is representative of that used in service including all aspects of processing and surface treatment and are often represented as points on a Haigh or "Modified Goodman diagram". (This point is qualified in the following paragraph.) The second category involves the

Paper prepared for the RTO AVT Specialists' Meeting on "Application of Damage Tolerance Principles for Improved Airworthiness of Rotorcraft", held in Corfu, Greece, 21-22 April 1999, and published in RTO MP-24.

introduction of damage into the material during production or during service usage. The three most common forms of damage, either alone or in combination, are LCF cracking, foreign object damage (FOD), and contact fatigue. To account for this damage, or to design for pure HCF, the concept of a threshold below which HCF will not occur is necessary because of the potentially large number of HCF cycles which can occur over short service intervals. This is due to the high frequency of many vibrational modes, often extending into the KHz regime. In fact, current design for HCF through the use of a Haigh diagram seeks to identify maximum allowable vibratory stresses so that HCF will not occur in a component during its lifetime. The current ENSIP specification requires this HCF limit to correspond to 10^9 cycles in non-ferrous metals, a number which is hard to achieve in service and even harder to reproduce in a laboratory setting. Consider that a material subjected to a frequency of 1 KHz requires nearly 300 hours to accumulate 10^9 cycles.

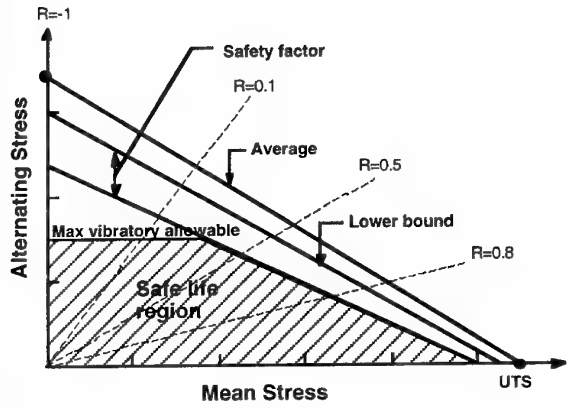

Fig. 1 Constant life diagram.

3. HCF MATERIAL ALLOWABLES

The diagram most used for design purposes in HCF is a constant life diagram as illustrated in Fig. 1, where available data are plotted as alternating stress as a function of mean stress for a constant design life, usually 10^7 or higher. This diagram, which should correctly be called a Haigh diagram, is commonly and incorrectly referred to as a Goodman diagram or a Modified Goodman diagram [2]. In the absence of data at a number of values of mean stress, it is often constructed by connecting a straight line from the data point corresponding to fully reversed loading, R=-1, with the ultimate tensile strength (UTS) of the material. Alternatively, the yield stress is used as the point on the mean stress axis. Data at R=-1 can be obtained readily from a number of techniques using shaker tables to vibrate specimens or components about a zero mean stress, while data at other values of mean stress are often more difficult to obtain, particularly at high frequencies. Alternatives to the straight line approximation in Fig. 2 involve the use of various curves or equations going through the yield stress or UTS point on the x-axis, or through actual data if available, to represent the average behavior. Scatter in the data can be handled by statistical analysis which establishes a lower bound for the data. On top of this, a factor of safety for vibratory stress can be included to account for the somewhat indeterminate nature of vibrations, particularly those of a transient type. Finally, design practices or specifications may limit the allowable vibratory stress to be below some established maximum value, independent of the magnitude of the mean stress. The safe life region, considering all of these factors, is shown shaded in Fig. 1. What this region provides, therefore, is an allowable threshold vibratory stress as a function of mean stress, the latter being fairly well defined because it is closely related to the rotational speed of the engine. If the vibratory stress is maintained within the allowable region on the Haigh diagram, there should be no failure due to HCF and, further, no periodic inspection required for HCF. Provided that the maximum number of vibratory cycles experienced in service does not exceed the number for which the Haigh diagram is established, 10^9 for example, then such a design procedure is one of "infinite" life requiring no periodic inspection.

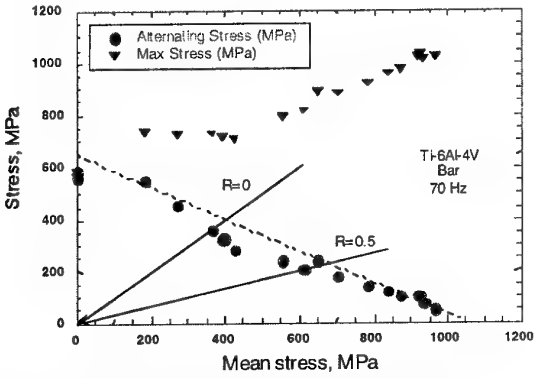

Fig. 2 Haigh diagram for Ti-6Al-4V bar.

There are some pitfalls in the use of a Haigh diagram in design, particularly when basing it only on data at R=-1. For example, Fig. 2 shows such a diagram for Ti-6Al-4V hot rolled bar where it can be seen that the straight line for alternating stress does only a fair job of representing the data. In addition to the alternating stress, the peak or

maximum stress is also shown. For high values of mean stress, the maximum stress is quite high, approaching the static ultimate stress of 1030 MPa for this material. Recent research on fatigue life at high mean stresses [3] has shown that at high mean stress, the fracture mode changes from one of fatigue to one of creep. Thus, in the creep regime, consideration should be given to the amount of time during which such vibrations occur, not only to the number of cycles. Allowable vibratory stresses, while very low in this region, should also be supplemented with consideration of maximum stresses. It is for these reasons that designers shy away from the high mean stress regime, often for reasons that cannot be quantified.

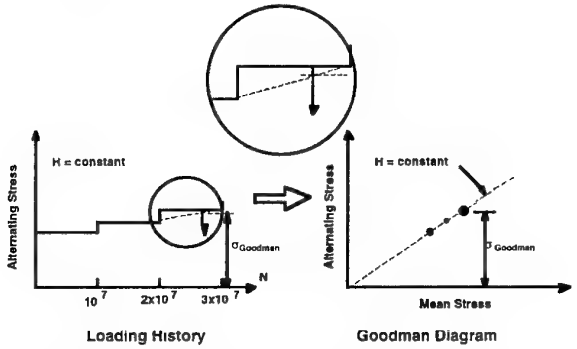

Fig. 3 Schematic of step-loading procedure.

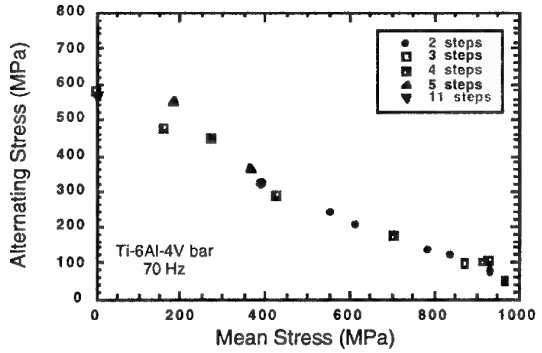

Fig. 4 Haigh diagram illustrating effect of number of steps on fatigue limit.

3.1 Obtaining material allowable data

One of the main concerns in establishing material allowables for HCF is the sparse amount of data available and the time necessary to establish data points for fatigue limits at 10^7 cycles or beyond. The conventional method for establishing a fatigue limit is to obtain S-N data over a range of stresses and to fit the data with some type of curve or straight line approximation. For a fatigue limit at 10^7 cycles, for example, this requires a number of fatigue tests, some of which will be in excess of 10^7 cycles. This is both time consuming and costly. One method for reducing the time is to use a high frequency test machine such as one of those which have appeared on the market within the last several years. In addition, the use of a rapid test technique such as one developed by Maxwell and Nicholas [4] involving step loading can save considerable testing time. It has been shown that such a technique provides data for the fatigue limit which are consistent with those obtained in the conventional S-N manner [4, 5]. The approach is illustrated schematically in Fig. 3 where a constant amplitude fatigue load is applied for a number of cycles corresponding to the number for which the fatigue limit is desired. If no failure occurs within this block of loading, the stress is raised and a second block is applied. The procedure is repeated until failure occurs within a block and the fatigue limit is established by a simple interpolation scheme involving the load levels of the final and prior blocks and the number of cycles in the final block. Data for a Haigh diagram obtained in this manner are shown in Fig. 4 where the number of blocks used for each data point is also indicated. It can be seen that there is no systematic trend for the value of the fatigue limit with the number of blocks. This is just one illustration of many that have shown that the so-called "coaxing" effect, where loading below the fatigue limit strengthens the material, does not exist in the Ti-6Al-4V material tested.

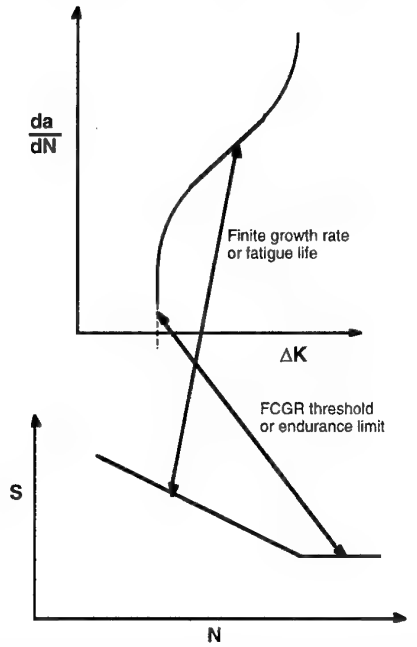

Fig. 5 Schematic illustrating threshold concept in fatigue and crack growth.

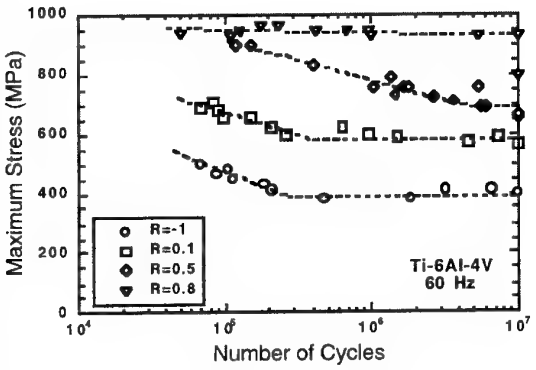

Fig. 6 S-N data at different values of R.

3.2 Threshold concept for HCF

Because of the large number of HCF cycles that may occur in service due to high frequency vibrations in a component, a threshold concept is necessary to insure structural integrity. Whether this threshold involves crack growth rates below some operational threshold, or the use of a fatigue limit corresponding to a large but fixed number of cycles, the concepts involve "infinite life," at least within the number of cycles that may be assumed to occur during the lifetime of a component. These could be either from steady state vibrations or from transient phenomena and would correspond to a different number of total expected cycles in general. The infinite life concept is illustrated schematically in Fig. 5 for crack growth and fatigue. In crack growth, a pre-existing or developed crack should not grow at a rate beyond some threshold rate so that crack extension can be neglected during the expected life of the material. Similarly, for a material without a crack, the stress level has to be maintained below a fatigue limit such that fatigue failure does not occur within an expected number of cycles. If the number of expected cycles can be established, and the crack growth rate and S-N curves can be estimated, then a threshold growth rate and a fatigue limit can be determined which are consistent with each other and account for "infinite" life for the expected number of cycles. In establishing such limits for fatigue, the shape of the S-N curve has to be taken into consideration. As an example, Fig. 6 shows S-N data for Ti-6Al-4V at several values of stress ratio, R. It is to be noted that the slopes of the curves are different, and the transition point where the curves become nearly flat differs depending on the value of R. Therefore, stress ratio becomes an important parameter in establishing the fatigue limit, just as is shown in the Haigh diagram where mean stress is used as the variable to establish allowable alternating stress.

4. DAMAGE CONSIDERATIONS

While methods appear to be available to quantify the fatigue limit of a material subjected to HCF, and to establish a threshold for a crack of an inspectable size, there are still issues remaining over how severe is the damage induced by LCF, FOD or contact fatigue and what material allowables should be used to account for such damage. Other modes of service-induced damage, such as creep, thermo-mechanical fatigue, corrosion, erosion, and initial damage from manufacturing and machining, must also be taken into account in establishing material capability and inspection intervals.

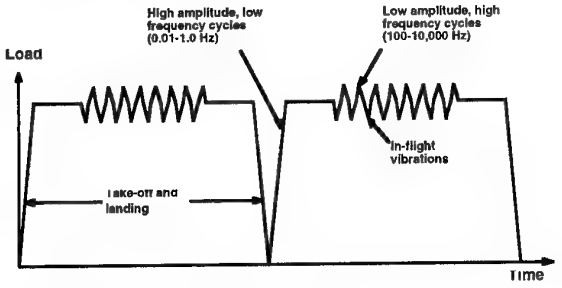

Fig. 7 Schematic of LCF and HCF.

4.1 LCF/HCF interactions

A representative turbine engine spectrum, shown schematically in Fig. 7, contains the simplest version of low and high cycle fatigue loading. The LCF loads or major cycles are those which represent takeoff and landing conditions whilst the HCF or minor cycles represent vibrations during flight. Of concern is what happens if cracks develop in a component due to LCF and then that component experiences HCF. It is important to know how the LCF degrades the fatigue limit, even when the LCF will not cause catastrophic failure by itself. Some preliminary experiments have shown, so far, that this may not be a major issue within the narrow limits of the parameters used in the investigation. Results are presented in Fig. 8 for the fatigue limit on Ti-6Al-4V plate which has been subjected to prior LCF for some fraction of the LCF life which is approximately 10^4 cycles at R=0.1. Under these conditions there is only a slight loss in fatigue limit stress up to 75% of LCF life. Note, however, that LCF life is itself a statistical variable. Much more work has to be conducted to establish LCF damage parameters for assessing remaining HCF life.

Another concern involving LCF is the effect of overloads and underloads on the subsequent HCF fatigue limit as illustrated schematically in Fig. 9.

When the peak stresses or stress ratio, R, of the HCF is different than that of the LCF, it is known from the literature that these prior underloads and overloads can accelerate or retard, respectively, a growing crack in a material compared to constant amplitude crack growth rates. What is not known, however, is whether or not such variable amplitude loading has any effect on the fatigue limit when there is no crack present or in the short crack regime where cracks exist but are too small to detect. This is another area where further work is needed.

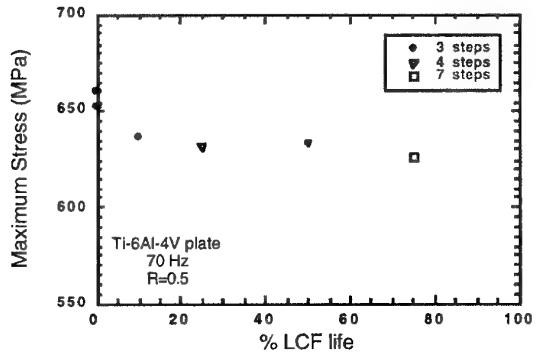

Fig. 8 HCF fatigue limit after applying LCF.

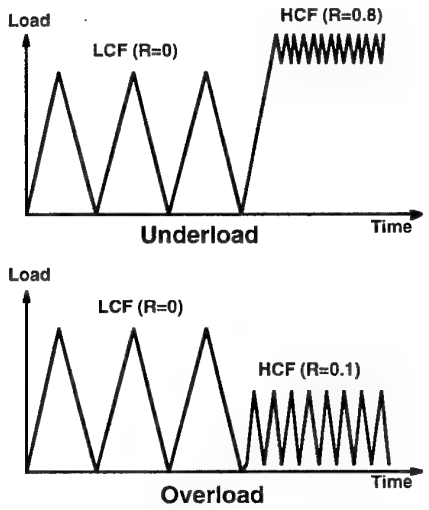

Fig. 9 Overload and underload considerations.

Another aspect to be considered in establishing fatigue limits for HCF is the frequency of loading in the laboratory and the frequencies encountered in vibrating components. Resonant and forced vibrations in engine components can often be in the kilohertz regime whereas laboratory testing is mostly conducted at 100 Hz or less because of equipment limitations. There have been developments over the last several years which have resulted in fatigue testing capability at frequencies up to 2 KHz, and ultrasonic resonant machines have been in existence for several years which have the capability to test typically at 20 KHz. These machines allow for testing at more realistic frequencies for applications and, more important, allow for data to be generated at larger numbers of cycles to failure than conventional machines. The data in Fig. 10 illustrate the capability to establish a fatigue limit corresponding to 10^8 or 10^9 cycles. In this particular case, there is little or no degradation of the fatigue limit when going to such a large number of cycles, but some recent experiments conducted at 20 KHz indicate that the fatigue limit may decrease for such a large number of cycles [6]. Again, this is an area where more work is required.

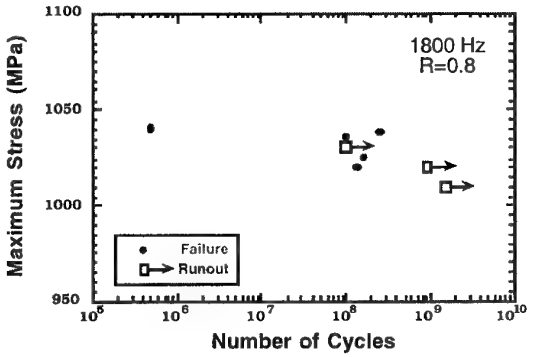

Fig. 10 S-N behavior of Ti-6Al-4V at 1800 Hz.

4.2 FOD and notches

Foreign objects impacting leading edges of rotating blades or static structures can produce damage in the form of notches or tears as shown schematically in Fig. 11. In addition to a geometric discontinuity which may look like a notch, there are residual stresses or strains at the root of the damaging notch from the impact which causes FOD. Whilst data exist on effects of notches on the S-N behavior of a material, there are fewer data on the effects of FOD and hardly any information on any change in the fatigue limit for a material which has been subjected to prestrain or damage due to FOD. Early data on titanium indicates that a tensile prestrain may increase the fatigue limit [7], but recent unpublished results in our laboratory indicate a possible decrease. The effect of precompression is also being investigated.

Attempts have been made to quantify FOD damage in the form of an equivalent K_t, but

relating that to actual material behavior is difficult. First, it is difficult to establish the effective value of K_t, particularly when residual stresses are produced and when small cracks are formed at the tip of the notch. Second, there are an unlimited number of notch geometries involving combinations of depth and radius of notch which will produce the same value of K_t for a given loading condition. Third, while some data exist on the reduction of fatigue life at a given stress due to FOD, there are few data available on the reduction of the fatigue limit, particularly in the very high cycle regime. These "regions of ignorance" are shown schematically in Fig. 11 as dashed lines. Recent work has provided some quantitative results on the fatigue notch factor, K_f (unnotched fatigue limit stress/notched fatigue limit stress) for machined notches in Ti-6Al-4V. Bellows et al. [8] report values of $K_f = 1.8$ and 2.1 for R= -1 and R=0.1 respectively using specimens with a notch having a $K_t = 2.5$ for 10^7 cycles at 60 Hz. Lanning et al. [9] report values of $K_f =$ 2.1, 1.8, and 1.3 for 10^6 cycles for R=0.1, 0.5 and 0.8 respectively, for K_t=2.8 at 50 Hz. If the notch root radius is a measure of the fatigue resistance of the material, then a plot such as Fig. 12 would show some repeatable functional form. For very small radii, for a fixed value of K_f as shown, the value of K_f should approach unity. For a large radius, K_f should approach the value of K_t which is 2.7 for the results shown. The results shown in Fig. 12 show that whatever functional form is used must account for differences depending on stress ratio, R.

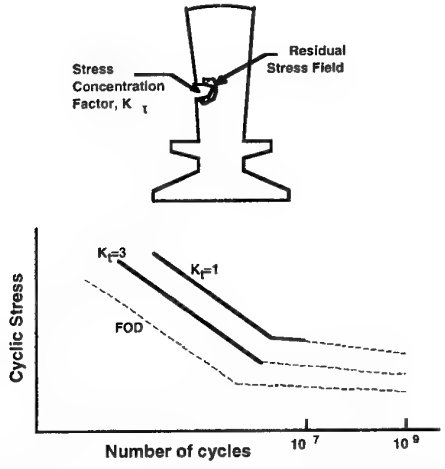

Fig. 11 Schematic of FOD concerns in design.

Data from studies of notch fatigue allow design limits for vibratory stress to be established for notches of a known K_t. But how do these relate to the performance of a material which has suffered FOD from a particle impacting at high velocities? Results for values of the fatigue limit in Ti-6Al-4V have recently been obtained using tension specimens which have a leading edge geometry similar to a fan or compressor blade. Tests on a leading edge (LE) specimen whose LE thickness is 0.75 mm (radius = 0.38 mm) have been conducted by impacting the LE with 1 mm diam. glass spheres at a velocity of 300 m/s and at incident angles between 0° and 60° [10]. Results are shown in Fig. 13 which shows the 10^7 cycle fatigue limit for the various conditions normalized with respect to the undamaged material at 2 values of R. It can be seen that normal incidence, 0°, is the least damaging for these impacts. The worst condition is when the impact angle is around 30° although a large amount of scatter is seen in the data. It is clear that experimental and analytical methods for assessing the extent of FOD damage must consider angle of incidence as an important parameter.

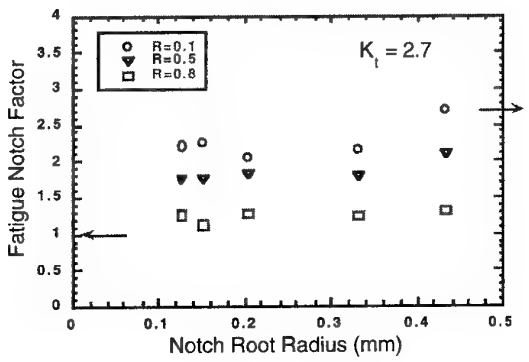

Fig. 12 Fatigue notch factor as a function of radius of notch.

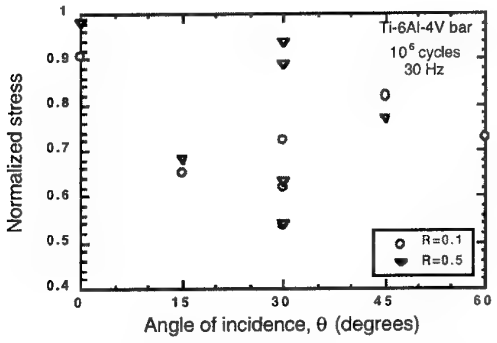

Fig. 13 Effect of incidence angle on fatigue limit of material subjected to FOD.

4.3 Contact fatigue and fretting

Contact fatigue in dovetail joints in the form of fretting is one of the most difficult and one of the

costliest problems in the U.S. Air Force related to HCF. Fretting fatigue occurs when there is small relative motion in the contact region between two surfaces. In the schematic of a dovetail, Fig. 14, it is seen that the contact region involves normal and shear loads as well as bending moments across the interface. In addition to the loads shown, there are axial stresses in both the blade and disk parallel to the contact plane. Superimposed on the loads from the steady centrifugal loading of the blade are vibratory stresses which can result from blade vibrations. Because of the nature of the stress fields in contact regions, there is always a region of relative slip near the edge of contact, shown schematically in Fig. 15. The general problem, therefore, involves normal contact forces, N, tangential contact forces, T, axial loading of the material, P, regions of stick and slip, and a relative displacement in the slip region. Depending on the magnitude of this relative motion and the stress fields produced by the steady and vibratory stresses, fretting fatigue can occur near the edges of the contact region. Whether fretting fatigue is due entirely to the relative motion, or whether the complex stress field contributes significantly to the process, is still debated. Nonetheless, laboratory experiments and field usage demonstrate that fretting fatigue can reduce the HCF material capability significantly.

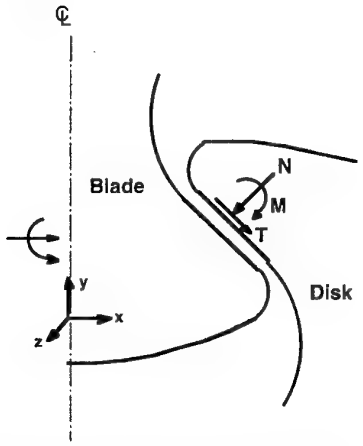

Fig. 14 Schematic of a dovetail region.

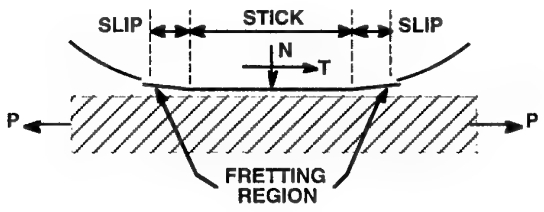

Fig. 15 Schematic of loads in contact region under fretting fatigue conditions.

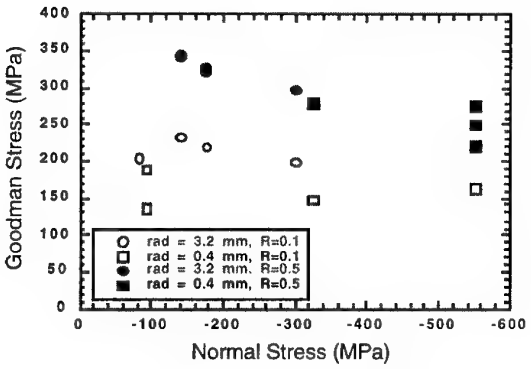

Fig. 16 Fatigue limit stresses under fretting.

Results for the fatigue limit stress corresponding to 10^7 cycles for specimens held in a fretting pad fixture [11] are presented in Fig. 16. The data shown represent the maximum stress, denoted by "Goodman stress", for tests conducted at two stress ratios using fretting pads with two different radii at the edge of contact. The data are plotted against the average normal (clamping) stress of the pad on the specimen. For comparison purposes, typical Goodman stress values for the Ti-6Al-4V used as the specimen and pad material are 600 and 825 MPa for R=0.1 and R=0.5, respectively. It can be seen from the figure that the values under fretting conditions are significantly lower than for the unfretted material. To quantify the reduction in fretting capability, an average knockdown factor (KF) is calculated as the unfretted fatigue limit stress divided by the fretting fatigue limit stress. This definition is similar to the one used for notches, K_f. Results to date conducted under limited conditions have shown that the larger contact radius produces the larger value of KF for both values of R=0.1 and 0.5. Second, tests at R=0.1 produce a higher value of KF than those conducted at R=0.5. While these trends and corresponding values of KF are significant and should be taken account of in design, there appears to be no systematic change in Goodman stress with value of clamping stress over the range of clamping stresses which cover roughly a factor of six as seen in Fig. 16. The authors conclude tentatively that the normal stress may not have much affect on the relative slip length in the contact region, but clearly more work has to be done to quantify all such effects. These results show, however, that use of a single factor of safety on the allowable alternating stress in a Haigh diagram, a procedure that has been used in design more than once, is not a rational approach and may be non-conservative for some contact stress conditions if the factor of safety is obtained

empirically for one specific condition. It should be pointed out that the values for KF range from 2.6 to 4.2 for the limited range of conditions studied.

5. HCF DAMAGE TOLERANCE

The ultimate goal is to be able to design for HCF in the presence of any type of damage or service usage which degrades the properties of materials under HCF loading. The concept is illustrated in Fig. 17 which shows, schematically, some type of damage which might affect material capability. Such damage state, denoted by D, will have a design life which is some fraction of the actual life under those conditions. The damage may be a continually increasing function, such as LCF, or may be a step function such as FOD. In either case, the material would be removed from service for cause (inspection) or because the design life is reached. Just prior to removal, the material has its least resistance to HCF. A damage tolerant design should address the HCF capability under the most severe and probable damage state, shown schematically in Fig. 17 as the critical damage state. Various approaches to implementing such an approach are discussed in the following sub-sections.

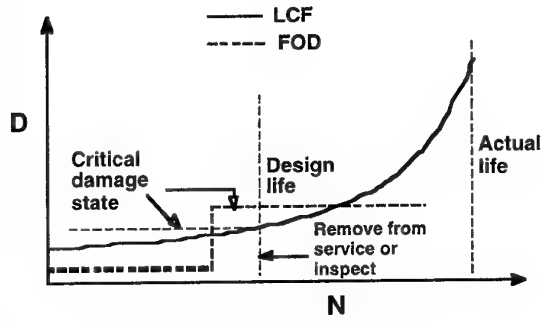

Fig. 17 Schematic of damage tolerance considerations in material allowables.

5.1 Crack growth thresholds

For damage in the form of cracks, from LCF, FOD, or fretting fatigue, the use of a fracture mechanics threshold to determine the allowable vibratory stress seems to be a promising approach for HCF, and follows the concept now being used successfully for LCF. Provided that an inspection can be made, and crack lengths measured, knowledge of the threshold for crack propagation can be used to assess the susceptibility of the material to HCF crack propagation. If the stresses are maintained below this limit, and the limit corresponds to a sufficiently low growth rate, perhaps 10^{-10} m/cycle or lower, then safe HCF life is assured. The potential growth of such cracks under LCF, and the time interval where such growth produces a crack where HCF might occur, must also be considered. This would establish the required inspection interval. One key issue in this proposed scenario is the determination of a suitable threshold for the types of cracks which may occur in service, some of which could be quite small. Various types of loading conditions can be used to determine a threshold, most of which are for long cracks.
Fig. 17 Schematic of damage tolerance considerations in material allowables.

6. CONCLUDING REMARKS

Damage tolerant approaches for HCF are still in the development stage. Whatever their final form, it seems clear that they will involve the use of a threshold concept, a criterion for a smooth or damaged material below which HCF will not occur. The criterion could be in the form of a stress or a stress intensity. From a maintenance and life extension point of view, it is important to be able to quantify the level of damage that may be present from other than HCF, such as from LCF, FOD, or fretting. This may be accomplished by inspection, analysis, probabilistics, or some combination of these. In addition, methods need to be established to predict the growth or extension of any such damage so that material capability limits are not exceeded before the next inspection or the component is removed from service.

7. REFERENCES

1. Engine Structural Integrity Program (ENSIP), MIL-STD-1783 (USAF), 30 November 1984.

2. Sendeckyj, G.P., "History of Constant Life Diagrams," High Cycle Fatigue of Structural Materials, T.S. Srivatsan and W.O. Soboyejo, Eds., TMS, 1998, pp. 95-107.

3. Morrissey, R.J., McDowell, D.L. and Nicholas, T., "Frequency and Stress Ratio Effects in High Cycle Fatigue of Ti-6Al-4V," Int. J. Fatigue, 1999 (special issue on HCF); see also Morrissey, R.J., "Frequency and Mean Stress Effects in High Cycle Fatigue of Ti-6Al-4V", WL-TR-97-4100, Wright-Patterson AFB, OH, 1997.

4. Maxwell, D.C. and Nicholas, T., "A Rapid Method for Generation of a Haigh Diagram for High Cycle Fatigue," Fatigue and Fracture Mechanics: 29th Volume, ASTM STP 1321, T.L. Panontin and S.D. Sheppard, Eds., American

Society for Testing and Materials, 1999, pp. 626-641.

5. Bellows, R.S., Muju, S. and Nicholas, T., "Validation of the Step Test Method for Generating Haigh Diagrams for Ti-6Al-4V, "Int. J. Fatigue, (special issue on HCF).

6. Nishijima, S. and Kanazawa, K., "Stepwise S-N Curve and Fish-Eye Failure in Giga Cycle Fatigue," Conference on Fatigue in the Gigacycle Regime, Paris, France, June 1998.

7. Romualdi, J.P. and D'Appolonia, E., "Effect of Range of Stress and Prestrain on the Fatigue Properties of Titanium," Proceedings of the ASTM, Vol. 54, 1954, pp. 798-815.

8. Bellows, R.S., Bain, K.R. and Sheldon, J.W., "Effect of Step Testing and Notches on the Endurance Limit of Ti-6Al-4V," Mechanical Behavior of Advanced Materials, MD-Vol. 84, D.C. Davis, et al., Eds., ASME, New York, 1998, 27-32.

9. Lanning, D., Haritos, G.K. and Nicholas, T., "Notch Size Effects in HCF Behavior of Ti-6Al-4V," Int. J. Fatigue, 1999 (special issue on HCF).

10. Ruschau, J., Thompson, S. and Nicholas, T., "Effects of Simulated FOD on Fatigue Strength of Ti-6Al-4V," presented at 4th National Turbine Engine High Cycle Fatigue Conference, Monterey, CA, 9-11 Feb. 1999.

11. Hutson, A. and Nicholas, T., "Fretting Fatigue of Ti-6Al-4V Under Flat on Flat Contact," Int. J. Fatigue, 1999 (special issue on HCF).

Damage Tolerance Characteristics of Composite Sandwich Structures

L. Lazzeri
Department of Aerospace Engineering
University of Pisa
Via Diotisalvi 2 - 56126 Pisa
Italy

U. Mariani
Head, Fatigue Office
Agusta S.p.A.
Via G. Agusta, 520 – 21017 Cascina Costa (VA)
Italy

SUMMARY

Current damage tolerance requirements impose strict constraints on the design of composite aircraft structures, since the various forms of defects taken into consideration must show 'no-growth' characteristics in the environmental and loading conditions expected in the operative life.

A research activity was carried out by Agusta, in collaboration with the University of Pisa, with the purpose of assessing the damage tolerance characteristics of typical composite sandwich structures used by the helicopter industry. A particular effort was dedicated to the study of delamination growth under compression loading, a basic step for understanding the damage tolerance behaviour of composite structures. The results of the numerical analysis carried out show that G, the Strain Energy Release Rate, is a suitable parameter for describing the behaviour of the delamination, but it is essential to consider its partition according to the fundamental modes.

1. - INTRODUCTION

Sandwich structures have been in the past, and are still at present, widely used in most aircraft and helicopter design, due to their inherently high specific strength and stiffness. This structural configuration is particularly efficient in the range of low load intensities, [1], and the interest for its application has grown since advanced composite materials have become commonly used for the thin skins. A milestone contribution to the understanding of sandwich design was given by Plantema, [2]. Further development has taken place in recent years, particularly as far as manufacturing technology and the delicate problem of fittings is concerned; it is worthwhile mentioning the recent review of design problems carried out by Zenkert, [3].

A sandwich composite structure may show many different failure modes for the skin and the core, which must be taken into account in the design phase: intralaminar and interlaminar matrix failures, fibre failures, global buckling, face wrinkling, shear crimping and core fracture. The problem becomes even more complex, if possible, when a prescribed load capability in the presence of manufacturing defects or impact damage must also be assured, as required by current Airworthiness Regulations, [4]. Usually, compliance with such Requirements is accomplished through the development of the so-called building block approach or pyramid of tests, [5-6]: a very large test program is devised and carried out, with hundreds of tests at coupon level (to produce a consistent data base and to define material allowables, also keeping environmental conditions into account), dozens of tests at element level (to verify the analysis methodology used for the strength evaluation of the different structural elements and to assess the variability of composite materials properties), and, finally, a reduced number of tests at subcomponent or component level. These kinds of tests are carried out not only to verify load paths and design methodologies, as well as static and fatigue strength and stiffness, but also to substantiate the acceptability of the maximum manufacturing discrepancies and the no-growth of the Barely Visible Impact Damage (BVID), whose relevant energy levels are determined in a specific preliminary activity.

The conclusion is that, due to the lack of reliable theoretical tools, the industries are more or less forced, for the design of primary composite structures, to use rather conservative strain allowables, obtained by means of the abovedescribed extensive test campaigns, a very expensive and time-consuming procedure.

The present paper summarizes the main results obtained by Agusta and the Department of Aerospace Engineering of the University of Pisa in a collaboration carried out within the framework of a wide research program, funded by the European Community. The main purpose of the research program was to obtain experimental data about the residual strength and residual fatigue life of damaged (impact and delamination) composite components. Such data is useful not only to assess the damage tolerance behaviour of selected configurations of practical interest, but also to verify the potentialities and capabilities of available analytical tools. Indeed, the results obtained are quite interesting, since they show that the very stringent no-growth requirement of current Airworthiness Regulations [4] can be, in certain circumstances, relaxed.

2. - DESCRIPTION OF THE RESEARCH PROGRAM

The purpose of this research was to increase the understanding of the damage tolerance behaviour of composite sandwich structures, which are inherently very susceptible to impact damage, [7], using experiments and analytical studies,

Paper presented at the RTO AVT Specialists' Meeting on "Application of Damage Tolerance Principles for Improved Airworthiness of Rotorcraft", held in Corfu, Greece, 21-22 April 1999, and published in RTO MP-24.

with the long term objective of developing reliable analysis methodologies.

Agusta has a wide experience in the field of the certification of composite structures; as an example, the Tail Unit of the EH-101 helicopter is made of a composite skeleton covered by sandwich panels, which were the object of a wide test activity during the certification process. The civil version of this helicopter was certified as a Safe Life structure, including BVID discrepancies, according to FAA AC 20-107A. The approach followed by Agusta in the certification process, described in [8-9], is in accordance with the building block approach or the pyramid of tests, but there was considerable interest in the assessment of damage tolerance capability, both on the part of Agusta/Westland and on that of the Airworthiness Authorities. It seemed therefore reasonable to carry out the major part of the tests of the present research using some specimen configurations which were developed by Agusta within the EH-101 Safe Life certification program, so that the test results could also be evaluated by means of a comparison with other meaningful data.

For this purpose, three different specimen configurations were used, all of them with the same core material but with differences in core thickness and in the lay-up of the skins. For the sake of brevity, in the present paper the panel configurations will be called A, B and C. All the specimens were manufactured by Agusta, using only one batch of material: the honeycomb core was made of Nomex, Euro-Composites ECA 3.2-48 (1/8"-3.0), while the material used for the skins was unidirectional carbon/epoxy Cyanamid 985-GT6-135 or fabric 985-GF3-5H-1000. Fig. 1 shows a drawing of a typical panel. The specimens are representative of parts of the real structure of the EH-101 Tail Unit, and they all have the peculiarity of having different thicknesses and lay-ups for the two skins, i.e. the complete panel is neither symmetrical nor balanced; table I summarizes the different lay-ups for the three configurations (outer and inner refer to the helicopter Tail Unit).

In the present research, attention has been focused on the evaluation of the effect of impact damage and on the assessment of delamination growth, under static and fatigue load conditions. Two types of damage were considered:
(i) impact damage, using different energy levels and impactor diameters, in order to assess the fatigue behaviour in the presence of BVID and Clearly Visible Impact Damage (CVID);
(ii) artificial delamination, introduced during manufacturing by means of a teflon insert at a given interface between the plies (only panels of type A and C).

The impact energy to be utilized was assessed by means of an analysis/evaluation of the frequency and severity of the possible hazards to which the structure was expected to be exposed, both in the production phase and in the operative life.

Impact damage was inflicted on the panels by means of the drop weight procedure. The energy level capable of producing BVID was assessed by means of appropriate susceptibility tests; both painted and unpainted panels were used for this purpose, in order to take into account the worst case of accidental damage during the manufacturing process and in service. BVID was assumed to be the impact damage visible from a distance of 1 meter. All the impacts were inflicted at the centre of each panel, on the thicker skin, since this is the outer skin of the real structure and therefore it is more likely to be accidentally impacted in service. The panel was supported at the edges for closer simulation of the in-service condition.

For a more complete information, some Clearly Visible Impact Damage (CVID) was also introduced; two types of CVID were studied: one obtained by using the same hemispherical impactor but increasing the BVID energy by 50%, the other using a pyramidal impactor, simulating a tool box, with the same BVID energy but obviously introducing CVID.

The second type of defect examined, the teflon insert, has two purposes: first, it is a rough and very simplified modelling of the damage introduced by impact; second, the evaluation of residual strength capability in the presence of delamination is particularly important in order to assess the tolerance of manufacturing defects, since many such defects (porosity, foreign object inclusion, ..) can be considered to be equivalent to a simple delamination.

In conclusion, the experimental activity comprised the following types of tests, classified according to the type of defect:
(a) static and fatigue tests (Constant Amplitude, Compression-Compression, R=5) on impact damaged specimens, using different energy levels and impactor geometry;
(b) static and fatigue tests (as before) on panels with an artificial delamination in the form of a teflon strip, as wide as the whole panel width;
(c) static and fatigue tests (as before) on panels with a circular teflon insert, in the centre of the specimen.

Moreover, tests on Double Cantilever Beam (DCB) and End Notch Flexure (ENF) standard specimens were carried out to assess the threshold and critical values of G, the Strain Energy Release Rate, for modes I and II.

Tab. II shows the different types of panels and defects included in the whole test program. The tests on type C specimens, with teflon inserts, were carried out at Pisa, while all the other tests were performed by Agusta.

3.- EXPERIMENTAL METHODOLOGY

3.1 Test apparatus

Servo-hydraulic actuators were used, of a load capacity of +/- 150 KN, and a stroke of +/- 15 mm. Since the panels were not symmetrical, particular attention had to be paid to the anti-buckling guides, as compression was unavoidably accompanied by bending. Experimental and also numerical analyses were carried out at the Department of Aerospace Engineering of Pisa in order to assess the possible influence of the geometry of the anti-buckling guides on the strain distribution in the panel: two different solutions were studied, one which provided support on the panel edges along a surface (L-shaped guides) and another which used two cylinders, each one constraining a single line of the specimen. The differences were negligible and all the tests done by Agusta were carried out with the L-shaped guides, while in all those carried out at Pisa University the cylindrical guides were used.

3.2 Non Destructive Inspection

After manufacturing, all the sandwich panels were inspected by means of a through-transmission UltraSonic technique in order to assess their integrity and compliance with standard Agusta production quality. After that impact damage was introduced, the extension of damaged area was assessed by means of U.S. inspection; an attenuation greater than 6 dB was assumed as a criterion for identification of damage.

3.3 Test procedure

All the tests were carried out in load control, considered to be representative of the operative conditions. A number of static test specimens were fitted with a particularly high number of strain gauges, in order to provide detailed information about

strain distribution. For all the other specimens, two couples of strain gauges, bonded back-to-back, were used: the first couple was positioned in the axial, vertical centreline, at a distance from the top equal to a quarter of the panel height (sufficiently far from the defect), and the other couple was bonded on the horizontal centreline, at a distance from the lateral free edge equal to a quarter of the panel width. The strain measured on the thick skin (the outer one) in this location was conventionally used to assess the stiffness of each panel and to define the fatigue loading. In the case of the teflon strip defect, the other strain gauge location was obviously used.

During the tests on delamination growth, carried out in Pisa on type C panels, the specimens were inspected in situ by means of U.S., using a contact probe and a gel as a couplant. Such an inspection was carried out by means of the pulse-echo technique, setting the instrument in such a way as to reveal the echo of the U.S. wave in its path back to the front skin, passing through the lateral walls of the Nomex cells; therefore, a fairly jagged delamination front was sometimes observed.

In the static tests, the specimen was loaded in steps, and after each step an U.S. inspection took place for the evaluation of delamination growth.

The delamination growth was measured, in the fatigue tests carried out in Pisa, at a prescribed number of cycles, while in all the tests carried out by Agusta, global damage was evaluated by continuously measuring the residual stiffness, by means of a LVDT, fixed to bonded brackets on the thick side.

In some cases, the end shortening and the maximum out-of-plane displacement under a given applied load were also measured, in order to obtain useful information for the calibration of the numerical models.

4. - TEST RESULTS

4.1 Fatigue behaviour of damaged specimens

Three different types of panels were used, as described above, to which different types of damage were introduced. The relevant S-N curves, based on about 20 tests each, in RTD conditions, are shown in figs. 2, where the maximum cyclic strain applied is divided by a reference strain value derived in compression static tests on integer specimens. For all the types of specimen, about 10 further specimens were tested in RTW (84% R.H.), after ageing up to saturation at 70° C and 84% R.H., in order to confirm the curve shape and to derive the knockdown factor due to humidity alone.

Fig. 2a concerns type A specimens, all tested by Agusta, and shows a relatively flat curve. For further investigation, specimens with a teflon disk insert (30 mm diam.) in the thick skin were also tested. The static strength of the BVID specimens and that of the teflon insert panels are quite similar, while the CVID specimens show a reduction both in the static strength, as could be expected, and in the fatigue strength. The results of the RTW tests, not reported, show a negligible environmental effect.

Fig. 2b shows the results of type B specimens, again all tested by Agusta; this time, with a greater thickness of the impacted skin, the CVID fatigue results are in the scatter band of the BVID specimens, while the reduction of the static strength is still considerable. In this case, too, the effect of the environmental conditioning (not reported) is quite small.

It is particularly interesting to observe the type C panel results, shown in fig. 2c, since they refer to a wider set of defects. As far as impact damage is concerned, the severity of the damage proved to have a large influence on static strength, giving evidence of the well-known notch sensitivity of composite materials. As far as the fatigue strength is concerned, even if few CVID results are available, the same observation made for the B specimens can be confirmed; it should be kept in mind that A specimens had the thinnest skin, about half of B and C configurations. The second type of defect, the teflon insert, allows us also to assess the effect of a weak bonding at the interface between skin and core, which proves to be the most detrimental from the fatigue point of view, while static strength is not affected to the same extent.

The fatigue results of impact damaged specimens fall in the middle of the two types of artificially delaminated panels; the average measurement of the damaged area for BVID panels was about 1200 mm^2, that is about twice the area of the 30 mm diam. disk, but also about five times less than the strip defect area.

In figs. 2 the test results, relevant to BVID panels, are fitted by a four parameter non-linear curve shape of the type:

$$S = S_1 + A * (N+C)^{-B}$$

where S_1 is the endurance limit (conventionally assumed to be at 10^9 cycles), N is the number of fatigue cycles and A, B, and C are parameters determined by fitting the test data.

4.2 Observations about delamination growth

In the static and fatigue tests carried out in Pisa on type C panels, information was also collected concerning delamination growth. The teflon insert was placed between the fifth and the sixth ply from the outside of the thick skin, thereby obtaining an outer sub-laminate $[0_2, +45, -45, +45]_T$ and leaving an inner sub-laminate $[0_3]_T$ in contact with the core.

An example of the evolution of the strip defect in a static test is shown in fig. 3, where the different positions of the delamination front over the panel width are shown for different loads. Similarly, a stable subcritical growth is also observed for the teflon disk specimens, which was much smaller in dimension and with a pronounced tendency towards preferential directions, i.e. a non homothetic growth. An example is shown in fig. 4. In both cases, out-of-plane displacement of the delaminated plies and panel end shortening were measured, in order to obtain useful data to calibrate the numerical models.

In fatigue tests, delamination grows to a much larger extent than in static tests, and the trend concerning the shape that emerged from the static tests finds a much clearer confirmation. Typical examples of the delamination growth at different number of cycles are shown in fig. 5 for the teflon strip specimens and in fig. 6 for the teflon disk specimen: in the last case, there is clearly an evolution towards a stable configuration of the delamination, a sort of butterfly shape.

Another interesting observation concerns the considerable influence of the occurrence of buckling on fatigue delamination growth: when buckling does not occur, the growth is negligible. At the very beginning of the series of tests on circular insert panels, a large scatter was observed in terms of applied strain versus life, with short lives associated with occurrence of buckling and long lives with no buckling occurrence, with a faint correlation with the applied cyclic strain level. Similar experimental observations were found in the literature [10-12] and attributed to a sort of vacuum effect, due to the autoclave procedure: in other words, the two sublaminates tried to separate but were restrained from doing so by the presence of a pressure differential, a vacuum, which was a function of the manufacturing quality (the presence of porosity reduces this effect). The problem was solved by drilling a small hole, 0.3 mm in diameter, in the outer sublaminate, in the centre of the teflon disk: the subsequent test results became quite consistent and correlated with strain level.

5. – ANALYSIS OF DELAMINATION GROWTH

If the delamination growth data from the teflon strip specimens are analysed in terms of growth rate vs. delamination length, a relatively "strange" result is obtained: the rate decreases with the dimension of the delamination, over most of the range examined. Fig. 7 shows a collection of such data, for the teflon strip specimen: the trend is quite clear. This behaviour is in contrast with the common experience, since usually, with the sole exception of a few specially designed specimens, under a constant load range applied, an increase in the crack (or defect) dimension is associated with a corresponding increase in the driving force and consequently also in the growth rate.

If the data concerning the circular insert are analysed, a similar, but more complex, situation is observed; as an example, fig. 8 shows what happens on the preferential directions of growth, shown in fig. 6.

These experimental results are quite useful, since they provide the opportunity to evaluate also from a quantitative point of view the models that have been proposed in the literature for the prediction of delamination growth; recent excellent reviews can be found in [13-14].

The use of the Strain Energy Release Rate, G, as the parameter capable of describing interlaminar fracture behaviour in composites, is receiving growing credit by the scientific community. In the present research a Finite Element analysis was carried out, using MSC/NASTRAN, to evaluate the capability of the approach. The problem is quite complex, due to the geometrical non-linearity, associated with the occurrence of buckling, and therefore requires long computing times. In the initial phases of the research, a complete model of the panel was used, adequately refined to obtain the required accuracy in the area of the delaminated plies. The load was introduced by means of a constant displacement on the loaded ends. No initial geometrical imperfection was introduced in the model. Sandwich skins and honeycomb were modelled by solid elements, which have produced better results, i.e. closer to the test results, in comparison with the use of shell elements for the skins. But the limits due to the very high number of degrees of freedom (d.o.f.) required have forced us to abandon the model of the complete panel, and to use a "superelement" (or global-local) approach, i.e. the use of a sub-model of the central region, described with a high number of d.o.f. (one element per layer). A preliminary analysis is carried out on a relatively coarse mesh of the complete structure, for the purpose of evaluating the displacements at the boundary nodes of the superelement; then a second analysis is carried out on the sub-model alone, under such displacements, which were applied in incremental steps. This approach has many advantages:

(a) a more refined mesh is used only for the area involved in the delamination, which requires a detailed description;

(b) the "shear locking" effect, i.e. a fictitious super-shear-stiffness, is reduced.

It must be borne in mind that it is very important to obtain an accurate description of the displacement field, since the evaluation of the contributions to G deriving from the different modes (opening, in-plane shear, out-of-plane shear) is greatly dependent on the out-of-plane displacement of the buckled sublaminate; in particular, the contribution of mode I, which is particularly important for delamination growth, is very sensitive to such a quantity. With the "superelement" approach it is possible to obtain out-of-plane displacement of the buckled sublaminate comparable with the test results.

Once the displacement and strain fields are evaluated, G is computed on the delamination front according to the virtual crack extension technique, [15], which proceeds according to the following steps. From the FEM analysis, by means of an integration routine on the stresses, the nodal forces are evaluated along the delamination boundary. The Multi Point Constraint element of NASTRAN is used for modelling the boundary; the nodes of these elements are then relaxed, thus simulating a growth of Δa. The FEM analysis is then repeated on this configuration, and again the nodal forces and displacements are computed. In this way, with an appropriate release of the various MPC rows along the delamination front, it is possible to evaluate G for any propagation shape. Since the forces along the front before the release are available, together with the nodal displacements after the release, the contributions to G according to the different fundamental modes can be easily evaluated along the delamination front. An 'ad hoc' program has been written in C++ language for carrying out automatically, and in an easy and reliable way, the numerical computations for mode I, II and III contributions. In order to simulate the delamination growth, it was considered appropriate to release the nodes along the crack front all together, because otherwise, when relaxing the nodes one by one, the values of the forces and displacements obtained were so small as to be of the order of numerical errors. Fig. 9a shows the distribution of G_I and G_{II} values in the 2-D specimen, for an applied load corresponding to an experimentally observed arrest of delamination growth. The contribution of G_{III} will not be shown, since it proved to be very small and negligible in comparison with those of the other two modes. If the analysis is repeated for different delamination lengths, a rather rapid decrease in mode I component is observed, while the mode II component increases. This effect explains why the delamination growth rate decreases, since a different mode partition of the total G occurs: the opening mode contribution, which is decreasing, is fundamental for the growth, since it is characterized by a lower resistance, i.e. a smaller threshold value, in comparison with the contribution of mode II. Fig. 9b shows how the points, that describe the overall severity of the solicitation on the delamination front, change their position in the G_I - G_{II} plane, moving towards the stable area as the delamination length increases.

In the case of the circular insert specimen, fig. 10 shows the distribution of G_I along the circular delamination front, obtained from the results of the analysis; it is qualitatively consistent with the directions of maximum growth.

These results confirm that the total value of the Strain Energy Release Rate alone is not a particularly meaningful parameter, but that it is very important to consider its contributions according to mode I and II; similar conclusions can be found in [16] and [17]. An important consequence is that a given delamination, subjected to fatigue loading, may evolve to a final dimension and shape that is a stable configuration; in other words, the applied load produces, along the delamination front, couples of contributions mode I/mode II to G that are globally below the mixed mode threshold for propagation. If this happens, composite structures can show interesting damage tolerance characteristics, at least when the defect is a simple delamination. Further research is therefore required, particularly to assess the delamination behaviour in realistic mixed mode conditions, both for what concerns the growth under fatigue loading and the fracture under static load conditions. There is an increasing interest in developing Mixed Mode test specimens and procedures, in order to fully characterize the resistance of a material to interlaminar fracture, considering also interaction between the two fundamental modes. In this respect, the Mixed Mode Bending test, developed by NASA [18-19], is the one that receives most credit, among others, by the composite community. The same authors have also proposed an interactive failure criterion for mixed-mode delamination, [20].

Within the framework of the present research, Agusta carried out Fracture Mechanics tests on DCB and ENF coupons, assessing the critical and threshold G values (for a stress ratio of 0.1) for pure mode I and pure mode II conditions: figs. 11 show the results. It is interesting to compare these values with the results of a very complex numerical analysis, carried out to evaluate the G distribution along the delamination contour of a "butterfly" stable delamination. Such results are shown in fig. 12, where it is observed that the contributions show preferential directions, where they are larger, i.e. the preferred directions of growth. But it is interesting to note that the numerically assessed peaks are just lower than the threshold values reported in figs. 11, particularly for mode I; slight differences in the R ratio (0.1 in the coupon tests and 5, symmetric to 0.2, in the sandwich panels) in this context can be neglected.

The results shown are quite interesting: the numerical approach is complex, non linear, needs to be calibrated with some experimental results, but can offer a powerful tool for evaluating the potential growth of delaminations under compression loading, both of a static and of a fatigue nature.

Another significant observation is related to the test methodology for defining threshold G values; two possibilities exist: to determine the "propagation arrest" or the "no onset of propagation" condition. The latter is usually preferred, since it is closer to the current damage tolerance design requirement, and, besides, testing is simpler and the fibre bridging problem is not meaningful, even if more specimens are required, while the "propagation arrest" procedure requires particular care, in the same way as a load shedding technique does, since the previous load history may influence the result. On the contrary, on the basis of the remarks made above, the "propagation arrest" technique seems to be preferable.

One last remark: in the full scale test of the EH-101 Tail Unit certain artificial delaminations showed a small growth, followed by an arrest. This behaviour was initially attributed to the resolution of the NDI method, but the foregoing considerations provide a more sound explanation.

6. - SUMMARY AND CONCLUSIONS

The results of the present research allow us to draw the following conclusions:

(a) impact damage remains by far the most dangerous type of defect for advanced composite materials; the type of damage associated with an impact is very complex and deleterious, since multiple delaminations are activated, in synergetic action with matrix intralaminar cracking and fibre failure;

(b) however, even if simple delamination is not so crucial for structural integrity, the understanding of the mechanisms that govern its growth, as well as the development of models for its analysis, is a significant step towards the solution of many important problems; just to quote one of the most meaningful, it is possible to give an appropriate answer, on a rational basis, to the definition of the maximum allowable defect that can be tolerated in the manufacturing process. There are important safety and economical concerns behind this question;

(c) the current approach, based on the test pyramid, is very time-consuming and expensive; if progresses in understanding the fracture behaviour of composites can reduce the experimental effort, significant economic advantages can be obtained, without reducing safety levels;

(d) a further effort is required to simplify the analythical effort and also in order to examine other load cases, such as the presence of shear stresses.

ACKNOWLEDGEMENT

The authors wish to thank Prof. A. Frediani for valuable discussions and also gratefully acknowledge the contributions given to this paper by the Ph.D. students M. d'Alessandro Caprice and E. Troiani and the final-year students G. Mearelli, S. Campigli and M. Pizzo.

7. - REFERENCES

[1] Gerard, G., 'Minimum weight analysis of compression structures', New York University Press, 1956.

[2] Plantema, F.J., 'Sandwich construction', J. Wiley & Sons, 1966.

[3] Zenkert, D., 'An introduction to sandwich construction', EMAS, Solihull, UK, 1995.

[4] F.A.A. Advisory Circular AC 20-107A, 'Composite Aircraft Structure', April 1984.

[5] Rouchon, J.R., 'Certification of large airplane composite structures - Recent progress and new trends in compliance philosophy', paper ICAS-90-1.8.1, in Proc. 17th ICAS Congress, Stockholm, pp. 1439-1447, 1990.

[6] Whitehead, R.S., 'Certification of primary composite aircraft structures', in "New materials and fatigue resistant aircraft design", Proc. of the 14th ICAF Symposium, Ottawa, D.L. Simpson ed., EMAS Ltd., Warley, pp. 585-617, 1987.

[7] Tsang, P.H.W. and Dugundji, J. 'Damage resistance of graphite-epoxy sandwich panels under low speed impact', J. of the American Helicopter Society, Vol. 37, No. 1, pp. 75-81, Jan. 92.

[8] Guzzetti, G., 'Certification approach and test of the EH-101 composite tail unit', 12th European Rotorcraft Forum, Amsterdam, 1994.

[9] Guzzetti, G. and Castano, D., 'Static and fatigue substantiation of the EH-101 composite tail unit', presented at the 50th Annual Forum of the American Helicopter Design, Washington, 1994.

[10] Gerharz, J.J., Shopfel, A. and Huth, H., 'Correlation between material properties and damage tolerance behaviour of composite structures', in "Durability and structural reliability of airframes", Proc. of the 17th ICAF Symposium, Stockholm, A.F. Blom ed., EMAS Ltd., Warley, pp. 733-58, 1993.

[11] Peck, S.O. and Springer, G.S., 'The behavior of delaminations in composite plates - analytical and experimental results', J. of Comp. Materials, Vol. 25, pp. 907-929, 1991.

[12] Guedra-Degeorges, D., Maison, S., Trallero, D. and Petitniot, J.L., 'Buckling and post-buckling behaviour of a delamination in a carbon-epoxy laminated structure: experiments and modelling', in "Debonding/delamination of composites", AGARD-CP-530, 1992.

[13] O'Brien, T.K. and Elber, W., 'Delamination and fatigue of composite materials: a review', in "Debonding/ delamination of composites", AGARD-CP-530, 1992.

[14] Gädke, M. et al., 'GARTEUR damage mechanics for composite materials: analytical/experimental research on delaminations', in "Debonding/delamination of composites", AGARD-CP-530, 1992.

[15] Tratt, M.D., 'Analysis of delamination growth in compressively loaded composite laminates', in "Composite materials: fatigue and fracture" (third volume), ASTM STP 1110, T.K. O'Brien ed., American Society for Testing and Materials, Philadelphia, pp. 359-372, 1991.

[16] Charalambides, M.N., Kinloch, A.J. and Matthews, F.L., 'Strength prediction of bonded joints', in "Bolted/bonded joints in polymeric composites", AGARD-CP-590, 1996.

[17] Davidson, B.D.: 'A prediction methodology for delamination growth in laminated composites - Part I: Theoretical development and preliminary eperimental results', DOT/FAA/AR-97/87, April 1998.

[18] Reeder, J.R. and Crews, J.H., Jr., 'The Mixed-Mode Bending method for delamination testing' AIAA Journal, Vol. 28, No. 7, July 1990, pp. 1270-1276.

[19] Reeder, J.R. and Crews, J.H., Jr., 'Redesign of the Mixed-Mode Bending delamination test to reduce nonlinear effects', J. of Composite Tech. & Res., Vol. 14, No. 1, Spring 1992, pp. 12-19.

[20] Reeder, J.R., 'A bilinear failure criterion for mixed-mode delamination', in "Composite materials: testing and design", ASTM STP 1206, American Society for Testing and Materials, Philadelphia, pp. 303-322, 1993.

Panel type	Core thick. (mm)	Outer skin	Inner skin
A	12.7	$(0/90)_f$, +45, -45, +45	$(0/90)_f$, -45, +45
B	9.5	0_2, +45, -45, +45, $((-45/+45)_f)_2$	-45, +45, -45, +45
C	12.7	0_5, +45, -45, +45	-45, +45, -45, +45

Table I – Lay-ups of the different panel configurations (f= fabric). The layers are listed from H/C towards the external.

Panel type	Defect
A	BVID, 15 J, impactor 20 mm CVID, 23 J, impactor 20 mm teflon disk, 30 mm diam., in the skin
B	BVID, 25 J, impactor 20 mm CVID, 38 J, impactor 20 mm CVID, 25 J, pyramidal impactor
C	BVID, 15 J, impactor 25 mm CVID, 23 J, impactor 25 mm CVID, 15 J, pyramidal impactor teflon strip, 30 mm wide teflon disk, 30 mm diam., in the skin teflon disk, 30 mm diam., at H/C-skin interface

Table II - Damage introduced in the various types of panel.

DAMAGE TOLERANCE TO LOW VELOCITY IMPACT OF LAMINATED COMPOSITES

G A O Davies, D Hitchings and X Zhang
Department of Aeronautics, Imperial College, South Kensington, London SW7 2BY, UK

Abstract

A strategy is developed for predicting easily the threshold energy for delamination caused by impact, whatever the nature of the laminated structure. The actual delamination and fibre damage is also predicted and the consequent compression-after-impact strengths. The latter strategies may be approximate but current research is pointing the way to more accurate solutions based on finding energy-release-rates around the delamination front.

1. Introduction

This specialist meeting is concerned with damage tolerance in helicopter structures. As the helicopter is an ideal fatigue machine and as most helicopter structures are still metallic (excluding rotor blades) it is natural that the emphasis should be on improving tolerance to cyclic loading and in using modern damage-tolerant methods to assess the time in which an inspectable crack will grow to an unstable situation which puts the structure at risk.

This paper is however aimed at laminated composite structures which have their own brand of damage susceptibility and which is serious without the threat of cyclic loading (indeed carbon-epoxy composites have a rather good fatigue performance compared with metals) and that is the threat of impact damage. It will become increasingly important as more helicopter fuselages and empanages are built out of carbon-epoxy materials: the Bell 427 for example has 70% composite airframe structure.

The effect of impact damage, particularly on the compressive strength of aircraft structures, has been known for more than 15 years. The traditional way of coping with impact damage has been to limit design allowable strains in compression to 0.3% or thereabouts, whereas the material can probably take 0.8% at least if dry at room temperature. Countless coupon tests have shown alarming reductions in the compression-after-impact (CAI) strength. Figure 1 shows the reduction of 70% for a thermoset resin, and less so for a thermoplastic. The second figure shows that the reduction in strength appears to be insensitive to the impact site (more of this later). Such tests on coupons are useful for comparing different materials for example, but are unsuitable for real structures where the nature of the structure can radically the alter the amount of damage, depending as it does on the history of the impact force and structural strains during the impact event. These will depend on the dynamic response which will in turn depend on the structural mass, stiffness, geometry, sub-structure, internal stress field etc. A flexible structure may not be as badly damaged as a locally stiff one for example. How then does one assess the amount of impact damage in a real structure without conducting a large set of very expensive impact tests, and in particular how to do this during the design phase when damage tolerance may be a key issue?

2. The Nature of Low-Velocity Impact Damage

This paper concentrates on low velocity impact which may cause significant damage by delamination in the middle region of a thin plate or it may cause tensile matrix and fibre failure on the back face, both of which are invisible to the outside observer. Barely visible impact damage (BVID) is a hidden menace. The aim is to have a – hopefully simple – analytical tool for predicting impact damage and the consequent Compression-After-Impact (CAI) strength.

Firstly it is necessary to define "low velocity". If the incident velocity is high enough (say ballistic or rotor blade damage) then high energy stress waves are set up through the thickness of the structure, sufficient energy may mean complete penetration, and the structural response will be very local and uninfluenced by the nature of the surrounding structure. Crudely it can be shown that these stress waves give rise to a strain of order V/C, where V is the impactor velocity and C is the speed of sound through the plate thickness – governed primarily by the density and modulus of the resin matrix. Local failure will occur if these strains are of order (say) 1%. Now for epoxy resins C is of order 2000m/sec which gives the threshold for V as 20m/sec. This is not commonly thought of as low, but experiments [Ref. 1] have shown a transition from low velocity behaviour, when the thin plate has time to respond away from the impact site, when the velocity increases from roughly 20 to 60 m/sec. Accidents like tools dropped from heights up to 4m correspond to impact velocities up to 9 m/sec. It is these that form the scope of this paper.

Figure 2 shows three zones of damage developing as the plate deforms under impact. The bending strains cause (1) tensile failure on the back face in which matrix cracks occur first (and then precipitate local delamination where the cracks meet an interface) and (2) delamination in the interior where the shear strains are a maximum and finally (3) compressive strains on the impacted surface. There may also be point (HERTZIAN) damage which is very local and does not debilitate the structure much, although up to 10% of the energy may be absorbed in this mode if the impact force is high. As far as the CAI strength is concerned, the internal delamination is the main threat, since the separated laminae may buckle locally and this local blister can then propagate. The distribution of these shear-driven delaminations can be complex, consisting of a series of overlapping oblongs or "peanuts" aligned in the direction of the fibres on the lower surface. Figure 3 shows an X-ray which reveals these multi-level delaminations. However, for this particular laminate with a quasi-isotropic stacking sequence $(+45, -45, 0, 90)_{4S}$, the envelope of the delamination is circular as revealed in the C-scan shown. Also can be seen the elongated delamination in the +45° direction, caused by tensile matrix cracking on the back face lamina. If we use the area enclosed by the envelope as a measure of the damage, we can construct a map of impact damage with incident energy. A very large number of tests were conducted [Ref. 2] on a variety of plates having quasi-isotropic lay-ups, thicknesses 1, 2, and 4 mm, dimensions ranging from 75 x 125mm (the so-called Boeing test specimen) to 200 x 200mm, with various boundary conditions, and including a few stiffened panels impacted between stiffeners. A map of damage against the incident energy is shown in Figure 4(a) to be chaotic, and illustrates the futility of using coupons to explain everything. It was thought at one stage that this sort of scatter should be attributed to variability in the composite structures' properties.

Paper presented at the RTO AVT Specialists' Meeting on "Application of Damage Tolerance Principles for Improved Airworthiness of Rotorcraft", held in Corfu, Greece, 21-22 April 1999, and published in RTO MP-24.

A very simple strategy can now be used to remove the effect of different dynamic responses of the many sizes of structure. We assume that the internal delamination is driven by shear stresses which are proportional to the impact force, and that, there is no coupling between the force history and the history of the bending strains (this turns out later not to be true). The force history was monitored during these impact tests and if we then plot damage against maximum force, the picture changes dramatically as shown in Figure 4(b). There are clearly three separate maps depending on the thickness only, and equally important the damage area for any particular plate thickness can occur anywhere in the zone band. It should therefore be possible to conduct just one set of coupon tests and use this map to predict the damage in any size of structure provided that the impact site is not near or over a local substructure. Thus the effect of dynamic response has been removed.

3. Prediction of Damage Threshold

Having shown that the damage depends primarily on the maximum impact force it is now tempting to try and predict what is clearly a threshold force, below which no damage occurs at all. One route is to model the laminated plate using a very fine finite element mesh and then solve the equations of motion to reconstruct the damage evolution during the impact event. If no approximations are to be made this means using finite elements as one brick element per lamina, so that if (say) the plate is 6mm thick (48 ply) and the damage zone is 20mm x 20mm (which is not large) we then need 48 x $(20 \div 1/8)^2$ = 1.3M elements. Although not difficult to set up this model, this is a very expensive simulation, and more importantly it will be extremely difficult to understand the answers and the underlying physics, possibly more difficult than interpreting experimental results. Nevertheless at Fort Worth Bell Textron Helicopters are trying this out. They are also using strength criteria which we now show to be flawed.

Suppose we attempt to use the interlaminar shear strength as a failure criteria, then the mean shear stress is a simple function of force and radius (stress = $P/2\pi rt$) and hence the area πr^2, varies continuously with P, quite unlike Figure 4(b). We therefore resorted to fracture mechanics which are capable of explaining sudden unstable propagation, and we are able to show that there is indeed a critical threshold force P_{crit} at which delamination will occur, and that this is independent of radius of the delamination circle [Ref. 3]

$$P_{crit}^{\ 2} = \frac{8\pi^2 Et^3 G_{IIC}}{9(1-\nu^2)} \qquad (1)$$

Notice that this force is a function of the plate stiffness (Et^3) and the mode II fracture toughness G_{IIC}, explaining why thermoplastics are less susceptible to damage since the fracture toughness may be two or three times that of a thermoset. Equation (1) is based on the highly simplifying assumption that the damage and the structural strains are axi-symmetrical which is approximately true for a quasi-isotropic lay-up, nevertheless Figure 5 shows that this equation is a reasonably accurate predictor. Thus if we wish to avoid delamination completely it is only necessary to find the maximum impact force and then use equation (1).

If we need only the force, and not a detailed history of the interior strain field, it is tempting to model the system as one degree of freedom – an impactor mass and a structural spring. This should be a reasonable model if the mass is heavier than the responding structure (which is likely) so that the structures' inertia forces can be ignored. The structure should then respond in a fundamental mode and simple harmonic motion ensures that the maximum force is readily evaluated. The computing effort would be negligible since a simple static solution would give the required equivalent spring stiffness. This approach has naturally been tried by many investigators [Ref. 4]. Unfortunately there are two reason why this may not work. Firstly the response of a real structure with discontinuities in stiffness may not be a single fundamental mode, and a mixture of harmonics may respond with no guarantee that the force history is sinusoidal with a clear maximum. Figure 6 illustrates just this point. A composite panel, 250mm x 250mm was supported as shown along four supports typical of the wing surface of a military multi-spar structure. The response in 6(a), using an impactor mass six times the panel mass, is far from sinusoidal (the peak and period are also wrongly estimated by the dynamic finite element solution due to damping at the four supports not being modelled correctly) contrast this behaviour with the same laminated plate stacking sequence but impacted in the much smaller standard Boeing rig, whose mass is now only 1/30 that of the impactor. A sinusoidal response would be an accurate approximation.

The other error source lies in ignoring the coupling between the bending strains and the shear-driven force response. If the plate is flexible enough, and if the incident energy is sufficiently high, then the bending strains may exceed the fibre allowable strengths and failure will then decrease the flexural rigidity locally and hence attenuate the force. To model this we presently need to use a finite element code, but there is no need to deploy an expensive model. In FE77 [Ref. 5] simple composite shell elements are used to assume the strain distribution through the shell thicknesses, as usual, linear, but each lamina at every level is monitored during the impact event, and if a conventional strain criteria [Ref. 6] is exceeded this element layer is deleted. The result is a quite gradual decrease in stiffness which has been shown to give force histories agreeing very well with many tests, sizes, and materials. Figure 7 shows the results of two such drop tests on the Boeing test specimens with (a) modest and (b) large incident energies. The C-scans show a conventional shear-driven circular enveloped for (a) but for (b) there is much delamination in the 45° direction under the laminate near the tensile back surface, which is a consequence of the massive matrix cracking in this region. The deflection in both cases exceed the plate thickness of 1mm and hence the code needed non-linear stiffness updates, but it also had the laminate-strength failure routine here referred to as "degraded" capability. The need for this is clear in Figure 7 (b) where the elastic undamaged prediction of 2400N is twice that of the true value of 1200N. It does look therefore that some FE modelling is unavoidable even if we wish only to find the force history and the threshold for delamination.

4. Prediction of Damage Extent

A thin-walled composite structure will still have residual compressive strength even when damaged, and there is therefore an incentive to predict the extent of this delamination even though Figure 5 has indicated the amount may be indeterminate as unstable fracture occurs. At the moment there does seem to be no alternative to using a non-linear dynamic finite element code to predict delamination, and also flexural degradation. This is nowadays accepted in crashworthiness studies on metal aircraft and automobiles, and DYNA 3-D (to name one) has become common usage in car and aero-engine impact studies. The problem in laminated

composites has been noted as the complex nature of the impact-induced delaminations. It will undoubtedly become routine as computing power becomes remorsefully cheaper and more accessible, and the commercial codes become more user-friendly in displaying damage and using it as an input to a residual CAI strength predictor. In the meantime we have assessed the accuracy of using a simpler description of damage. Using the success of the single equivalent circular delamination which led to equation (1) we assumed this form ab initio. Thus a delamination level was assumed and just two layers of shell elements arranged each side of it, with fictitious links joining the element node points, and which could be broken as the equivalent forces reach a value derived from the interlaminar shear strength or the peeling strength. This should predict the initiation of delamination but we need a fracture (energy release rate) criteria to propagate. The results were encouraging as Figure 8 indicates.

A more ambitious study was the damage threshold for impact over a stiffener in a top-hat stiffened compression panel. This is much more complex and not amenable to the simple analysis used for plate impact. Here the structure is locally very much stiffer than a single plate thickness and hence a much higher impact force is generated for a given energy. However a structure is better able to resist such a force since it will locally behave like a stiff beam many times stiffer than the thin plate, hence we may expect a higher threshold energy, in this case 9J. However, as Figure 9 shows the shear stress rises to a peak and is then constant along the stiffener all the way to the nearest support, there being virtually no diffusion to the surrounding panel. This is potentially very dangerous as complete separation of a stiffener can reduce the buckling load of the stiffened panel by 75%. However as is indicated in 9(a) we need to unpick nodes and establish the energy release rate to see if the peak shear of 83MPa will propagate along the stiffener. This code development is underway.

5. Compression After Impact Evaluation

Knowing the damage extent, we can feed this into a FE code which is capable of predicting the propagation of delamination when the structure is loaded in compression. The initial buckling of the delaminated zone is straightforward (Figure 10) but this local "blister" will move no further until the applied load is increased and the blister forces and moments around its periphery increase with load until there is a point at which the potential energy release rate G at some point exceeds the fracture toughness, G_C, and propagation occurs. G is predominantly mode I (peeling) but the critical value may be a combined form of mode I and mode II release rates. In the case shown the energy release rate is a maximum at the two extremities of the transverse axis of the blister so it will propagate at right angles to the applied load direction. Two methods are available for evaluating G. One is the virtual crack extension or closure in which the perimeter edge forces do work over a test perturbation of the delamination. The other is the use of hypothetical interface elements which may be thought of as representing an adhesive but whose force/displacement law is stipulated to contain G as the work done when the crack moves [Ref. 7]. Unfortunately both of these methods require a very fine mesh to evaluate G accurately and they need to be updated as the front propagates. This is a non-trivial task, and the strategy is the subject of a current research programme ADCOMP supported by the European Union. There is however an alternative, very much cheaper way, [Ref. 8] which make the unlikely assertion that a delamination zone can be approximated by a clean circular hole of the same area. This latter problem can be solved using a fracture mechanics approach but deploying the kink-band failure mode known to be the dominant mode of failure in compression. Figure 11 show the success of this approximation. Thus there is no easy route through

$$\text{impact} \rightarrow \text{damage} \rightarrow \text{CAI strength},$$

but the physics is clearly being modelled correctly, i.e. mode II is the dominant creator of delamination damage whilst mode I is the dominant CAI failure mechanism. This should be borne in mind when the damage tolerance is to be improved by stitching, Z-pins, or a tougher resin.

6. Cyclic Loading

The propagation of delamination under cyclic loading can be simulated using the well known Paris law if we can evaluate G, and therefore the stress intensity factor K. Figure 12 shows how this is done [Ref. 9] but it needs to be said that the same fine mesh restriction is necessary once more. Work to be done is to incorporate a mixed mode I plus II law and a mixed damaged zone due to shear and peeling stresses.

7. Conclusions

The traditional industrial way of finding damage tolerance has been to establish CAI strength against impact energy using tests of coupons or components. It is clear that this can be simulated with one extra stage.

$$\frac{1}{2}mV^2 \rightarrow \text{damage extent} \rightarrow \text{CAI strength}$$

The effect of size and all the other scale effects can be eliminated by converting energy to maximum impact force. This is all that needs to be done if the threshold delamination is sufficient. It the energy is greater than this threshold then current research points the way to evaluating the damage extent and the consequent CAI strength.

8. Acknowledgements

Most of this work has been supported by the Defence Research Agency in the UK, British Aerospace (Military and Aerostructures) and by the European Union, and their help is very gratefully acknowledged.

9. References

[1] Godwin W. and Davies G.A.O. *"Impact behaviour of thermoplastic composites"*. CADCOMP 88, Southampton (April 1988).

[2] Davies G.A.O. and Zhang X. *"Impact damage prediction in carbon composite structures"*. Int. Jnl. Impact Engng., **16**, 1, pp149-170 (1995).

[3] Davies G.A.O. and Robinson P. *"Predicting failure by debonding/delamination"*. AGARD Conference Proceedings 530.

[4] Abrate S. *Impact on composite structures"*. Pub. C.U.P. ISBN 0521 473896 (1998).

[5] Hitchings D. *"FE77 general purpose modular finite element system for static and dynamic, linear and non-linear analysis"*. Dept. of Aeronautics, Imperial College (1993).

[6] Chang F-K. and Chang K-Y. "A progressive damage model for laminated composites containing stress concentrations". Jnl. Composite Materials, **21**, pp834-855 (1987).

[7] Mi Y., Crisfield M.A. and Davies G.A.O. *"Failure modelling in composite structures"*. 5th ACME Conference, Ed. Crisfield, Imperial College, (April 1997).
[8] Soutis C., Curtis P. and Fleck A. *"Compression failure of notched carbon fibre composites"*. Proc. Roy. Soc. (A), **440** (1993).
[9] Kônig M and Krüger R. *"Delamination growth under cyclic loading"*. ECCM-8, Naples, June (1998).

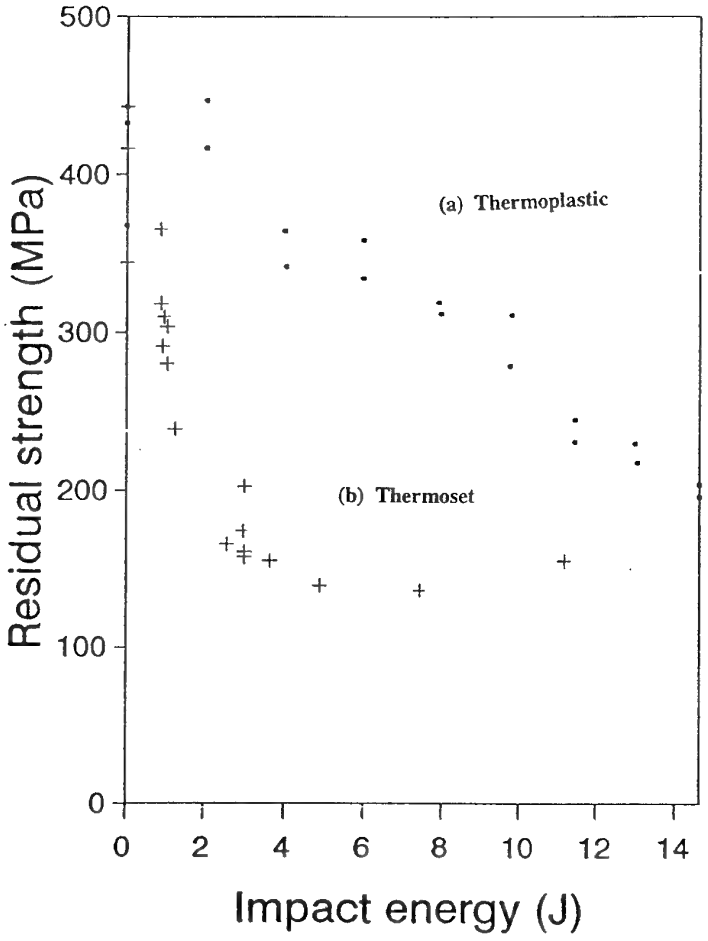

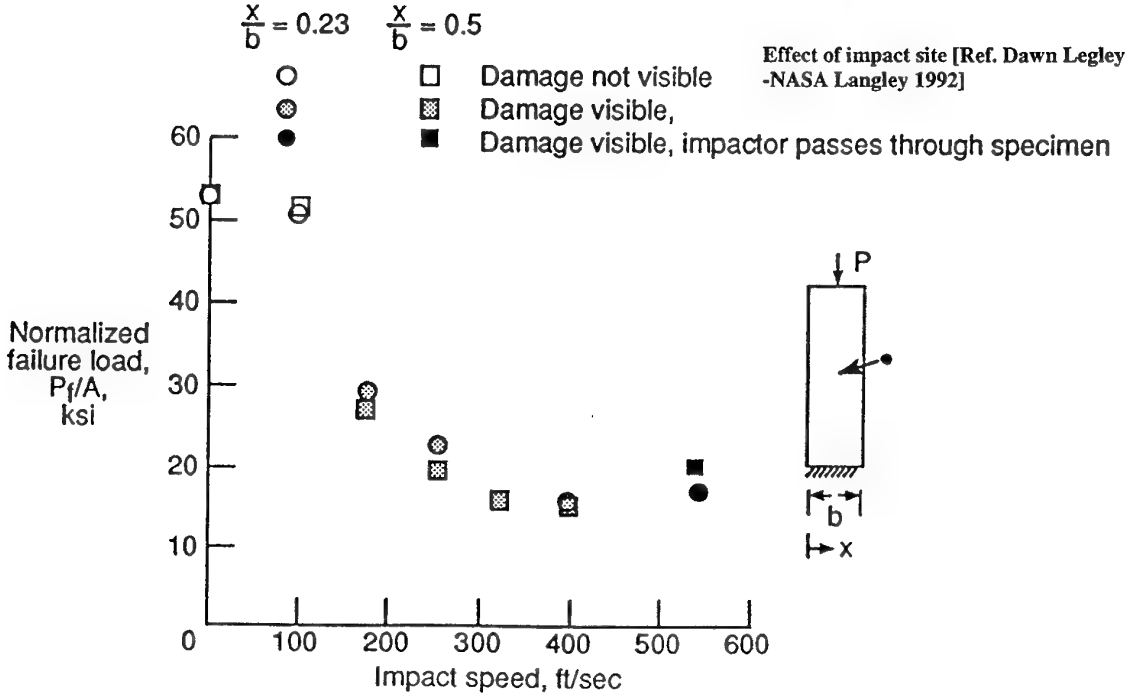

Effect of impact site [Ref. Dawn Legley -NASA Langley 1992]

Figure 1 Compression strength after impact

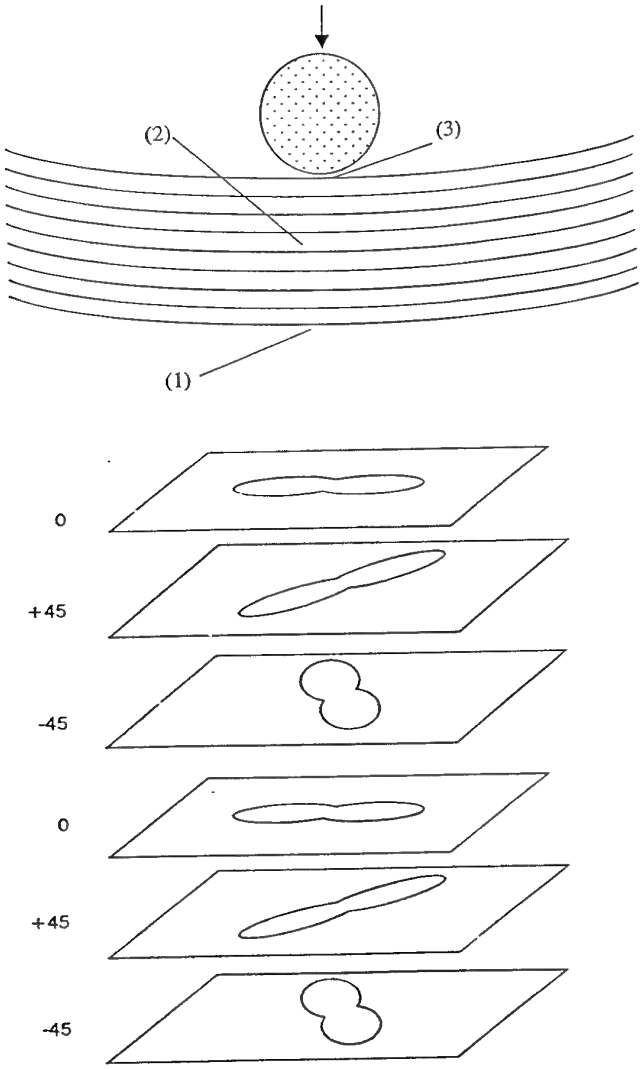

Figure 2 Low velocity impact damage zones

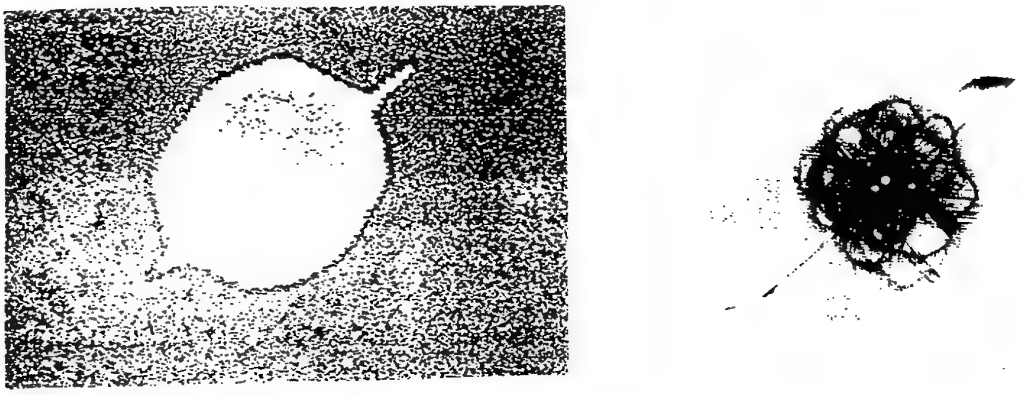

Figure 3 Internal delamination in the form of overlapping peanut shapes

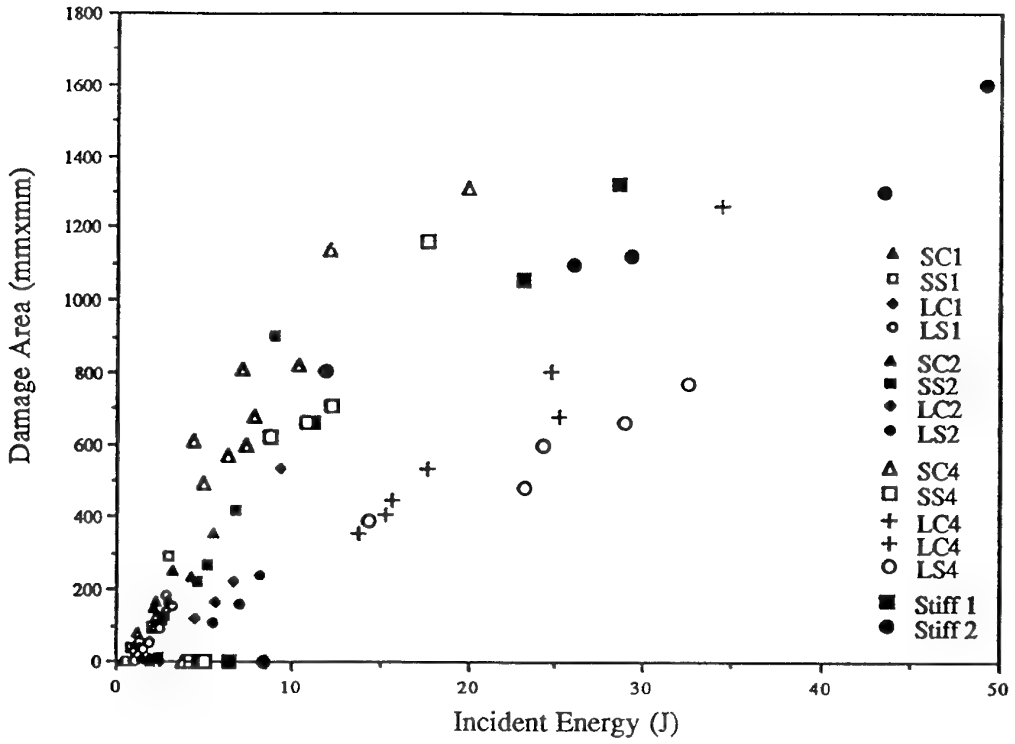

Figure 4(a) Map of damage against energy

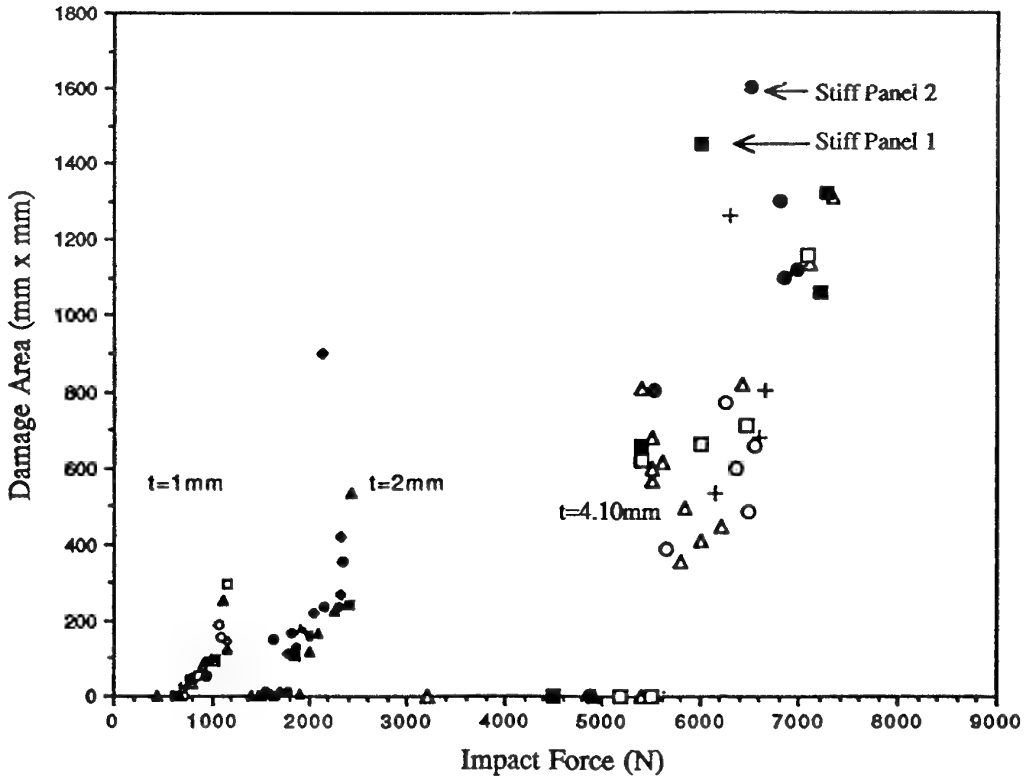

Figure 4(b) Map of damage against force

Fracture-based predictions for delamination in a variety of plate dimensions and support conditions

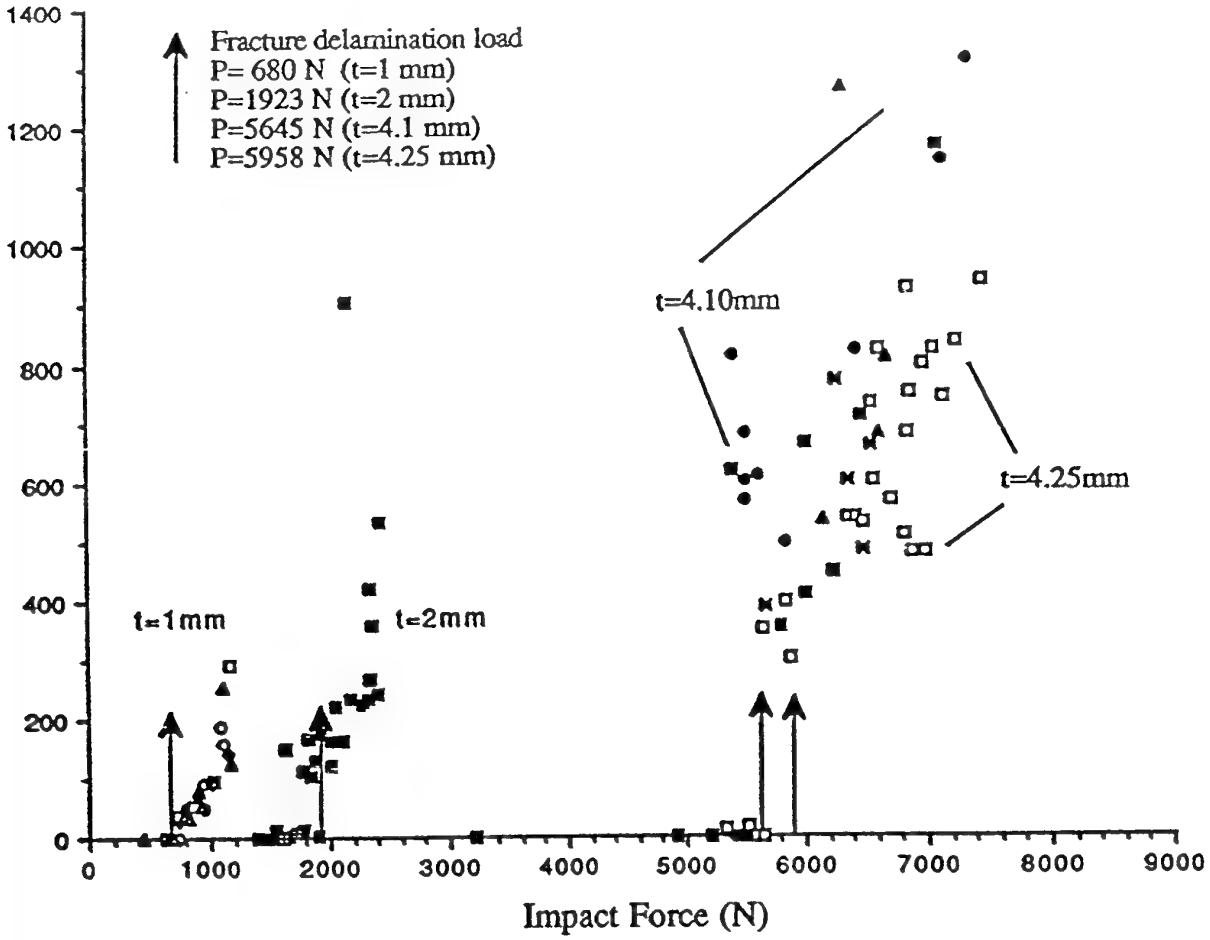

$$P_{crit}^{\ 2} = \frac{8\pi^2 E t^3 G_{IIC}}{9(1-\nu^2)}$$

Figure 5 Simple force threshold predictions

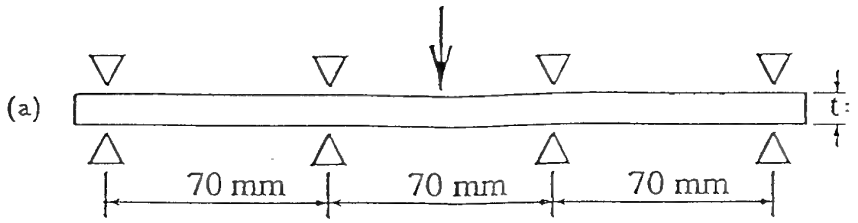

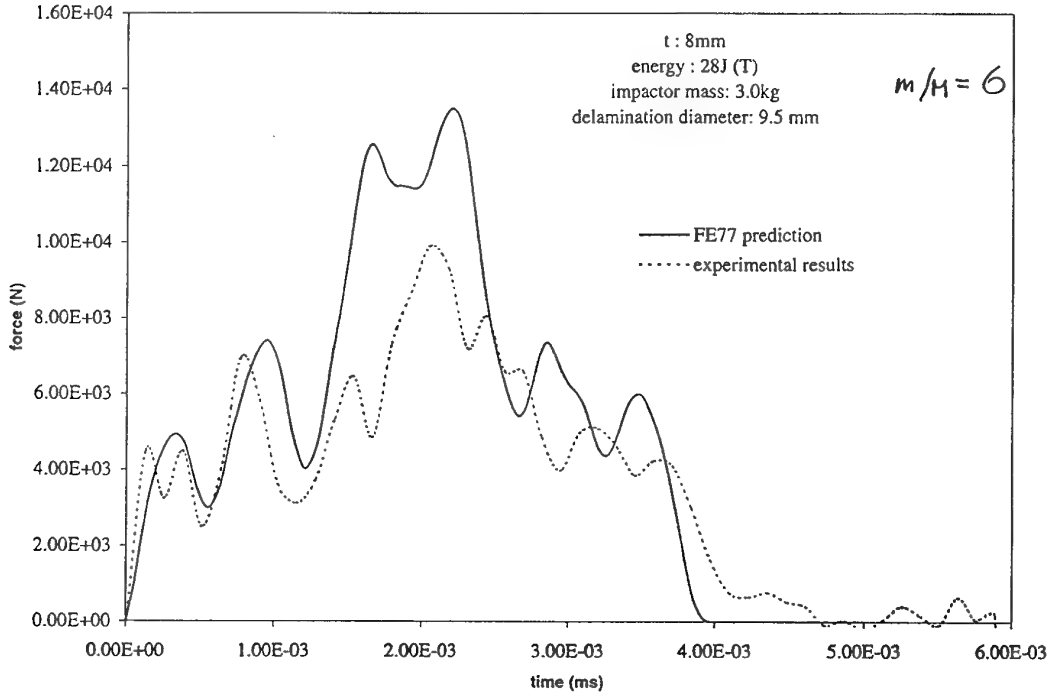

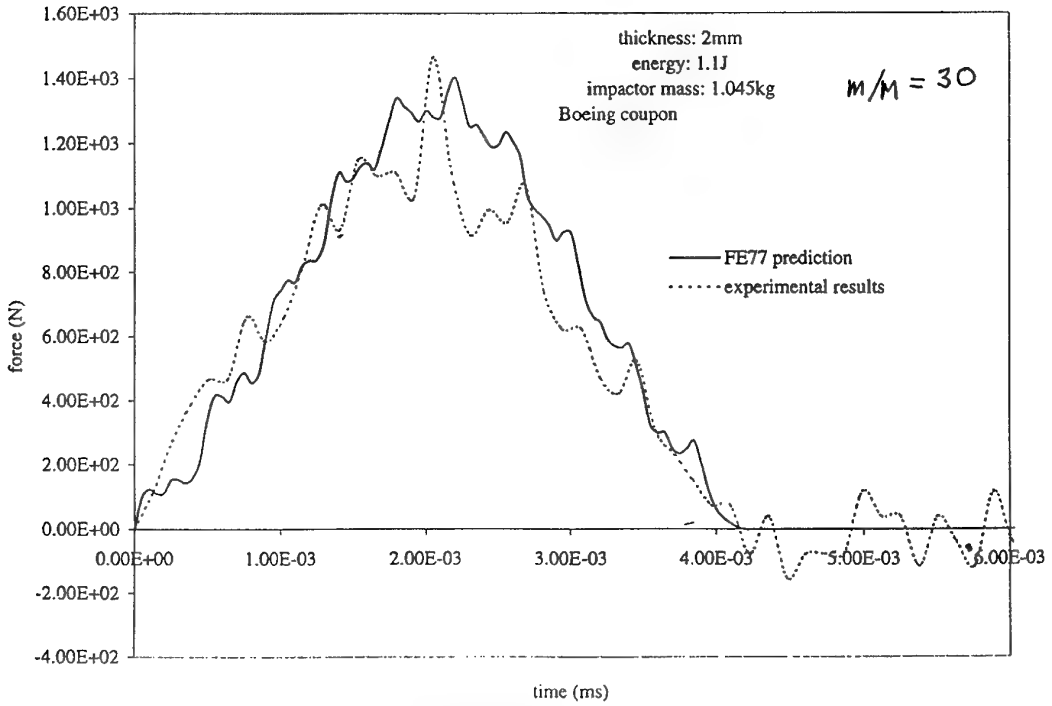

Figure 6 Effect of higher harmonic response on force history

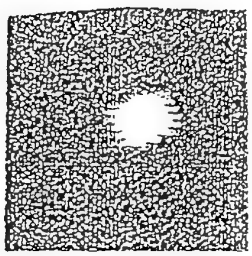

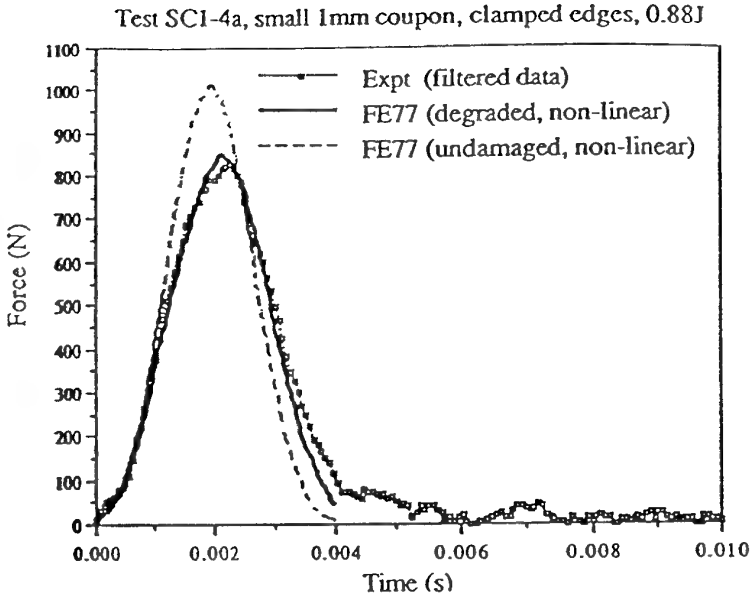

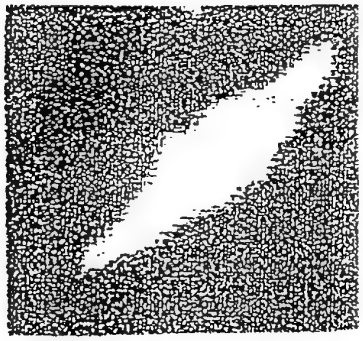

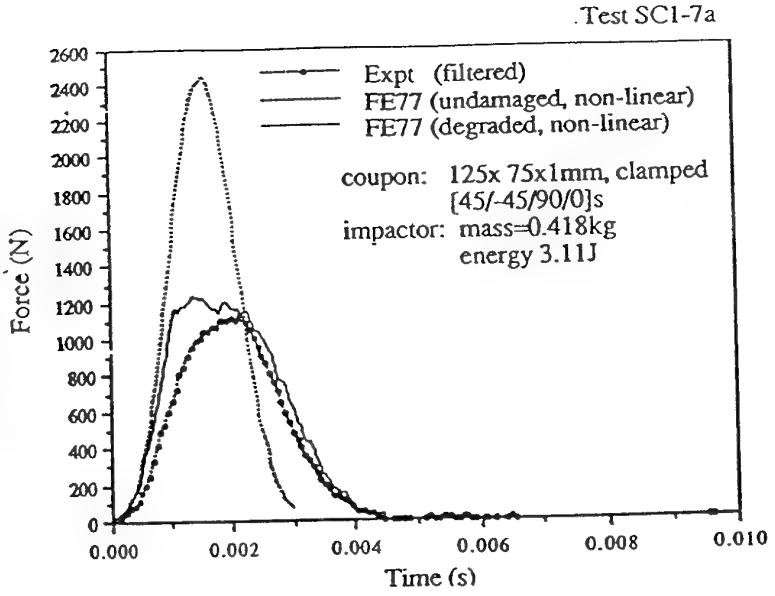

Figure 7 FE force predictions with and without extensive flexural damage (a) 0.88J (b) 3.11J

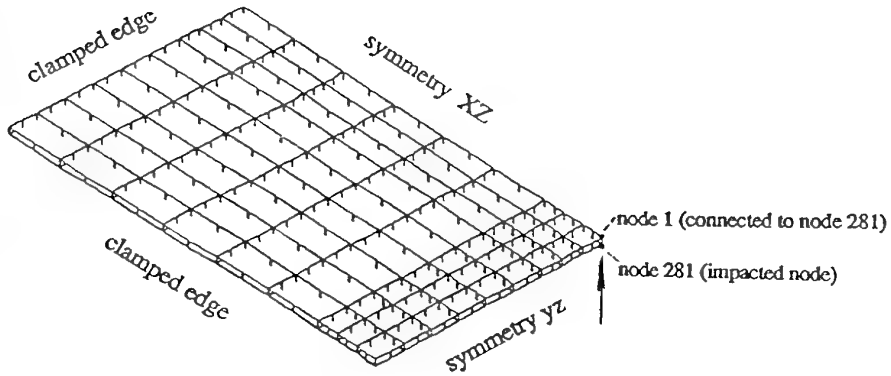

FE model of one quarter plate for delamination simulation.

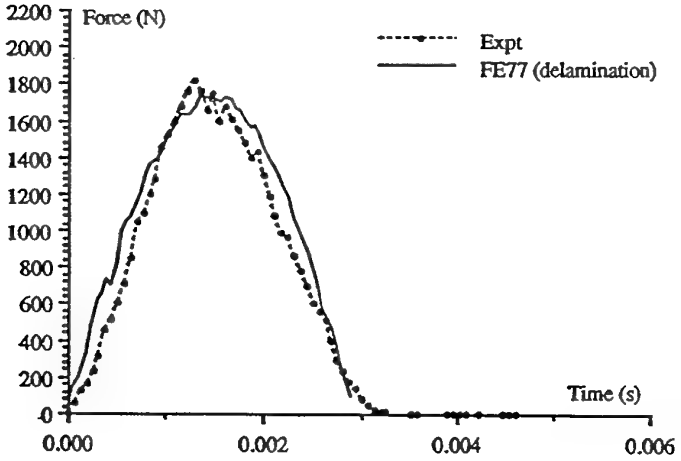

Comparison of predicted and measured force histories.

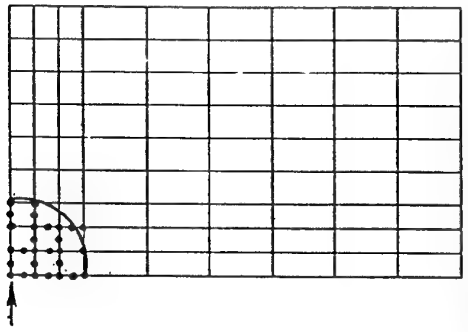

predicted delamination area = 160 mm^2.

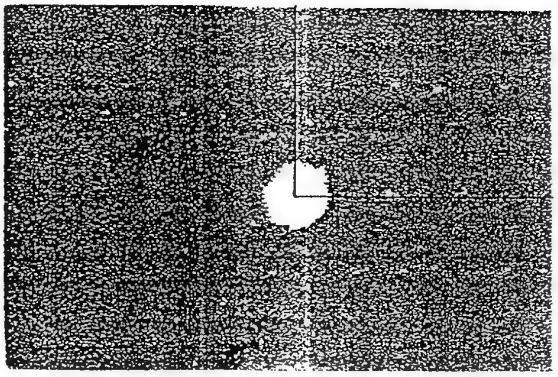

C-scan detected damage area = 140 mm^2.

Figure 8 Predictions of delamination size using just one array of breakable links

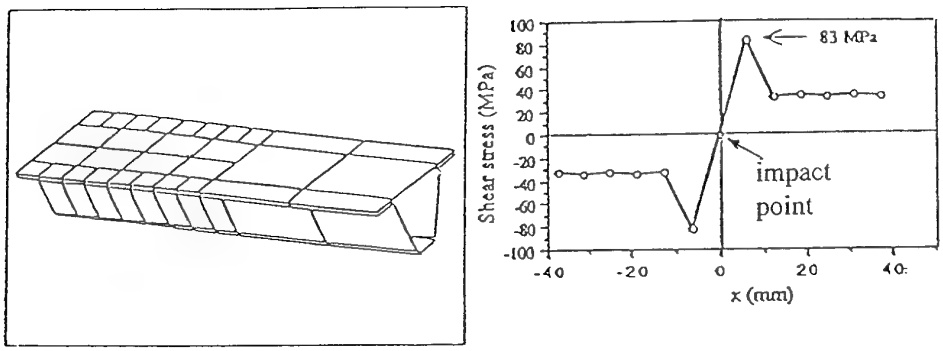

(a) Distribution of shear along the stiffener

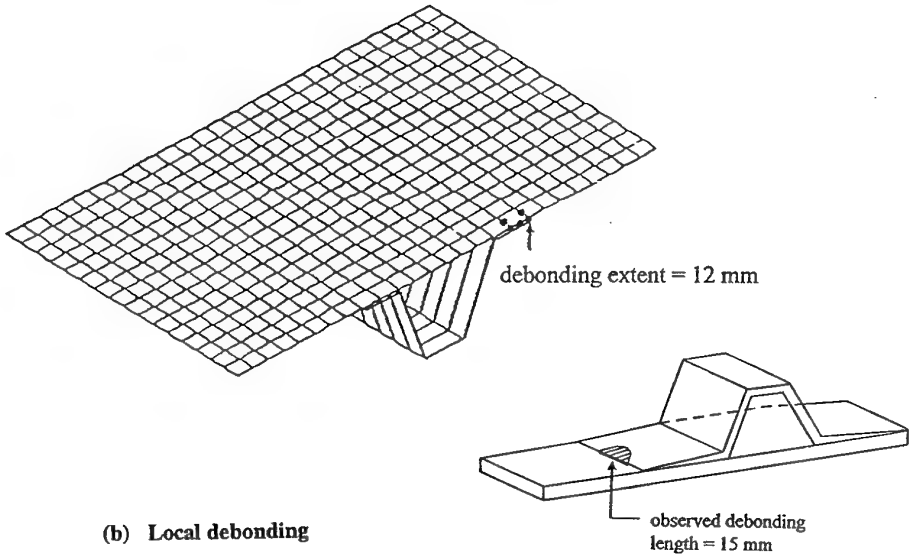

(b) Local debonding

Figure 9 Prediction of debonding at stiffener interface

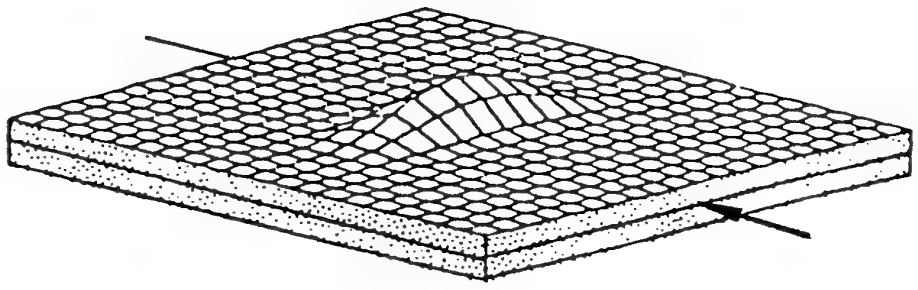

Figure 10 Buckling of delaminated zone

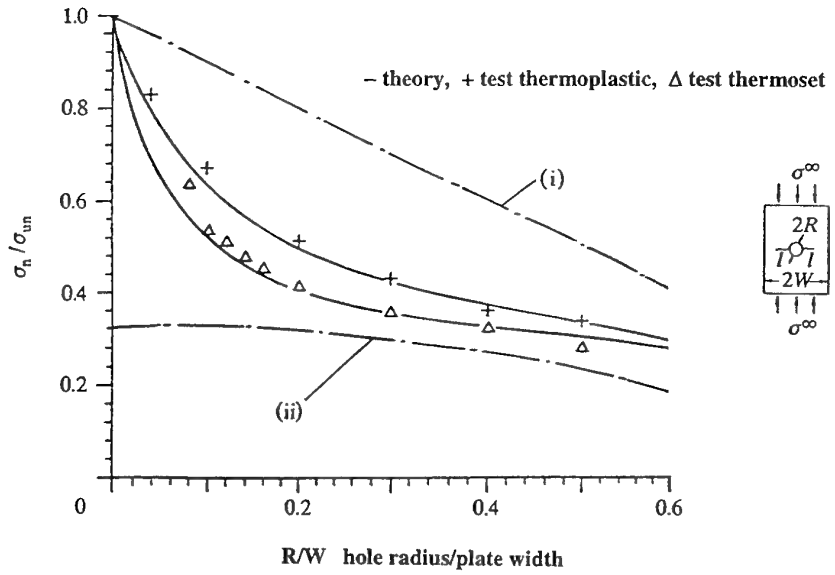

Figure 11 Open hole model for CAI prediction (i) fully ductile material (ii) completely brittle material

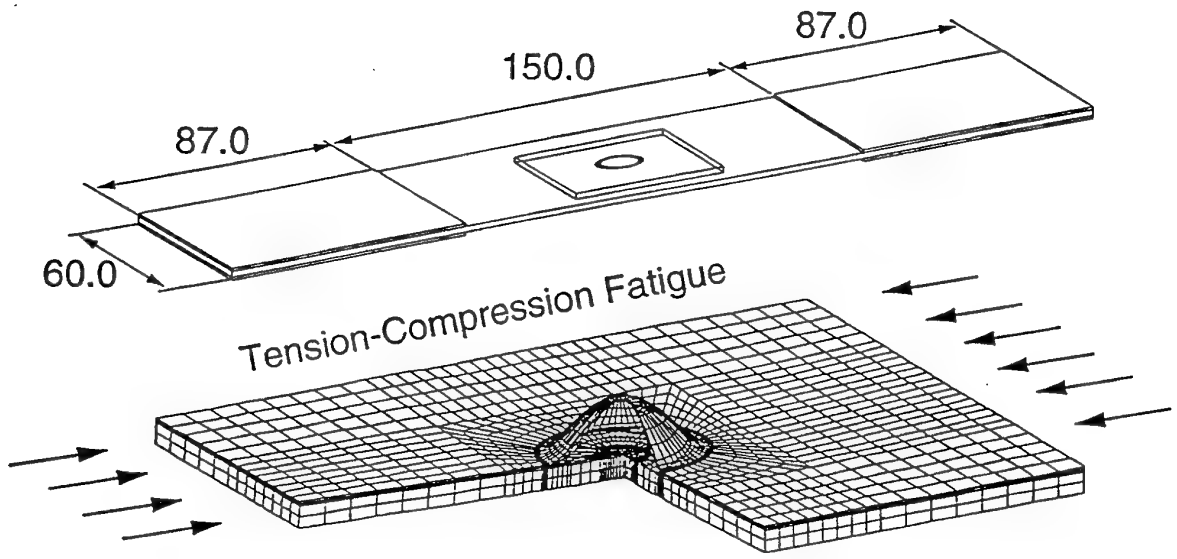

Figure 12 FE model for fatigue delamination [Ref. 9]

APPLICATION OF DAMAGE TOLERANCE TO INCREASE SAFETY OF HELICOPTERS IN SERVICE

Bogdan R. Krasnowski*
Dept. 81, M.S. 1342
Bell Helicopter Textron, Inc. BHTI
P.O. Box 482
Fort Worth, Texas 76021, United States

INTRODUCTION

In the past, all helicopters have been designed to safe-life requirements. Introduced in October 1989, FAR 29.571 at Amendment 28 requires damage tolerance substantiation for transport category helicopters. Therefore, the majority of helicopters currently in service were designed to safe-life requirements. In general, the safe-life approach has proven to be adequate. However, there have been a number of field problems with cracking components, which lend themselves to the application of a damage tolerance approach. Damage tolerance analysis allows addressing the safety of the cracking components by

- Evaluation of the field cracking, supported by the laboratory evaluation of the field-returned cracks.
- Establishment of the inspection interval in conjunction, if necessary, with operation limitations.
- Specification of fixes to be applied to the structure to either increase the inspection limit and/or lift the operation limitations.

To accomplish the above listed tasks, crack growth analysis is performed using the appropriate usage spectrum and the flight load survey data. If necessary, usage spectrum reviews and additional flight load surveys could be required. The crack growth analysis results are verified by the laboratory evaluation of the cracked components, and if necessary by the additional crack growth testing of the field-returned components with cracks or the pre-cracked components.

GENERAL CONSIDERATIONS

Safe Life

The safe life of a helicopter component is the service time in flight hours that will precluded the initiation of fatigue cracks. The safe life is calculated using the usage spectrum, flight-measured loads, and the fatigue strength determined from full-scale fatigue testing of as-manufactured components. To ensure high reliability of the calculated life, the fatigue strength of the component is reduced by three standard deviations, which would correspond to approximately one component out of a thousand with a fatigue crack. The reliability of safe-life helicopter components is, in general, higher than 0.999, determined by the fatigue strength reduction, as other elements of analysis, usage spectrum, and measured flight loads are conservative, i.e., are above their average values.

The reliability of the safe life is not known, as its determination would require consideration of other sources of randomness besides fatigue strength—such as usage spectrum, flight loads, and damage accumulation (Miner's Rule). The safe life does not account directly for such events as the presence of cracks due to manufacturing, maintenance, environment, or discrete damage.

Therefore, the reliability of the safe life could be lower than calculated if the above mentioned events are relevant, i.e., if their combined probability is of the same order as the probability of having a fatigue crack. The reliability of safe-life components can be increased by lowering their replacement times or decreasing their usage.

Damage Tolerance

Damage tolerance of a helicopter component is ensured by inspection or part removal before a crack grows critical. The inspection interval or removal time is calculated for the assumed crack using the usage spectrum, flight-measured loads, and the material crack growth data. The damage tolerance starts where the safe life ends, i.e., when there is a crack; it also accounts for events not covered by the safe life, such as cracks caused by manufacturing, maintenance, environment, or discrete damage.

In general, the reliability of components designed to damage tolerance requirements is higher than that of components designed to safe-life requirements. The reliability of damage tolerance is not known, as its determination would require consideration of the following variables: crack growth data, flight loads, usage spectrum, initial crack sizes, and inspectable crack sizes (Ref. 1). The reliability of damage tolerance components can be increased by more frequent inspection, a more thorough inspection method, or both.

Scope of Damage Tolerance Application to Safe-Life Components

Overall, the safe-life approach yields components with an adequate reliability level. However, there are situations where the reliability level of safe-life components needs to be increased, for example,

*Principal Engineer, Fatigue and Fracture Group.

Paper presented at the RTO AVT Specialists' Meeting on "Application of Damage Tolerance Principles for Improved Airworthiness of Rotorcraft", held in Corfu, Greece, 21-22 April 1999, and published in RTO MP-24.

a. Components having field problems.

b. Components that are susceptible to damage due to manufacturing, maintenance, environment, etc.

c. Components whose reliability has been adequate to the design requirements such as usage, quality, maintenance, environment—but which needs to be increased due to increased requirements.

The components in group (a) are of the primary importance, as they are proven threats to the safety of the fielded fleet, whereas components in groups (b) and (c) are only potential field problems.

The only way to increase reliability of safe-life components is to decrease the retirement life or their usage. For components of group (a) this could mean grounding of the fleet; for components of groups (b) and (c), this would mean severe economic and logistic impact. Another option is to re-evaluate these components using a damage-tolerance approach, which allows realistic evaluation of actual and potential field cracking problems, and determination of measures that would allow an increase in the components' reliability to an acceptable level. Usually, the acceptable level of reliability is defined by the damage tolerance requirements (Refs. 2, 3, and 4). The following measures alone or in combination could increase reliability of any safe-life component:

- Inspection program
- Limitation of the operation envelope
- Modification of maintenance program
- Modification of manufacturing processes
- Structural modification
- Redesign

PARTICULAR APPLICATIONS TO FIELD PROBLEMS

Fatigue cracking of any safe-life component during its service can mean that this component's fatigue life does not meet the safe-life requirements. That requires immediate action to determine the cause of cracking and to ensure the safety of remaining in-service components. To accomplish that, a thorough post-failure investigation needs to be performed, including the following data about the component in question:

- Failure data
  - Total time
  - Type of usage
  - Maintenance records, etc.
- Fleet survey data
  - Service history
  - Maintenance history
- Field investigation of the failed part
  - Failure origin and its extent
  - Metallurgical evaluation
  - Conformity check
  - Striation count

Once the post-failure examination excludes any straightforward reason, the safe-life evaluation of the fatigue life should be examined. Fig. 1 presents a flow chart of safe-life methodology. The shorter-than-calculated fatigue life could be due to

a. More severe usage, e.g., logging, higher GAG rate, high altitude operations.
b. Higher loads, e.g., rotor out-of-balance loads, residual loads due to assembly.
c. Lower fatigue strength due to corrosion, fretting, manufacturing defects, casting anomalies, etc.
d. Miner's Rule.

The first three elements of the safe-life methodology are easy to evaluate. The effect of Miner's Rule, which combines the load spectrum with the fatigue strength, cannot be directly assessed since partial damage used to accumulate the fatigue damage cannot be measured. Miner's Rule assumes that damage accumulation is independent of the damage size, and does not account for the load sequence. There are a number of publications that showed large variability induced by the application of Miner's Rule (Refs. 5, 6, 7). In general, this could lead to either shorter or longer calculated fatigue life. It could be a suspect of premature failures in cases involving both high and low cycle loads, as Miner's Rule cannot account for the load sequence.

Damage tolerance analysis (Fig. 2) offers capabilities not available in safe-life analysis, as it considers that the growth of a crack depends on its size, and accounts for the presence of damage (the initial crack) and the load sequence.

The post-failure evaluation and examination of the fatigue life analysis, allowed to define and verify data for the crack growth analysis in terms of selection of the critical location, assumed initial damage, appropriate usage spectrum, and appropriate flight load survey data and crack growth predictions. If necessary, usage spectrum reviews and additional load surveys could be required, as well as an additional crack growth testing of (1) the field-returned components with cracks or (2) the pre-cracked components. The results of the crack growth analysis can be used to determine an appropriate

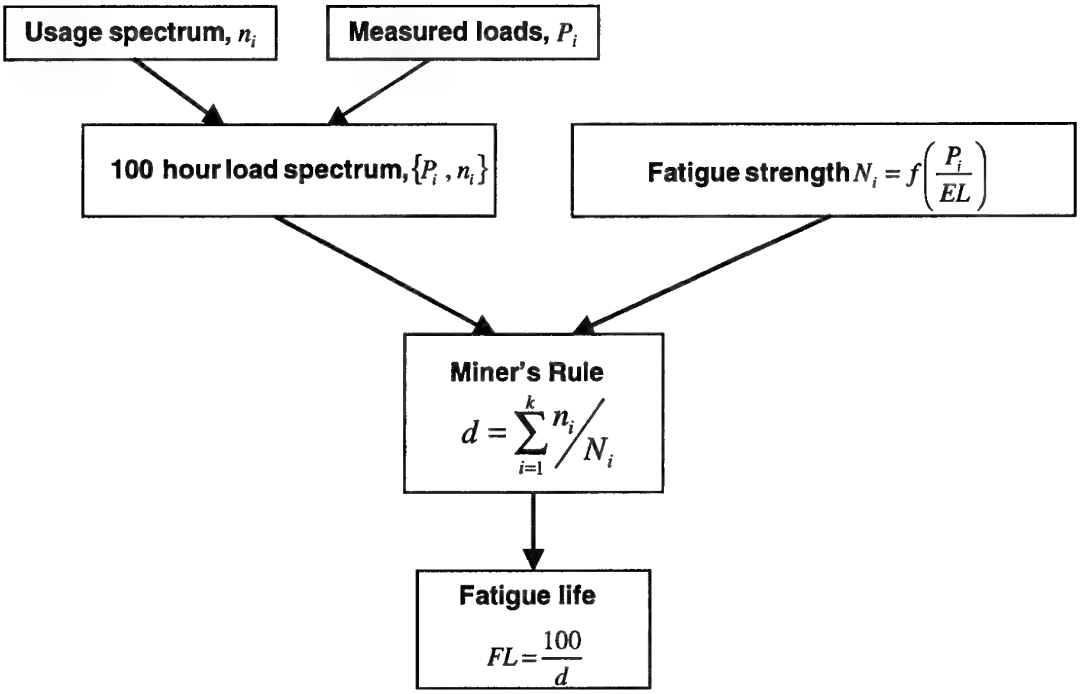

Fig. 1. Safe-life methodology.

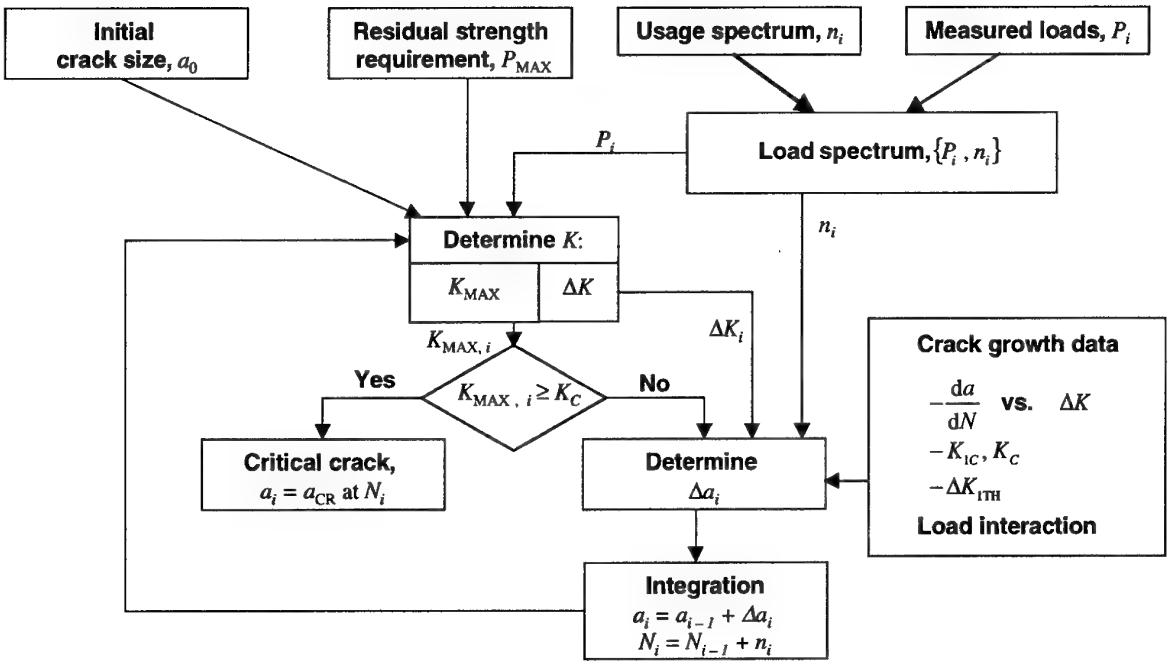

Figure 2. Damage tolerance methodology.

inspection interval to restore safety to the acceptable level defined by the damage tolerance requirements. Crack growth analysis can be performed for various scenarios of initial cracks, load spectrum, and part geometry to address options available to tackle the problem, which would include

a. Inspection using various inspection methods.
b. Limitation of the operation envelope.
c. Structural modifications.

In case the first option (a) yields an unacceptable inspection interval, the remaining options (b) and (c) can be exercised in order to increase an inspection interval to the acceptable level.

EXAMPLES

Severe Load Spectrum: Monocoque Tailboom

Fatigue cracking of the skin was detected at the outboard section of the tailboom (Fig. 3). The cracking

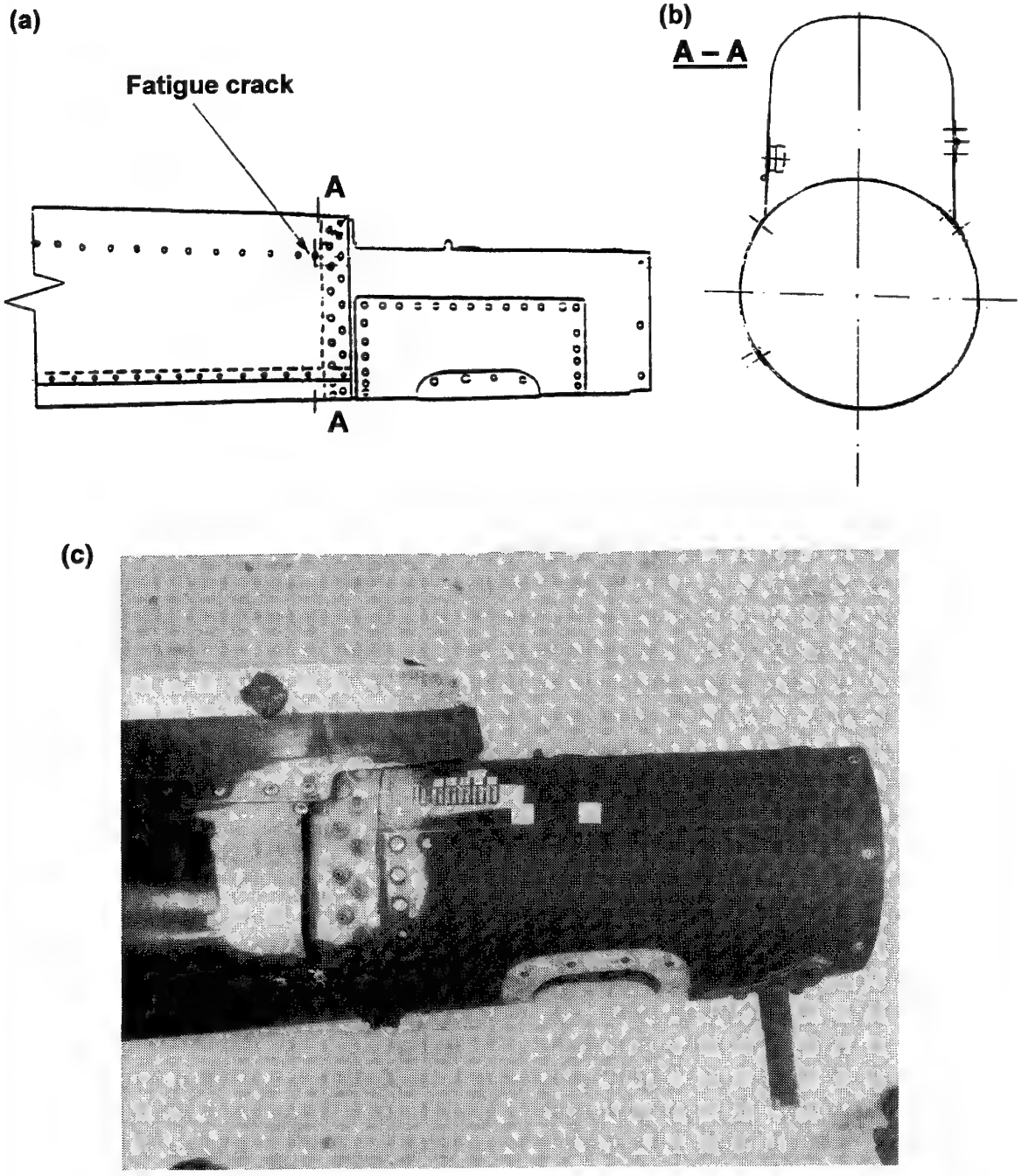

Figure 3. Tailboom: geometry, critical section, and crack-growth test result.

originated at the hole of the last rivet attaching the drive shaft cover support to the skin. The cracking was caused by high vibratory loads at this section, being the result of the combined action of the main rotor and tail rotor excitations. The flight load survey with the strain gauges at the critical areas of the tailboom was flown for the baseline tailboom and a modified tailboom. The modified tailboom incorporated "dynamic fixes" which changed the dynamic response of the tailboom and lowered both magnitude and frequency of the vibratory loads at the critical area of the tailboom. Also, to extend the inspection interval, the skin thickness of the critical area has been increased. Based on the strain data from the flight survey, an inspection interval was determined using the crack growth analysis for the crack in the cylindrical shell, without considering the beneficial effect of the drive shaft cover supports on crack growth.

To verify crack growth analysis and to extend the inspection interval, field-returned tailbooms with fatigue cracks were tested under the flight load spectrum. The crack growth test results confirmed the conservatism of early crack growth results and showed the beneficial effect of the drive shaft cover supports as an additional load path (Fig. 3c). The test results allowed extension of the inspection interval and addressing of the load variability at the tailboom critical section.

Discrepant Components Due to Manufacturing: Tail Rotor Blade

A number of tail rotor blades (Fig. 4) were produced with excessive sanding of the skin around the doubler tip, which caused fatigue cracking of the skin. The flight load survey data were available for the beamwise and chordwise bending moments at the station near the area affected by sanding. The stress spectra at the critical areas were determined, followed by the crack growth analysis of the blade with a cracked skin. The inspection intervals were established for blades with plain spars (Fig. 3b), and spars reinforced with glass fibers, (Fig. 3c). The presence of the reinforcement substantially increased the inspection interval.

The inspection intervals ensured the structural integrity of the blade, allowing for corrective action to fix the problem without affecting the operation of the fleet and its readiness.

Components Made of Material Susceptible to Stress Corrosion: Main Rotor Grip

The main rotor grips on older helicopters was made of 2014-T6 aluminum alloy (Fig. 5). This material shows low resistance to stress corrosion, which could cause problems in highly stressed areas—particularly when accompanied by high residual stresses. The lugs of the main rotor grip with thermally fitted bushings are highly loaded by centrifugal force and beamwise and chordwise moments. The crack growth analysis of the grip was performed to establish an inspection interval to increase its reliability. Subsequently, the main rotor grip material has been changed to 7075 T73 aluminum alloy, which shows higher resistance to stress corrosion.

Components Redesigned to Meet Increased Structural Integrity Requirements: Main Rotor Pitch Link

The main rotor pitch link (Fig. 6) was originally designed with an aluminum tube, which failed due to fatigue cracking. The pitch link was redesigned with the aluminum tube replaced by a steel one. Both designs have infinite safe life. To show the higher reliability of the redesigned pitch link, crack growth analysis was performed to show its damage tolerance (Ref. 8). The crack growth analysis was verified by crack growth testing of selected elements of the pitch link, rod end "banjo" (Fig. 6b), and the threaded shank (Fig 6c). Also, material crack growth data were generated by crack growth testing of center cracked panels made of the pitch link material, 15-5PH stainless steel heat treated to 155–170 ksi minimum ultimate tensile strength.

CONCLUSIONS AND RECOMMENDATIONS

The damage tolerance of safe-life helicopter components can be evaluated using crack growth analysis. To accomplish that, load spectrum, stress distributions, stress intensity factor solutions, and material crack growth data are required.

Crack growth analysis determines inspection intervals that can be used to ensure structural integrity and to increase reliability. Inspections can be used to address field problems resulting from fatigue cracking and to prevent such occurrences. In the latter case, the decision to introduce inspections should be based on the criticality of the components and their sensitivity to inherent or external damages, and to variations in usage and loading.

The ultimate goal of any structural integrity requirements, whether safe-life, or damage tolerance, is to ensure an acceptable level of safety. The level of safety can be measured by reliability, which is the probability of not failing. Therefore, reliability is the common denominator which can be used to verify adherence to structural integrity requirements, to evaluate various approaches, both structural and methodological, and to optimize structures with regard to structural integrity. It is recommended that guidelines be established to evaluate reliability of fatigue critical components for both metal components (Ref. 1) and composite components (Refs. 9, 10).

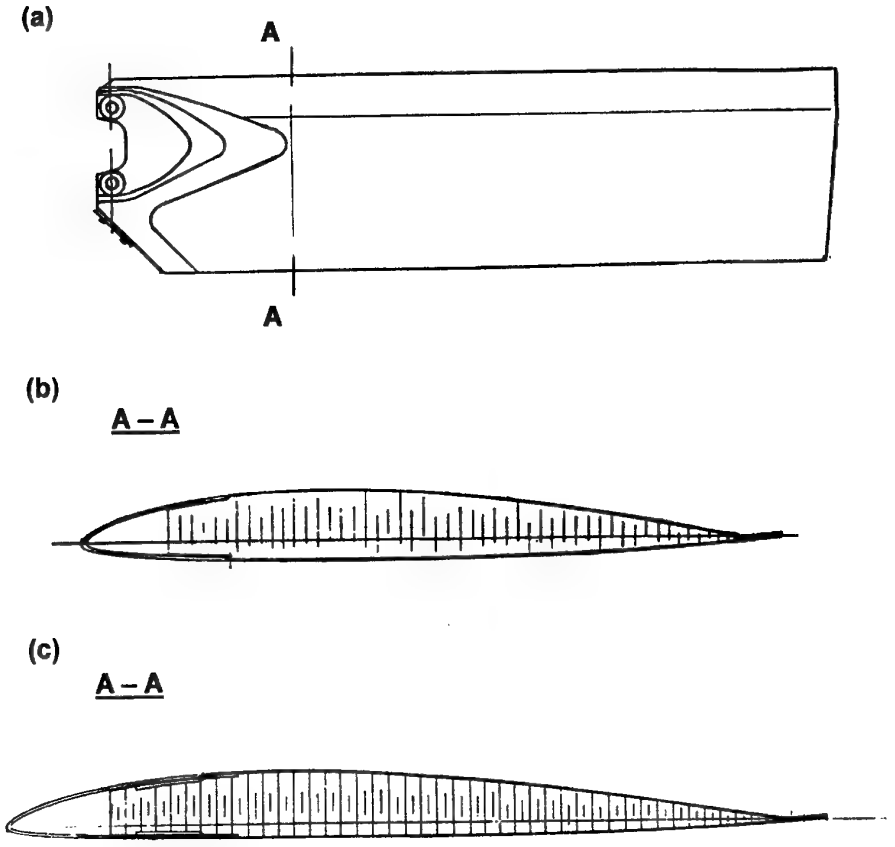

Figure 4. Tail rotor blade: geometry and critical section.

ACKNOWLEDGEMENTS

The author wishes to thank Mr. B. H. Dickson and Mr. D. J. Reddy for valuable support, and Mr. C. M. Gatlin, Jr. for help in preparation of this paper.

REFERENCES

1. Krasnowski, B. R., "Reliability Requirements for Rotorcraft Dynamic Components," *Journal of the American Helicopter Society*, Vol. 36, No. 3, 1991.
2. MIL-A-83444 (USAF), "Airplane Damage Tolerance Requirements."
3. FAA Advisory Circular No. 29-2B, Appendix 1, "Fatigue Evaluation of Transport Category Rotorcraft Structure (Including Flaw Tolerance)."
4. Dickson, B. H., ed., "Rotorcraft Fatigue and Damage Tolerance," white paper prepared for TOGAA, January 1999.
5. Shutz, W., and P. Heuler, "Miner's Rule Revised," in AGARD Proceedings "An Assessment of Fatigue Damage and Crack Growth Prediction Techniques," Sept. 1993.
6. Svensson, T., and M. Holmgren, "Numerical and Experimental Verification of a New Model for Fatigue Life," *Fatigue Fracture Engineering Material Structures*, Vol. 16, No. 5, 1993.
7. Leipholz, H. H. E., "On the Modified S–N Curve for Metal Fatigue Prediction and Its Experimental Verification," *Engineering Fracture Mechanics*, Vol. 23, No. 3, 1986.
8. Krasnowski, B. R, K. M. Rotenberger, and W. W. Spence, "A. Damage Tolerance Method for Helicopter Dynamic Components," *Journal of the American Helicopter Society*, Vol. 36, No. 2, 1991.
9. Krasnowski, B. R., and S. P. Viswanathan, "Reliability Analysis of Composite Rotorcraft Components", *Journal of the American Helicopter Society*, Vol. 37, No. 3, 1992.
10. Krasnowski, B. R., "Reliability and Durability of Aircraft Structures Made of Fiber-Reinforced Plastics," Chapter 27 in *Performance of Plastics*, ed. W. Brostow, Munich and Cincinnati: Hauser Publisher, 1999 (forthcoming).

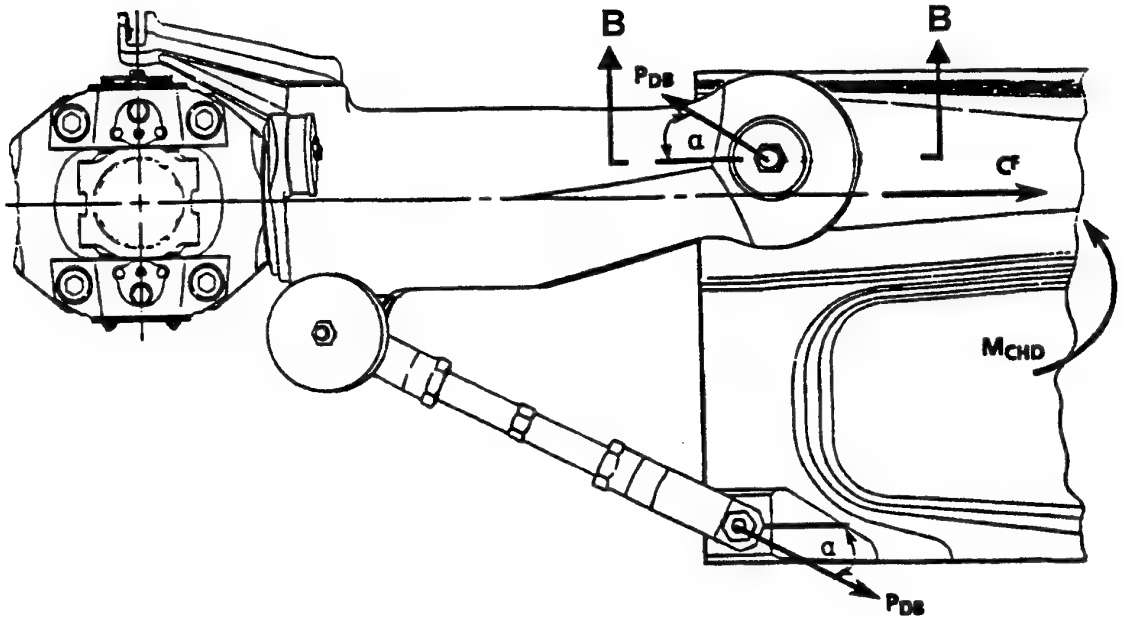

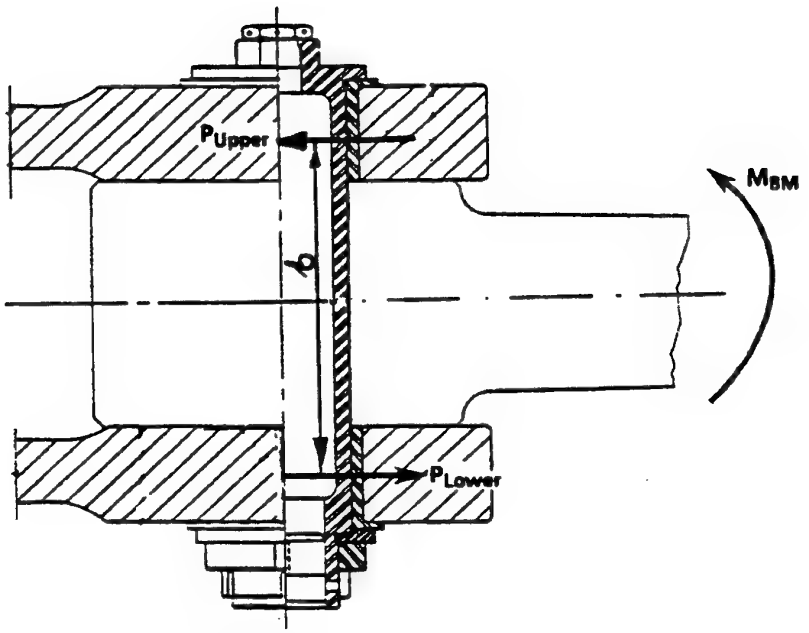

Section B – B

Figure 5. Main rotor grip: geometry and loading.

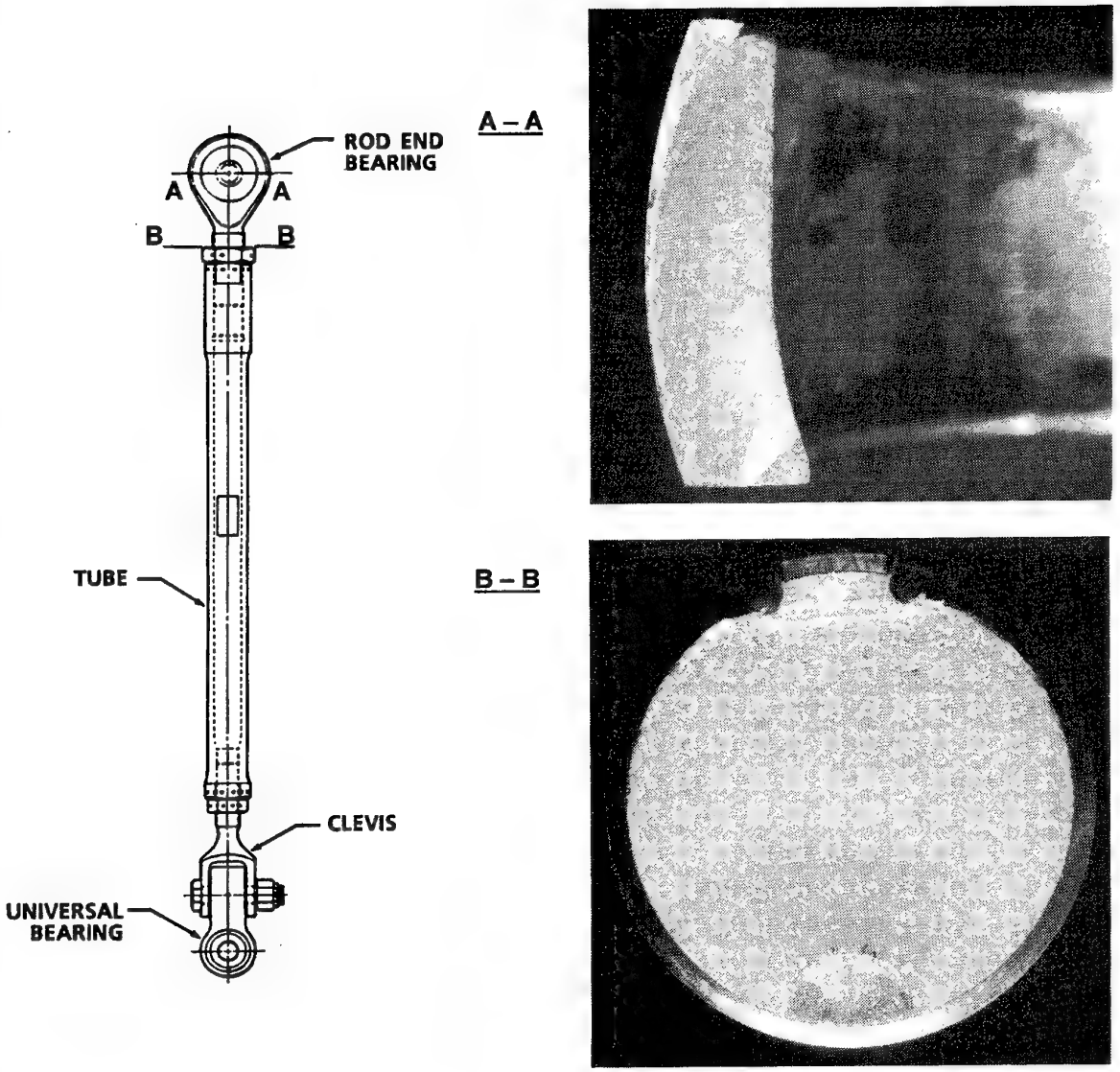

Figure 6. Main rotor pitch link: geometry and crack-growth test results.

AGUSTA Experience on Damage Tolerance Evaluation of Helicopter Components

Ugo Mariani – Fatigue Office
Luigi Candiani – Accidents Investigation Office

AGUSTA A Finmeccanica Company
Via Giovanni Agusta 520
21017 Cascina Costa di Samarate (VA) - ITALY

ABSTRACT

Within the fatigue evaluation of the EH101, Agusta has carried out a specific program of flaw tolerance evaluation of the primary loading path. The program is close to completion and this paper provides a summary of the most relevant results.
For composite components, damage size was increased considering both manufacturing discrepancies greater than the minimum quality standard and impact damages clearly detectable during visual inspections. The favourable data achieved are based on the 'no growth' concept.
The metal parts of the main rotor head were evaluated by enhanced safe life method and fail safe capability. The slow crack growth approach was instead applied for the Rear Fuselage End Fittings, which connect the Tail Unit.
All these evidences can be used in addition to the comprehensive safe life evaluation of the aircraft to improve the maintenance and the repair actions.
Based on this experience, application of flaw tolerance criteria will be carried out on the new helicopters in development phase.

INTRODUCTION

Since 1989 the Civil Rule for Transport Helicopter requires the flaw tolerance evaluation of the fatigue critical parts, wherever practical. For this reason the certification basis of the EH101 was amended with specific requests of Flaw Tolerance evaluation by the three Airworthiness Authorities involved in the program: the Registro Aeronautico Italiano, the British Civil Aviation Authority and the U.S. Federal Aviation Administration. The structural substantiation of the most relevant components of primary loading path was therefore improved to verify their strength in case of improbable and undetected accidental damage.
The reasonable expectance in the near future is that the maintenance manual could take advantage of the flaw tolerance data to improve the evaluation of the inspection intervals by test data and analysis, which properly address the structural strength of damaged parts. The present standard instead takes into account mainly experience and engineering judgement, supported by data from prototypes and lead fleet helicopters. Up to now the purpose to provide a more rational and traceable criteria for the EH101 was achieved by an engineering approach which establishes inspection intervals of the Structural Significant Items (SSI) for accidental damage according to fractions of the retirement life, computed using tables which grade the reduction factor based on the safe life, the static strength margin of safety, the probability of having an accidental damage and the visibility for inspection. Table 1 details the approach for the SSI Accidental Damage Analysis.

An overview of the EH101 flaw tolerance evaluation results is provided hereafter.

MAIN AND TAIL ROTORS

The Main Rotor Head is made by the Main Rotor Hub, with a titanium core and carbon fibre-epoxy loop windings enclosed by glass-epoxy box. Two different configurations of blade grips can be used: the foldable configuration for naval variants, made by Inboard and Outboard Tension Links, with hybrid titanium frames and composite plates, and the 'one-piece' design Civil Tension Link made by a full carbon and glass fibre-epoxy laminate. Most of the Main Rotor Blade shear loads are reacted by the titanium Support Cone, via the Elastomeric Bearings.
The Tail Rotor is a 'see-saw' made by carbon fibre-epoxy Blades and the composite Hub, made by carbon fibre loops windings with glass fibre-epoxy wrap.
Both Main and Tail Rotor have Elastomeric Bearings, providing relevant damage tolerance capabilities.

All the composite parts were evaluated according to AC 20-107A , proving a flaw tolerance demonstration considering:

- Barely Visible Impact Damages (BVID), assumed as the damage visible at the distance of 1 metre caused by dropping a blunt tool of 25 mm diameter, with a maximum realistic energy of 50 Joules, whichever the less;
- environmental ageing consistent with 20 years of service life at T = 24°C and 84% RH
- manufacturing discrepancies at maximum size accepted by production standards, to assure testing components representative of the minimum quality standard.

Static strength was proved at Ultimate Load at the end of the service life.
Additional evaluations for damage tolerance were carried out increasing damage size to a level clearly detectable by visual inspections or exceeding the size of the manufacturing discrepancies beyond the production standards, with the purpose to improve the Accidental Damage Analysis.
Metal parts were evaluated for fatigue according to safe life approach. Additional evaluations were carried out to address the flaw tolerance capabilities for Clearly Detectable Damage of the M.R. Hub titanium core, the Damper Hub Attachments, the Support Cones and the Tension Links titanium frames.

The Table 2 summarises the Agusta components of the EH101 which were evaluated for Damage Tolerance.
Figure 1 points out the Main Rotor Head components evaluated for Damage Tolerance capabilities.

Paper presented at the RTO AVT Specialists' Meeting on "Application of Damage Tolerance Principles for Improved Airworthiness of Rotorcraft", held in Corfu, Greece, 21-22 April 1999, and published in RTO MP-24.

M.R. Hub

The M.R. Hub, figure 2, assures connection of the 5 blades and transfers the loads to the mast through a splined coupling. It is a hybrid metal-composite structure made by a titanium core and 10 small plus 2 large carbon fibre-epoxy loop windings enclosed by an external wrapped glass-epoxy box. The hub is a 125°C autoclave cured component.

Composite and metallic parts were evaluated for DT capabilities according to a full scale spectrum test with intentionally induced manufacturing discrepancies and localised fatigue failures due to the safe life testing phase.
No damage growth in the service life was proved by tests in composite parts, which were impacted for Barely Visible Impact Damage (BVID) at energy of 50 J with a spherical impactor ϕ=25 mm, and for Clearly Visible Impact Damages (CVID) with a sharp tool made by a 90° pyramid, figure 3.
In addition, scratches and delaminations in the glass wrap due to amplified loading of safe life test showed a slow flaw growth behaviour in the start-stop cycles of the D.T. testing phase, and no damage growth at flight loads, figure 4. The test achieved the target of 10.000 hours for the Navy spectrum, the most severe for the higher start stop loads due to the blade folding cycle, proving a safe inspection interval of 2500 hours using a life safety factor of 4.

After the safe life test, tolerance to fretting and fail safe capabilities in the titanium core were checked removing the solid lubricant and 10% of the Hub teeth in the splined coupling with the M.R. Mast and testing at amplified Torque, figure 5. The test achieved the Civil variant design target of 40.000 h for the start-stop torque loading cycles, proving also no high frequency fatigue damage by the S/N curve for the fretting failure mode. A mean strength reduction by 2 standard deviations, appropriate for Enhanced Safe Life approach, was used instead of the normal reduction by 3 standard deviations for pristine components, considering the structural redundancy demonstrated and the relevant flaws under test.
Flaw Tolerance capabilities of the Aluminium Upper and Lower Plates was checked removing 4 out of 15 bolts on both plates in the splined area and testing the Support Cone coupling area with relevant cracks and fretting due to the initial safe life phase of testing, figure 6. The Al Plates proved fail safe capabilities for bolts failures achieving the target for both Civil and Navy usage spectra and proved in addition more than 1000 hours of Enhanced Safe Life for the Support Cone coupling area with severe fretting and cracks. The pristine component has unlimited fatigue life and this evaluation could be used to improve the evaluation of inspection intervals in service for Clearly Detectable Damages.

In addition, the M.R. Hub fatigue test proved the capability of the composite arm to sustain for at least 3 flight hours the full spectrum of shear loads of the M.R. Blade. This should allow, from the structural point, the safe landing of the aircraft in the remote event of a Support Cone failure, considered immediately detectable in flight due to the increased vibration level. Residual strength up to limit load was proved without failure of the composite arm, showing also that no stiffness degradation occurred in the M.R. Hub composite parts.

M.R. Damper Hub Attachments

The M.R. Damper Hub Attachment is made by an upper and a lower Al-Alloy plate, bonded to the Hub and additionally fitted by three bolts, figure 7.
After having initiated a crack in the safe life test at amplified loads, the crack grew in the upper plate reaching the bolt hole. No further crack initiation occurred for 200 flight hours at max flight load, using $1/(1-2\sigma)$ load safety factor, appropriate for the Enhanced Safe Life evaluation. Residual strength was proved up to limit load, considering the partial failure already occurred.
An additional Rogue Flaw was intentionally made by a corner saw cut of 2 mm depth in the lower plate, in the section which has showed a further failure mode during the safe life tests. Even in this case the 200 h inspection interval was confirmed.
The evaluation was not improved since both failure modes are easily detectable during visual inspections of the M.R. Hub.

M.R. Support Cone

The M.R. Support Cone connects the Pitch Change Arm to the Rotor Hub. It is made by Titanium with a vulcanised Elastomeric Centering Bearing, which allows the pitch movement of the blade, figure 8. The Support Cone is connected to the Hub core via two Special Bolts and four Stud Bolts.
The structural significant sections were taken into account for the flaw tolerance evaluation of this component, according to the failure modes showed in the safe life tests:

- the Stud Bolts failure, which was proved as not fatigue critical due to redundancy of the two Special Bolts
- fretting of the Special Bolts
- fretting in the lugs of the Special Bolts
- flaws in the lugs of the Special Bolts, simulating flaws that could be done during assembling and maintenance operations, figure 9. Flaws made by 'V' grooves of 0.35 and rogue flaw 0.50 mm dept were made in the test components using a sharp tool to minimise plastic deformation at the flaw tip. Constant amplitude loading tests were carried out to determine the Wohler curve of the flawed specimens for the 'Enhanced Safe Life' calculations.
- the same flaws were made also in the cylindrical part of the Support Cone, for simulation of improper manufacturing or maintenance operations.

The retirement life of the component is determined by the fretting failure mode in the Support Cone lug.
The rogue flaw in the lug reduces the fatigue strength of the pristine components by 1.25, the flaws in the other sections did not show relevant fatigue strength reduction. The Enhanced Safe Life evaluation for surface flaws in the lug did not show any additional fatigue life reduction. Figure 10 shows the fatigue test data.

M.R. Inboard and Outboard Tension Links

The M.R. Inboard Tension Link is a hybrid structure composed by two carbon and glass-epoxy composite plates bonded and bolted to a titanium forged frame in the outer folding section.
The M.R. Outboard Tension Link is a hybrid structure composed by a titanium forged frame with two glass-epoxy composite plates bonded to the upper and lower metal frame plates.
Figure 11 shows the two components, designed to allow blade folding for the Navy requirements.
Flaw Tolerance of the composite plates to 50 J impact damages, manufacturing discrepancies and environmental ageing were proved to address the retirement life, proving also ultimate load static strength after fatigue in hot-wet ageing.
Tolerance to CVID by sharp impact at 50 J was additionally proved by full size test for 500 flight hours with residual static

strength test up to limit load. Additional tests of composite lug structural elements have not shown fatigue strength reduction between test specimens with impact damages and with manufacturing discrepancies greater than production quality standards.
Full size lug structural elements were tested for evaluation of fatigue strength reduction due to rogue flaws in the lugs of the folding section. The specimens were flawed by 'V' grooves 0.5 mm deep, made by milling machine, simulating severe scratches in the lug contact sections. The scratches did not reduce the fatigue strength if they were made out of the net-tension area. An additional type of flaw was evaluated considering improper repair, simulated in the lug elements by 'U' grooves made by grinding wheel. The test data proved a relevant fatigue life reduction, but without additional reduction of the endurance value. Figure 12 compares the Wohler curves.
Full size tests of the Outboard Tension Link verified the capability of the composite plate to provide a redundant loading path after local failure of the titanium lug, figure 13, proving at least 40 hours of fail safe capabilities at maximum flight loads and residual static strength up to limit loads. An Equivalent capability is expected by the outer lug section of the Inboard Tension Link.
In both components the fatigue crack in the titanium lug is detectable by detailed inspection.

M.R. Civil Tension Link

The M.R. Civil Tension Link is a hybrid structure made by carbon and glass-epoxy composite plates, very similar to the Inboard Tension Link used on Navy configuration. This is a full composite component Civil Certified according to the Flaw Tolerance evaluation taking into account 50 J impact damages, manufacturing discrepancies and environmental ageing and proving ultimate load static strength after fatigue in hot-wet ageing.
Tolerance to CVID by sharp impact at 50 J was additionally proved by full size test for 500 flight hours with residual static strength test up to limit load, figure14.

Elastomeric Bearings

Two types of Elastomeric Bearings, Centering and Spherical, are installed on the M.R. Head, providing the drag, pitch and flap hinges of articulation and transmitting the blade shear loads to the Hub. The Spherical Bearing transmits part of the blade shear loads due to its radial stiffness and it can provide a redundant loading path for the flight completion in case of failure of the Centering Bearing, as proved by test.
The Tail Rotor Elastomeric Thrust Bearing allows blade motions and the coupling with the T.R. Hub.
The qualification tests provided data for the durability assessment and relevant evidences supporting the slow damage growth capability taken into account to address the periodic inspections. The driving parameter is the failure mode shown during tests with a progressive wearing out of the elastomer, with rubber loss.

An additional test was carried out to provide comprehensive data on the strength and stiffness degradation after fatigue damage, high temperature and contamination by potentially aggressive fluids, like hydraulic fluid and lubricating oil. The tests followed three phases: accelerated fatigue damage at amplified loads, damage propagation monitoring with and without contamination, residual static test for strength and stiffness evaluation up to limit load, figure 15. Initially two specimens were planned, but due to the very positive results all the test plan could be carried out with one specimen only, covering the routine inspection intervals for fluid contamination and improving to 900 flight hours the evaluation of slow structural degradation due to fatigue loading, initially set at 300 h. A life safety factor of 3 was considered due to structural redundancy.
The Tail Rotor Bearing was used since this provides the higher ratio between external surface exposed to contamination and rubber volume.

Tail Rotor Hub

The Tail Rotor Hub is made by a carbon fibre-epoxy loop windings with internal glass-epoxy plates, wrapped by a glass-epoxy cross ply. The Flaw Tolerance to 50 J impact damages, figure 16, manufacturing discrepancies and environmental ageing was proved by tests to address the retirement life, proving also ultimate load static strength after fatigue in hot-wet ageing.
A critical sections are protected in service by the blade cuff and therefore no additional investigation for Clearly Visible Damages was carried out.

Tail Rotor Blade

The Tail Rotor Blade is made by carbon fibre–epoxy. In addition to the Flaw Tolerance evaluation of the Spar, considering BVID up to 50 J, manufacturing discrepancies and environmental ageing, a specific test was carried out to address the fail safe capability for large cracks in the trailing edge skin, covering 10 flight hours of spectrum test factored for scatter and environment with the trailing edge removed from the specimen, figure 17. Residual static strength was then proved up to limit load.
A daily visual inspection for cracks in the trailing edge was required, without any special tool, covering the accidental damage on the blade skin.

Rear Fuselage

Three different variants of Rear Fuselage were designed according to three basic configuration of the aircraft: Civil, Utility and Naval. The structures are conventional metal fuselages made by Al-Alloys stringers and skin panels. The Utility variant has a ramp door for cargo operations.
Fail safe capabilities for the airframe were preliminary evaluated supporting 1000 hours of visual inspection and will be improved by a comprehensive analysis.

The most relevant evidences for damage tolerance were provided by the spectrum test of the Naval subcomponent, made by the Rear Folding Beams and the last bays of the fuselage. This configuration provides a foldable joint with the Tail Unit structure. In the safe life test a rig failure occurred during the folding phase, overloading the Rear Upper Folding Beam which failed with a large crack which cut through the Beam critical section, near the Actuator Lug, figure 18. The test was continued for the flight loading phase proving 50 hours of fail safe capability, with a life safety factor of 4. The crack is easily detectable by visual inspection while the Tail Unit is folded and this has an average occurrence of 4 hours in the usage spectrum.

The equivalent subcomponent for the Civil variant showed 500 hours of slow crack growth for fatigue crack starting from the fillet of the boss in the development configuration, figure 19. Inspection by Ultrasonic can detect the crack with the Tail Unit installed.

Tail Unit Structure

The composite Tail Unit is a structure made by panels of carbon-epoxy skins with honeycomb core. Metal attachments are used in the coupling areas with the gearboxes, the tailplane and the forward structure (the Rear Fuselage). The skins are jointed using both bonding and rivets, to provide redundant load path in case of weak bonding. The Tail Unit was substantiated by analysis and tests, using test data on structural elements, subcomponents and full size specimens representative of the structure in dry and environmentally aged conditions.

Tolerance to Barely Visible Impact Damages (BVID) was proved by static and fatigue tests up to conservative but still realistic energies established by an hazard assessment, with a maximum energy level of 50 J near metal attachments and a minimum of 10 J on upper sandwich panel, protected in service by the fairings.

Tolerance to manufacturing discrepancies was proved by test using items properly manufactured with artificial flaws, like Teflon inserts for delaminations and debondings.

Tolerance to moisture absorption due to hot-wet environment was demonstrated by static and spectrum tests of subcomponents after accelerated aging up to moisture saturation at 84%RH, since the low thickness skin could reach moisture saturation in service. This was determined by diffusivity calculations according to Fick's law at the worst hygrothermal environment assumed of 26°C of temperature and 84% RH.

After local failure caused by safe life tests, subcomponents were fatigue tested to evaluate their tolerance to delaminations, disbondings, rivet failures and cracks in the skins or in the metal attachments caused by amplified loading or intentionally done after the basic fatigue tests.

These tests were related to the vertical fin and the tailplane attachments area, figures 20 and 21. They proved no flaw growth or redundancy of the loading path in sections of load concentration.

Additional tests for the composite structure were carried out on damaged panels and structural elements as a relevant background for selection of artificial damages to be applied in the subcomponent and full size test. The comprehensive evaluation was carried out by the spectrum tests on the full size structure, after completion of the one lifetime safe life test with BVID and manufacturing discrepancies. Sharp impacts were added to the structure at the maximum energy established by the hazard assessment, causing Clearly Detectable Damages, mainly skin indentation and core crushing. Considering the low probability of having the combination of a highly damaged structure with bottom of scatter strength, the DT test was carried out with safety factors computed on a B-basis. An additional load amplification factor of 1.1 was applied to account for environmental conditioning. Residual static strength was checked at limit load.

Since the loading spectrum has relevant occurrences of both maneuver and vibratory loads, no practical application of slow flaw growth capability was envisaged, since damage would grow very fast, and the test was therefore carried out to check the no growth or the structural redundancy.

An inspection interval of 600 flight hours was proved for Clearly Detectable Damages.

CONCLUDING REMARKS

The helicopter loading spectra of the dynamic components are strongly affected by rotor induced loads, which have relevant amplitude and high frequency. If damage grows due to the flight loads from a size detectable in service, the crack propagation rate would require frequent inspections in single load path components.

For this reason most of the evaluations carried out for the EH101 main load path were focused on 'no damage growth' approach. This was determined for composite parts mainly by testing of damaged components, addressing the retirement life with BVID, environmental aging effects and manufacturing discrepancies covering the minimum quality item. The flaw tolerant evaluation was then improved by increasing the damage size considering Clearly Detectable Damages, and verifying an applicable inspection interval by no growth demonstrations or by proving structural redundancy.

The Enhanced Safe Life methodology was applied for metal parts to establish a time to crack initiation from relevant flaws, clearly detectable by inspection.

Based on this experience Agusta is addressing the flaw tolerance evaluation for NH90 and the substantiation criteria of the new helicopter AB139.

REFERENCES

1) J.P.Waller, R.S. McLellon, "U.S. Army Requirements for Damage Tolerance of Composite Helicopter Structure", 13th ICAF, 1985.

2) A. Cardrick, R. Maxwell, S. Morrow, "The Application of Fatigue Damage Tolerance Concepts to Helicopters: the Approach Proposed by the UK Military Airworthiness Authorities", American Helicopter Society Specialists' Meeting, 1984.

3) R.S. Whitehead, "Certification of Primary Composite Aircraft Structures", 14th ICAF, 1987.

4) J. W. Lincoln, "Damage Tolerance for Helicopters", 15th ICAF, 1989.

5) J. Rouchon, "Certification of Large Airplane Composite Structures, Recent Progress and New Trends in Compliance Philosophy", ICAS, 1990.

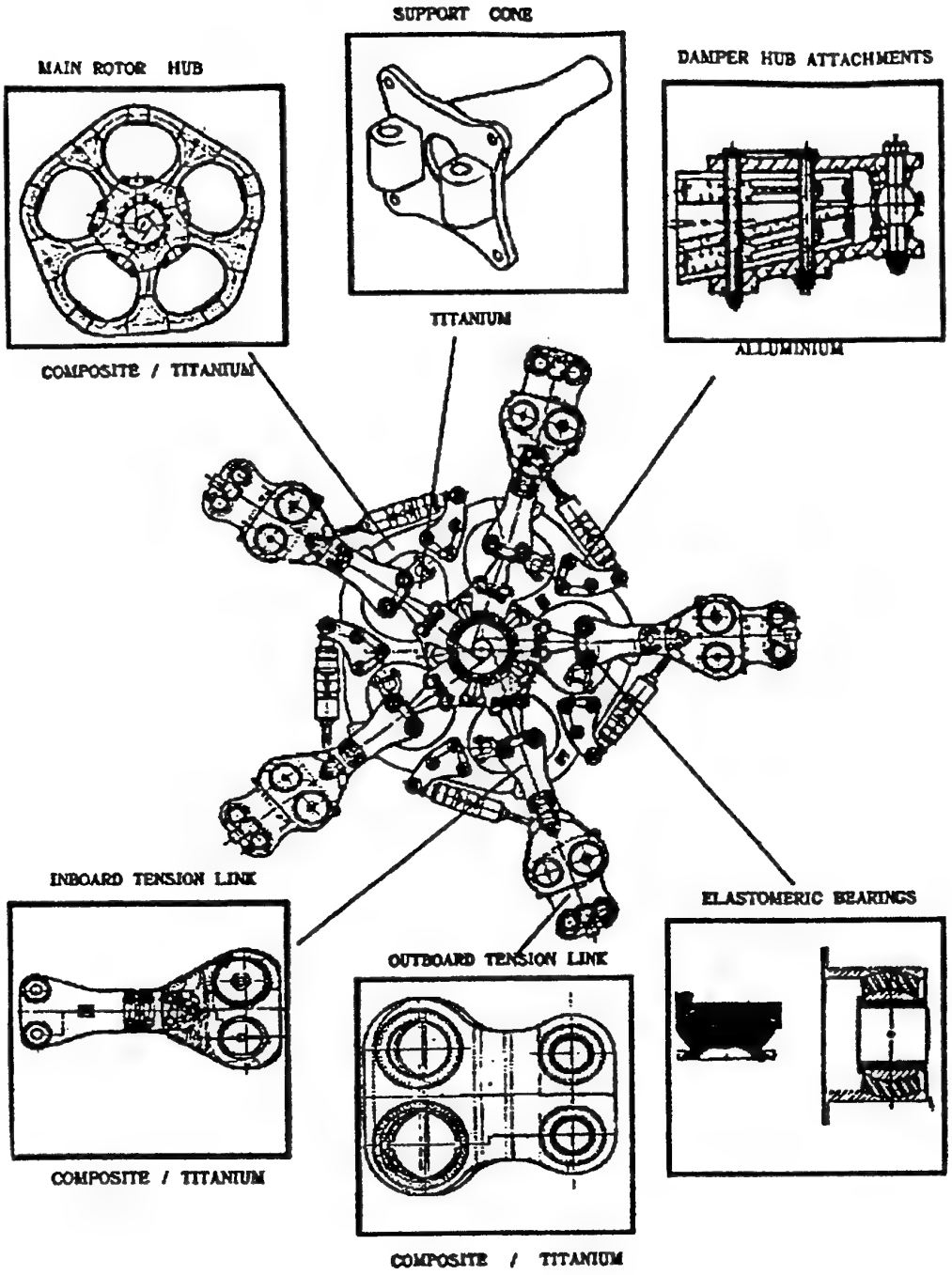

Figure 1 - EH101 Main Rotor Head - Components verified for Damage Tolerance capabilities.

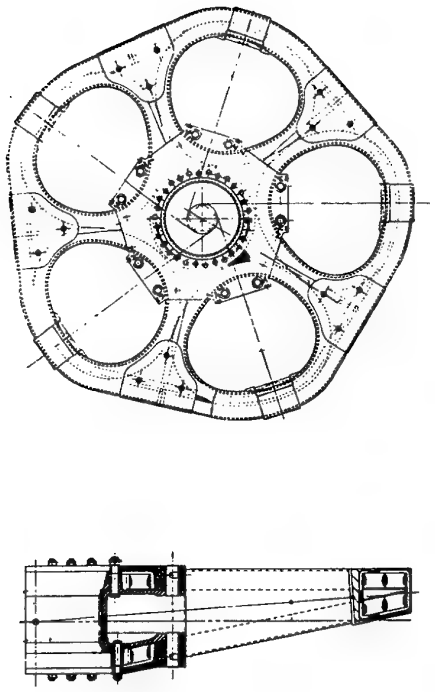

Figure 2 - Main Rotor Hub

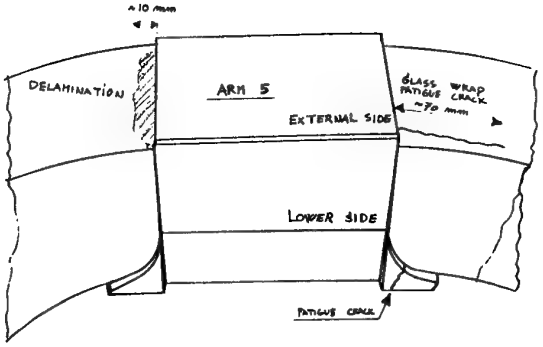

Figure 4 - M.R. Hub Damages after Safe Life Test

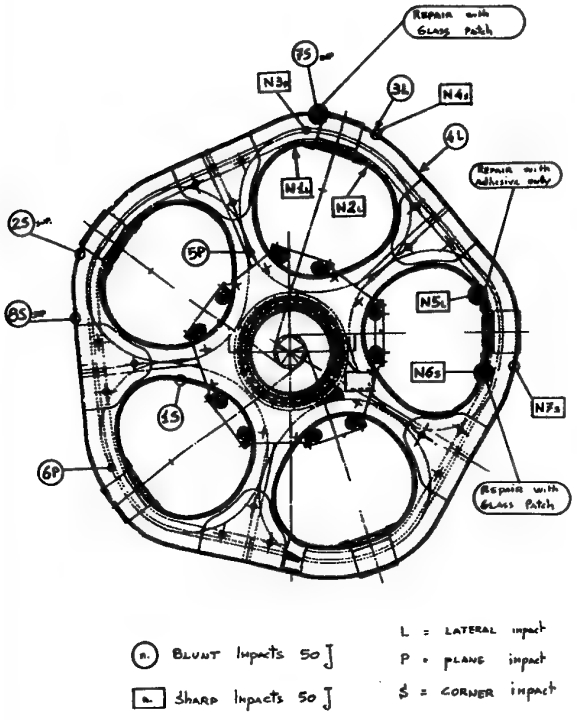

Figure 3 - M.R. Hub Impact Damages

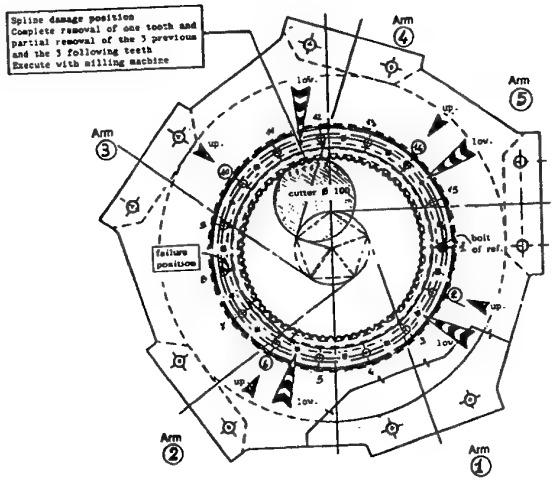

Figure 5 – Flaws in M.R. Hub Splined Coupling

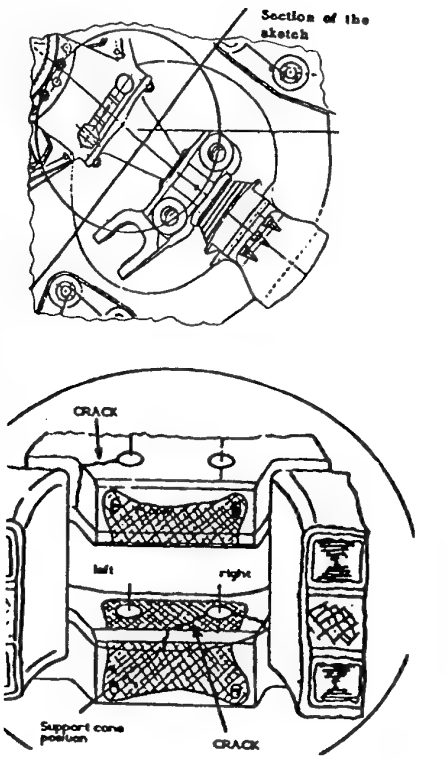

Figure 6 - M.R. Hub Flaws in Aluminium Plates and Titanium Core

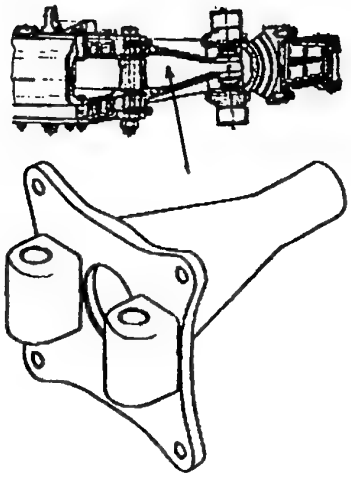

Figure 8 - M.R. Support Cone

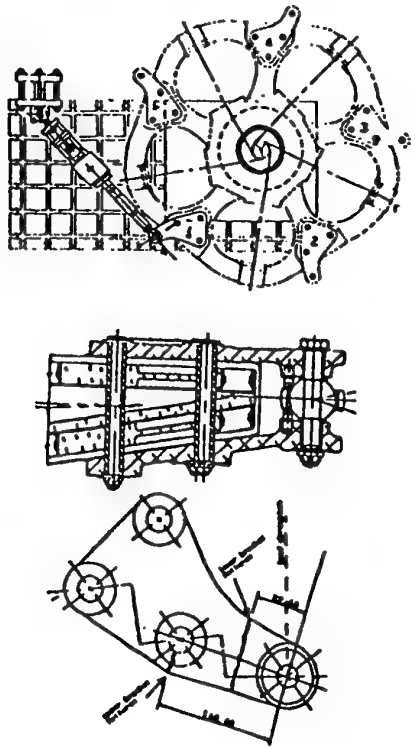

Figure 7 - M.R. Damper Hub Attachments

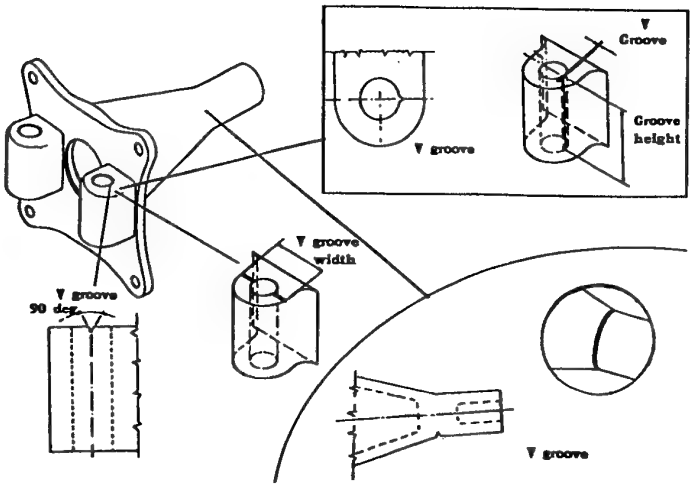

Figure 9 - M.R. Hub Support Cone - 'V' grooves of flawed components for fatigue tests

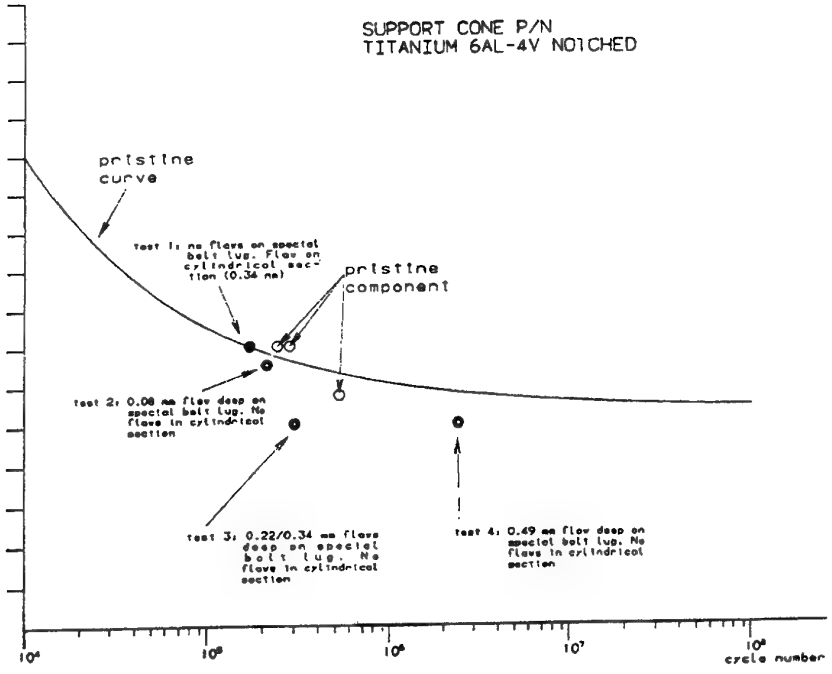

Figure 10 - M.R. Hub Support Cone Flaw Tolerance Data

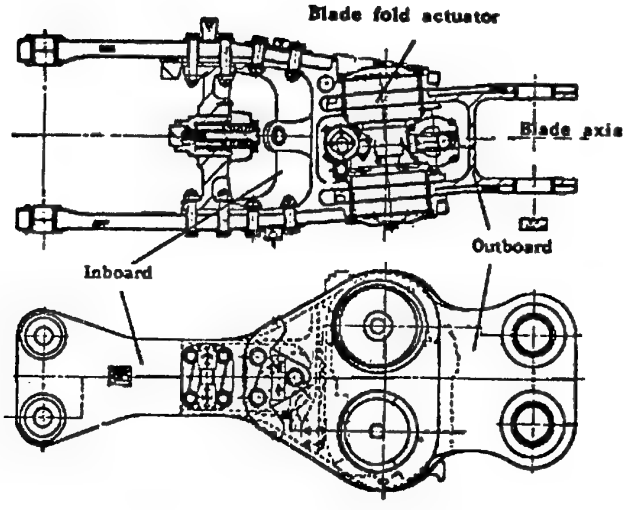

Figure 11 - M.R. Inboard and Outboard Tension Links

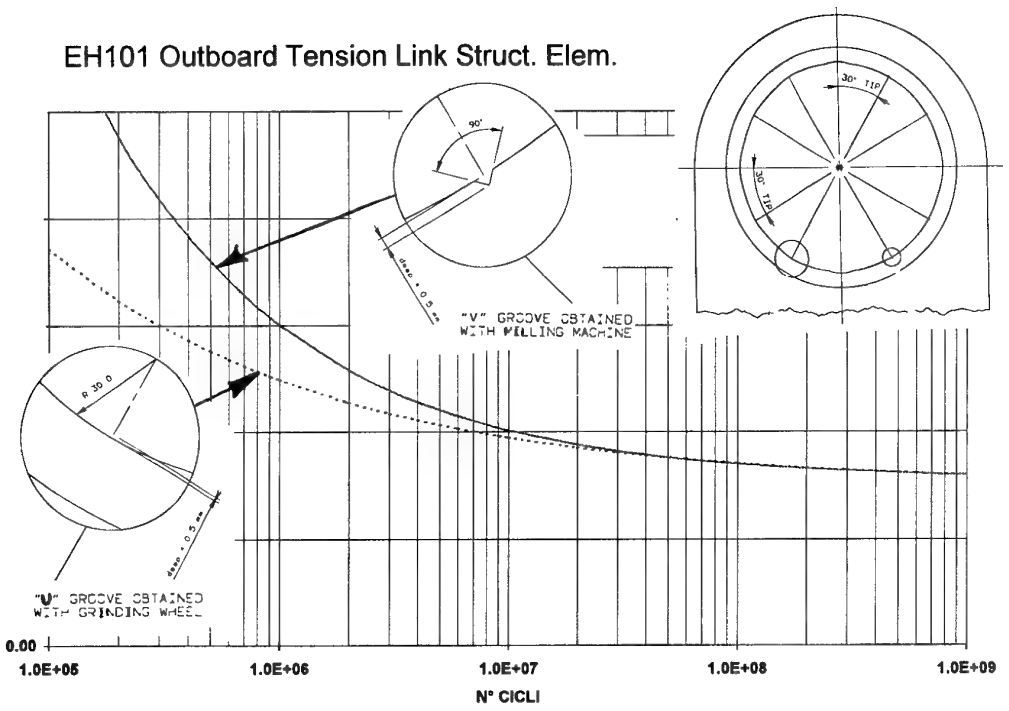

Figure 12 – Titanium Lug Elements - Flaw Tolerance Data

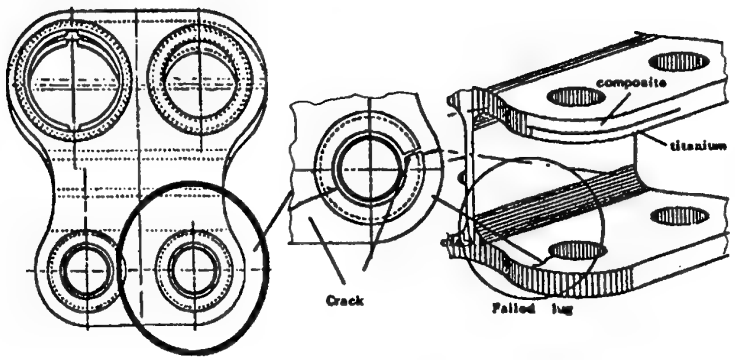

Figure 13 - M.R. Outboard Tension Link fatigue crack of the titanium lug

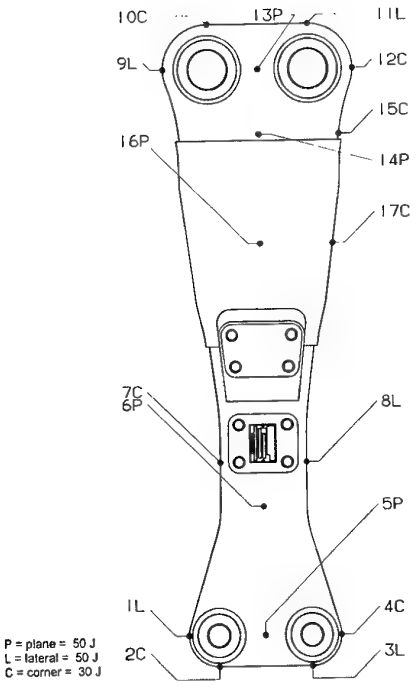

Figure 14 - M.R. Civil Tension Link Impact Damages for D.T. Test

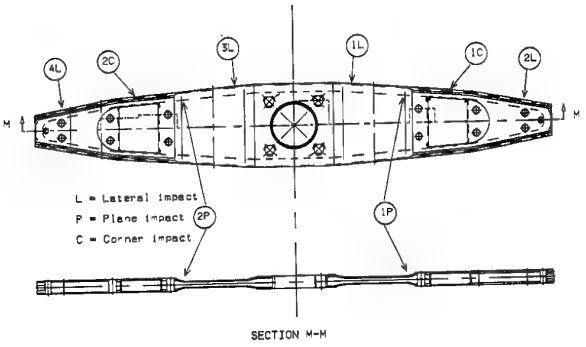

Figure 16 – Tail Rotor Hub Impact Damages for Test

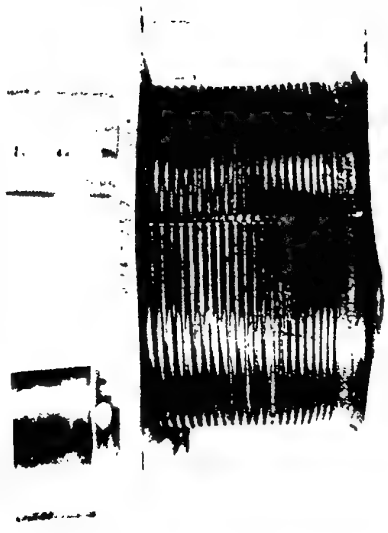

Figure 15 – Tail Rotor Elastomeric Bearing in Contamination Tests

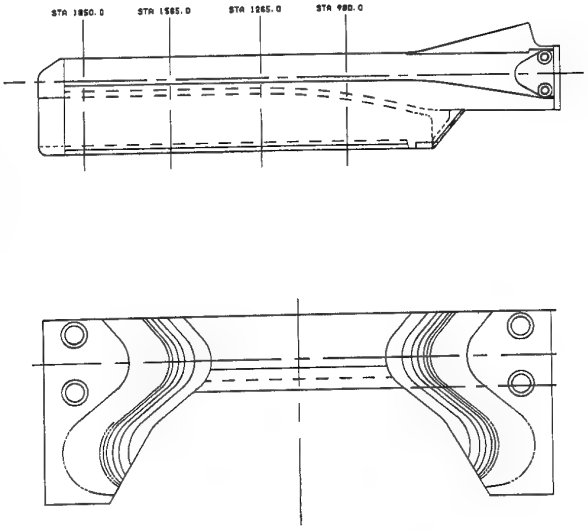

Figure 17 – Tail Rotor Blade D.T. of Trailing Edge

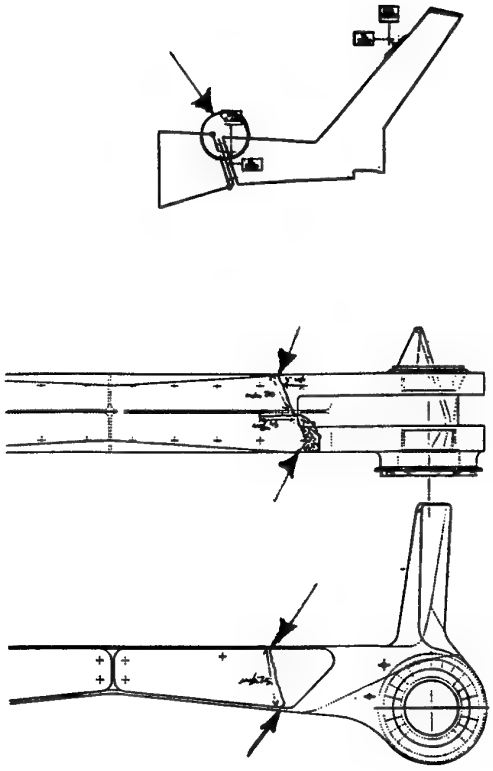

Figure 18 – Naval Rear Fuselage D.T. of Folding Beams

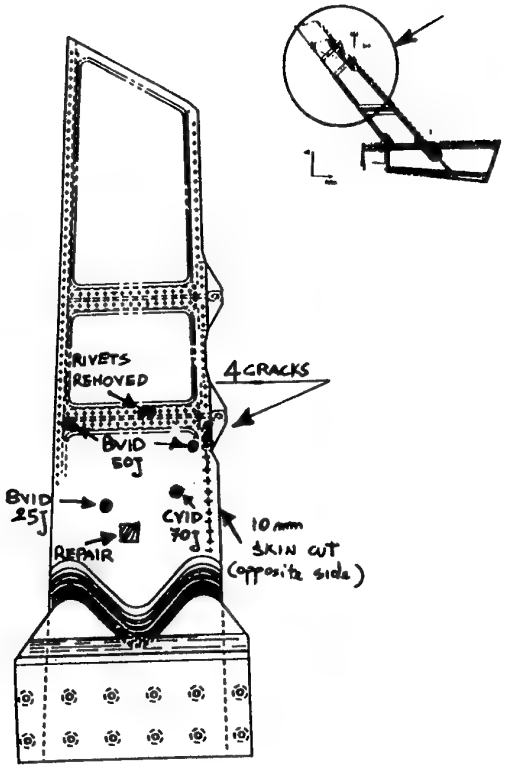

Figure 20 - EH101 Tail Unit subcomponent for flaw tolerance test - Fin Area and 90° Gearbox Attachments

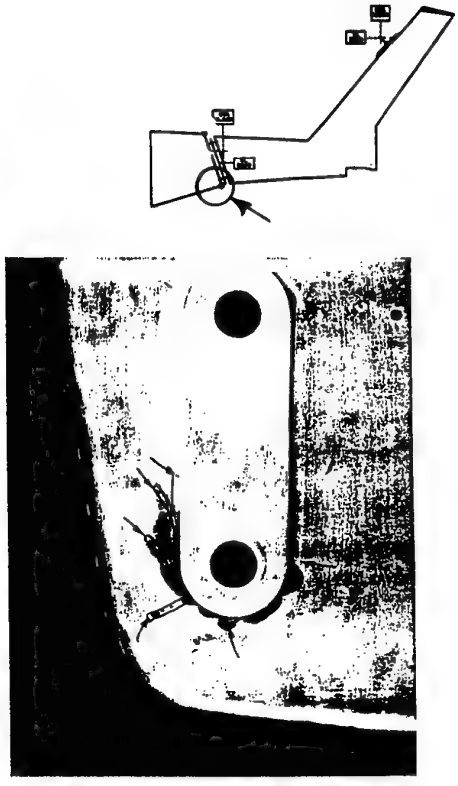

Figure 19 – Civil Rear Fuselage – End Fittings Slow Crack Growth

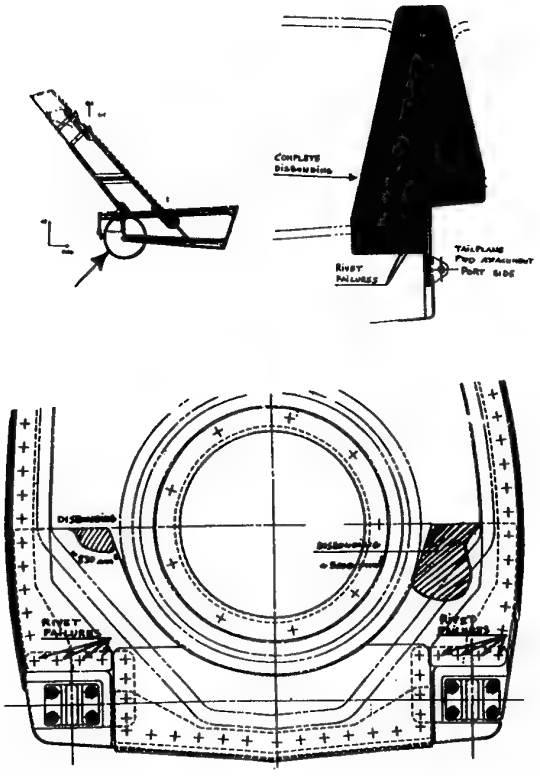

Figure 21 - EH101 Tail Unit subcomponent for flaw tolerance test - Tailplane FWD Attachments Area

Factor K Related To The Likelihood Of Accidental Damage And Visibility For Inspection		Likelihood of Accidental Damage		
		Probable	Possible	Unlikely
Visibility of SSI for Inspection	Poor	5	4.5	4
	Adequate	4.5	4	3.5
	Good	4	3.5	3

Factor H Related To The Sensitivity To Damage		Static Strength Margin Of Safety (MS)		
		MS ≤ 0.33	0.33 < MS ≤ 1.00	MS > 1.00
Safe Life (L)	L ≤ 2500	4	3	2.5
	2500 < L ≤ 10000	3.5	2.5	2
	10000 < L ≤ 40000	2.5	2	1.5
	40000 < L	2	1.5	1

SSI Accidental Damage Analysis By The Factored Safe Life Method:

Inspection Interval = (Undamaged SSI Safe Life) / (H × K)

Table 1 - SSI Accidental Damage Analysis by the Factored Safe Life Method -

COMPONENT	N° OF TESTS FOR SAFE LIFE OF METAL COMPONENTS AND FLAW TOLERANCE OF COMPOSITE COMPONENTS	N° OF TESTS FOR DAMAGE TOLERANCE
MAIN ROTOR HUB	2 Full Scale 10 Structural Elements	1 Full Scale
M.R. DAMPER HUB ATTACHMENTS	5 Full Scale	2 Full Scale
M.R. SUPPORT CONE	4 Full Scale	4 Full Scale
M.R. INBOARD TENSION LINK	4 Full Scale 30 Structural Elements	2 Full Scale 10 Struct. Elements
M.R. OUTBOARD TENSION LINK	3 Full Scale 20 Structural Elements	3 Full Scale 12 Struct. Elements
M.R. CIVIL TENSION LINK	2 Full Scale	1 Full Scale
MAIN AND TAIL ROTOR ELASTOMERIC BEARINGS	9 Full Scale	2 Full Scale
TAIL ROTOR BLADE	6 Full Scale	2 Full Scale
TAIL ROTOR HUB	2 Full Scale 30 Structural Elements	2 Full Scale

Table 2 - Main and Tail Rotor Test Plan for Damage Tolerance -

Application of Damage Tolerance to the EH101 Airframe

(April 1999)

David Matthew
GKN Westland Helicopters Ltd
Yeovil
England
BA20 2YB

Summary

This paper presents the work carried out by GKN Westland Helicopters in the damage tolerance evaluation of the EH101 airframe. A comprehensive programme of crack growth testing and analysis was undertaken and is described in this paper. A simplified analysis method was developed and used to predict flaw growth in the Main Load Path structure of the EH101. The analysis showed that high frequency vibratory loads exceed the crack growth threshold at relatively short crack lengths. This has been confirmed by a full-scale airframe crack growth test in which a 4mm crack was propagated under representative loading. These results have led to the adoption of the 'Flaw Tolerant (Enhanced) Safe Life' approach for fatigue critical components on the EH101 airframe.

1. Introduction

The EH101 is a modern medium/large three engined helicopter that has just entered service with the Royal Navy and will shortly enter service with the RAF. Civil rear-ramp utility variants are also in production. The EH101 has undergone an extensive development programme that included a full-scale factored load fatigue test. Failure modes observed during this test were eliminated from the production standard by design changes. A stand-alone fatigue test of a production standard lift frame, together with analysis using fine mesh finite element modelling, demonstrated the effectiveness of the changes. Safe Lives in excess of 10000 hours have been demonstrated for civil and military variants. Consequently, the EH101 has one of the best qualified helicopter airframes in service today.

As part of the civil certification activity of the EH101-510 variant, the Airworthiness Authorities also required damage tolerance evaluations of all fatigue critical components to be carried out. This is in keeping with the current thinking of regulatory bodies, who favour a flaw growth damage tolerance approach over Safe Life or even Flaw Tolerant Safe Life approaches.

A programme of work and analysis was commissioned to develop a viable approach to flaw growth damage tolerance for the Main Load Path structure of the EH101 Helicopter. Figure 1 shows the cabin fuselage and highlights the lift frames that form the Main Load Path structure. The frames are machined from cold compressed aluminium lithium forgings (8090 T852).

The programme of work involved a series of crack propagation tests to generate material data and to provide crack growth data that would enable the validation of the analysis method. Crack growth under a realistic usage spectrum at key sites on the Main Load Path was predicted and inspection intervals generated.

This paper presents the manner in which GKN Westland Helicopters have developed crack growth analysis methods for the EH101 Main Load Path. The initial conclusions drawn from applying this method to the EH101 are then discussed.

2. Test Programme

The testing programme involved a series of crack propagation tests. The initial phase of testing generated the required crack growth material data. In subsequent tests, cracks were grown in a variety of specimens ranging from structural elements to a full-scale airframe test.

The principle aims of the test programme were to:-

- Generate crack growth material data.
- Evaluate the crack growth characteristics of the aluminium-lithium Main Load Path components.
- Generate crack growth data under progressively more realistic geometry and loading.

The most effective method for introducing initial flaws in the test specimens was established by a series of coupon tests. Flaws were introduced by spark erosion or by using a 0.5mm grinding wheel. The effect of chemical etching and initial flaw size was also investigated. The main observations were as follows:-

- 25% higher loads were required to initiate cracks from ground flaws compared to spark eroded flaws.
- Chemical etching reduced the load required to initiate cracks by 5% at spark eroded flaws and by 7.5% at ground flaws.

Paper presented at the RTO AVT Specialists' Meeting on "Application of Damage Tolerance Principles for Improved Airworthiness of Rotorcraft", held in Corfu, Greece, 21-22 April 1999, and published in RTO MP-24.

- A higher stress intensity was required to initiate 1.3mm flaws compared with the 2.6mm flaws.

Each of the crack growth tests was modelled using linear elastic fracture mechanics and the analytical predictions compared with the test results. The modelling techniques were refined and the accuracy of the predictions established.

2.1 Generation of Material Data

The Main Load Path structure is machined from aluminium-lithium alloy (8090-T852). This material has been developed specifically to meet the requirements of GKN Westland Helicopters. The crack growth material data required for the damage tolerance evaluation was generated by the GKN Westland Helicopters Materials Laboratory.

Compact tension specimens were machined from production forgings and tested at R-ratios of 0.1, 0.4, 0.7 and 0.9 under constant amplitude load. This testing formed part of the collaborative project 'Robust Crack Growth Model for Rotorcraft Metallic Structures' funded by the UK Department of Trade and Industry as part of the LINK initiative.

The data generated by the testing included:-

- Crack growth rate versus stress intensity range (da/dN versus ΔK)
- Threshold stress intensity range (ΔK_{TH})
- Plane strain / plane stress fracture toughness (K_{IC} & K_C)

2.2 Structural Elements Tests

The purpose of these tests was to prove that the data derived from the CT specimens can be used in the analysis of complex structures. The tests also investigated the crack growth characteristics of the machined aluminium-lithium forgings on the EH101.

The structural element shown in Figure 2 represents the geometry of the roof frames in the region of a lightening hole. Six structural elements were tested under constant amplitude loading. Three structural elements were machined from aluminium-lithium alloy plate (8090 T8771) and three from a cold compressed aluminium-lithium alloy forging (8090 T852). Spark eroded initial flaws were located at either the lightening hole or the corner of the flange. A Potential Drop system was used to monitor crack growth.

A further two lightening hole structural elements were tested by Cranfield University under a complex variable amplitude load spectrum. Crack growth from an initial flaw at the edge of the lightening hole was monitored using a Potential Drop system.

As part of the DTI LINK project, the structural elements have been extensively analysed using various crack growth models. The analysis and conclusions are reported in Reference 1.

2.3 Full-Scale Component Tests

A production roof frame and side frame have also been tested with flaws at four locations (see Figure 3). The load was applied as a block loading programme representing the low frequency manoeuvre loads produced by forward flight, climb, and spot turn conditions. Each flaw site was tested sequentially and the crack growth monitored using crack growth gauges. Each flaw site was repaired using composite patches before beginning testing at the next flaw site.

Cracks were successfully grown at three out of four of the flaw sites. At the first three flaws, elevated loads and large initial flaws were needed to initiate crack growth. At the fourth flaw, located at a bolt hole, crack growth could not be initiated, even when the initial flaw was 5mm deep.

2.4 Full-Scale Complete Airframe Test

The final stage of testing was to grow a crack in the Main Load Path of a complete EH101 airframe (see Figure 4). The aim of this test was to identify the effect of any load redistribution and to more accurately represent the multiple mode loading that occurs in a complete airframe under flight loads.

The development standard fatigue test airframe, used in the safe-life fatigue qualification of the EH101, was retro-fitted with a production roof frame and fore/aft roof beam. High and low frequency loading was applied to the airframe using hydraulic actuators. The flaw was located on the top flange of the roof frame and the flaw growth monitored using crack growth gauges.

A crack was initiated from an initial corner flaw of 4mm with large amplitude crack initiation loads. Once initiated, the crack was grown under high and low frequency loads representative of a level flight cruise condition. At a length of 10.5mm, fast fracture occurred and the crack grew as far as the nearest lightening hole where it arrested. Testing has resumed with the aim of establishing if a crack can be initiated from the lightening hole. A crack self-initiated from and total failure of the frame occurred after very few load cycles. Figure 5 shows the crack propagation up to fast fracture and the final state of the crack.

The test demonstrated that there was very little load redistribution up to the point when fast fracture occurred. After the partial failure to the lightening hole, the load in the adjacent structure increased by about 20%.

3. Analysis Method

The tests described in Section 2 generated a large amount of measured crack growth data with progressively more realistic geometry and loading. The results provided a bench mark to enable fracture mechanics analysis techniques to be developed.

Linear Elastic Fracture Mechanics (LEFM) is used extensively in fixed-wing applications to successfully apply the 'Fail Safe Considering Flaw Growth' approach to damage tolerance. The successful application of this approach to helicopter metallic structures is complicated by a number of factors:-

- Helicopter load spectra contain large amplitude high frequency vibratory loads - fixed wing spectra contain predominantly low frequency manoeuvre loads.
- Critical crack lengths in helicopter components are much shorter than in fixed wing components.
- The versatility of helicopters results in missions that are more complex and involve more manoeuvres than in typical fixed wing operations.

In order to apply the 'Fail Safe Considering Flaw Growth' approach an economically viable analysis method was required that was suitably conservative.

The first step was to select suitable crack growth modelling software with the following features:-

- Commercially available and fully supported
- Allow entry of complex load spectra
- Allow entry of user defined stress intensity solutions
- Retardation and acceleration modelling
- Conservative
- Simple to use

These requirements led to the selection of KRAKEN which is a module of the nSoft software produced by nCode International Ltd. KRAKEN uses a modified Willenberg model to model the effect of load interaction on crack growth rates.

The three inputs necessary to predict flaw growth using a model such as KRAKEN are:-

- Material data
- Load Spectrum
- Stress Intensity Factor (Compliance Curve)

The methods used to derive each of these inputs for the analysis of the test results, and in the damage tolerance evaluation of the EH101, are described in the following subsection.

3.1 Material Data

Crack growth material data at R-Ratios of 0.1, 0.4, 0.7, and 0.9 were generated using compact tension specimens. KRAKEN represents the growth rate versus stress intensity range relationship in the following manner (Reference 2):

$$\frac{da}{dN} = C\Delta K_{eff}^{m}$$

$$\Delta K_{eff} = K_{maxeff} - K_{mineff}$$

$$K_{maxeff} = K_{max} + K_{fs}$$

$$K_{mineff} = \text{Greater of } K_{cl} \text{ or } K_{min}$$

The equations have additional terms to represent retardation, acceleration, short cracks etc.; these have been omitted for clarity.

ΔK_{eff} = Effective stress intensity range
K_{fs} = Additional stress intensity from static fracture modes
K_{max} = Apparent maximum stress intensity
K_{min} = Apparent minimum stress intensity
K_{IC} = Material fracture toughness
K_{cl} = Stress intensity at crack closure

C and *m* are material parameters t calculated by regression analysis of the growth rate and stress intensity range measured by the CT specimen tests.

The threshold stress intensity range for aluminium-lithium alloy (8090 T852) was measured at R-Ratios of 0.1, 0.4,0.7 and 0.9 and represented in KRAKEN as shown by Figure 6.

3.2 Stress Intensity Solutions

The most time consuming phase in the analysis process is often the generation of stress intensity solutions. A number of methods have been used to generate stress intensity solutions. Various methods were used in the analysis of the structural elements and 'single frame test'; predicted crack growth was compared with that measured on test to assess the relative accuracy of each method. In Figure 7, stress intensity solutions generated for the lightening hole structural element are compared. It can be seen that the 3D finite element model gives the best representation of the stress intensity solution generated from the test data.

As part of the DTI Link Project, 'Robust Crack Growth Model for Rotorcraft Metallic Structures', the generation of stress intensity solutions using boundary elements was also investigated. This investigation showed that this method is promising but is, at present, very time

consuming and the results too difficult to interpret. For these reasons, boundary element analysis was not used in the analysis of the Main Load Path.

The damage tolerance assessment of the main load path had to be completed in a short time scale. Ideally, each flaw site would have been modelled using fine mesh finite element models and the stress intensity solutions calculated by the strain energy release rate method. This method was used at locations that could not be approximated to a standard solution. Other locations were analysed using standard or test generated stress intensity solutions.

The critical locations of the main load path can be divided into four types of geometric feature. The methods used to derive the stress intensity solution for each type of feature were:

Lightening holes	Calculated from a crack growth test on a structural element by matching growth rates.
Flanges	Derived using standard solutions for a corner crack and through crack.
Cutouts	Fine mesh 2D FE model used to derive solution using the strain energy release rate.
Bolt holes	Derived from standard solutions for loaded bolt holes.

3.3 Load Spectra

A spectrum of low frequency manoeuvre load and high frequency vibratory load was generated for each of the analysed locations. The spectra were derived from measured flight strains. High frequency were those occurring at the blade passing frequency of 17.85 Hertz.

A load survey was undertaken using production EH101 aircraft incorporating comprehensive strain gauge installations. The load survey included each manoeuvre in the civil variant usage spectrum. Conservatively, the maximum vibratory load measured in a manouevre was assumed to apply for the whole manoeuvre. In KRAKEN, the load history effect has been shown to have very little influence on crack growth under helicopter load spectra. For this reason, the sequencing of the load spectra was ignored. Figure 8 shows a load spectrum for a typical roof beam strain gauge.

The relationships between the stress at the analysis locations and the stress at the strain gauges were calculated using a fine mesh finite element model of the EH101 airframe. This relationship was used to derive a stress spectrum at the flaw.

4. Analysis of Cabin Main Load Path

The crack growth under the aircraft loads was predicted at each analysis location using KRAKEN. Inspection intervals were calculated based on the predicted flaw growth.

4.1 Selection of Flaw Sites

The selection of flaw sites was based on experience from the Main Load Path airframe fatigue test and by using a fine mesh finite element model of the airframe. The most highly stressed of each type of feature was identified using the finite element model. Typically a flange, lightening hole, and bolt hole were analysed on each component.

4.2 Initial Flaw Size

The crack growth was predicted from 1.3mm (0.05 inch) radial corner cracks. This is in accordance with USAF General Specification for Aircraft Structures, MIL-A87221.

4.3 Failure Criteria

The component was considered to have failed when the first of the following conditions occurred:-

- The crack tip stress intensity at limit load exceeded the fracture toughness, leading to fast fracture.
- Limit load caused nett section yield.

At all of the Main Load Path analysis locations, fast fracture was the critical factor. The limit load at an analysis location was identified using a finite element model of the aircraft that was run with all limit load cases.

4.4 Generation of Inspection Intervals

Threshold and repeat inspection intervals were calculated from the predicted flaw growth. The threshold inspection interval was one-third of the crack growth period from the initial flaw size to the detectable flaw size. The repeat inspection interval was one-third of the crack growth period from the detectable flaw size until failure. The analysis only considered growth in the primary component.

The detectable flaw size was based on an eddy current inspection method.

5. Discussion of Results

The analysis of the EH101 Main Load Path predicted that the vibration levels present in helicopter airframes are sufficient to cause rapid growth at relatively short crack lengths. This has been confirmed by the result from the full-scale airframe test. The lightening holes tended to exhibit slow initial growth because of the thickness of the flange around the hole. Even with the slow initial flaw growth, the time for the cracks to grow to failure was not sufficient to allow the generation of acceptable inspection intervals.

This analysis was conservative on several grounds; these include:-

- The KRAKEN fit to the growth rate versus stress intensity material data can be conservative at high R-Ratios.
- The representation of the vibratory load in the load spectra is conservative for transient manoeuvres where the amplitude does not remain constant.
- No account was made for load redistribution unloading a component as its stiffness reduces.

Refining the analysis would reduce these conservatisms but this would not affect the point at which high frequency load becomes damaging. For the 'fail-safe design considering flaw growth' approach to be viable, high frequency loads must be of a magnitude that ensures that they are not damaging until much greater crack lengths. The point at which the high frequency load exceeds the crack growth threshold is therefore the crucial factor.

The Main Load Path analysis considered flaw growth in the primary load path only. The regulations permit failure of the primary load path if it can be demonstrated that the secondary load path can still sustain limit load. The limit load carrying capability of the EH101 airframe would be compromised by the total failure of the roof frame tested in the full scale airframe test. The full scale test has confirmed that the total failure would occur, a damage tolerance approach based on flaw growth in the secondary load path would therefore not be viable.

6. Conclusions

The EH101 has one of the best qualified helicopter airframes in service today. However, the work reported in this paper shows that the 'Fail Safe Design Considering Flaw Growth' approach to damage tolerance is not viable. It is probable that this conclusion is true for all helicopters and not just the EH101.

The quick and conservative method used to analyse the EH101 Main Load Path generated short inspection intervals. The short inspection intervals were due to high frequency loads causing rapid crack growth at relatively short crack lengths. The full-scale airframe test confirmed that the predicted growth rates are realistic and that the roof frame would completely fail. The complete failure of the roof beam rules out a secondary load path flaw growth approach to damage tolerance. For this reason a 'Fail Safe (Enhanced) Safe Life' approach has been adopted for the EH101 Main Load Path.

GKN Westland Helicopters have demonstrated that accurate predictions of crack growth in helicopter metallic structures are possible. However, due to the complex nature of helicopter structures and load spectra, the generation of accurate predictions is very time consuming.

The DTI LINK Project 'Robust Crack Growth in Rotorcraft Metallic Structures' (Reference 1) has demonstrated that crack growth models need to be developed further before they can be reliably applied to helicopter structures. A number of issues are being addressed by a collaborative project with the same partners as the DTI LINK Project. The project will focus on the following:-

- Stress intensity solution generation.
  Existing generation methods involving fine mesh finite element or boundary element analysis are very labour intensive.

- Crack growth model
  Models need to accurately predict growth rates over a range of R-Ratios. KRAKEN, for instance, can be very conservative with high R-Ratio loads.

- Threshold stress intensity
  Little is known about the scatter that can be expected in threshold data. Also, the threshold behaviour of shorter cracks is not fully understood.

7. References

1. DTI LINK Project - "Robust Crack Growth Model for Rotorcraft Metallic Structures" - Final Report GKN Westland Helicopters Ltd. Research Paper RP1011 June 1998

2. nSoft Version 4 "KRAKEN Users Manual" 1996 nCode International Ltd., Sheffield UK.

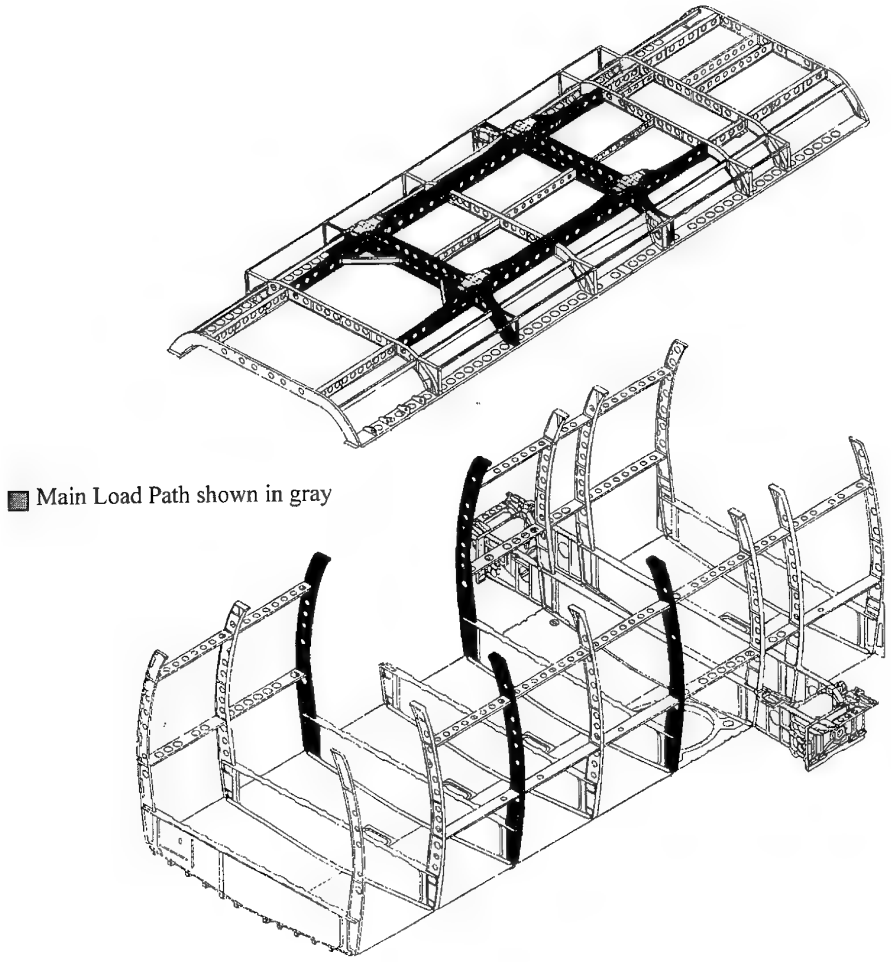

Figure 1 Main Load Path Structure

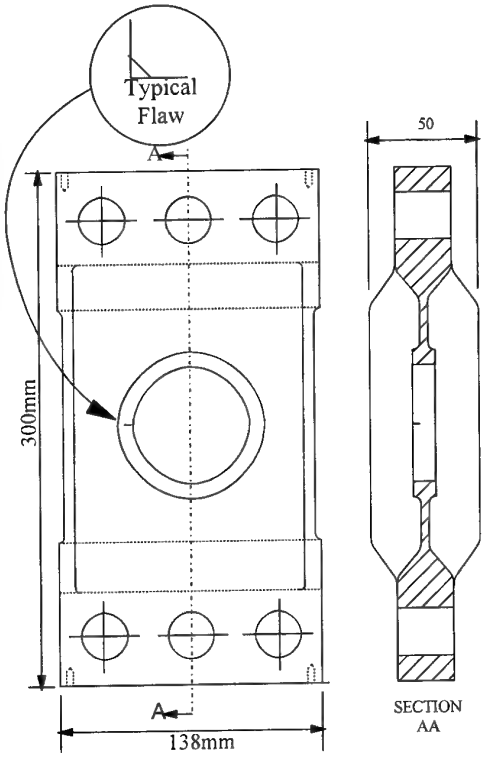

Figure 2 Lightening Hole Structural Element

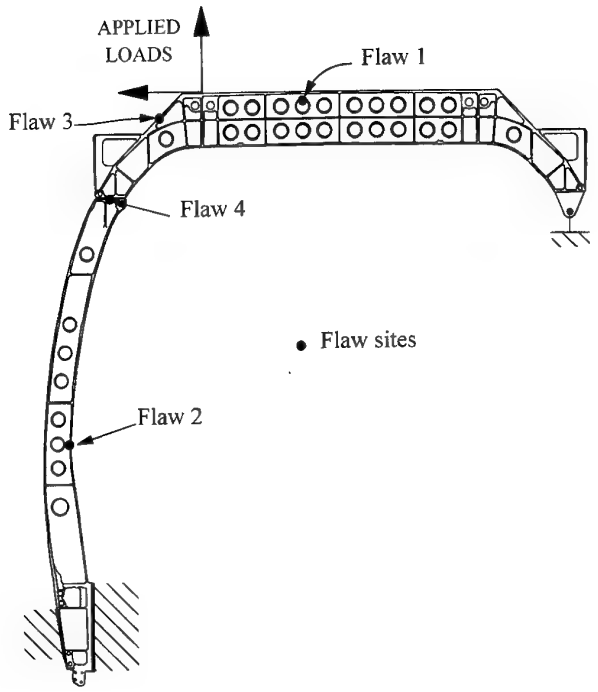

Figure 3 Single Frame Crack Growth Test

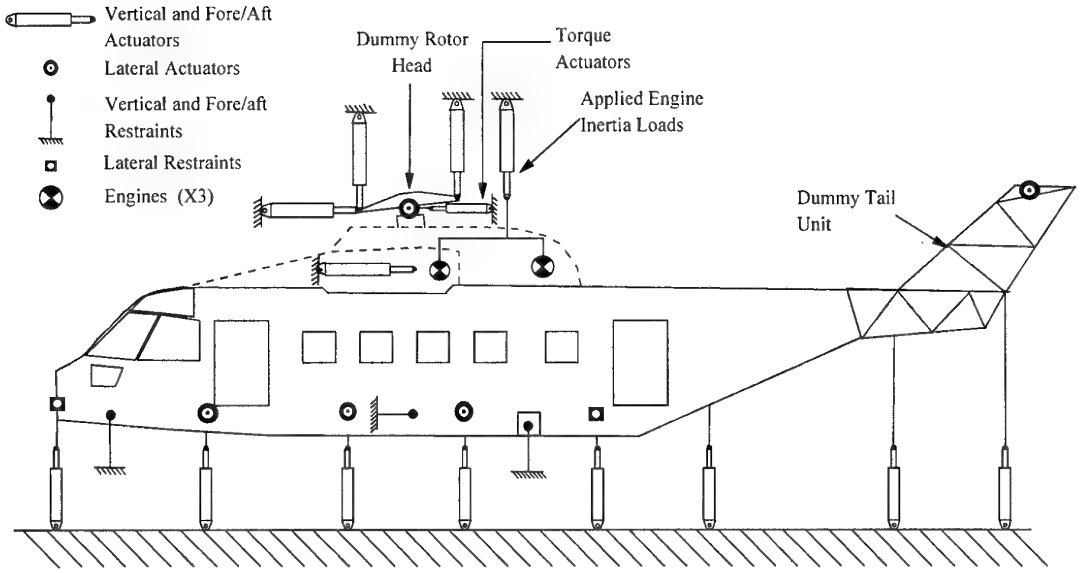

Figure 4 Full AIrframe Fatigue Test Rig

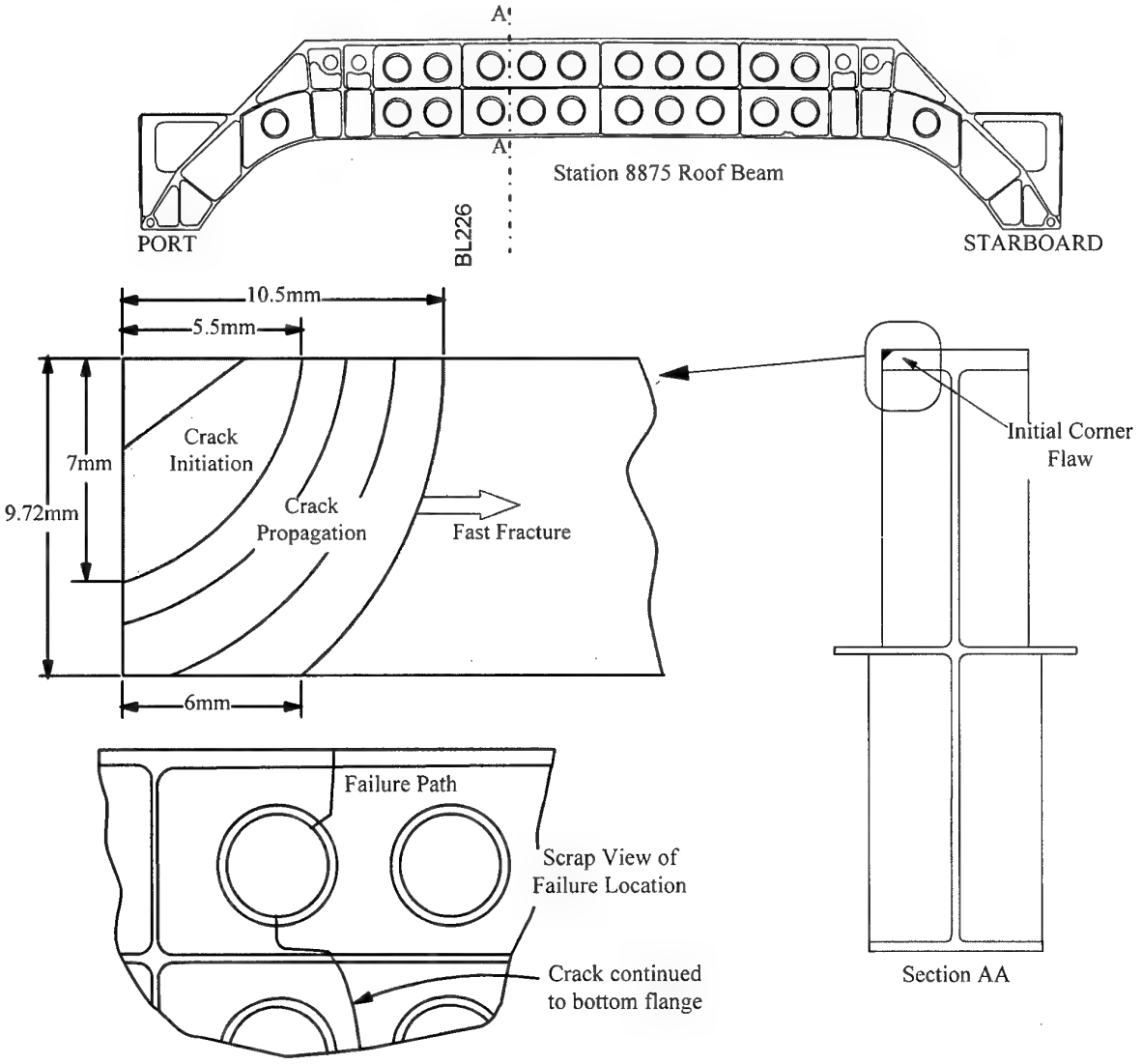

Figure 5 Full AIrframe Fatigue Test - Crack Propagation

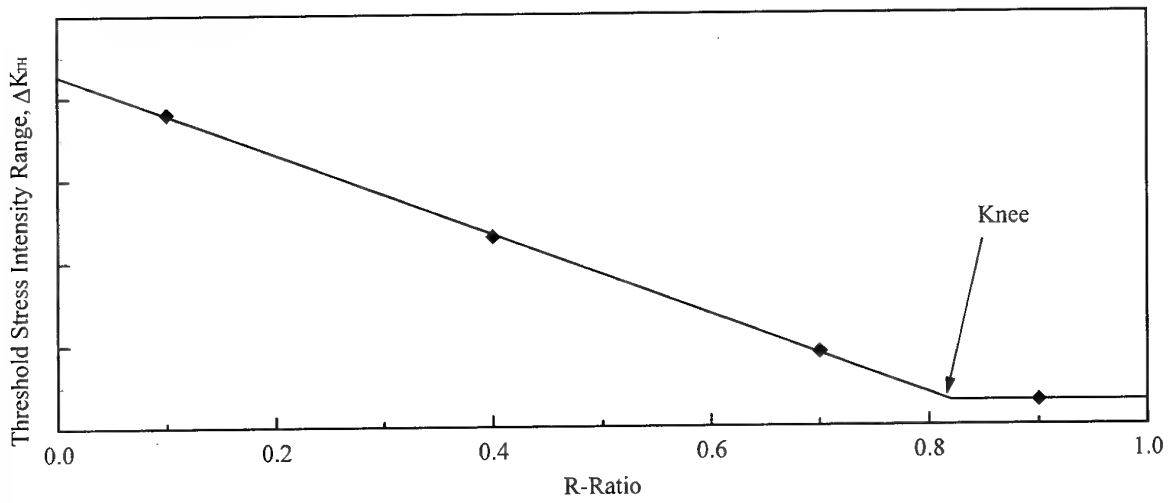

Figure 6 Kraken Representation of ΔK_{TH}

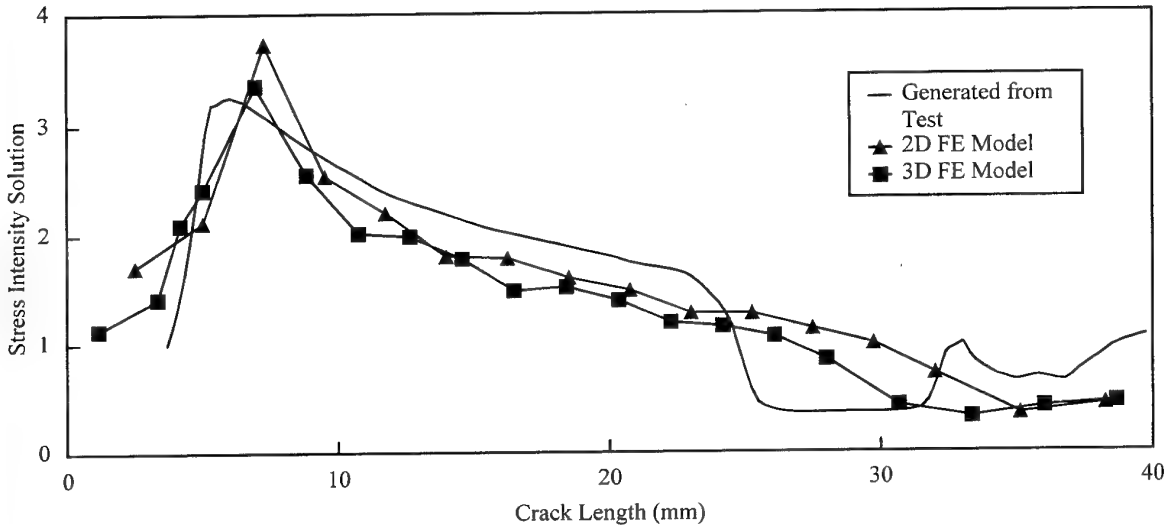

Figure 7 Stress Intensity Solutions for a Flanged Lightening Hole

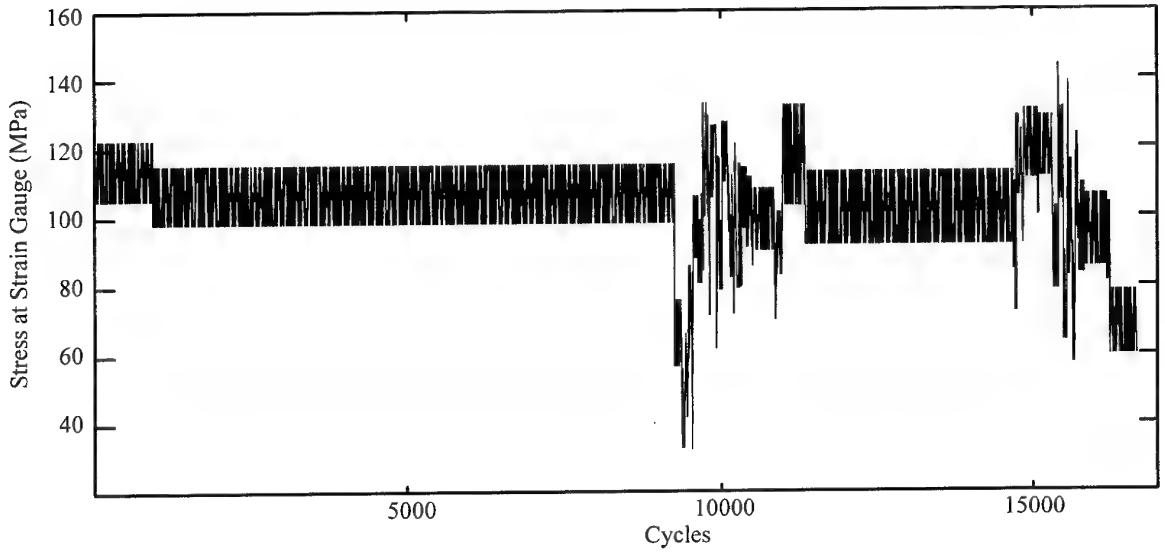

Figure 8 Typical Load Spectrum

Fatigue Substantiation and Damage Tolerance Evaluation of Fiber Composite Helicopter Components

H. Bansemir, S. Emmerling
Eurocopter Deutschland GmbH
81663 München, Germany

ECD-0096-99-PUB

ABSTRACT

Helicopter rotor systems are dynamically loaded structures with many composite components such as main and tail rotor blades and rotor hubs. The new civil helicopter EC135 has a bearingless main rotor system certified according to the 'Special Condition for Primary Structures Designed with Composite Material' of the German airworthiness authority LBA containing increased safety demands. This special condition addresses subjects like

- demonstration of ultimate load capacity including consideration of manufacturing and impact damages
- fatigue evaluation for parts suitable or unsuitable for damage tolerance method and the related inspection procedures
- investigation of growth rate of damages that may occur from fatigue, corrosion, intrinsic and manufacturing defects or damages from discrete sources under repeated loads expected in service
- residual strength requirements
- consideration of the effects of material variability and environmental conditions like hot/wet strength degradation etc.
- substantiation of bonded joints

The fatigue tolerance evaluation and damage tolerance substantiation for composite structures are shown in this paper. The fulfillment of the 'Special Conditions' is demonstrated for the main rotor blade of the EC135.

TABLE OF CONTENTS

1. INTRODUCTION

In 1967 the BO105, a product of the former helicopter division of MBB, now Eurocopter Deutschland, flew for the first time. Three years later this light twin helicopter was certified by the German Luftfahrtbundesamt (LBA). Up to now almost 1500 BO105 multipurpose helicopters have been manufactured and are flying in more than 40 countries. The worldwide first serial hingeless main rotor system was a key element of this helicopter, using the advantages of the newly developed fiber glass technology. Thus the flapping and lead-lag hinges could be eliminated. The innovative rotor design included new materials such as titanium for the rotor hub and fiber glass epoxy for the main and tail rotor blades. The substitution of the hinges was a big step towards weight reduction and cost-saving due to the reduction of parts. Another benefit of the rotor system was the improved handling qualities and flight manoeuverability especially in gusty weather conditions. The pitching motion, however, is still carried out using roller bearings, which require some effort in manufacturing and service.

The first flight of the BK117 of MBB / Kawasaki Heavy Industries took place June 13, 1979. Since that time about 375 helicopters are flying worldwide. The rotor system of this helicopter is identical to the BO105 except the rotor blade design which includes a different geometry but mainly equivalent glass/epoxy and carbon/epoxy composite materials.

Figure 1: The Multi-Purpose Helicopters BO105 and BK117

In 1991/92 Eurocopter started the development of the multipurpose light twin helicopter EC135. The main rotor was derived from the BO108 technology (Ref. [1-4]), whereas the tailboom with the Fenestron anti-torque system was developed by Eurocopter France. The first prototype carried out its maiden flight in February 1994, powered by two Turbomeca Arrius 2B engines, whereas the second prototype began flight testing two months later, powered by the alternative Pratt & Whitney PW206B engines.

After extensive testing of three prototypes, structures and systems and with the help of validated analysis, the type certification was issued in June 1996 by the LBA and in July 1996 by the DGAC and FAA. Since that date EC135 helicopters with certified basic and optional equipment have been delivered to customers all over the world.

2. DYNAMICALLY LOADED ROTOR BLADES

The basic design features of the multi-mission helicopter EC135, a 3D drawing and the overall dimensions, are shown in Figure 3 and Table 1.

Paper presented at the RTO AVT Specialists' Meeting on "Application of Damage Tolerance Principles for Improved Airworthiness of Rotorcraft", held in Corfu, Greece, 21-22 April 1999, and published in RTO MP-24.

Figure 2: The New Multi-Mission Helicopter EC135

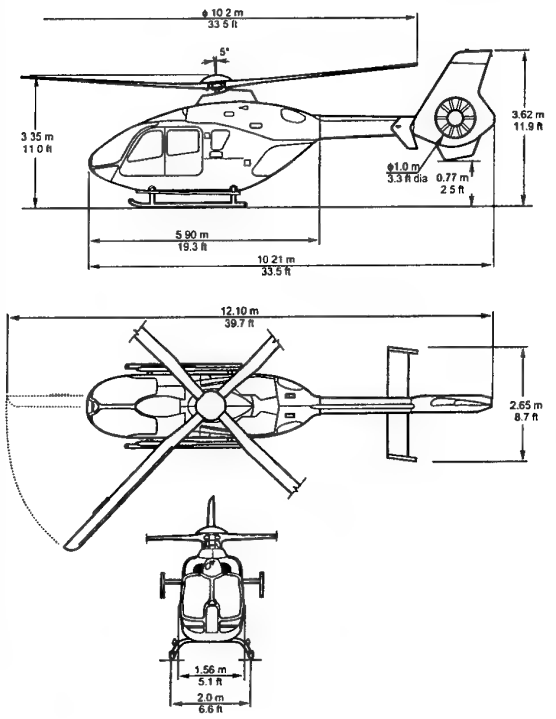

Figure 3: 3D-View Drafting of the EC135

Main emphasis was laid on the design of the dynamic components in order to achieve unlimited life with high flaw tolerance. Thus the direct operating costs can be reduced. Most of the components were designed for on-condition maintenance.

One of the most significant development features of the EC135 is the Bearingless Main Rotor (BMR) shown in Figure 4. The BMR shows a 50 kg weight reduction and 40 % less parts count compared to the BO105 rotor. The fully composite design (fiber glass and graphite epoxy) has characteristic fail safe design features such as a blade root attachment of the flexbeam consisting of two double lugs and a two load path attachment of the tuning masses to the blade. The flexbeam of the BMR shows an equivalent flapping hinge offset of about 9% of the blade radius. The rotor is a soft inplane design. The elastomeric damping devices provide sufficient inplane damping and the system control cuff - flexbeam - control rod produce adequate pitch-lag coupling [4].

Whereas the rotor hub of the EC135 has an exceptionally simple design, the structure of the blade root has become rather complicated as it has to take on the tasks of the hinges and bearings of a conventional rotor. This blade root is also called flexbeam and is the key element of the bearingless rotor. A skilful design, however, allows the local separation of the different tasks in the flexbeam.

Table 1: Main Characteristics of the EC135 with Arrius 2B1 Engines

Empty Weight of Aircraft	1465	kg	3230	lbs
Max. Take-Off Weight	2720	kg	6000	lbs
MTOW with External Load	2900	kg	6393	lbs
Max. Continuous Power	2x 283	kW		
Take-Off Power	2x 308	kW		
2.5 min OEI	1x 411	kW		
Rotor RPM	100 – 104	%		
Blade Tip Speed	211 – 219	m/s		
Max. Cruising Speed SL ISA	257	km/h	139	kts
Never Exceed Speed SL ISA	278	km/h	150	kts
Hover in Ground Effect	4040	m	13250	ft
Hover Out of Ground Effect	3100	m	10200	ft
Rate of Climb	8.4	m/s	1650	ft/min
Maximum Range	620	km	335	nm
Maximum Endurance	4:33	hrs		

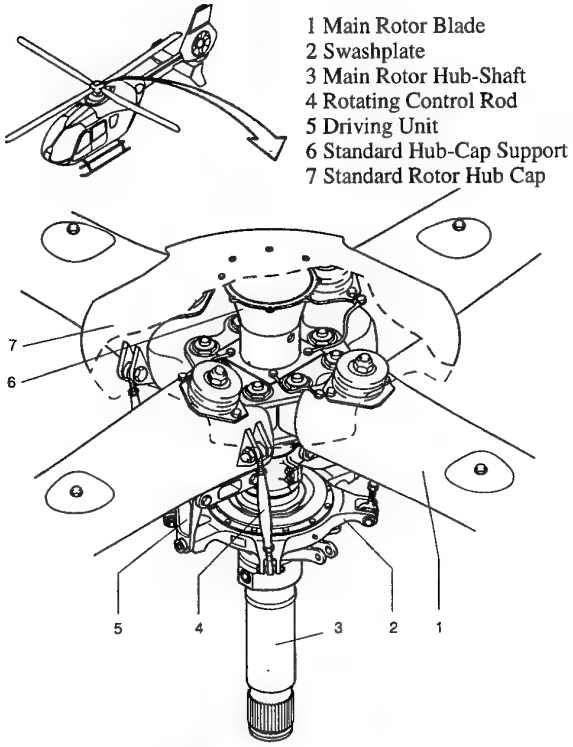

Figure 4: The Bearingless Main Rotor System with Elastomeric Dampers

The blade and its inner part are shown in the Figures 5 and 6. It is a GFRP (glass fiber reinforced plastic) prepreg design using E-Glass and a 120°C epoxy system. It consists of unidirectional tapes orientated in the longitudinal direction. These are mainly responsible for the longitudinal and bending stiffnesses and carry the greatest part of the centrifugal force and the bending moments, whereas the ±45° layers in the shear

web and the blade skin have to carry the greatest part of the shear loads including torsional moment.

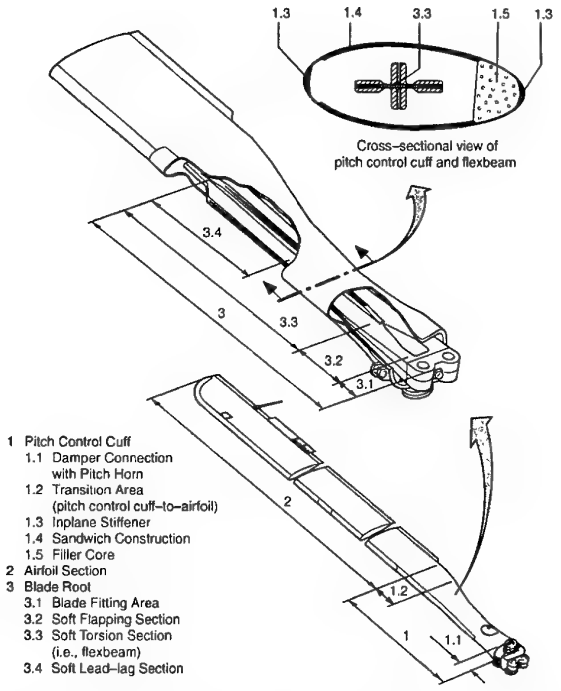

Figure 5: The Blade of the Bearingless EC135 Main Rotor

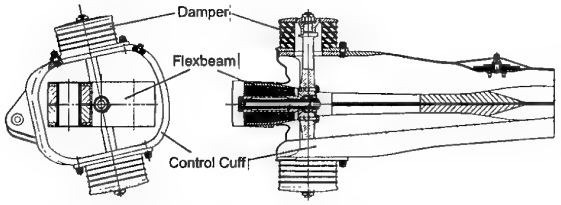

Figure 6: Blade Attachment Area with Control Cuff and Dampers

At radius station R = 110 mm the blade is connected with the help of two bolts to the rotor hub. The loads are transferred via two double lugs at the relatively stiff blade attachment area. A tapered transition area leads to the flat 'flapping hinge' section. This section has to allow the flap angles by bending.

In the following transition area the layers are shifted to the cruciform shape of the torsional element. This has a short length of about 0.5 m and replaces the blade bearings. Its slim and deeply slit cruciform cross section results in an extremely low torsional stiffness of the flexbeam of 4.2 Nm/° without and of 7.2 Nm/° with centrifugal force.

The cruciform shape of the torsional element has special advantages. Warping restriction can be avoided, and the flapping and lead-lag stiffnesses can be tuned independently from each other. In addition the relatively high flapping stiffness of the torsional element reduces the static sag of the non-rotating rotor. Therefore no blade stop is needed.

The total mass of the blade is almost 40 kg including about 7.5 kg of additional masses for the tuning of frequencies and the reduction mainly of the lead-lag bending moments.

These tuning masses are locally built in at several radius stations. Apart from the blade tip mass, they are enclosed by thermoplastic casings. Great care was taken to ensure a fail safe fixation of these masses in the blade structure, as they locally generate high additional centrifugal forces. Each of two separate load paths can completely transfer the loads. Besides large-sized bonding areas being the first load path the masses are completely surrounded by blade structure, lugs, C-profiles etc., so that the centrifugal forces can also be totally carried via form-locking, even if the bonding had failed.

Main emphasis was laid on an excellent fail safe behaviour not only of the tuning masses but also of the complete rotor blade. The following table summarizes some of its characteristic features [3,4].

Table 2: Characteristic Fail Safe Design Features of the EC135 Main Rotor Blade

1. Flexbeam
   - Complete spar including flexbeam manufactured in one shot
   - 2 'double lugs' at the blade attachment

2. Control Cuff
   - Integral with blade skin
   - Double shear bonding of control cuff halfs
   - Form-locking design and double shear bonding of the connection to the pitch lever

3. Connection Control Cuff and Flexbeam (R = 1172 mm)
   - 2 load paths: a) large bonding areas
     b) form-locking design

4. Tuning Masses
   - 2 load paths: a) large bonding areas
     b) masses completely enclosed by supporting structures

3. QUALITY ASSURANCE METHODS APPLIED FOR COMPOSITE ROTOR BLADES

At Eurocopter Deutschland computed tomography (CT) is used for the quality assurance of the rotor blades of BO105, BK117 and EC135 [7], see Figure 7 and Figure 8.
For the EC135 blades CT was also used during the design phase and has been performed for each blade at the beginning of the serial production.

Originally CT was developed for the medical field. To create a cross section image, an X-ray beam rotates around the object in a complete circle. From several projection directions attenuation profiles of the beam are measured. With these data a computer calculates the image of the cross section slice having the thickness of the X-ray beam of about 1.5 mm. During the rotor blade examination cross section images are produced at various radius stations. When these stations are close together, e.g. in the lug area, vertical and horizontal cuts in radial direction can also be computed.

CT is a very effective non-destructive testing (NDT) method to check the quality of fiber composite parts. Damages or defects like cracks or waves in the laminate of at least 0.2 mm size can be detected. By the determination of special CT numbers the local material density can be established. Thus e.g. it can be checked if dark spots in a cross section consist of resin or critical air inclusions. With the help of CT, the manufacturing quality of the EC135 blade could be improved significantly.

A test specification for the EC135 main rotor blade describes in detail, in which area which kinds of damages are allowed. If a new type of damage occurs seeming to be eventually critical, a component test is performed. This test has to prove, if the damage affects the life of the structure. When it does, this damage is not accepted for the serial blade quality.

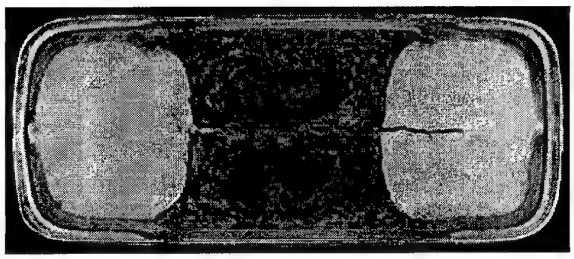

Figure 7: Non-Destructive Testing of the BO105/BK117 Attachment Lug Area by Means of Computed Tomography

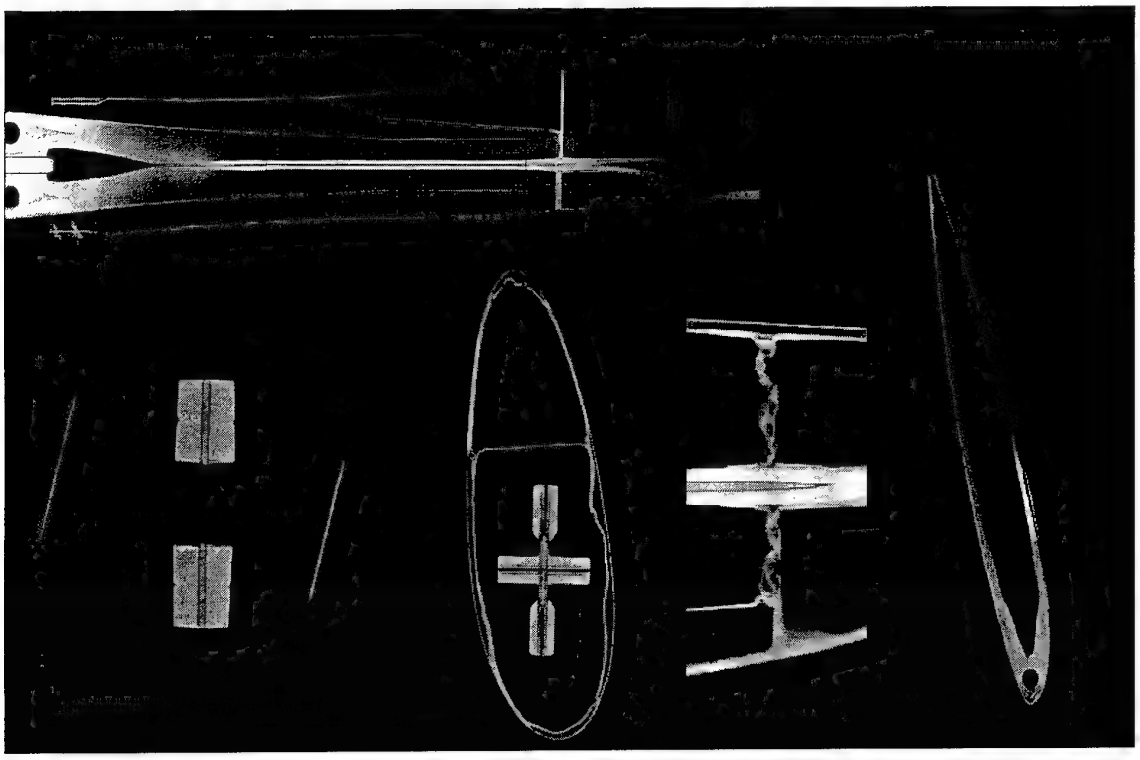

Figure 8: Non-Destructive Testing of the EC135 Main Rotor Blade with Manufacturing Defects at an Early Development Stage by Means of Computed Tomography

4. GENERAL CERTIFICATION REQUIREMENTS AND SUBSTANTIATION PRINCIPLES

The EC135 has been certified according to Joint Aviation Requirements JAR27 'Small Rotorcraft'. However, as the primary structure includes composite materials, the German airworthiness authority Luftfahrtbundesamt issued a Special Condition 'Primary structures designed with composite material' that had to be fulfilled additionally. The special condition adresses subjects like

- demonstration of ultimate load capacity including consideration of manufacturing and impact damages
- investigation of growth rate of damages that may occur from fatigue, corrosion, intrinsic defects, manufacturing defects or damages from discrete sources under repeated loads expected in service
- fatigue evaluation for parts suitable or unsuitable for damage tolerance method and the related inspection procedures
- residual strength requirements
- consideration of the effects of environmental conditions and material variability
- substantiation of bonded joints

In general the fatigue substantiation of dynamically loaded structures is based on the Safe Life procedure. As derived and stated in the Helicopter Fatigue Design Guide (see also [5]), the service life is determined from the usually applied substantiation procedure:

- Establishment of a safe fatigue strength working curve
- Derivation of load spectrum from inflight measurements
- Calculation of the service life by means of Miner's linear damage accumulation hypothesis.

In accordance with the fatigue evaluation of Transport Category Rotorcraft Structures FAR29.571 (Table 3) multiple load paths were established whenever possible.

Table 3: Fatigue Evaluation of Transport Category Rotorcraft Structure (Including Flaw Tolerance) according to FAR29.571

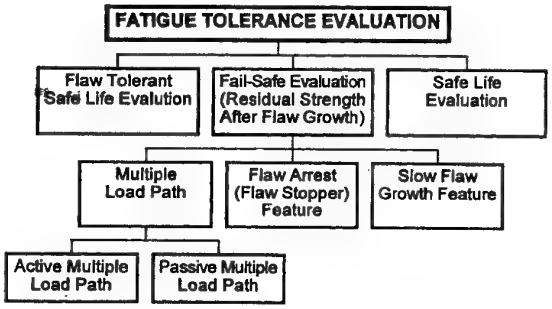

For the dynamically loaded EC135 rotor blade the Flaw-Tolerant Safe Life Method was used for substantiation. In addition fail safe features were incorporated into the design to ensure sufficient residual strength capability after flaw growth. The composite structures were predamaged with the help of impactors up to 25 Joule.

The no-crack-growth ability of the fuselage composite parts was demonstrated by tests.

The rotor blade of the EC135 is an integrated composite structural element with multiple load paths in several areas and for several load cases. In Figure 10 blade sections are shown with the critical load and failure situation. The blade sections with intrinsic, manufacturing and impact damages were tested with dynamic loads. With the help of the performed tests S/N working curves for the flexbeam were established.

The S/N-curve expressed in amplitude values is represented by the following relation:

$$S_A = S_{A\infty} + \frac{S_{A,ult} - S_{A\infty}}{\exp\left[\left(\frac{\log(N)}{\alpha}\right)^{\beta}\right]}$$

where $S_{A\infty}$ is the endurance limit, $S_{A,ult}$ the ultimate value, N the number of cycles and α, β are the shape parameters for the adjustment of the curve [5].

The S/N-curve for torsion of the flexbeam is shown in Figure 9.

The flight tests yielded the necessary load spectra. A complete spectrum contains the working loads (High-Frequency-Spectrum) and the GAG loads (Ground-Air-Ground-Spectrum). The damage ratios and the resulting lives of the structures were calculated according to Miner's linear damage accumulation hypothesis.

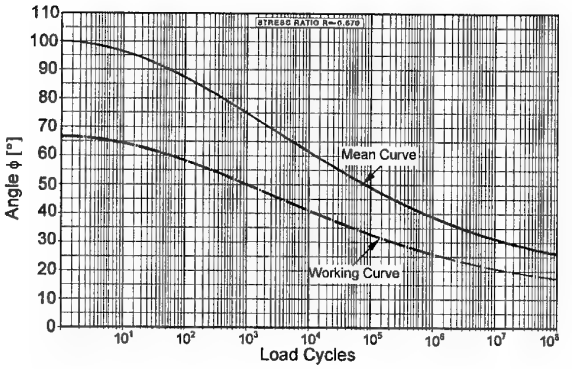

Figure 9: S/N-Curve for Torsional Angle of the Flexbeam

5. ESTABLISHMENT OF BASIC MATERIAL FATIGUE AND DAMAGE TOLERANCE DATA

The material stiffness and strength properties of the fiber composite materials were measured at ECD itself with the help of standardised coupon tests. The basic unidirectional stiffnesses and strengths were determined by long and short beam coupon specimens.

For the static strength substantiation interlaminar failure had to be avoided up to limit load. Up to ultimate load, however, no fiber failure was allowed. The strength degradations due to high temperature and moisture had also to be taken into account. For the fatigue strength substantiation room temperature conditions could be used. For the residual strength test with limit load after fatigue test the hot/wet degradation had to be considered again. As the blade is a fail safe structure, B-values could be taken for the substantiation [8].

Table 4 describes the tested material specimen types, the hot/wet conditions for the EC135 certification and the proceeding for the use of the allowables agreed with the certification authorities.

Table 4: Material Properties and Environmental Conditions

1. Material stiffness and strength properties determined by coupon tests:
   a) bending specimens (long beam type)
   b) shear specimens (short beam type)

2. Environmental conditions
   a) 75°C and 85% relative humidity (hot/wet conditions)
   b) room temperature conditions for fatigue strength substantiation

3. Allowables for material strength
   a) Ultimate load and residual strength
      - hot/wet conditions
      - $\sigma_{\parallel}$ decisive (fiber crack)
      - No interlaminar failure (τ_{ILS}) allowed up to limit load
   b) Flight loads
      - room temperature conditions
      - B-values for substantiation of blade as fail safe structure

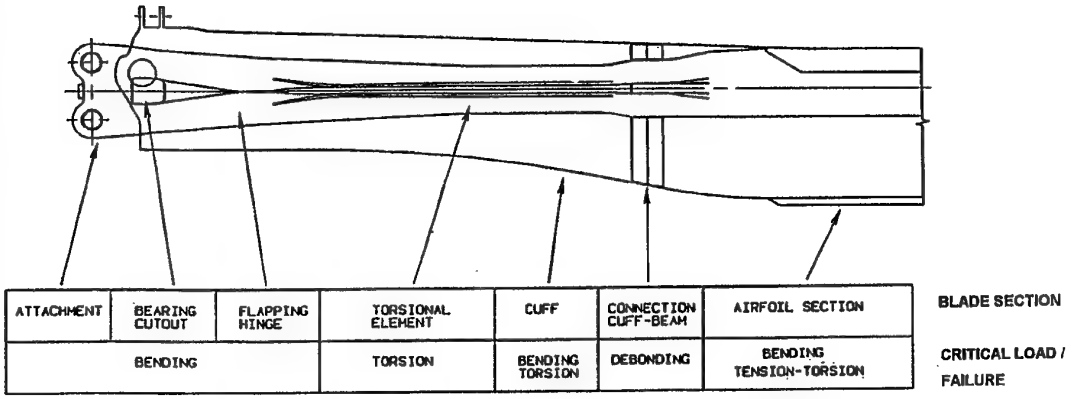

Figure 10: Critical Load / Failure Areas of the EC135 Main Rotor Blade

As seen in Figure 10, the sections of the rotor blade are loaded in different ways. As the rotor blade cannot be tested dynamically as complete structure, several sectional areas were tested according to their critical load and failure behaviour. Thus for each section S/N-curves were derived and transformed to working curves taking into account 99.9 % survivability and 95 % confidence level.

As also seen in Figure 10 the root of the blade is mainly loaded either by bending or by torsion. The failure modes of the blade were established with the help of structural dynamic tests.

Delaminations due to torsional and bending stresses are important failures, which are studied by means of coupons and structural parts. In Figure 11 the three delamination modes I, II, and III are shown. By design the delamination mode I was eliminated if possible. Basic equations for bonded and tapered joints are derived in Figure 11. The relation between the transferable stress $\sigma_{||}$ and the peak shear stress τ_{max} was analysed by means of the classical shear-lag theory and by fracture mechanics. For bonded joints the fracture mechanic property G_{II} is proportional to thickness of the adhesive and the square of the peak shear stress divided by the shear modulus of the adhesive [8, 9, 10].

To establish experimentally the energy release rates for mode I, mode II and mixed mode I/II a variety of test specimens as shown in Table 5 have been developed [12].

Comparative investigations between the Transverse Crack Tension TCT and End Notch Flexure ENF test configuration [15] showed a much better aptitude of the TCT specimen to indicate the static and dynamic delamination behaviour of unidirectional composites. Compared with the ENF specimen the TCT specimen is less complicated in fabrication and the tests include no shear deformation and no frictional effects which can be observed with the ENF tests. Especially while investigating the crack growth behaviour the TCT test has the advantage of maintaining an energy release rate independent from the crack length which is not true for the ENF tests.

In opposite to the TCT specimen with inner fiber interruption as shown in Table 5 a modified TCT specimen with outer fiber interruption shown in Figure 12 was created to investigate the mixed mode I/II.

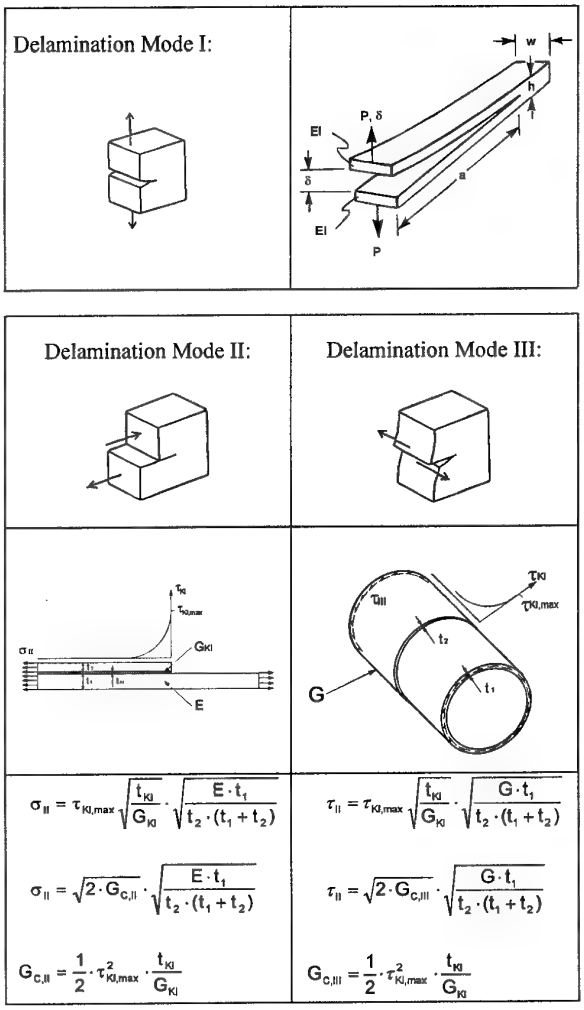

Figure 11: Delamination Modes of Overlaps and Joints and Relevant Delamination Formulas for Mode II and III

Table 5: Tests for Experimental Determination of Energy Release Rates for Mode I, Mode II and Mode I / II

Mode	Sign / Designation	Test Configuration
I	DCB double cantilever beam	
II	TCT transverse crack tension TCT transverse crack tension-compression	
II	SBS schort beam shear	
II	ENF end-notched flexure	
I/II	CLS crack lap shear	
I/II	EDT edge delamination tension EDTC edge delamination tension-compression	
I/II	HDT hole delamination tension HDTC hole delamination tension-compression	
I/II	ENT edge notch tension ENTC edge notch tension-compression	

Figure 12: Modified TCT Specimen with Outer Fiber Interruption

For the analysis of delamination initiation and delamination propagation due to dynamic tension loads TCT test specimens with inner and outer fiber interruption shown were used. The test specimen with inner fiber interruption corresponds to the pure delamination mode II, whereas the specimen with outer fiber interruption takes the influence of mode I on mode II into consideration.

The delamination stress σ_U (upper value) for the stress ratio R = 0.1 versus load cycles is shown in Figure 13 for the outer fiber interruption. The specimens for establishment of this curve were fabricated of E-Glass/913 unidirectional prepreg material, which is used for the flexbeam of the EC135 helicopter. The delamination onset curve is described by the four parametric Weibull formula:

$$\sigma = \sigma_{unl} + \frac{\sigma_{ult} - \sigma_{unl}}{\exp\left[\left(\frac{\log N}{\alpha}\right)^{\beta}\right]} \qquad \text{with}$$

Ultimate Delamination Stress	σ_{ult}
Delamination Endurance Limit	σ_{unl}
Curve parameter	α
Curve parameter	β

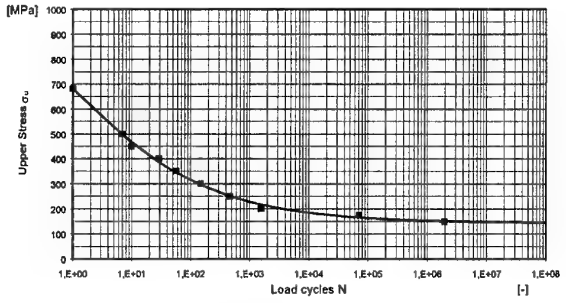

Figure 13: S/N-Curve for Delamination Strength of Unidirectional E-Glass/913

The relation between the stress σ_{II} and the energy release rate G_{II} with the specific parameters of the tested specimen reads:

$$G_{II} = \frac{1}{4} \cdot \frac{\sigma^2}{E} \cdot \frac{h \cdot t}{h - t} \qquad \text{with}$$

Young's modulus	E	= 41.5	GPa
Specimen thickness	h	= 1.25	mm
Thickness of interrupted plies	t	= 0.25	mm

The delamination growth rate was determined for materials widely used in the helicopter structures of ECD. The logarithmic linear relationship between the delamination growth rate da/dN and the energy release rate G_{II} in the range of stable delamination growth was derived from the test results. The range of stable delamination growth is bounded by the threshold value of G_{IIth} and the critical value G_{IIc}. Below G_{IIth} there is no crack propagation and above G_{IIc} the crack grows instantenously.

$$\frac{da}{dN} = c \cdot G_{IImax}^{n}$$

with c and n being material constants describing the position and the slope of the curve.

Figure 14 shows the delamination growth rates versus energy release rate for E-Glass/913, carbon T300/913 and R-Glass/913 UD prepreg materials. In general it can be deducted from the gradient of the curves that materials with higher stiffness show more sensitivity of the crack propagation velocity against increasing cyclic energy release rate.

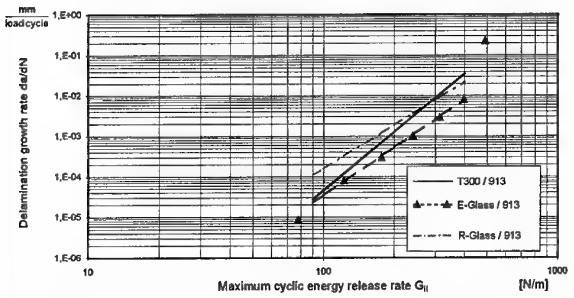

Figure 14: Delamination Growth Rate da/dN versus Energy Release Rate G_{II}

Figure 15 which is taken from [12] shows the comparison of the carbon fiber materials T300/914C and M40/Code69. Here this trend can be seen more clearly due to the higher difference in modulus between the two fiber types. In addition a difference in the threshold and critical value of G_{II} is obvious. The higher the modulus is, the higher is the threshold and the lower is the critical value of G_{II}. That is, the band between the threshold and the critical value of G_{II} becomes narrower. Thus the endurance limit comes closer to the static strength with increasing stiffness of the material. This effect can also be observed in the fatigue curves of high modulus carbon fibers.

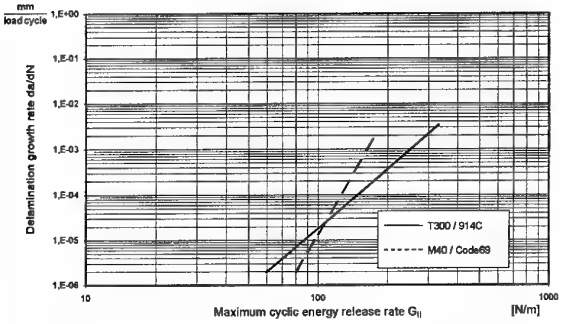

Figure 15: Delamination Growth Rate da/dN versus Energy Release Rate G_{II} according to [12]

In Table 6 the test results for the critical energy release rate G_{IIc} are listed for E-Glass/913, T300/913 and T300/M18. In addition the value for E-Glass/913 with an additional layer of adhesive between the continuous and interrupted layers is shown. This intermediate bonding layer ameliorates the critical value substantially. This effect can be easily transferred into design solutions to improve areas prone to delamination. The comparison of the two resin systems for the carbon laminates emphasizes the importance of the resin properties for the delamination strength of fiber composite components.

Table 7 summarizes the curve parameters of the delamination S/N curves and the crack propagation curves of E-Glass/913, R-Glass/913 and T300/913. The links between the both types of curves are the static delamination strength σ_{ult} and the delamination endurance limit σ_{unl} which can be transformed into the critical and threshold value G_{IIc} and G_{IIth} respectively.

Table 6: Critical Energy Release Rate G_{II} for Several Unidirectional Composites

Unidirectional Material	Young's Modulus E [GPa]	H [mm]	T [mm]	Critical Energy Release Rate G_{IIC} [N/m]
E-Glass/913	41.5	1.3	0.26	914
E-Glass/ 913 with Bonding Layer	40.3	1.4	0.26	1944
T300 / 913	126.4	1.3	0.26	791
T300 / M18	133.1	1.3	0.26	958

Table 7: Delamination Onset and Propagation Curve Parameters

Material	σ_{unl} [MPa]	σ_{ult}[MPa]	α [-]	β [-]	c [*]	n [-]
T300/913	315	884	3.166	1.496	2.852	4.793
E-Glass/913	149	650	1.772	1.174	0.287	3.915

* Dimension of c: $[(m/N)^n \cdot mm/load\ cycle]$

6. BASIC STRUCTURAL BEHAVIOUR

For the blade design, the cross section characteristics were calculated at various radius stations with the help of a two-dimensional finite element (FE) program. This ECD own code computes the six different stiffnesses corresponding to the forces and moments in the three coordinate directions. Additionally it also calculates the normal and shear stress distributions for any load combination. Figure 16 shows a typical FE modelization of the airfoil section.

Figure 16: Cross Section FE Model of the Airfoil Section

This FE analysis yields good results. However, it assumes that the cross section remains constant over a greater length.

In order to determine additional stresses e.g. due to strong cross section variations or special load introduction areas, such as the glass fiber lug the fixation with the help of a titanium fitting, are treated by special tools and calculation procedures.

A critical load situation of the BK 117 root area is the dynamic lead-lag motion. The interaction between the glass fiber composite loop and the titanium fitting due to centrifugal force and lead-lag-moment was modelled in finite elements. The stresses in the composite loop were calculated with the program system MARC in an iterative process. The contour of the titanium fitting was optimised in order to reduce stress peaks in the loop.

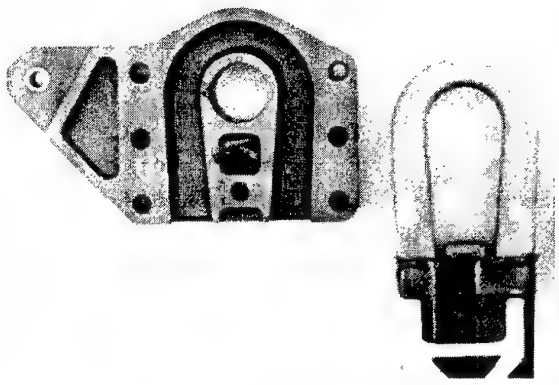

Figure 17: BO105/BK117 Blade Root Glass Fiber Loop and Titanium Fitting

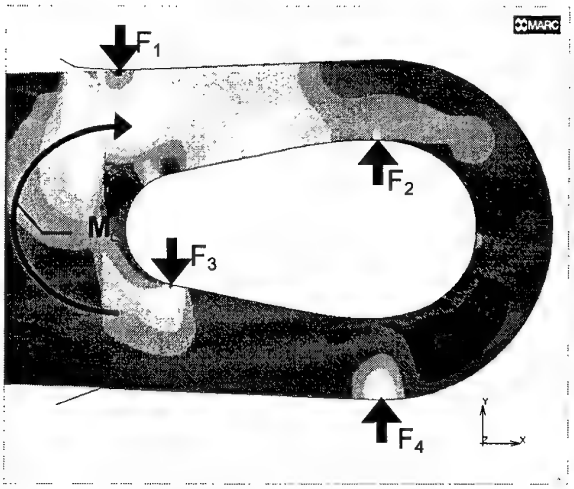

Figure 18: Transverse Stresses in the Loop due to Lead-Lag Bending Moment

For the Flexbeam of the EC 135 a three-dimensional Finite Element (FE) model was developed in order to determine additional stresses e.g. due to strong cross section variations.

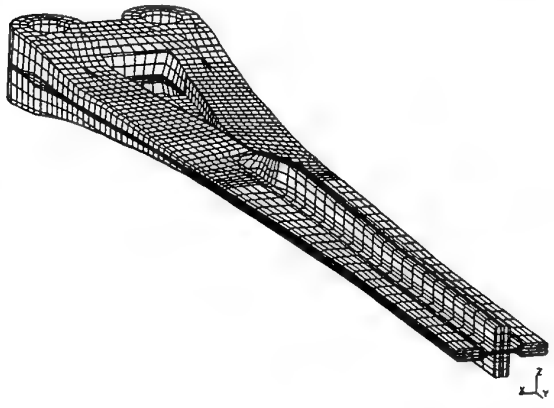

Figure 19: Three-Dimensional FE Model of the Prototype Flexbeam

Furthermore flaws, which had been detected in component tests, were introduced into the three-dimensional FE-model in order to determine the criticality to the overall strength behaviour of the blade root [15].

7. DYNAMIC STRENGTH COMPONENT TESTING AND DEMONSTRATION OF LIMIT LOAD CAPACITY

It is not possible to test a complete blade realistically at all possible load combinations in a testing machine. Therefore the blade was subdivided into several components each of them being tested under its critical load conditions. For each test type several specimens with intrinsic, manufacturing and impact damages were tested at different load levels. The impact energy for flexbeam and control cuff was 25 J. This means a 2.5 kg impact mass falling from 1 m height.

For the static ultimate load tests the influence of high temperature and moisture had to be taken into account according to the 'Special Condition'. The strength degradation was determined by coupon tests, see chapter 4. The static component tests were then performed at room temperature with loads increased by the hot/wet degradation factors. The maximum loads were simultaneously applied to cover the worst case possible.

After the fatigue tests residual strength tests had to be performed. Limit load capacity was proven there, also including load amplification factors to simulate hot/wet conditions.

Table 8 summarises the process for the component tests taking into account the requirements of the 'Special Condition'. These tests were the basis for the life calculations.

Table 8: Process for the (Sub-)Component Tests

1. Component specimens
   - Specimens with intrinsic, manufacturing and impact damages

2. Tests
   - Separate component tests for critical areas
   - Constant amplitude tests at different load levels
   - Test monitoring
   - Documentation of: Type of damage
     Damage begin
     Size
     Location
     Growth rate

3. Residual strength test with predamaged specimens after fatigue test
   - Proof of Limit Load capacity
   - Load amplification factor to simulate hot/wet conditions

Figure 20 shows a bending specimen of the flexbeam in its upper and lower test position. It is pretensioned by a centrifugal force of about 150 kN and simultaneously loaded by flapping and lead-lag moments (number a of the flexbeam tests from above). At the left side the blade attachment area is clamped into a fork simulating the rotor hub. At the right side two hydraulic cylinders introduce the maximum transverse forces and flapping and lead-lag moments simultaneously. This test mainly simulates the load conditions between blade attachment and 'flapping hinge'.

During the development phase the flexbeam was continuously improved and the S/N-curve concerning bending could be raised by about 20%.

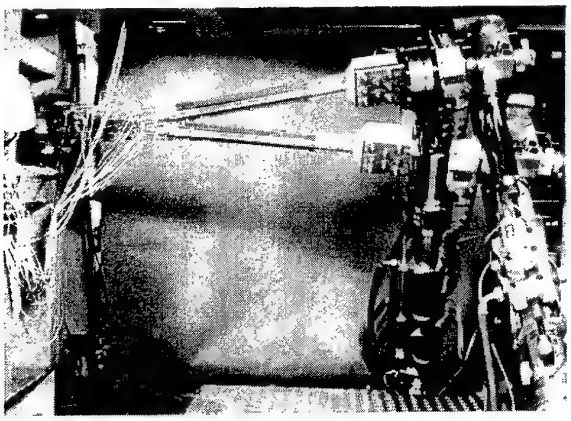

Figure 20: Flexbeam Specimen Loaded by Bending Moments and Centrifugal Force

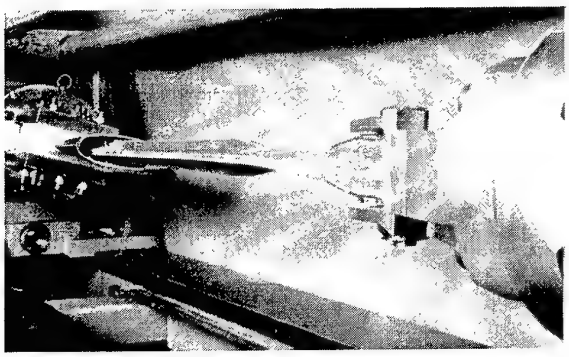

Figure 21: Flexbeam Unloaded

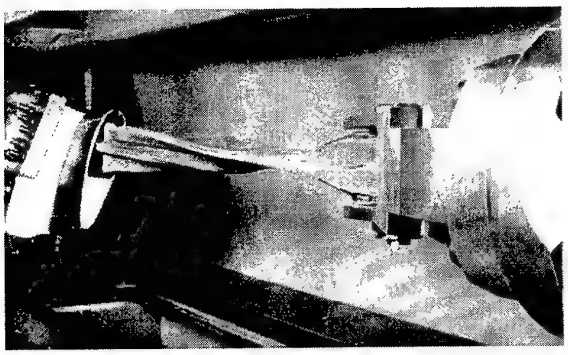

Figure 22: Flexbeam Loaded by Centrifugal Force and Twisted by 100 °

The torsional capability of the flexbeam was proved in another test sequence. Figure 21 shows the specimen unloaded. The cuff is almost completely removed. At the right side the blade attachment area of the flexbeam is clamped. (To the left it is followed by the flat 'flapping hinge' and the torsional element with its slit cruciform cross section.) In Figure 22 the specimen is pretensioned by a centrifugal force of 150 kN and is twisted by 100°. This means a torsional angle of 2°/cm length of the torsional element. The specimen showed no failure, the test was only limited by the capacity of the testing machine. This test proved the outstanding qualities of the EC135 flexbeam.

8. SUMMARY

During the last decades the former helicopter division of MBB and now Eurocopter Deutschland has consequently developed the main rotor systems towards simplification, improved reliability, increased life, lower weight and reduced service and maintenance costs. It started with the hingeless rotor of the BO105 and continued to the bearingless rotor of the EC135. However, this became only possible by using the outstanding qualities of glass fiber composites with regard to strength and flexibility.

As the certification authorities demand for an improved damage tolerant behaviour, especially for dynamically loaded structures, basic damage tolerance material data were studied. The basic delamination growth data for several unidirectional fiber/epoxy combinations were determined with the help of TCT test specimens. The gained database allows sizing of dynamically loaded flexbeams. The load case of flap bending corresponds to the mode II whereas the torsional load case corresponds to mode III. The outstandingly low crack growth behaviour of composite materials and improved methods of quality assurance, such as computed tomography (CT), reduce life cycle costs and improve the structural safety of helicopters remarkably.

REFERENCES

[1] Huber, H., and Schick, C.,
'MBB's BO108 Design and Development',
46th Annual Forum & Technology Display of the American Helicopter Society, Sheraton Washington Hotel, Washington D.C., 21-23 May 1990

[2] Attlfellner, S.,
'Eurocopter EC135 Qualification for the Market',
22nd European Rotorcraft Forum, Brighton, UK.,
17-19 September 1996

[3] Bansemir, H., and Mueller, R.,
'The EC135 - Applied Advanced Technology',
AHS, 53rd Annual Forum, Virginia Beach, USA,
29 April - 1 May 1997

[4] Pfeifer, K., and Bansemir, H.,
'The Damage Tolerant Design of the EC135 Bearingless Main Rotor',
24th European Rotorcraft Forum, Marseilles, France,
15-17 September 1998

[5] Och, F.,
'Fatigue Strength',
AGARDograph No 292, Helicopter Fatigue Design Guide, Nov. 1983 ISBN 92-835-0341-4

[6] Rauch, P., and Charreyre, A.,
'Damage - Tolerant Tail Rotor Blade for AS 332 L2 Super Puma Helicopter'
19th European Rotorcraft Forum, 14-16 September 1993, Cernobbio (Como), Italy

[7] Oster, R.,
'Computed Tomography as a Nondestructive Test Method for Fiber Main Rotor Blades in Development, Series and Maintenance',
23rd European Rotorcraft Forum, Dresden, Germany,
16-18 September 1997

[8] Notzon, T.,
'Analyse und Versuche an geschäfteten Laminaten',
Diplomarbeit an der Universität der Bundeswehr München / Eurocopter Deutschland 1993

[9] Rapp, H.,
'Berechnung von Delaminationen in Aufdoppelungen und Ausschäftungen',
ECD-DE133 (Internal Report) - 1993

[10] Wisnom, M. R.,
'Delamination in Tapered Unidirectional Glass Fiber Epoxy at Static Tension Loading',
Proc. AIAA Structures,
Structural Dynamics and Materials Conference,
Baltimore, April 1991, pp. 1162 - 1172

[11] Sigh, G.C., and Paris P.C.,
'Stress Analysis of Cracks',
ASTM STP 381, p.60, 1985

[12] Prinz, R., and Gädke, M.,
'Characterization of Interlaminar Mode I and Mode II Fracture in CFRP Laminates',
Proc. Internat. Conf.: Spacecraft Structures and Mechanical Testing, Noordwijk, 1991

[13] Cui, W. C., Wisnom, M. R., and Jones, M.,
'A Comparison of Fracture Criteria to Predict Delamination of Unidirectional Glass / Epoxy Specimens with Cut Central Plies',
5th Int. Conf. on Fiber Reinforced Composites,
Newcastle, March 1992

[14] Murri, G. B., O'Brian, T. K., and Salpekar, S A.,
'Tension Fatigue of Glass / Epoxy and Graphite / Epoxy Tapered Laminates',
46th Annual AHS Forum, Washington D.C., May 1990

[15] Boelingen, M., and Nawrath, C.,
'Bruchmechanische Analyse des Biege- und Drillstrukturelements des Hauptrotorblattes für einen Mehrzweckhubschrauber',
Diplomarbeit an der Universtät der Bundeswehr München / Eurocopter Deutschland 1995

Rotorcraft Damage Tolerance Evaluated by Computational Simulation

Christos C. Chamis*
National Aeronautics and Space Administration
Lewis Research Center, Cleveland, Ohio 44135-3191

Levon Minnetyan
Clarkson University, Potsdam, New York 13699-5710

Frank Abdi
AlphaStar Corporation, Long Beach, CA 90804

ABSTRACT

An integrally stiffened graphite/epoxy composite rotorcraft structure is evaluated via computational simulation. A computer code that scales up constituent micromechanics level material properties to the structure level and accounts for all possible failure modes is used for the simulation of composite degradation under loading. Damage initiation, growth, accumulation, and propagation to fracture are included in the simulation. Design implications with regard to defect and damage tolerance of integrally stiffened composite structures are examined. A procedure is outlined regarding the use of this type of information for setting quality acceptance criteria, design allowables, damage tolerance, and retirement-for-cause criteria.

KEYWORDS: Composites, Composite Shells, Composite Structures, Computational Simulation, Damage, Degradation, Durability, Fracture, Integrated Stiffening, Laminates, Structural Degradation.

INTRODUCTION

Laminated composite structures are used in many aerospace applications such as rotorcraft components, advanced aircraft fuselage, rocket motor cases, pressure vessels, containment structures, and other components with various shapes and sizes. In these applications composite structures are required to withstand significant in-plane loads. Additionally, composite structures are required to possess sufficient bending stiffness to resist buckling. Discussion in the current paper is focussed on integrally stiffened composite structures subjected to in-plane loads and internal/external pressures. Damage initiation, growth, accumulation, and propagation to fracture is simulated for composite panels and cylindrical shells with and without integrated stiffening layups. The influence of integrated stiffeners is examined with regard to out of plane stiffness contribution as well as damage progression and structural durability assessment under applied loading. Changes in the damage initiation load and the structural fracture load are quantified due to the presence of integrated stiffeners.

Integrally stiffened composite structures are manufactured by adding additional plies or braids that are designed to improve both the out-of-plane stiffness and buckling resistance of composite structural components. Integrated stiffening is typically obtained within the manufacturing process of a composite material. The layup of a laminated composite or the braid structure of a braided composite may be spatially concentrated to obtain a stiffening of the composite in the desired orientations. Integrally stiffened composites would display logical patterns of ply/braid concentrations. For example, a rectangular composite panel may be stiffened by adding bands of layers with fibers along the diagonals of the panel. Another example is the superposition of lattice type periodic angled stiffeners over a smooth composite plate layup during the manufacturing process. Integrated stiffening of composites may be obtained by hand layup of composite tape, filament winding, or by automated braiding processes. The distinguishing feature of an integrally stiffened composite is that the stiffening system has been manufactured simultaneously as part of the stiffened composite structure.

Paper presented at the RTO AVT Specialists' Meeting on "Application of Damage Tolerance Principles for Improved Airworthiness of Rotorcraft", held in Corfu, Greece, 21-22 April 1999, and published in RTO MP-24.

Critical components of a structure are required to remain safe and be able to function under loading after experiencing some damage. The cause of damage may be an accident, defect, or unexpected overloading. Damage tolerance of a structure is quantified by the residual strength, that is the additional load carrying ability after damage. Composite structures are well suited for design with emphasis on damage tolerance as continuous fiber composites have the ability to arrest cracks and prevent self-similar crack propagation. It is difficult to design and certify a composite structure because of the complexities in predicting the overall congruity and performance of fiber composites under various loading and hygrothermal conditions.

Design considerations with regard to the durability of fiber composite structures require an a priori evaluation of damage initiation and fracture propagation mechanisms under expected loading and service environments. Concerns for safety and survivability of critical components require a quantification of the structural fracture resistance under loading. A significant design parameter with regard to composite damage tolerance is the laminate configuration. In general, quasiisotropic laminates yield better damage tolerance. However, in many cases a quasiisotropic laminate may not be the most efficient with regard to structural strength and performance when there is no damage. For a rational design process it is necessary to quantify the structural damage tolerance for a candidate design. The ability of designing composites with numerous possible fiber orientation patterns, choices of constituent material combinations, ply drops and hybridizations, render a large number of possible design parameters that may be varied for an optimal design. Damage initiation and progression characteristics are much more complex for integrally stiffened fiber composites compared to homogenous or orthotropic materials. The structural fracture process of a fiber composite depends on many parameters such as laminate configuration, fiber volume ratio, constituent stiffness/strength/hygrothermal parameters, stiffening system, and the fabrication process. Recent developments in computational simulation technology have made it possible to evaluate the details of progressive damage and fracture in composite structures. Computational simulation enables assessment of the damage initiation and propagation loads. A damage energy release rate is evaluated globally during simulation by computing the work done per unit damage created. The damage energy release rate is used to quantify the structural damage tolerance at different stages of degradation. The influence of local defects or flaws and effects of the fabrication process in terms of residual stresses are taken into account.

An important feature of computational simulation is the assessment of damage stability or damage tolerance of a structure under loading. At any stage of damage progression, if there is a high level of structural resistance to damage progression under the service loading, the structure is stable with regard to fracture. The corresponding state of structural damage is referred to as *stable damage*. On the other hand, if damage progression does not encounter significant structural resistance, it corresponds to an *unstable damage* state. Unstable damage progression is characterized by very large increases in the amount of damage due to small increases in loading. Whereas during stable damage progression the amount of increase in damage is consistent with the increase in loading.

Internal damage in composites is often initiated as cracking due to normal stresses transverse to fiber orientation. At the presence of stress concentrations or defects, initial damage may also include fiber fracture. Further degradation is in the form of additional fiber fractures that usually lead to structural fracture. Because of the numerous possibilities with material combinations, composite geometry, fiber orientations, and loading conditions, it is essential to have an effective computational capability to predict the behavior of composite structures for any loading, geometry, composite material combinations, and boundary conditions. The predictions of damage initiation, growth, accumulation, and propagation to fracture are important in evaluating the load carrying capacity and reliability of composite structures. Quantification of the structural fracture resistance is also required to evaluate the durability/life of composite structures.

Laminated composite design practice has been based on extensive testing with attempts to apply formal fracture mechanics concepts to interpret test results. In certain cases interpretation of laminated composite test data via fracture mechanics has been satisfactory. However, in most cases fracture mechanics methods have significantly mispredicted the strength of fiber composites. Reconciliation of test results with fracture mechanics has required significant modifications of effective fracture toughness and specific, laminate configuration dependent, effective stress concentration field parameters. Additionally, required adjustments of fracture mechanics parameters have had to be reassessed with every change in constituent and laminate characteristics. The complete evaluation of laminated composite fracture requires an assesment of ply and subply

level damage/fracture processes.

Continuous fiber composites in general have the ability to arrest cracks and prevent self-similar crack propagation. For most fiber reinforcement configurations, cracks and other stress concentrators do not have as important an influence in composites as they do for homogeneous materials. Another important aspect is the multiplicity of design options for composites. The ability of designing composites with numerous possible fiber orientation patterns, choices of constituent material combinations, ply drops, hybridizations, and integrated stiffening options render a large number of possible design parameters that may be varied for an optimal design.

The present approach by-passes traditional fracture mechanics to provide an alternative evaluation method, conveying to the design engineer a detailed description of damage initiation, growth, accumulation, and propagation that would take place in the process of ultimate fracture of an integrally stiffened fiber composite structure. Results show in detail the damage progression sequence and structural fracture resistance during different degradation stages. This paper demonstrates that computational simulation, with the use of established material modeling and finite element modules, adequately tracks the damage growth and subsequent propagation to fracture for an integrally stiffened fiber composite structure.

METHODOLOGY

Computational simulation is implemented via the integration of three modules: (1) composite mechanics, (2) finite element analysis, and (3) damage progression tracking. The overall evaluation of composite structural durability is carried out in the damage progression module (Minnetyan et al 1990) that keeps track of composite degradation for the entire structure. The damage progression module relies on the composite mechanics code (Murthy and Chamis 1986) for composite micromechanics, macromechanics and laminate analysis, and calls a finite element analysis module that uses anisotropic thick shell elements to model laminated composites (Nakazawa et al 1987).

A computational simulation cycle begins with the definition of constituent properties from a materials databank. Composite ply properties are computed by the composite mechanics module. The composite mechanics module also computes through-the-thickness structural properties of each laminate. The finite element analysis module accepts the composite properties that are computed by the composite mechanics module at each node and performs the analysis for a load increment. After an incremental finite element analysis, the computed generalized nodal force resultants and deformations are supplied to the composite mechanics module that evaluates the nature and amount of local damage, if any, in the plies of the composite laminate. Individual ply failure modes are determined using failure criteria associated with the negative and positive limits of the six ply-stress components ($\sigma_{\ell 11}$, $\sigma_{\ell 22}$, $\sigma_{\ell 33}$, $\sigma_{\ell 12}$, $\sigma_{\ell 13}$, $\sigma_{\ell 23}$), a modified distortion energy (MDE) combined stress failure criterion. The MDE failure criterion is expressed as:

$$F = 1 - \left(\frac{\sigma_{\ell 11\alpha}}{S_{\ell 11\alpha}}\right)^2 - \left(\frac{\sigma_{\ell 22\beta}}{S_{\ell 22\beta}}\right)^2 + K_{\ell 12\alpha\beta}\frac{\sigma_{\ell 11\alpha}}{S_{\ell 11\alpha}}\frac{\sigma_{\ell 22}}{S_{\ell 22}} - \left(\frac{\sigma_{\ell 12S}}{S_{\ell 12S}}\right)^2 \quad (1)$$

where α and β indicate tensile or compressive stress, $S_{\ell 11\alpha}$ is the local longitudinal strength in tension or compression, $S_{\ell 22\alpha}$ is the transverse strength in tension or compression, and

$$K_{\ell 12\alpha\beta} = \frac{(1 + 4\nu_{\ell 12} - \nu_{\ell 13})E_{\ell 22} + (1 - \nu_{\ell 23})E_{\ell 11}}{[E_{\ell 11}E_{\ell 22}(2 + \nu_{\ell 12} + \nu_{\ell 13})(2 + \nu_{\ell 21} + \nu_{\ell 23})]^{1/2}} \quad (2)$$

The type of failure is assessed by comparison of the magnitudes of the squared terms in Equation (1). Depending on the dominant term in the MDE failure criterion, fiber failure or matrix failure is assigned.

The generalized stress-strain relationships for each node are revised according to the composite damage evaluated by the composite mechanics module after each finite element analysis. The model is automatically updated with a new finite element mesh and properties, and the structure is reanalyzed for further deformation and damage. If ply failure criteria indicate new or additional damage during a load increment, the damage tracking module degrades the composite properties affected by the damage and reanalizes the structure under the same load. When there is no indication of further damage under a load, the structure is considered to be in equilibrium. Subsequently, another load increment is applied leading to possible damage growth, accumulation, or propagation. In the computational simulation cases presented in this paper, analysis is stopped when commencement of the damage propagation phase is indicated by laminate fracture. Laminate fracture is predicted when major principal failure criteria are met for all plies

at a node. After laminate fracturing, the composite structure is anticipated to enter a final damage propagation stage that leads to ultimate structural fracture or collapse.

During progressive damage tracking the following terminology is utilized to describe the various stages of degradation in the composite structure: (1) *damage initiation* refers to the start of damage induced by loading that the composite structure is designed to carry; (2) *damage growth* is the progression of damage from the location of damage initiation to other regions; (3) *damage accumulation* is the increase in the amount of damage in the damaged regions with additional damage modes becoming active; (4) *damage propagation* is the rapid progression of damage to other regions of the structure; (5) *structural fracture* is the ultimate disintegration of the specimen.

INTEGRALLY STIFFENED PANEL

A graphite/epoxy laminated composite plate with integrated ±45° intermittent lattice stiffeners was investigated with damage and fracture propagation due to tension, compression, and in-plane shear loads. The response of the integrally stiffened composite panel was compared with that of an unstiffened skin plate. The unstiffened plate was given additional skin thickness such that the material volume was the same as the material volume of the integrally stiffened plate. The additional plies of the unstiffened plate were given fiber orientations of ±45°, same as the fiber orientations of the integrated stiffeners. Both the unstiffened and integrally stiffened panels were made of AS-4 graphite fibers in a high modulus high strength epoxy matrix (AS-4/HMHS). Ply layup of the unstiffened panel was $[\pm 45/0/90/\pm 45]_S$. The stiffened panel had a skin layup of $[0/90/\pm 45]_S$. The stiffener plies were added to the top of the skin as $[+45]_8$ or as $[-45]_8$. Ply thickness was 0.127 mm (0.005 in). The fiber volume ratio was V_f=0.60 and the void volume ratio vas V_v=0.01. The cure temperature was T_{cu}=177°C (350°F). The fiber and matrix properties were obtained from a databank of composite constituent material properties resident in the composite mechanics module (Murthy and Chamis 1986). The fiber and matrix properties corresponding to this case are given in Tables I and II, respectively. The HMHS matrix properties are representative of the 3501-6 resin. These in-situ properties are similar to those identified by Sobel et al (1993) with experimental correlation.

The panels had identical planar geometry with a width of 305 mm (12.0 in.) and length of 457 mm (18 in.). Each finite element model contained 117 nodes and 96 uniformly sized square elements. Figure 2 shows the finite element model with diagonal lines along the ±45° stiffener bands. Numbers at nodes indicate the laminate type number at that node for the integrally stiffened panel. Laminate type 1 had a layup of $[0/90/\pm 45]_S$, representing the skin. Laminate type 2 had the skin layup plus $[+45]_8$ representing the +45 stiffened nodes. Laminate type 3 had the skin layup plus $[-45]_8$ representing the -45 stiffened nodes. Laminate type 4 had the skin layup plus $[+45_8/-45_8]$ representing intersection nodes for +45 and -45 stiffeners. Panels were assumed to be simply supported for structural response; i.e. the left end nodes of the panel were restrained against all displacement components and the right end nodes were restrained against displacement normal to the plane of the panel. Additionally, the right end nodes were constrained to have uniform displacement in the plane of the panel via duplicate node specifications.

Structural response characteristics of the integrally stiffened panel were evaluated in terms of the buckling load and the bending stiffness. Analysis of the integrally stiffened panel under uniaxial compression indicated a buckling load of 1,114 N (250 lbs). The buckling load of the unstiffened panel was only 213 N (48 lbs). Therefore the buckling resistance of the integrally stiffened panel was 5.2 times that of the unstiffened panel with the same amount of composite material. Similarly, the bending rigidity was significantly improved due to integrated stiffeners. Figure 3 shows a comparison of the midspan deflections of unstiffened and integrally stiffened panels due to uniform bending moment applied to the simply supported right end of the panel. Figure 3 shows that the integrally stiffened panel was 7.2 times stiffer than the unstiffened panel in bending.

Next, the in-plane progressive damage and fracture responses were compared for the unstiffened and stiffened panels. Figure 4 shows damage progressions of unstiffened and integrally stiffened panels subjected to tension. Damage initiation for the integrally stiffened panel occurred in the 90° skin plies due to transverse tensile fractures. Damage initiation for the unstiffened panels was also in the 90° plies due to transverse tensile fractures. In both cases the MDE combined stress failure criterion was activated. However, the damage initiation load for the integrally stiffened panel was approximately one third of the damage initiation load for the flat panel with the same material volume. Figure 5 shows the

displacements in tension. The uniaxial stiffnesses of the unstiffened and integrally stiffened panels are approximately the same prior to damage initiation. However, stiffness of the integrally stiffened panel degrades quickly due to damage initiation and progression. Figure 6 shows damage progressions of the unstiffened and integrally stiffened panels under uniaxial compression. Damage initiation for the integrally stiffened panel occurred at the edge of the panel at midspan where +45 and -45 stiffeners converged (laminate type 4). The damage initiation modes included the transverse tensile and longitudinal compressive failures of the 90° skin plies, in-plane shear failures of the ±45° skin plies, as well as the in-plane shear failures of the +45 stiffener plies near the skin. Damage initiation for the unstiffened panels under compression was in the 0° plies due to longitudinal compressive fractures. The damage propagation load of the unstiffened panel was more than five times that of the integrally stiffened panel. The initial stiffnesses of the unstiffened and integrally stiffened panels in compression were the same as observable from Figure 7. However, the stiffness of the integrally stiffened panel degraded at a much lower loading compared to degradation load of the flat panel. Figure 8 shows the damage progressions of unstiffened and integrally stiffened panels under in-plane simple shear loading. Damage initiation for the integrally stiffened panel was due to longitudinal compressive failure of a +45 skin ply at a type 3 stiffened node. On the other hand, damage initiation for the flat panel under shear was due to transverse tensile failures of the 90° plies. As it was in tension and compression, also in shear the integrally stiffened panel degraded at a lower load compared to the flat panel. Figure 9 shows the load-displacement relationships in shear. Computational simulation results depicted in Figure 9 indicate that in shear, the initial stiffness of the flat panel was slightly higher than that of the integrally stiffened panel.

INTEGRALLY STIFFENED COMPOSITE SHELL

A composite cylindrical shell with and without integrated ±45° intermittent lattice stiffeners was investigated with damage and fracture propagation due to axial tension, as well as internal and external pressure loads. The response of the integrally stiffened shell was compared with that of an unstiffened shell. The unstiffened shell was given additional skin thickness such that the material volume was the same as the material volume of the integrally stiffened shell. The additional plies of the unstiffened shell were given fiber orientations of ±45°, same as the fiber orientations of the integrated stiffeners. Both the unstiffened and integrally stiffened shells were made of AS-4/HMHS composite. Ply layup of the unstiffened shell was $[\pm 45/0/90/\pm 45]_S$. The stiffened shell had a skin layup of $[0/90/\pm 45]_S$. The stiffener plies were added to the top of the skin as $[+45]_8$ or as $[-45]_8$. Ply thickness was 0.127 mm (0.005 in). The fiber volume ratio was V_f=0.60 and the void volume ratio vas V_v=0.01. The cure temperature was T_{cu}=177°C (350°F).

Each cylindrical shell finite element model contained 400 nodes and 384 uniformly sized square elements. Figure 10 shows the finite element model for a cylindrical shell. The shell was simulated subject to increasing levels of internal and external pressurizations as well as axial loading. To represent the axial stresses produced in the closed end pressure vessel, boundary nodes at one end of the cylinder were subjected to force resultants in the axial direction, whereas the boundary FEM nodes were restrained in the axial direction at the opposite end. The uniformly distributed axial tension was such that the generalized axial stresses in the shell wall were half those developed in the hoop direction.

Figure 11 shows a comparison of damage progressions for the integrally stiffened and unstiffened composite shells under axial tension. Figure 11 indicates that ultimate strength of the integrally stiffened cylindrical shell is approximately 60 percent of the ultimate strength of shell without integral stiffeners. Additionally, damage initiation for the integrally stiffened shell begins at only 10 percent of the ultimate load. On the other hand, damage initiation for the unstiffened shell corresponds to a loading level that is approximately 97 percent of its ultimate load. Figure 12 shows the exhausted cumulative damage energy based on depleted energies of the local failure modes. The exhausted damage energy represents a similar pattern of damage progression as the percent damage volume depicted in Figure 12. Figure 13 shows the damage energy release rates (DERR) based on the incremental work done by applied loading during damage progression of the integrally stiffened cylindrical shell. Peak values in the DERR levels indicate significant damage events. The first peak in DERR corresponding to damage initiation for the integrally stiffened shell occurred due to transverse tensile fractures in the 90° skin plies. The steep increase in DERR at approximately 11 kN (2.5 k) axial tension corresponds to a partial separation between skin and

stiffener plies.

Figure 14 shows comparison of damage progressions for integrally stiffened and unstiffened cylindrical shells subjected to external pressures. The ultimate pressure for the integrally stiffened shell is approximately 75 percent of the ultimate pressure for the unstiffened shell. Damage initiation for the integrally stiffened shell occurs at 23 percent of its ultimate pressure. On the other hand damage initiation for the unstiffened shell occurs at approximately 94 percent of its ultimate pressure. Also, the volume of damage in the integrally stiffened shell at ultimate pressure is much greater than the volume of damage in the unstiffened shell at ultimate pressure.

SUMMARY OF RESULTS

This section summarizes some of the insights gained by the present investigation as applicable to graphite/epoxy laminated composite structures with integrated stiffeners, as follows:

1. Integrated stiffeners may be used to increase the out-of-plane stiffness properties significantly.
2. The improvement of out of plane stiffness is paid for by the degradation of in-plane damage tolerance and durability characteristics.
3. Damage initiation occurred much sooner for the integrally stiffened composite structures subjected to in-plane tension, compression, or shear.
4. Damage initiation occurred in the skin plies for all cases considered.
5. For the integrally stiffened composites, damage initiation was within the skin at stiffened nodes.

GENERALIZATION OF PROCEDURE

The present computational simulation method is suitable for the design and continued in-service evaluation of composite structures. Composite structures with different constituents and ply layups can be evaluated under any loading.

Structural health monitoring is based on damage tolerance requirements defined via the computational simulation method. A damage tolerance parameter is described as the state of damage after the application of a given load level, normalized with respect to the damage state corresponding to ultimate fracture. Identification of damage progression mechanisms and the sequence of progressive fracture modes conveys useful information to evaluate structural safety. Computational simulation results can be formulated into health monitoring criteria, increasing the reliability of composite structures. The simulated failure modes and the type of failure provide the necessary quantitative and qualitative information to design an effective health monitoring system. Computed local damage energy release rates are correlated with the magnitudes of acoustic emission signals and other damage monitoring means such as piezoelectric stress sensors and strain gages that are an integral part of a composite structure. Fiber optics data networks embedded in the composite structure would transmit the detected local damage information to an expert system that provides feedback and reduces power to delay failure.

The basic procedure is to simulate a computational model of the composite structure subjected to the expected loading environments. Various fabrication defects and accidental damage may be represented at the ply and constituent levels, as well as at the laminate level. Computational simulation may be used to address various design and health monitoring questions as follows:

1. Evaluation of damage tolerance: Computational simulation will generate the damage that would be caused due to overloading by the type of load the structure is designed to carry. On the other hand, a fabrication defect or accidental damage produced by inadvertent loading that is not an expected service load can be included in the initial computational model. Once the composite damage is defined, damage tolerance can be evaluated by monitoring damage growth and progression from the damaged state to ultimate fracture. Significant parameters that quantify damage stability and fracture progression characteristics are the rate of damage increase with incremental loading, and the changes in the structural response characteristics with loading. Identification of damage initiation/progression mechanisms and the sequence of progressive fracture modes convey serviceable information to help with critical decisions in the structural design and health monitoring process. Determination of design allowables based on damage tolerance requirements is an inherent use of the computational simulation results. Simulation of progressive fracture from defects allows setting of qual-

ity acceptance criteria for composite structures as appropriate for each functional requirement. Detailed information on specific damage tolerance characteristics help establish criteria for the retirement of a composite structure from service for due cause.

2. Determination of sensitive parameters affecting structural fracture: Computational simulation indicates the damage initiation, growth, and progression modes in terms of a damage index that is printed out for the degraded plies at each damaged node. In turn, the damage index points out the fundamental physical parameters that characterize the composite degradation. For instance, if the damage index shows ply transverse tensile failure, the fundamental physical parameters are matrix tensile strength, fiber volume ratio, matrix modulus, and fiber transverse modulus; of which the most significant parameter is the matrix tensile strength (Murthy and Chamis, 1986). In addition to the significant parameters pointed out by the ply damage index, sensitivity to hygrothermal parameters may be obtained by simulating the composite structure at different temperatures and moisture contents. Similarly, sensitivity to residual stresses may be assessed by simulating the composite structure fabricated at different cure temperatures. Identification of the important parameters that significantly affect structural performance for each design case allows optimization of the composite for best structural performance. Sensitive parameters may be constituent strength, stiffness, laminate configuration, fabrication process, and environmental factors.

3. Interpretation of experimental results for design decisions: Computational simulation allows interactive experimental-numerical assessment of composite structural performance. Simulation can be used prior to testing to identify locations and modes of composite damage that need be monitored by proper instrumentation and inspection of the composite structure. Interpretation of experimental data can be significantly facilitated by detailed information from computational simulation. Subscale experimental results may be extended to full prototype structures without concern for scale effects since computational simulation does not presume any global parameters but is based on constituent level damage tracking.

CONCLUSIONS

On the basis of the results obtained from the investigated flat composite plate, integrally stiffened panel, integrally stiffened and unstiffened composite cylindrical shell examples and from the general perspective of the available computational simulation method, the following conclusions are drawn:

1. Computational simulation can be used to track the details of damage initiation, growth, and subsequent propagation to fracture for unstiffened and integrally stiffened composite structures.
2. For the considered integral stiffening system, out-of-plane structural response characteristics such as the buckling load and the bending stiffness are significantly improved.
3. In-plane load carrying capability of a composite panel is reduced due to damage initiation and progression processes caused by the presence of integrated stiffeners.
4. Computational simulation, with the use of established composite mechanics and finite element modules, can be used to predict the influence of composite geometry as well as loading and material properties on the durability of composite structures.
5. The demonstrated procedure is flexible and applicable to all types of constituent materials, structural geometry, and loading. Hybrid composites and homogeneous materials, as well as laminated, stitched, woven, and braided composites can be simulated.
6. Computational simulation by CODSTRAN represents a new global approach to progressive damage and fracture assessment for any structure.

REFERENCES

1. C. C. Chamis and G. T. Smith, "Composite Durability Structural Analysis," NASA TM–79070, 1978.

2. T. B. Irvine and C. A. Ginty, "Progressive Fracture of Fiber Composites," *Journal of Composite Materials*, Vol. 20, March 1986, pp. 166-184.

3. L. Minnetyan, C. C. Chamis, and P. L. N. Murthy, "Structural Behavior of Composites with Progressive Fracture," *Journal of Reinforced Plastics and Composites*, Vol. 11, No. 4, April 1992, pp. 413-442

4. L. Minnetyan, P. L. N. Murthy, and C. C. Chamis, "Progression of Damage and Fracture in Composites under Dynamic Loading," NASA TM–103118, April 1990, 16 pp.

5. L. Minnetyan, P. L. N. Murthy, and C. C. Chamis, "Composite Structure Global Fracture Toughness via Computational Simulation," *Computers & Structures*, Vol. 37, No. 2, pp.175-180, 1990

6. L. Minnetyan, P. L. N. Murthy, and C. C. Chamis, "Progressive Fracture in Composites Subjected to Hygrothermal Environment," *International Journal of Damage Mechanics*, Vol. 1, No. 1, January 1992, pp. 60-79

7. L. Minnetyan, C. C. Chamis, and P. L. N. Murthy, "Damage and Fracture in Composite Thin Shells," NASA TM–105289, November 1991

8. C. C. Chamis, P. L. N. Murthy, and L. Minnetyan, "Progressive Fracture of Polymer Matrix Composite Structures: A New Approach," NASA TM–105574, January 1992, 22 pp.

9. L. Minnetyan, J. M. Rivers, P. L. N. Murthy, and C. C. Chamis, "Structural Durability of Stiffened Composite Shells," Proceedings of the 33rd SDM Conference, Dallas, Texas, April 13-15, 1992, Vol. 5, pp. 2879-2886

10. L. Minnetyan and P. L. N. Murthy,"Design for Progressive Fracture in Composite Shell Structures," Proceedings of the 24th International SAMPE Technical Conference, Toronto, Canada, October 20-22, 1992, pp. T227-T240

11. P. L. N. Murthy and C. C. Chamis, *Integrated Composite Analyzer (ICAN): Users and Programmers Manual*, NASA Technical Paper 2515, March 1986.

12. S. Nakazawa, J. B. Dias, and M. S. Spiegel, *MHOST Users' Manual*, Prepared for NASA Lewis Research Center by MARC Analysis Research Corp., April 1987.

13. L. Sobel, C. Buttitta, and J. Suarez, "Probabilistic & Structural Reliability Analysis of Laminated Composite Structures Based on IPACS Code," Proceedings of the 34th SDM Conference, LaJolla, California, April 19-22, 1993, Vol. 2, pp. 1207-1217

TABLE I: AS-4 Fiber Properties:

Number of fibers per end = 10000
Fiber diameter = 0.00762 mm (0.300E-3 in)
Fiber Density = 4.04E-7 Kg/m^3 (0.063 lb/in^3)
Longitudinal normal modulus = 200 GPa (29.0E+6 psi)
Transverse normal modulus = 13.7 GPa (1.99E+6 psi)
Poisson's ratio (ν_{12}) = 0.20
Poisson's ratio (ν_{23}) = 0.25
Shear modulus (G_{12}) = 13.8 GPa (2.00E+6 psi)
Shear modulus (G_{23}) = 6.90 GPa (1.00E+6 psi)
Longitudinal thermal expansion coefficient = -1.0E-6/°C (-0.55E-6 /°F)
Transverse thermal expansion coefficient = 1.0E-5/°C (0.56E-5 /°F)
Longitudinal heat conductivity = 301 kJ-m/hr/m^2/°C (4.03 BTU-in/hr/in^2/°F)
Transverse heat conductivity = 30.1 kJ-m/hr/m^2/°C (.403 BTU-in/hr/in^2/°F)
Heat capacity = 0.712 kJ/kg/°C (0.17 BTU/lb/°F)
Tensile strength = 3.09 GPa (448 ksi)
Compressive strength = 3.09 GPa (448 ksi)

TABLE II: HMHS Matrix Properties:

Matrix density = 3.40E-7 Kg/m^3 (0.0457 lb/in^3)
Normal modulus = 4.14 GPa (600 ksi)
Poisson's ratio = 0.34
Coefficient of thermal expansion = 0.72E-4/°C (0.40E-4 /°F)
Heat conductivity = 0.648 kJ-m/hr/m^2/°C (0.868E-2 BTU-in/hr/in^2/°F)
Heat capacity = 1.047 KJ/Kg/°C (0.25 BTU/lb/°F)
Tensile strength = 71.0 MPa (10.3 ksi)
Compressive strength = 423 MPa (61.3 ksi)
Shear strength = 161 MPa (23.4 ksi)
Allowable tensile strain = 0.02
Allowable compressive strain = 0.05
Allowable shear strain = 0.04
Allowable torsional strain = 0.04
Void conductivity = 16.8 J-m/hr/m^2/°C (0.225 BTU-in/hr/in^2/°F)
Glass transition temperature = 216°C (420°F)

LIST OF FIGURE CAPTIONS

Figure 1 Computational Simulation Cycle

Figure 2 Finite Element Model with Square Elements
Diagonal Lines are along the Integrated Stiffeners; AS-4/HMHS$[0/90/\pm45]_S$
Width = 305 mm; Length = 457 mm

Figure 3 Deflections of Panels due to Bending
Graphite-epoxy: AS-4/HMHS$[0/90/\pm45]_S$
Solid line: flat panel
Dashed line: integrally stiffened panel

Figure 4 Damage Progression under Uniaxial Tension
Graphite-epoxy: AS-4/HMHS$[0/90/\pm45]_S$
Solid line: flat panel
Dashed line: integrally stiffened panel

Figure 5 Displacements under Uniaxial Tension
Graphite-epoxy: AS-4/HMHS$[0/90/\pm45]_S$
Solid line: flat panel
Dashed line: integrally stiffened panel

Figure 6 Damage Progression under Compression
Graphite-epoxy: AS-4/HMHS$[0/90/\pm45]_S$
Solid line: flat panel
Dashed line: integrally stiffened panel

Figure 7 Displacements under Uniaxial Compression
Graphite-epoxy: AS-4/HMHS$[0/90/\pm45]_S$
Solid line: flat panel
Dashed line: integrally stiffened panel

Figure 8 Damage Progression under In-plane Shear
Graphite-epoxy: AS-4/HMHS$[0/90/\pm45]_S$
Solid line: flat panel
Dashed line: integrally stiffened panel

Figure 9 Displacements under In-plane Simple Shear
Graphite-epoxy: AS-4/HMHS$[0/90/\pm45]_S$
Solid line: flat panel
Dashed line: integrally stiffened panel

Figure 10 Finite Element Model of Cylindrical Shell
AS-4/HMHS$[0/90/\pm45]_S$

Figure 11 Damage Progression under Axial Tension
Graphite-epoxy: AS-4/HMHS$[0/90/\pm45]_S$
Solid line: unstiffened shell
Dashed line: integrally stiffened shell

Figure 12 Exhusted Damage Energy under Tension
Graphite-epoxy: AS-4/HMHS$[0/90/\pm45]_S$
Solid line: unstiffened shell
Dashed line: integrally stiffened shell

Figure 13 Damage Energy Release Rates under Tension
Graphite-epoxy: AS-4/HMHS$[0/90/\pm45]_S$
Solid line: unstiffened shell
Dashed line: integrally stiffened shell

Figure 14 Damage Progression under External Pressure
Graphite-epoxy: AS-4/HMHS$[0/90/\pm45]_S$
Solid line: unstiffened shell
Dashed line: integrally stiffened shell

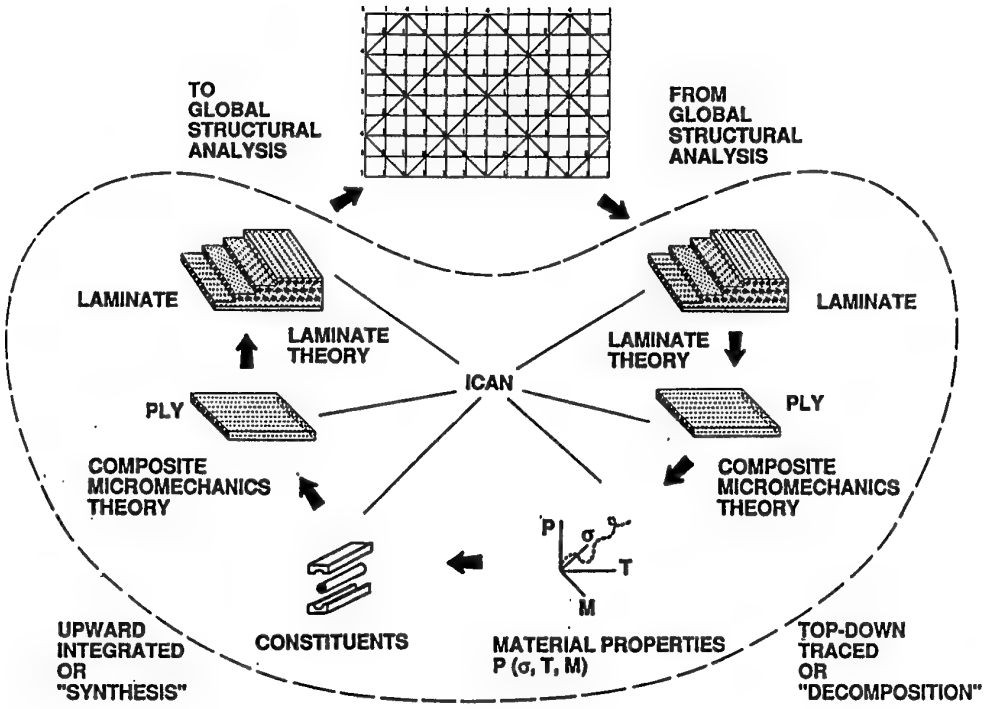

Figure 1 Computational Simulation Cycle

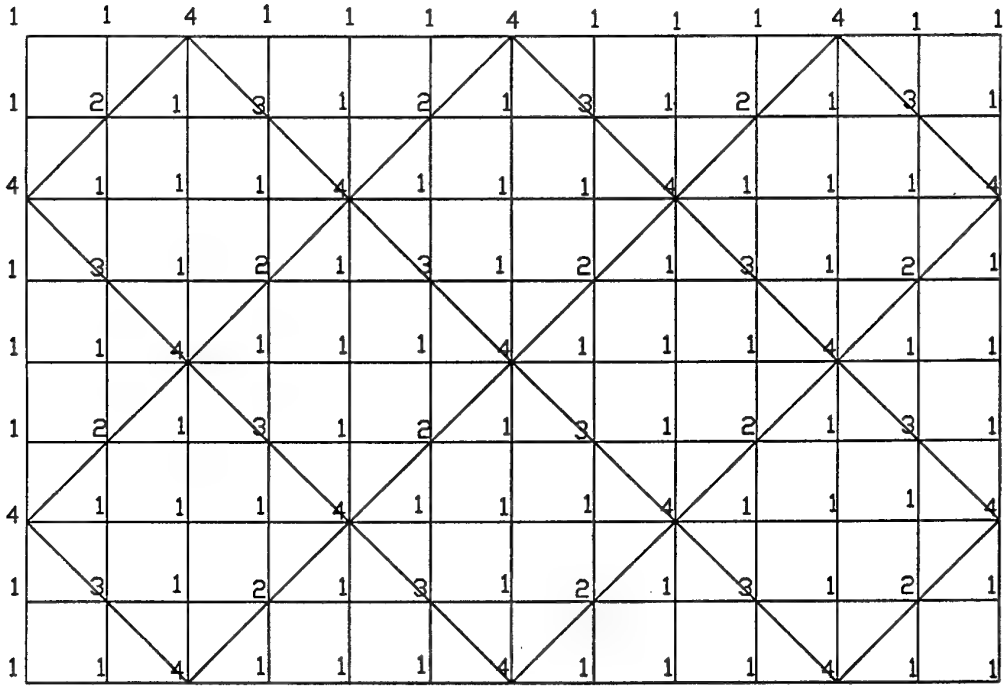

Figure 2 Finite Element Model with Square Elements
Diagonal Lines are along the Integrated Stiffeners
AS-4/HMHS$[0/90/\pm45]_S$; Width = 305 mm; Length = 457 mm

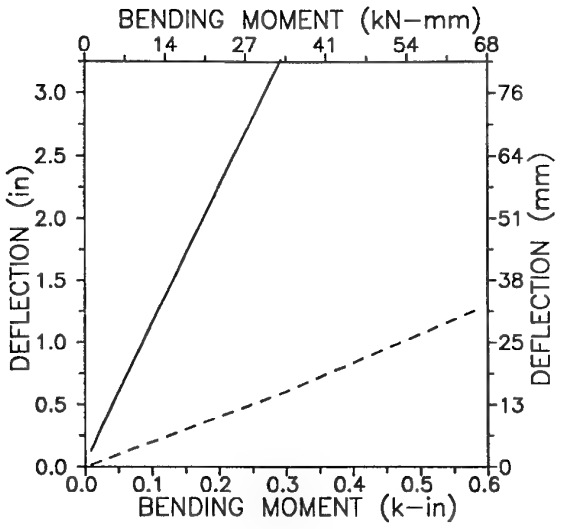

Figure 3 Deflections of Panels due to Bending
Graphite-epoxy: AS-4/HMHS$[0/90/\pm45]_S$
Solid line: flat panel
Dashed line: integrally stiffened panel

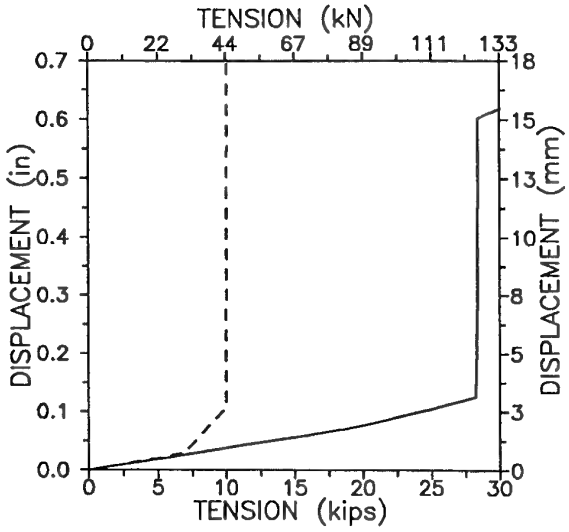

Figure 5 Displacements under Uniaxial Tension
Graphite-epoxy: AS-4/HMHS$[0/90/\pm45]_S$
Solid line: flat panel
Dashed line: integrally stiffened panel

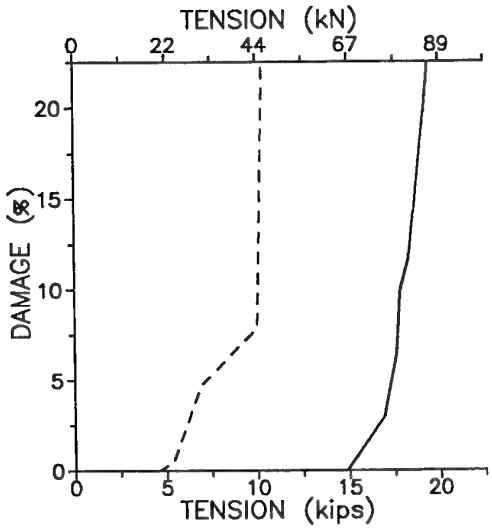

Figure 4 Damage Progression under Uniaxial Tension
Graphite-epoxy: AS-4/HMHS$[0/90/\pm45]_S$
Solid line: flat panel
Dashed line: integrally stiffened panel

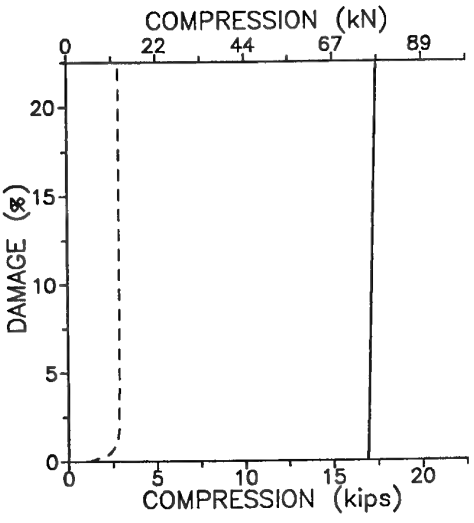

Figure 6 Damage Progression under Compression
Graphite-epoxy: AS-4/HMHS$[0/90/\pm45]_S$
Solid line: flat panel
Dashed line: integrally stiffened panel

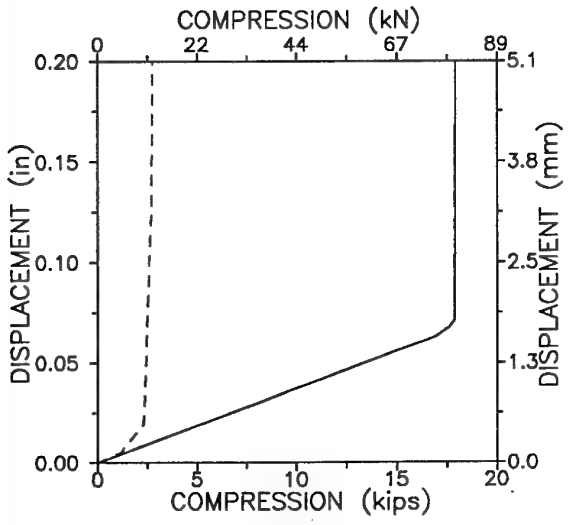

Figure 7 Displacements under Uniaxial Compression
Graphite-epoxy: AS-4/HMHS[0/90/±45]$_S$
Solid line: flat panel
Dashed line: integrally stiffened panel

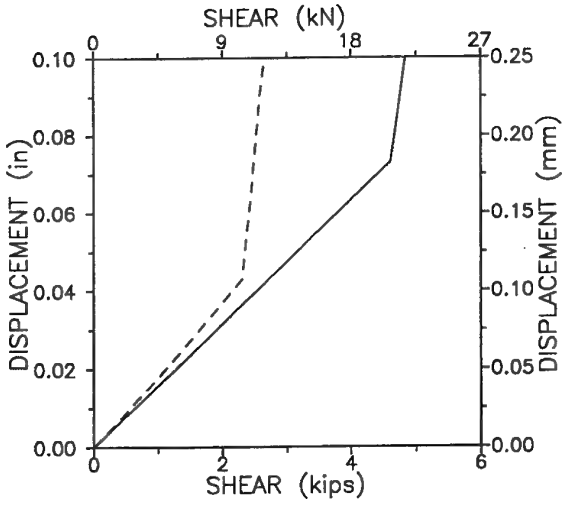

Figure 9 Displacements under In-plane Simple Shear
Graphite-epoxy: AS-4/HMHS[0/90/±45]$_S$
Solid line: flat panel
Dashed line: integrally stiffened panel

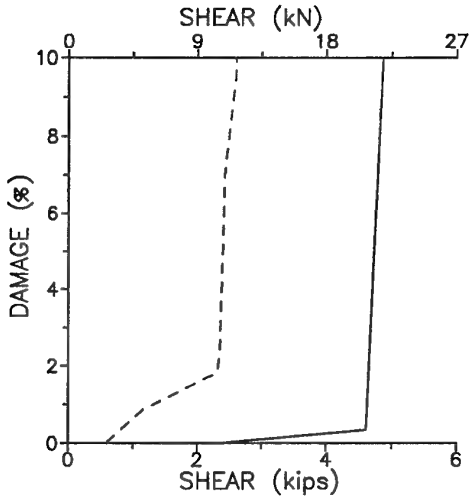

Figure 8 Damage Progression under In-plane Shear
Graphite-epoxy: AS-4/HMHS[0/90/±45]$_S$
Solid line: flat panel
Dashed line: integrally stiffened panel

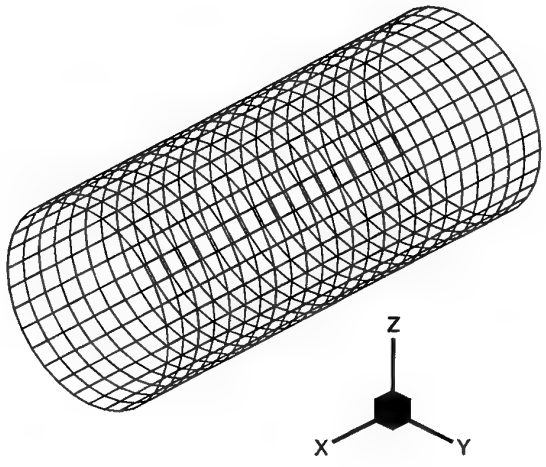

Figure 10 Finite Element Model of Cylindrical Shell
AS-4/HMHS[0/90/±45]$_S$

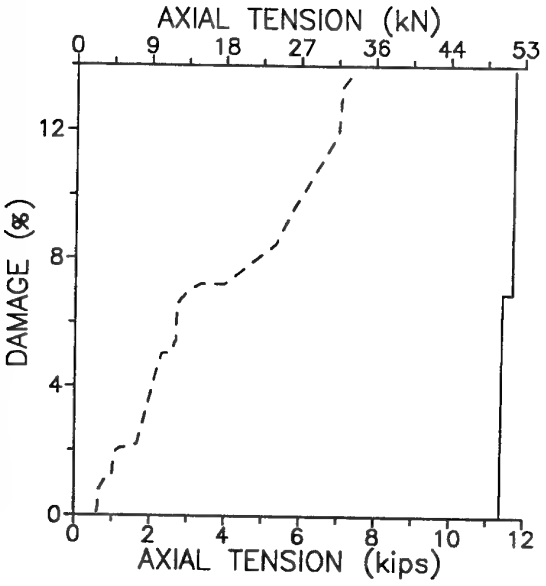

Figure 11 Damage Progression under Axial Tension
Graphite-epoxy: AS-4/HMHS$[0/90/\pm45]_S$
Solid line: unstiffened shell
Dashed line: integrally stiffened shell

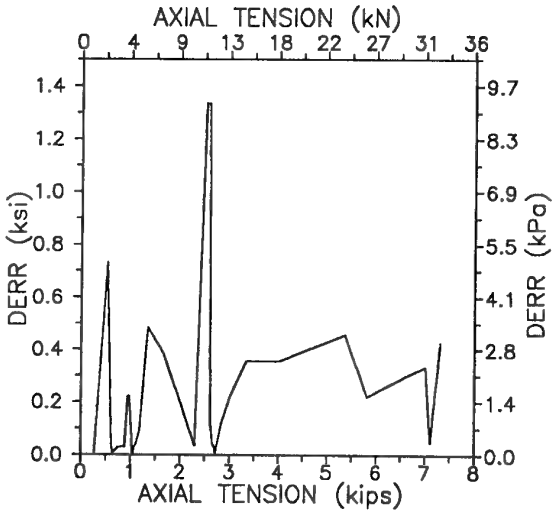

Figure 13 Damage Energy Release Rates under Tension
Graphite-epoxy: AS-4/HMHS$[0/90/\pm45]_S$
Solid line: unstiffened shell
Dashed line: integrally stiffened shell

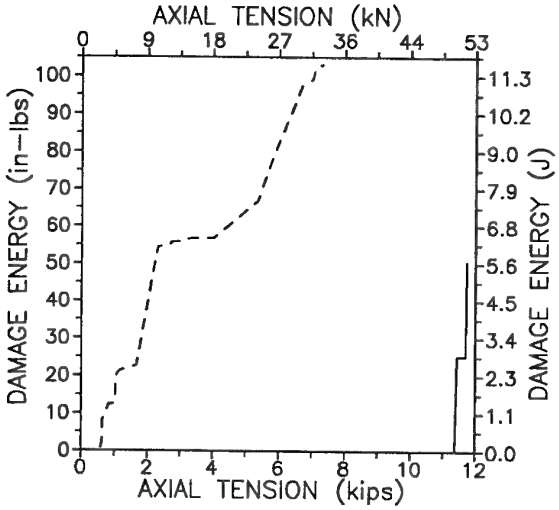

Figure 12 Exhusted Damage Energy under Tension
Graphite-epoxy: AS-4/HMHS$[0/90/\pm45]_S$
Solid line: unstiffened shell
Dashed line: integrally stiffened shell

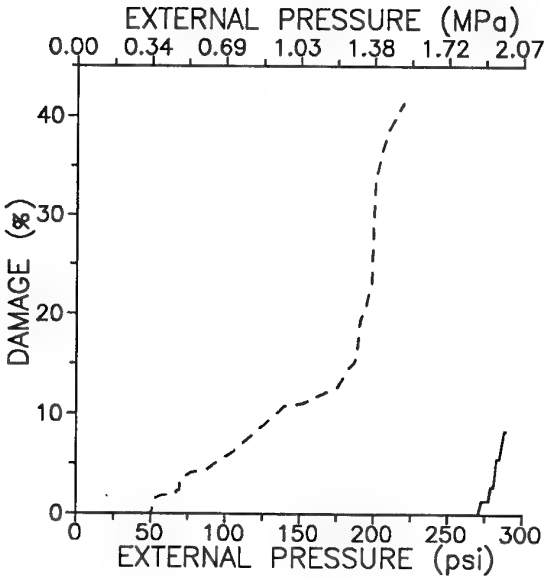

Figure 14 Damage Progression under External Pressure
Graphite-epoxy: AS-4/HMHS$[0/90/\pm45]_S$
Solid line: unstiffened shell
Dashed line: integrally stiffened shell

The US Navy's Helicopter Integrated Diagnostics System (HIDS) Program: Power Drive Train Crack Detection Diagnostics and Prognostics, Life Usage Monitoring, and Damage Tolerance; Techniques, Methodologies, and Experiences

Andrew Hess
William Hardman
US Naval Air Warfare Center
Aircraft Division
Patuxent River, Md 20670-1534
United States

Harrison Chin
John Gill
BFGoodrich Aerospace
54 Middlesex Turnpike
Bedford, MA 01730
United States

The evolution of automated diagnostic systems for helicopter mechanical systems has been greatly advanced by the Navy, in a program of systematic testing of drive train components having known anomalies (seeded faults) while simultaneously executing a suite of diagnostic techniques to identify and classify the mechanical anomalies. This program, called the Helicopter Integrated Diagnostic System (HIDS) was carried out using both an iron bird test stand and SH-60B/F flight vehicles. The SH-60 HIDS program has been the Navy's cornerstone effort to develop, demonstrate, and justify integrated mechanical diagnostic system capabilities for its various helicopter fleets. The objectives of the original program were to:

1. Acquire raw data for multiple cases of "good" and seeded fault mechanical components on a fully instrumented drive train to support the evaluation of diagnostic algorithms and fault isolation matrices. Data is being acquired from 32 vibration channels simultaneously at 100 kHz per channel while a continuous usage monitoring system records parametric steady state data from the power plant and airframe.
2. Analyze vibration and other diagnostic indicators to evaluate sensitivity and performance of all available diagnostic methods when analyzing well-documented parts and their associated failure modes. Evaluate relative effectiveness of these various diagnostic methods, indicators, and their associated algorithms to identify and optimize sensor location combinations.
3. Demonstrate the ability to integrate and automate the data acquisition, diagnostic, fault evaluation and communication processes in a flight worthy system.
4. Integrate and evaluate comprehensive engine monitoring, gearbox and drive train vibration diagnostics, advanced oil debris monitoring, in-flight rotor track and balance, parts life usage tracking, automated flight regime recognition, power assurance checks and trending, and automated maintenance forecasting in a well-coordinated on-board and ground-based system.
5. Provide an extensive library of high quality vibration data on baseline and seeded fault components. This data can be made available to anyone wanting to prove their diagnostic techniques or develop new capability.
6. Provide a "showcase", state-of-the-art, fully functional Integrated Mechanical Diagnostic system to act as a catalyst demonstration which might lead to interest in a fleet wide production application.

This paper will describe the HIDS program background, development, system capabilities, and accomplishments; but will also focus on the most recent demonstrated drive train crack detection diagnostic techniques; aircraft component life usage monitoring philosophies and capabilities; and damage tolerance methodologies. Data and results from both the seeded fault "iron bird" test cell rig and flight test aircraft will be presented. Experience, results, and lessons learned will be emphasized. HIDS initiated functions and capabilities being applied to the commercial off-the-shelf (COTS) SH-60 Integrated Mechanical Diagnostics System (IMDS) production program will be described. Conclusions and lessons learned that can be applied to future Helicopter Usage Monitoring Systems (HUMS) and/or Integrated Mechanical Diagnostic (IMD) systems will also be discussed.

Introduction

Background

The U. S. Navy and U. S. Marine Corps rotary wing operators have long had a requirement to improve readiness through more effective maintenance, eliminate losses of aircraft and personnel, and dramatically reduce maintenance related costs. The requirements to extend the service life of aircraft and the limitations on manpower have increased the urgency of effecting these types of improvements. A major cause of the Class A mishaps (loss of aircraft and/or personnel) in Navy helicopters are caused by

Paper prepared for the RTO AVT Specialists' Meeting on "Application of Damage Tolerance Principles for Improved Airworthiness of Rotorcraft", held in Corfu, Greece, 21-22 April 1999, and published in RTO MP-24.

engine and drive train failures. The need to accurately identify and diagnose developing faults in mechanical systems is central to the ability to reduce mechanically induced failures and prevent excessive maintenance. The Navy has successfully developed and deployed engine monitoring systems in fixed wing aircraft, notably on the A-7E and subsequent fighter/attack aircraft. These Engine Monitoring Systems (EMS) have positively impacted flight safety, aircraft availability, and maintenance effectiveness. The Navy also successfully demonstrated a promising automatic mechanical fault diagnostic capability on its gearbox overhaul test stands in Pensacola, Florida.

The U.S. Navy would clearly benefit from a reliable state-of-the-art on-board diagnostic capability for rotary wing aircraft. An advanced prognostic capability would provide even further benefits. Based upon the Mission Need Statement (Ref. 1), such a system is expected to enhance operational safety and significantly reduce life cycle cost. The system accomplishes this through it's ability to predict impending failure of both structural and dynamic drive system components and consequently direct on-condition maintenance actions and/or alert the pilot to conditions affecting flight safety.

While diagnostic capabilities to detect a specific impending component failure are relatively straightforward, prognostic capabilities are less mature and can provide a much larger benefit payoff. Any system considered for fleet-wide implementation should have both capabilities to maximize effectiveness. Any program to demonstrate and validate diagnostic capabilities must also address some degree of prognostics. This program attempts to do both.

There is currently considerable activity underway to develop integrated health and usage monitoring systems, particularly for helicopter subsystems (transmissions, rotor head, engines, tail drive systems, etc.). A major challenge is acquiring and managing large quantities of data to assess the health and usage of the aircraft system.

A significant disadvantage of first generation commercial systems in 1992 was the lack of raw data acquired to validate and optimize the full, Integrated Mechanical Diagnostic (IMD) functionality. As a result, these systems exhibited false alarms and missed calls and did not routinely collect the supporting raw data that would enable improvement of the diagnostic accuracy. Raw data acquisition is necessary in any development effort, in order to reliably indicate mechanical and rotor system faults, avoid false alarms, and develop structural and mechanical system usage routines. These are some of the keys to preparing a production IMD system for deployment.

Present Work

The Naval Air Warfare Center Aircraft Division leads a very comprehensive and continuing program to evaluate helicopter diagnostic, prognostic, and usage technologies. The SH-60 was originally selected as the test vehicle because it offered the best availability of test assets and the highest potential for eventual production support, because of its large fleet of aircraft among the Navy, Army and Coast Guard. The program designated Helicopter Integrated Diagnostic System (HIDS) uses state-of-the-art data acquisition, raw data storage, and algorithmic analysis provided under contract by Technology Integration Inc. [TII - now part of BFGoodrich Aerospace (BFG)] to evaluate the propulsion and power, rotor, and structural systems. Cockpit instruments and control positions are recorded during the entire flight for usage monitoring and flight analysis. Rotor track and balance is performed via the trackerless ROTABS system. Analysis of vibration signals acquired from a comprehensive suite of accelerometers assesses dynamic component health.

The program reported herein was structured to evaluate two functionally equivalent TII/BFG systems at the following test sites:

1. Flight Testing: Flight tests were conducted at NAWCADPAX (Naval Air Warfare Center, Patuxent River, Maryland). Demonstrate the integration of a comprehensive integrated diagnostic system which performs rotor track and balance, mechanical and rotor system diagnostics, and dynamic and structural component usage monitoring. Evaluate the operability of the demonstration system and provide a foundation for the user interface requirements functional specification for fleet procurement. In addition, evaluate a real time engine performance estimation algorithm provided by General Electric Aircraft Engines in cooperation with Dr. Peter Frith of the Australian Mechanical Research Laboratory (AMRL) via implementation onboard the HIDS flight test aircraft.

2. Ground Testing: Conduct fault detection validation testing in the unique NAWCAD full scale Helicopter Transmission Test Facility (HTTF) which currently consists of the entire SH-60 power drive system (engines, transmission and tail drive system). Evaluate and validate the TII/BFG system and associated algorithms to detect seeded faults while building a base of raw data for evaluating other fault detection methods. In addition, the program is evaluating other advanced technologies in parallel with the TII system. The information generated from this testing will form a body of knowledge from which

specifications can be written to procure effective production versions of the integrated diagnostic system.

One purpose of this paper is to describe the overall program, diagnostic system, NAWCAD HTTF, seeded fault testing, flight testing and major accomplishments to date. A second purpose is to discuss both diagnostic and potential prognostic capabilities demonstrated during this development experience. Thirdly, possible impacts of HIDS type systems on damage tolerance concerns for aging aircraft will be briefly discussed. Finally, several lessons learned that that can be applied to future production HUMS and IMDS programs will be identified.

Description

This section will describe the systems and facilities used in support of the HIDS program. The test articles are the diagnostic and prognostic technologies. The SH-60 test facilities were used to exercise various diagnostic and prognostic technologies and evaluate their relative performance.

HIDS Diagnostic System

In 1993, the NAWCAD awarded a competitive contract on the Broad Agency Announcement to TII for two functionally equivalent integrated diagnostic systems. (TII elected to make a substantial investment in the program through providing Commercial Off the Shelf (COTS) hardware and software.) One system was configured for rack mounting in the HTTF and the other is flyable ruggedized commercial grade hardware. The TII system uses an industry-standard open architecture to facilitate modularity and insertion of new hardware and software. TII has divided the system into two main avionics units, the commercial off-the-shelf KT-1 aircraft parameter-usage monitor and the KT-3 vibration acquisition, analysis and rotor track and balance system. System architecture and data flow is shown in Figure 1. Though not a production type unit, the vibration acquisition system is essential to acquire the raw data necessary to substantiate the diagnostics technology and obtain enough knowledge to write the minimum acceptable production specification.

Structural Usage Monitor: The TII/BFG system performs aircraft usage monitoring, engine condition monitoring, drive shaft and gearbox condition monitoring, chip detector monitoring and rotor track and balance. Data is stored to a PCMCIA card providing the usage spectrum of the aircraft, engine performance information, flight regimes for trending gearbox vibration information and an actual record of the mission. This data is available for post-processing, enabling recalculation of regime recognition and structural usage parameters.

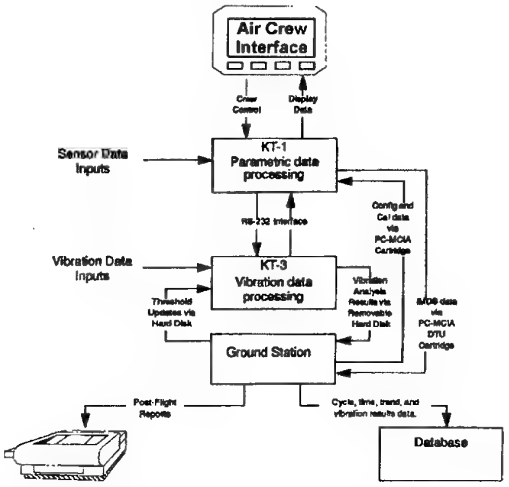

Fig. 1. Diagnostic System Architecture.

Engine Performance: The HIDS Cockpit Display Unit (CDU) depicted in Figure 2 interfaces with the pilot to execute and display results of automated NATOPS T700 engine health checks and the engine Power Performance Index (PPI). The PPI is a fourth order best fit curve representing an engine degraded 7.5% from the specification line, and can provide a warning to the pilot when an engine has degraded due to salt ingestion, sand erosion or other foreign object damage (FOD).

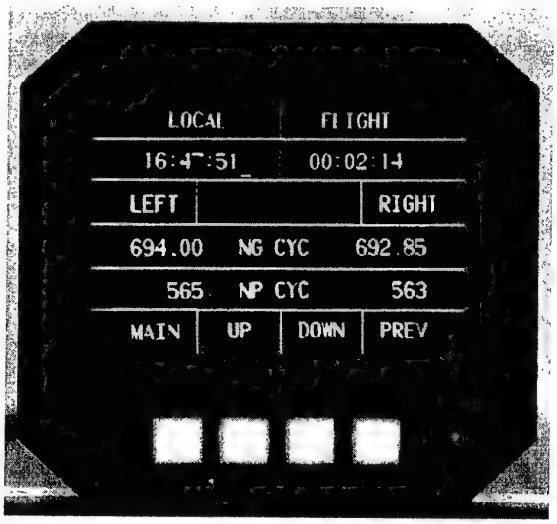

Fig. 2. Central Display Unit.

Vibration Based Mechanical Diagnostics: The focal point of this program was to explore a wide

variety of diagnostic methods based upon vibration inputs, in a manner that would lead to a rational selection of reliable "production" techniques with a high confidence in accurate detection with low false alarm rates. Vibration data recorded at both Trenton, NJ and Patuxent River, MD uses the same acquisition system, sensors, mounting and accelerometer locations. The data sets are digital time series records, recorded simultaneously for up to 32 channels (accelerometers and tachometers), at 100,000 samples per second, 0-50Khz bandwidth, for 30 seconds. This proof-of-concept system records five sets of raw data per flight for post flight data analysis in the ground station. Drive system accelerometer locations are shown in Figure 3 for the input and main modules and Figure 4 for the tail section. The mechanical diagnostic system algorithms provided by TII/BFG under investigation are "classical," model based diagnostics. That is, the model is composed of the Sikorsky proprietary gear and bearing tables for the SH-60B drive system. No fault or anomaly detection training is required. The system provides three significant contributions to the development and verification of diagnostics for helicopters:

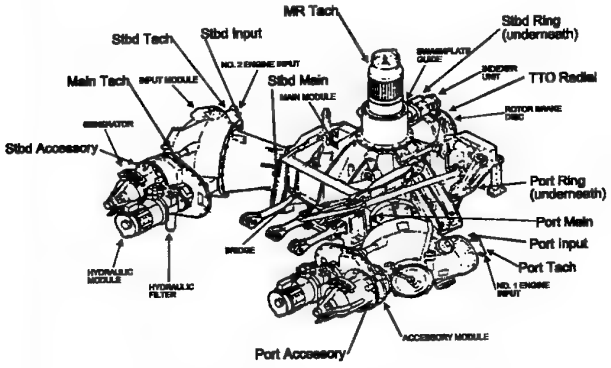

Fig. 3. Accelerometer Locations on Input and Main Modules.

1. First, the system acquires data from all channels simultaneously. This makes it possible to use multiple channels to analyze a single component; an essential element of false alarm reduction. Today, the HIDS system is the only flying data acquisition system that has demonstrated the ability to record the raw and processed data set for an entire aircraft propulsion and power drive system. The HIDS system saves raw time series data, for all channels including tachometers for post flight evaluation and future algorithm development. This minimizes the possibility that a malfunction in the preprocessing could contaminate the database.

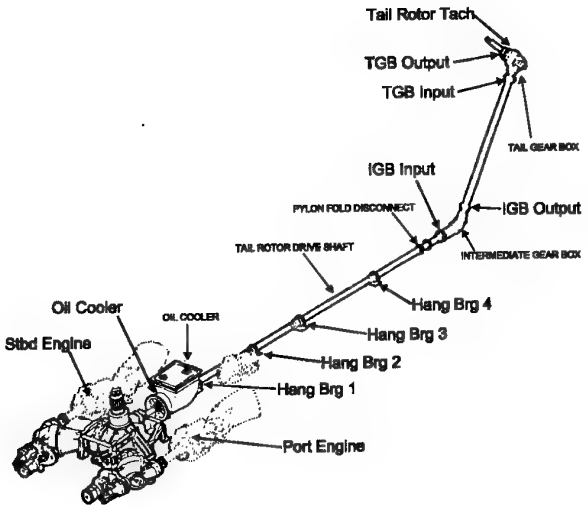

Fig. 4. Accelerometer Locations on the Tail Drive System.

2. Second, the system has the capability to automatically adjust to provide good signal to noise ratios for all channels. The system starts each acquisition with a one-second acquisition, and internally sets the gains based upon the measured signal amplitude to maximize dynamic range. The gain for each channel is recorded with the raw data for future analysis.

3. Third, is the capability for on-board processing. All gears, bearings and shafts are analyzed and the diagnostic results are written to the aircraft parameter data file according to flight regime. The raw data files can be held in RAM until the analysis is complete, then discarded if no anomalies are identified by the limit check. If a parameter is deemed to be in "maintenance" or "alarm" status by exceeding preset limits, the component of concern would have all of the accelerometers that are used for its analysis plus the aircraft tachometer saved as raw digital time series data for post flight investigation. When data is taken in response to a pilot-activated switch, raw data is written to disk with all of the analysis results. The HIDS program is in the process of determining alarm limits and algorithm sensitivities to achieve this goal and level of integration.

Vibration Based Prognostics: Though it is often difficult to separate diagnostic and prognostic performance in a seeded fault program such as this, one of the by-products of this testing was the demonstration of the potential and performance of prognostics.

As a working definition for this paper: prognostics is the capability to provide early detection of the precursor and/or incipient fault condition to a component or sub-element failure condition; and to have the

technology and means to manage and predict the progression of this fault condition to component failure. The early detected, "incipient" fault condition, is monitored, "tracked", and safely managed from a "small" fault as it progresses to a "larger" fault, until it warrants some maintenance action and/or replacement. Through this early detection and monitoring management of incipient fault progression, the health of the component is known at any point in time and the future failure event can be safely predicted in time to prevent it.

Applying many of the same algorithms and techniques used for vibration based mechanical diagnostics, a significant degree of component failure prediction and prognostics was demonstrated during these tests. Often the extrapolation of vibration frequency data, statistical parameters and/or diagnostic indices trends is the technique used to enable failure prediction. It is of course key to have sensors, algorithms, and diagnostics indicators (or indices) that are sensitive and accurate enough to "see" the precursor or incipient "small" component fault. It is equally important to have a reliable experience database of examples of similar types of "faults" so that the failure progression rate is understood. Using this experience database knowledge and the understanding of various types of failure progressions will enable the intelligent settings of alarm thresholds. It is envisioned that in most cases, the alarm thresholds for safety-of-flight (cockpit warning) will be significantly higher than for maintenance. Establishing these alarm thresholds is a very necessary step in implementing future failure event prediction and enabling prognostics. Without having the benefit of an extensive experience database of actual component failures with fault progression data and/or a comprehensive "seeded fault" trials as the SH-60 HIDS program, establishing these alarm thresholds approaches the realm of "magic".

There are other important elements needed in the "diagnostic tool kit" or "bag of tricks" before prognostics can be successfully implemented. One of these can be called "Model Based" diagnostics or prognostics. Another can be grouped as a series of approaches and techniques to handle data scatter and manage false alarms. Model based techniques require a detailed and accurate understanding of the underlying physics of the system to model how a specific component, system, or machine, operates in normal and degraded conditions. Using measured parameters, real or calculated, against this accurate model, enables the determination of relative "health" of the component monitored at any point in time. Some of the approaches applied to deal with inherent data scatter and to manage false alarms include: fuzzy logic and neural network techniques; data fusion; and multiple indications (either sensor or algorithm indices driven) required prior to alarm. At times, and with varying degrees of application and success, all of these approaches and techniques were tried during this program.

Rotor Track and Balance: The ROTABS system promises to negate the need for on-board trackers and utilizes higher order mathematics and a significantly larger data set to resolve the adjustments required to keep the rotor system in track and balance. ROTABS does not collect or use track data to compute rotor adjustments. On other aircraft types, the system has demonstrated the ability to maintain track limits while simultaneously optimizing vibration in 6-degrees-of-freedom at 1/rev and selected harmonics thereof. Results obtained during HIDS testing have been presented in detail (Ref. 3).

A continuous monitoring of the in-flight rotor track and balance condition will alert the maintainers of out-of-limit conditions that, among other things, will result in high vibration stress conditions. By keeping the rotor system in a "better" track and balance condition, overall vibration levels on all aircraft structural components and subsystems will be reduced. This could significantly increase the life of many of these aircraft structural components and subsystems. In particular, avionics systems could see a large improvement in life. This capability alone would positively impact several damage tolerance issues on aging aircraft.

Groundstation: The HIDS groundstation houses maintenance, pilot, and engineering windows to support complete health and usage functionality. Tools are provided for parts and maintenance tracking, rotor track and balance, mechanical diagnostics, flight parametric data and flight regime replay, pilot flight logs, and projected component retirement times. During a flight data download, the groundstation calculates flight regimes from downloaded parametric data, and updates life usage on pre-selected serialized components in a database upon aircraft data download. Functions to trigger usage based maintenance and component replacement are designed into the system. Historical data replay provides regime, event and exceedance information along with all aircraft parameters for the entire flight. Pilot control inputs are displayed along with all aircraft parameters for the entire flight. Pilot inputs are recorded along with other parameters, which are essential for understanding events during a flight. The ground station has been shown to reduce the paperwork associated with daily operations and to direct maintenance personnel to the faulty component identified by diagnostics.

Description of the Test Cell

The NAWCAD HTTF has been described in detail (Ref. 4). The facility was originally located in Trenton, NJ and has now been transferred to the new Propulsion Systems Evaluation Facility (PSEF) at NAWCADPAX. The test cell uses aircraft engines to provide power to all of the aircraft drive systems except the rotors. Power is absorbed through both the main rotor mast and tail rotor shaft by water brake dynamometers. The main rotor shaft is loaded in bending, tension and torque to simulate flight conditions. There is a speed increasing gearbox between the main rotor mast and the water brake, which raises the main rotor speed by a factor of 32. This currently allows water brakes to extract up to 8,000 shaft horsepower (SHP) and will soon be upgraded to handle up to 18,500 SHP. The complete aircraft lubrication system is used with the oil cooler, oil cooler blower and blower drive shaft part of the system assembly. The tail drive system is installed and power is extracted from the tail at operating speed. The tail water brake can extract up to 700 SHP.

The tail drive system installation allows balance and alignment surveys on the blower, tail drive shafts and disconnect coupling. Aircraft viscous damper bearing assemblies support the installation. The length of the test cell limits the number of tail drive shafts, so two of the aircraft shafts are not installed. The test cell also supports the aircraft accessories. Generators and hydraulic pumps are mounted on the accessory gearboxes and loaded to simulate aircraft operation (see Figure 5). This is a significant capability, especially when diagnostics using vibration acquisition is the test objective. Vibration signatures collected from the HTTF include frequency content from all dynamic components of the loaded power drive system. The complex signal is representative of the aircraft environment.

Since this cell has the ability to operate all the aircraft mechanical systems together, the diagnostic system can record all component "signatures" to a database. This database can then be interrogated to determine system health, and system performance rather than a diagnostic evaluation of a single component or fault. This is a significant improvement over single component regenerative rigs that tend to have two gearboxes that generate the same frequencies (and cross talk) bolted to a single stand and none of the adjacent mechanical systems.

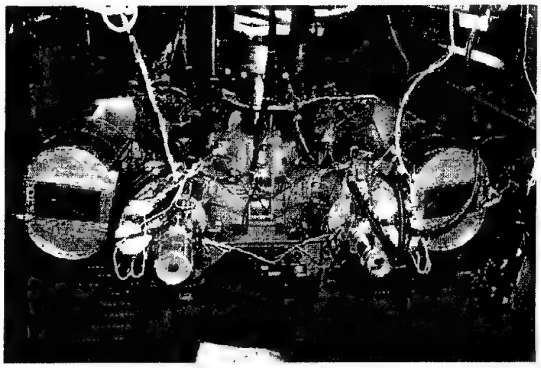

Fig. 5. Main Transmission Assembly including Accessories.

Aircraft Installation

The HIDS installation is the first health and usage monitor with advanced gearbox diagnostics to be placed on-board a US military helicopter. The system has a menu driven cockpit display (see Figure 2) for pilot information/interface. The usage monitor is built on an open architecture, 1/2 ATR short box, which has unused slots for future integration of selected vibration monitoring functions. Downloads from the aircraft are accomplished via the data transfer unit (DTU), a Type II PCMCIA card. The vibration analysis system is housed in a vibration isolated chassis with removable hard drive and full VME chassis. This system is necessary for the development program to acquire all of the raw data that generates an airborne warning or alarm for either confirmation of the fault, or development of additional algorithms that identify a data problem that resulted in a false alarm. A significant benefit of this system is the comprehensive database, which is a powerful resource for diagnostic development. This same system was used to support data collection for the first phase of the IMD program.

Evaluation

The SH-60 was selected for this program since it offered the best availability of test assets and highest potential for support due to the large fleet of aircraft between the Navy, Army and Coast Guard. The HTTF drive system includes two General Electric T700 engines, the main transmission, oil cooler and the tail drive system.

Test Objectives

To insure a comprehensive test effort, the planning for this test program included support from in-

dividuals and organizations involved with the design of the H-60 aircraft and diagnostic systems. The team developed and documented the program plan (Ref. 4). All seeded fault test planning was discussed with Sikorsky drive system engineering prior to execution. Team discussions led to the objectives and test sequence previously described in detail (Ref. 3). A subset of these is summarized below.

1. Evaluate the ability of the diagnostic system to identify localized faults in an entire drive system.

2. Evaluate the diagnostic algorithms for cracked gear fault identification and sensitivity.

3. Quantify the level of signal for a known defect size to develop operational limits and trending for the SH-60 drive system.

4. Evaluate the diagnostic systems sensitivity to defects and faults in tail drive shafts and bearings.

5. Evaluate the diagnostic systems sensitivity to bearing defects in gearboxes.

6. Evaluate variability of data across flight regimes (including torque and weight variations).

7. Evaluate sensor placement sensitivity for the various defects. The objective is to minimize the total number of sensors required to identify faults large enough to require maintenance action and to increase robustness via use of secondary sensors.

8. Evaluate the potential for detecting misalignment, bad pattern and improper shimming during assembly that may be the cause of premature damage in mechanical systems.

9. Develop seeded fault data library that can be used to evaluate systems in the future without repeating the test program.

10. Evaluate as many currently available propulsion and power drive system diagnostic technologies as possible in the HTTF and assess their relative effectiveness.

11. Evaluate the data collected on-board the aircraft with the test cell data to validate the pertinence of test cell proven algorithms for use on-board an aircraft.

12. Categorize diagnostic results with respect to aircraft flight regime to define optimized system acquisition and processing requirements.

13. Demonstrate ability of the diagnostics to reduce component "false removals" and trial and error maintenance practices.

14. Demonstrate methods that improve the accuracy of component condition assessment and reduce false alarms.

Vibration Monitoring Test Plans

Testing of the diagnostic system was divided between two Navy activities that could exercise as much of the entire diagnostic system as possible. The NAWCAD HTTF and operational SH-60 aircraft both operated the entire propulsion and power drive system during testing. Test plans were designed to maximize the return on investment when the system is evaluated in a single type of test vehicle.

Reliable fault identification from vibration signatures is a well documented, but difficult task. In many test cases, the researcher has been able to show that a given process can successfully identify a fault in a small scale test. Production use in complicated systems that have varied operational parameters with time has proven to be much more difficult to implement without false alarms and missed detections. In order to maximize the potential benefit of the HIDS program, early program decisions drove the diagnostic system to be a state-of-the-art data collection and processing system. Goals included acquiring the raw data, and using it as a foundation to allow rational selection and evaluation of diagnostic parameters such as data rate, sample length, degree of redundancy required, etc., and also to identify the anomalies that result in inconsistent system performance. The vibration acquisition system and the HTTF have been combined to create a unique mechanical diagnostics laboratory.

The NAWCAD HTTF personnel began acquiring seeded fault assets at the program inception. These parts had been removed from the overhaul process for discrepancies and were set aside for test rather than scrapped. This provided tremendous cost savings by avoiding purchase of good parts for artificially seeded fault specimens, while supplying naturally created faults for test. Sikorsky Aircraft parts from prior bench qualification tests are also available for test. These parts are "bench test only" assets since they experienced over-torque conditions during test. The program has over two full sets of Not For Flight Asset (NFFA) gearboxes. The spares can be implanted with faults while another gearbox is tested.

The testing initially concentrated on the tail drive system to verify the TII/BFG diagnostic system operation and performance. Subsequent testing has been performed on all drive system components, including artificially implanted and naturally occurring faults. The test conditions have consisted of sequentially varying power settings throughout the normal range of operation. It is essential to understand the sensitivity of the diagnostic algorithms as a function of changing aircraft power. Ambient temperature variation effects are included in the analysis. The first data set from each run is taken before the oil warms up at low torque to obtain a database that can be compared to flat pitch maintenance ground turns for troubleshooting.

Test runs to evaluate component assembly (i.e. build-up variation) requires gearbox disassembly, assembly and test sequences without changing any parts. All four of the input and main gearbox assemblies in the database were tested for sensitivity to bolting being loosened, housings jacked apart, and then reassembled with the same components.

System Installation

The HIDS system is capable of accommodating multiple configurations. The HTTF and aircraft Bureau Number (BUNO) 162326 installations are the same for a majority of the inputs. The aircraft has many additional parameters that are not present in the test cell, such as flight parameters including altitude, airspeed, pitch, roll and heading. Also, the aircraft system measures fuel quantity while the test cell system measures fuel flow. Aircraft 162326 was made available for instrumentation in the spring of 1994 and the entire system was installed by 1 August 1994. The initial installation was completed with a majority of parameters in good operation and a system that functioned and passed installation acceptance tests. Several modifications have been incorporated since the commissioning. Performing checkout of system functionality at the HTTF tested the aircraft system changes, and many of the aircraft discrepancies were found to be in areas where the aircraft was different from the HTTF. The interface documentation was updated and validated accordingly. In March of 1997, the next generation HIDS system was installed on PAX aircraft 804 for continued analysis and development. When the IMD schedule was accelerated, the HIDS system supported the effort on the SH-60 platform, while an improved variant was utilized for the CH-53E.

Vibration Data Analysis

The HIDS program has correlated the seeded fault test data acquired in the HTTF to NAWCAD flight data. The diagnostic system user interface and its ability to detect faulty components in a full drive system were evaluated using the HTTF data. The operational characteristics, rotor track and balance and user interface were evaluated on the NAWCAD-PAX aircraft.

Data was recorded at both sites using the same acquisition system, sensors, mounting, and accelerometer locations. The data sets are digital records, recorded simultaneously on all channels at 100,000 samples per second for 30 seconds. This system is believed to exceed the requirements for a total on-board health and usage monitoring system. However, by exceeding the requirements for data acquisition under known conditions, HIDS will provide the rationale to specify the minimum system requirements needed to achieve the low false alarms and complete functionality goals. This system can store and analyze large amounts of meaningful raw data and has significant value when new aircraft types or newly overhauled aircraft require a new baseline.

Two means of collecting vibration data are being implemented at HTTF. The TII/BFG diagnostic system saves raw digital data, while Metrum VHS digital tape recorders are used for making parallel raw data tapes. The test cell does not provide the airframe inputs or the rotor pass vibration inputs, but these frequencies are relatively low compared to the engine and gearmesh frequencies. The impact of this limitation on component- specific algorithms is restricted to the lowest speed components.

The TII/BFG diagnostic system has a comprehensive scientific development environment that aids the user in evaluating and tuning diagnostic system performance. Trending of indicators and adjustment of limits is a useful part of the system, and the flexibility to add and develop new algorithms is also noteworthy. This ability makes it possible to review and modify the processing in the ground station to optimize on-board system performance.

The HIDS program, by taking advantage of these tools for diagnostic system development and verification has an excellent opportunity to properly bound the operational issues that have limited the successful implementation of currently available health and usage monitoring system. Extensive analysis and algorithm development of the baseline and fault raw data continuously improves the performance of the system through scientific understanding of the mechanics of the helicopter, and through detailed study of the events that have resulted in false alarms. By utilizing the database, HIDS has been able to develop and

validate quality assurance routines that identify maintenance required to the diagnostic system rather than an on-board alarm.

Damage Tolerance Concerns

The actual operational lives for aircraft and their subsystem components are now commonly being extended well past their original design lives. This trend has been increasing in recent years because of reduced defense budgets and growing operational demands. Services are having to operate longer, in some cases much longer, with the aircraft and systems they already own. Thus, a pressing problem becomes how to best manage damage tolerance issues in a fleet of ever aging aircraft.

One of the most important damage tolerance issues is the accurate accounting for life usage accumulation on components with design life limits. Gas turbine engines, gearboxes, helicopter rotor assemblies, and other stressed airframe parts are all subject to finite design limits on life limited components. The data acquisition and life usage monitoring capabilities of HIDS type systems provide an excellent means to track damage accumulation and effectively manage parts life consumption on aging aircraft.

Another important damage tolerance issue is the problem of dealing with secondary damage. Diagnostic capabilities provided by HIDS type systems will identify the small faults and component failures early, before they become significant contributors to more severe secondary damage.

Accomplishments

Accomplishments Summary

The COTS usage monitoring hardware and software have been successfully installed and operated in both the HTTF and NAWCADPAX BUNO 162326 and 164176. The HIDS aircraft flew with engine algorithms and recording cockpit instrumentation, control positions and alarm panel indications. The cockpit display can notify the pilot when there is an exceedance and the ground station reiterates those exceedances during data download into the ground station. The system has functioned as a flight data recorder providing a complete history of the flight. The ground station tracks serialized part numbers and times, correlates maintenance performed and part change data, and has a variety of report and plotting options. The system has continued to improve towards, and provide valuable data for, defining the specification of a production Navy system.

The usage monitor and maintenance tracking system is also being used in the test cell to track what faulted components were run on any given day. The system has a list of all gear and bearing serial numbers which we can correlate to the faults. All component changes are tracked chronologically and the files are maintained by the test cell mechanics.

The 32 channel simultaneous sampling vibration acquisition system has proved to be reliable and robust for both test stand and flight activities. The system recorded data in aircraft BUNO 162326 as a not-to-interfere secondary test. The hardware installation required that the system be stood on end to fit into the aircraft during the initial installation, and later was moved from the front of the aircraft to the rear. Data has been acquired from three airframes for the main gearbox and one aircraft for the entire system. A total of 85 hours of flight and 254 data sets have been recorded on aircraft 326. The HTTF has operated for 396 hours of diagnostic system evaluation. Seven main gearboxes, seven input modules, two accessory modules, three intermediate gearboxes, four tail gearboxes and six engines have been tested and 31 faults have been run in the test cell. Extensive investigation into signal quality and gain control has provided good confidence of data acquisition quality. The analysis has provided a significant diagnostic capability for the detection of degraded components.

The data library consists of over 2000 sets of 32 channel simultaneous acquisitions of raw time series data with tachometers and accelerometers recorded together, providing a rich database to enhance diagnostic techniques. Multivariate techniques are being investigated to exploit the additional information inherent in the relationships between indicators and to increase the robustness of health evaluation calls.

Compliance with Objectives (Examples)

1. Evaluate the ability of the diagnostic system to identify localized faults in an entire drive system. The HIDS system has demonstrated the ability to identify localized faults on a number of H-60 drive system components. The engine high speed shaft/input module interface (see Figure 7) has been a problem area, where the difficult to inspect Thomas Coupling disc pack has suffered several failures. The Figure 8 engine high speed shaft (with cracked Thomas Couplings) was removed from the fleet and tested at Trenton. Figure 9 illustrates baseline test data with good driveshafts, and the degraded component installed at the starboard engine location for one acquisition at run number 31. The HIDS system detects the fault and isolates it to the starboard side. This provides a rationale for providing a cockpit alert for critical, rapidly degrading components. The

HIDS system also detected a fleet removed input module suspected of being an every-other-tooth gearmesh candidate. These gearboxes were emanating a strong tone at one-half the normal gearmesh frequency, and it was believed this tone was contributing to premature removals of the mating T700 engines due to torque reference shaft wear. Figure 10 exhibits a gear health indicator (algorithm) of such a component tested at Trenton which shows baseline and fault (run numbers 149 through 170) data.

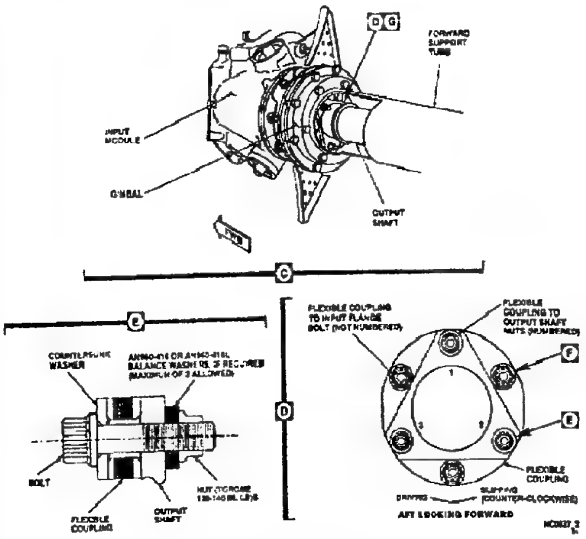

Fig. 7. High Speed Shaft Interface.

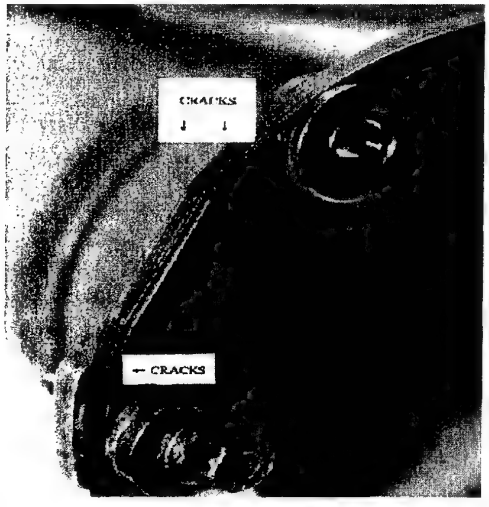

Fig. 8. Cracked Thomas Coupling.

2. Evaluate the diagnostic algorithms for cracked gear fault identification and sensitivity. A critical part of the HIDS program is to demonstrate the detection of catastrophic gear faults. The most serious of which are root bending fatigue failures. Depending upon gear design, this type of crack can either propagate through the gear tooth causing tooth loss, or through the web causing catastrophic gear failure and possible loss of aircraft.

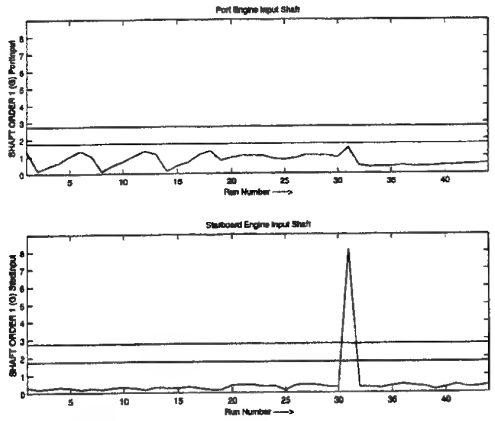

Fig. 9. Degraded Shaft at Position 31.

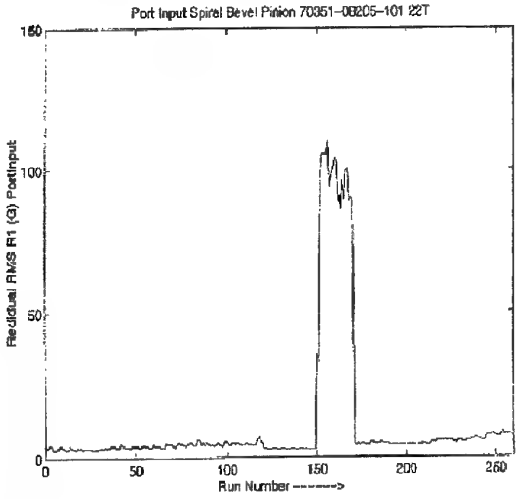

Fig. 10. Response for Half Gearmesh Anomaly.

A means used in the helicopter community to promulgate this type of investigation is to weaken the tooth by implanting an Electronic Discharge Machine (EDM) notch in the gear tooth root. This action creates a localized stress concentration at the tooth root in an effort to initiate a crack. The HIDS team had previously attempted this test on other gear teeth, but with no success. Discussions with the transmission design departments at Agusta Helicopters and Boeing Helicopters assisted us in

determining optimum notch placement. Figure 11 is a cutaway of the SH-60 intermediate gearbox. Two EDM notches (.25" Length x .006" Width x .040" Depth) were implanted along the length of the intermediate gearbox (IGB) gear tooth root by PH Tool of New Britain, PA. The location of the notches is critical as they were implanted where the gear tooth root bending stress is greatest.

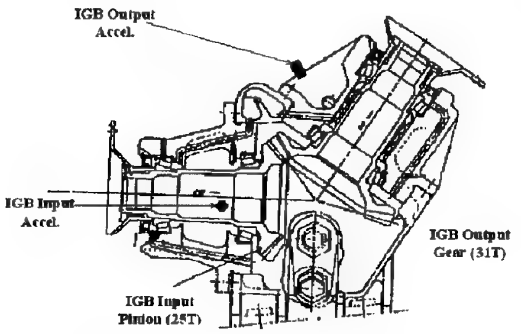

Fig. 11. SH-60 Intermediate Gearbox Cutaway.

The test was run at 100% tail power for a total of 2 million cycles, when testing was terminated prior to gearbox failure when a gross change in the raw FFT spectra was observed on the HP36650 Spectrum Analyzer. Subsequent to test termination the gearbox was disassembled and inspected. The input pinion's faulted tooth exhibited a crack initiating from the tooth root and extending through the gear web and stopping at a bearing support diameter. Figure 12 exhibits the subject pinion at the end of the test. There is a void at the toe end of the notched tooth where a large section of the tooth broke off, and a through web crack extending to the bearing support diameter. No indication from the gearbox chip indicator was observed.

A review of the diagnostic results shows the TII/BFG model based algorithms successfully detect the presence of the gear tooth fault. Figures 13, 14 and 15 respectively exhibit "Component Condition" and the early and late responding health indicators from which it was derived. After indicating a healthy gear for roughly 267 minutes (most acquisitions were acquired 15 minutes apart), the indicator levels raised steadily for the next 139 minutes, thereafter exhibiting sharp changes in level until test termination at 548 minutes (Ref. 5 discusses indicator results of another pinion tooth fault). Test results illustrated an EDM notched tooth behaves much like adjacent teeth until the part is fatigued and a crack develops. The crack effectively weakens the tooth in bending, causing the faulted tooth to share load unequally with adjacent teeth. Depending upon the crack path, other dynamic anomalies are manifested. Also, synchronous averaging techniques employed in model based diagnostics can "filter out" non-synchronous vibration providing a health determination of a specific component.

Fig. 12. Cracked Intermediate Gerabox Pinion.

A root bending fatigue propagation test was repeated on a main transmission input pinion. This test promised to be a more challenging effort for several reasons. First, the main transmission module is a larger and more complex system than the intermediate gearbox. The background noise is greater and the fault is located deep inside a larger housing. The gear form was also different. The intermediate gearbox pinion has a large web, where the main module pinion teeth are closer to the shaft centerline and therefore has a great deal of support at the tooth root. These observances made, the HIDS team determined to investigate the crack propagation properties of the more robust gear form.

Two EDM notches were implanted in the root of one geartooth and run for 12 million cycles at 110% power, removed and inspected, and then tested for another 10 million cycles. After 12 million cycles, small cracks less than 2mm in length emanating from the notch corners were present. Figure 16 exhibits the pinion after another 10 million cycles. A large part of the faulted tooth has broken off, and a crack propagated the length of the part forward (toe end), and aft (heel end) to the bearing support. No indication from the gearbox chip indicator was observed.

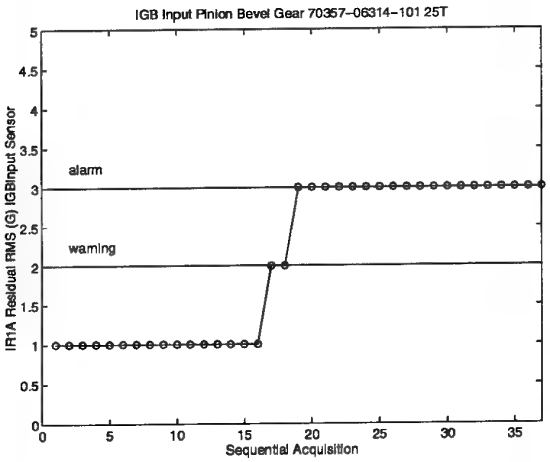

Fig. 13. IGB Pinion Component Condition.

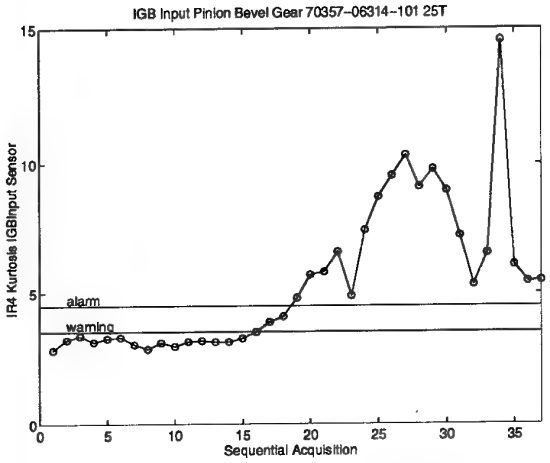

Fig. 14. Early Responding Health Indicator.

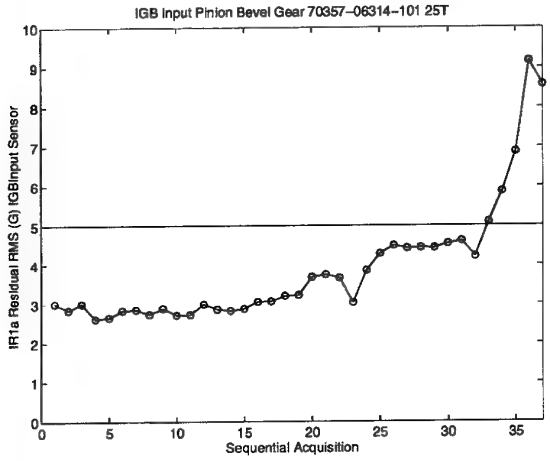

Fig. 15. Late Responding Health Indicator.

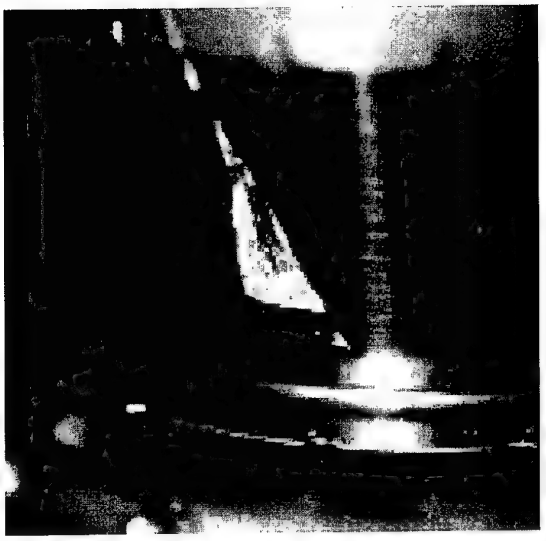

Fig. 16. Main Transmission Input Pinion Crack.

Figure 17 shows an indicator response for the test. Run numbers 1-206 are data from the first gearbox build, and run numbers thereafter from the second. It is interesting that key fault response indicators reached only half the level as for the IGB fault. Speculatively speaking, this may be due to the fault being deeper inside the gearbox, but is most probably due to the other main module pinion emanating "healthy" synchronous gearmesh tones and masking indicator response.

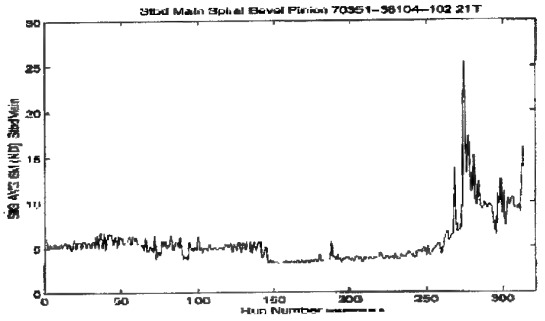

Fig. 17. Response to Main Module Pinion Fault.

It is presumed the steep increase can be attributed to either the gear tooth breaking off, or the crack propagating through the web. It is indeed impressive that these components held together considering their condition and the loads transmitted.

These tests demonstrated (1) the HIDS diagnostic algorithms successful early detection of root bending fatigue failures, (2) chip detectors are unreliable for the detection of classic gear failures caused by root bending fatigue, (3) H-60 drive system components

are particularly robust, and (4) root bending fatigue cracks on gear tooth forms such as the main module pinion can propagate through the web (vice only the tooth) to a catastrophic condition.

3. Quantify the level of signal for a known defect size to develop operational limits and trending for the SH-60 drive system. As discussed above, the IGB root bending fatigue failure provided excellent results in component fault detection and condition assessment. Figures 13, 14 and 15 exhibit the gear "Component Condition" indicator, and two gear health indicators which determine the component condition. The IR4 Kurtosis indicator provides early warning of a local gear tooth anomaly, and the IR1a indicator is excited as the gear tooth crack has propagated to a severe condition. These indicators could therefore be integrated into the diagnostics package as early warning and impending failure indicators respectively.

4. Evaluate diagnostic system sensitivity to defects and faults in tail drive shafts and bearings. Hanger bearing assemblies are used to support the helicopter tail drive shaft. The main components of the assembly consist of a grease-packed sealed ball bearing that is pressed into a viscous damper bladder and supported by a housing that mounts to an airframe interface. The bearing is expected to be lightly loaded since it doesn't support any significant radial or axial loads, though those imposed from imbalance and misalignment occur in-service. Figure 18 shows the hanger bearing assembly and associated accelerometer installed at the number 2 location in the tail drive system. Since the viscous damper is in the vibration transmission path, there was concern it would inhibit the transmission of high frequency tones from the bearing to the vibration sensor.

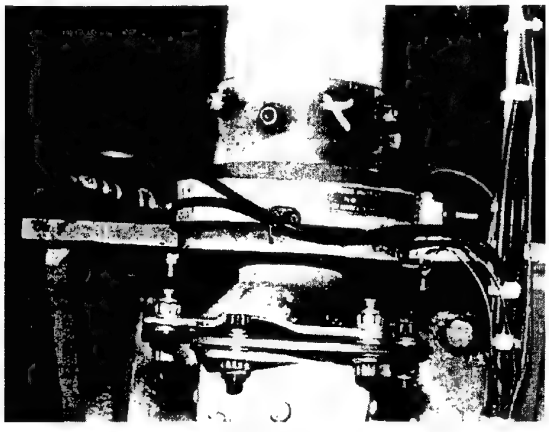

Fig. 18. Hanger Bearing Assembly.

A fleet removed hanger bearing with a very light click was installed in the HTTF. There was considerable opinion that the click was due to dirt in the bearing. 12.7 drive system operating hours were accumulated and 129 data points were acquired. Figure 19 shows a representative envelope spectral plot for the fleet rejected hanger bearing. A fault clearly exhibits itself by the strong tones at frequencies specific to the inner and outer race defect frequencies and also at shaft speed. By comparison, fault-free hanger bearings did not generate bearing defect frequencies. The Figure 20 indicator is derived from the information contained in the spectral plot, and presents data from four different bearings which were installed in the #2 hanger bearing location. Data from the fleet rejected bearing is easily identifiable between run numbers 199 through 325. Note that the viscous damper attenuation concern did not materialize.

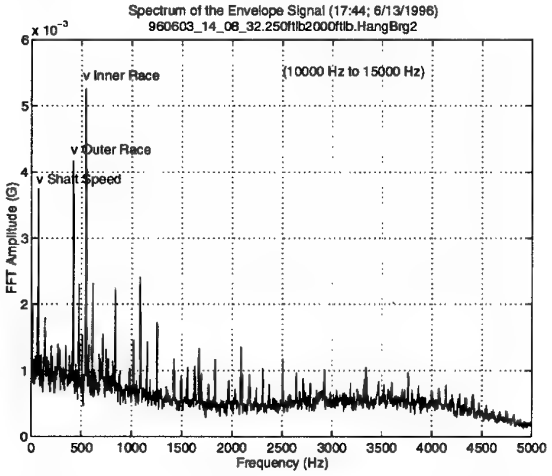

Fig. 19. Rejected Hanger Bearing Spectral Plot.

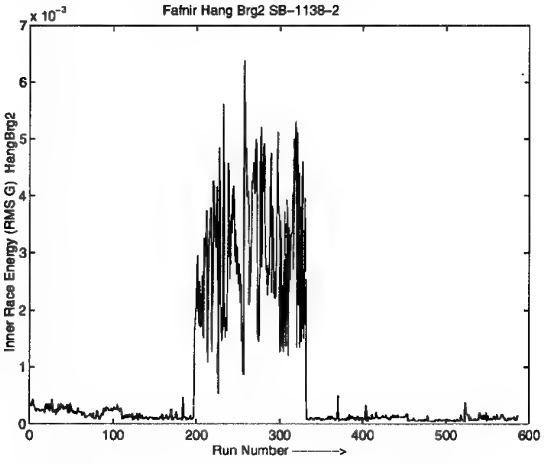

Fig. 20. Hanger Bearing Inner Race Energy.

Posttest inspection of the bearing revealed that the inner ring was fractured as shown in Figure 21. Also, the bearing was found to have about 1.5 grams of grease remaining, which is within the range normally found in bearings operating to their 3,000 hour overhaul life. Hanger bearings with inner race fractures have been known to eventually purge all the grease through the fracture leading to overheating, seizure, and loss-of-aircraft.

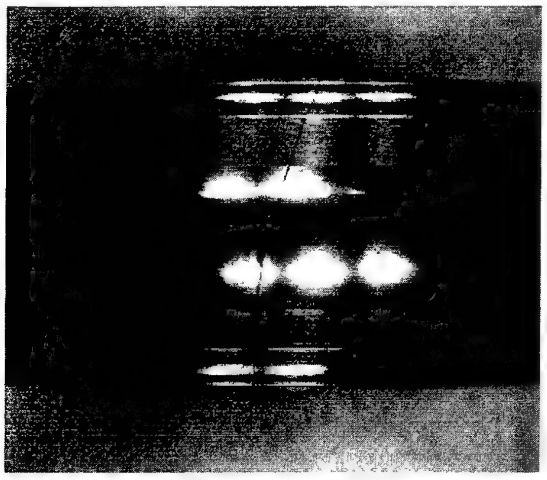

Fig. 21. Post-Test Condition of Hanger Bearing.

5. Evaluate the diagnostic systems sensitivity to bearing defects in gearboxes. The spalled integral raceway bearing (P/N SB 2205) is the most common dynamic component cause for gearbox removal in the H-60 community. This fault is particularly challenging as it is located deep inside the main transmission, (see Figure 22) suggesting it would be difficult to detect. Figure 3 illustrates the SH-60 main transmission system and respective vibration accelerometer locations. The Figure 23 fleet rejected component was installed in the HTTF starboard location. Bearing condition for the starboard and port main accelerometer locations are presented in Figures 24 and 25 respectively. The starboard main condition indicator toggles into the alarm position when the fault is implanted at acquisition number 254 and reverts back to the okay position when the fault is removed at acquisition number 300. The port main indicator is also sensitive to this fault because the sensor is located on the same structural housing member, and is rotated about 90 degrees around the housing from the starboard main sensor. The port indicator serves as a confirmation of the starboard condition. Enveloped kurtosis is the main indicator used to evaluate bearing condition for this fault. One of the keys to obtaining meaningful results with this technique is to envelope an appropriate frequency range. The frequency range used in this analysis was determined analytically as well as experientially. Figures 26 and 27 respectively exhibit the Kurtosis values of the primary (stbd main) and secondary (port main) sensors for the bearing SB-2205 fault.

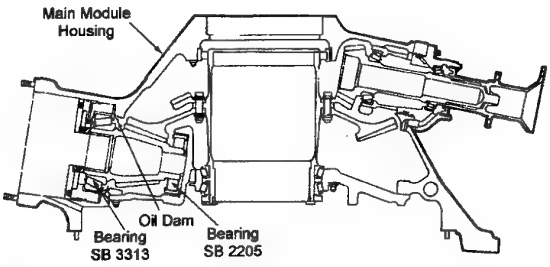

Fig. 22. Locations of SB-2205 and SB-3313 Bearings in the Main Module.

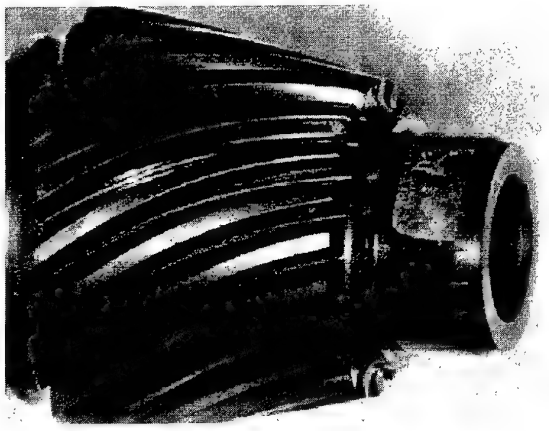

Fig. 23. Main Module Input Pinion with Spalled Integral Raceway Bearing SB 2205.

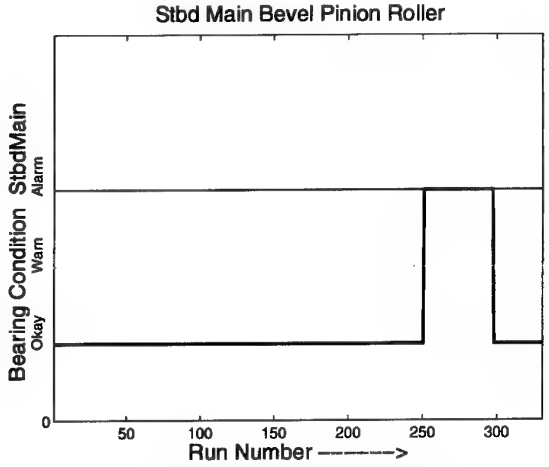

Fig. 24. SB 2205 Condition Call from Starboard Sensor.

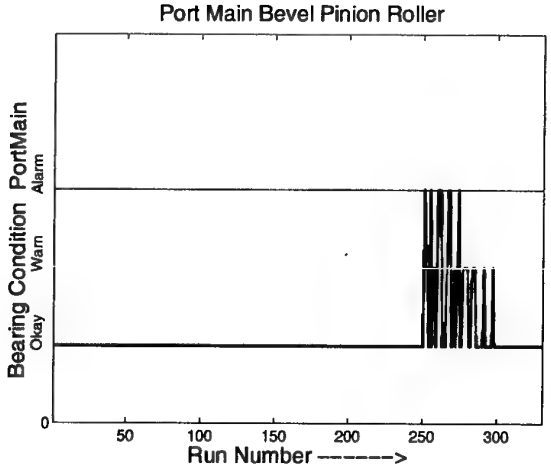

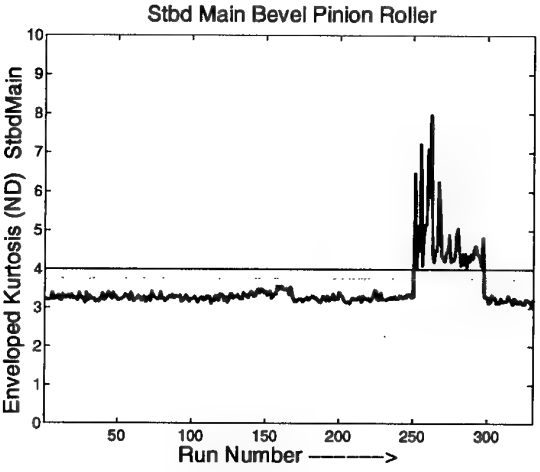

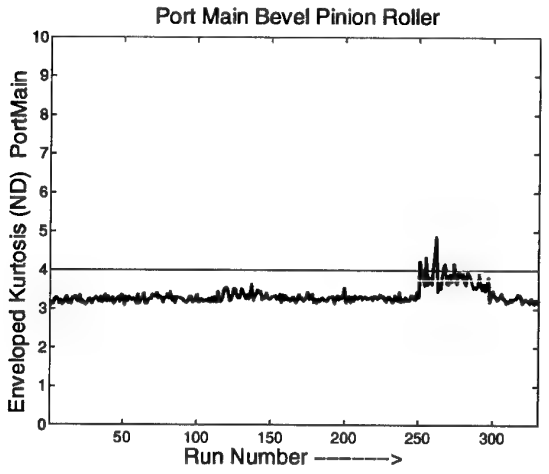

Prognostics could effectively be applied to the failure of this component. The SB2205 fault progresses in a repeatable manner from a small, localized spall into a larger one that will eventually encompass a good portion of the inner race diameter. At this point, the chip detector will provide an indication of a failure somewhere in the gearbox with no indication of fault location or severity. On the other hand, the model based bearing indicators identify the presence of the fault early in this process. As the fault becomes progressively larger, the statistical indicators in Figures 28 and 29 are among the dominant indicators that identify the degraded condition. By carefully tracking the progression of this fault, maintenance and mission planning can be conducted in an effective manner, and unscheduled downtime can be effectively reduced.

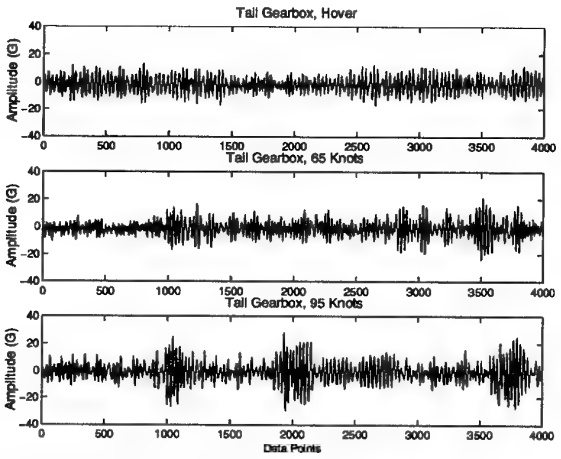

6. Evaluate variability of data across flight regimes (including torque and weight variations). Figure 28 exhibits time domain tail gearbox vibration data at different flight regimes. There is considerable difference in the signal between forward flight and hover. This introduced considerable scatter in the algorithm indicators. It was determined a large main rotor 4/rev component (rotor wash) is interacting with the tail pylon in forward flight, which is causing this data instability. This and other flight regime nuances are being investigated.

7. Evaluate sensor placement sensitivity for the various defects. The objective is to minimize the total number of sensors required to identify faults large enough to require maintenance action and to increase robustness by verifying use of secondary sensors. The test of bearing SB 2205 provided an interesting study for sensor placement. At the time of

test, the stbd main was the primary sensor for the stbd SB-2205 bearing, and the stbd input sensor was the secondary. Test results however showed otherwise. Figure 29 shows that the enveloped kurtosis of the stbd input sensor does not respond to the fault, whereas the port main sensor does (see Figure 27). Based on results from this test, the port main sensor was then mapped as the secondary sensor for the stbd SB 2205 bearing.

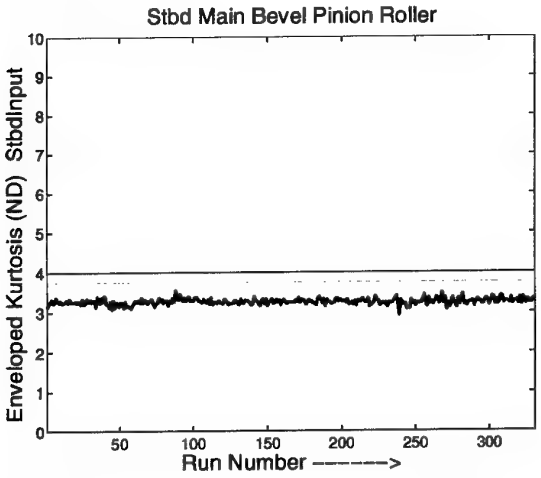

Fig. 29. SB 2205 Starboard Input Kurtosis Trend.

8. Evaluate the potential for detecting misalignment, bad pattern and improper shimming during assembly that may be the cause of premature damage in mechanical systems. Misalignment and imbalance testing have been performed on a number of drive system components. Specifically, the engine high speed shaft/input module assembly has been investigated under these conditions and findings were documented (Ref. 6). Other similar tests (some naturally occurring) were recorded. Gearbox gear pattern shim surveys were also performed. Test results are pending data review.

9. Develop seeded fault data library that can be used to evaluate systems in the future without repeating the test program. The HIDS program has provided a wealth of knowledge and understanding of the implementation of mechanical diagnostics. Though not immediately quantifiable, the HIDS testing has identified many optimized test methods and fleet implementation issues. Though not eliminating the need of seeded fault testing for other drive systems, the scope of work can be more precise and reduced. For the Integrated Mechanical Diagnostics Commercial Operational Savings and Support Initiative (COSSI), the HIDS data is being distributed to various institutions to develop and evaluate transmission planetary system gear and bearing algorithms.

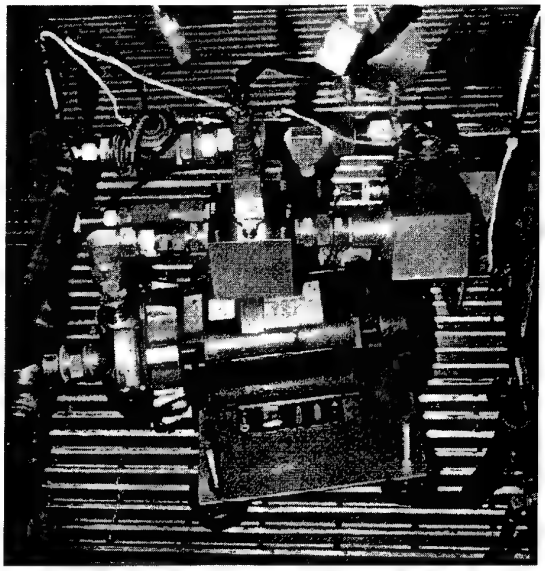

Fig. 30. Test Rig for Oil Monitoring Evaluation.

10. Evaluate as many currently available propulsion and power drive system diagnostic technologies as possible in test cell 8W and assess their relative effectiveness. Engineering evaluation testing of Stress Wave Analysis, Electrostatic Engine Exhaust Monitoring, Inductive Oil Debris Monitoring, Quantitative Oil Debris Monitoring, Optical Oil Debris Monitoring, and Acoustic Emission have been done in parallel with HIDS testing evaluation at Trenton. Two of these efforts are US Army SBIR efforts. As a means to evaluate the IDM and QDM MKII oil debris monitoring systems simultaneously, a modified main transmission lubrication scavenge apparatus was provided by Vickers Tedeco (See Figure 30). The system attaches to the main transmission module at the normal chip detector location and a positive displacement pump adds sufficient head to pump the oil through an external plumbing arrangement. Sump oil enters the pump, IDM, QDM MKII, and finally the production main module chip detector and returns to the transmission. A fine mesh screen is included to capture particles that are not captured by the QDM MKII and main module magnetic detectors. The Figure 23 main transmission input pinion with a spalled integral bearing raceway was used as a tool to generate debris for the evaluation. This test (Ref. 7) found the fault generated particles much smaller (5-20 microns) than what a typical bearing fault (>100 microns) is known to produce. This evaluation provided sensitivity and performance information.

11. Evaluate the data collected on-board the aircraft with the test cell data to validate the pertinence of test cell proven algorithms for use on-board an aircraft. As part of the HIDS program, drive system vibration data was acquired on 22 and 23 May and 30 August 1995 from SH-60 BUNO 164176 at NAWC-ADPAX. Data was also collected on two other SH-60 aircraft using the same data acquisition system. The data was acquired primarily to support a next generation diagnostic effort based on neural network technology and designated the Air Vehicle Diagnostic System (AVDS) program. The intent was to acquire raw vibration data on fault-free aircraft to use as a means for baselining the neural network process. For aircraft BUNO 164176 a total of 46 separate acquisitions were taken at several different flight conditions including ground turns, hover in-ground effect, hover out-of-ground effect, straight and level and descent. Torque ranged from 28-100%. Approximately one month after the May data had been acquired from BUNO 164176, HIDS project personnel were informed that the aircraft had a history of setting off the main transmission chip detector light. The chip detector events prompted an analysis of vibration data collected from BUNO 164176 using HIDS diagnostic algorithms. The same analysis was also conducted on one of the other aircraft, namely BUNO 162326, to provide a baseline for comparison to aircraft BUNO 164176. Representative envelope spectral plots of baseline and faulted aircraft data are shown in Figures 31 and 32 respectively. The fault clearly exhibits itself by the strong tones at frequencies specific to the main bevel pinion tapered roller bearing (SB 3313) both in the test cell and the aircraft. The Roller Energy indicator for the aircraft data is displayed in Figure 33.

The analysis clearly indicated a fault in the rolling elements of the starboard main bevel input pinion tapered roller bearing, P/N SB 3313 (see Figure 22 schematic for location) and represented a safety-of - flight concern. Further confirmation of fault location was provided by chip elemental analysis, conducted by Sikorsky Aircraft, which determined that the chips were CBS 600 steel indicating that this bearing was one of several possible sources of the chips. Based on the analysis, the HIDS team strongly recommended that flight operations on aircraft BUNO 164176 cease and the main gearbox could be removed and sent to the HTTF for continued testing. The data collected in the test cell environment was compared to flight test data (see Figure 34 for test cell data). Moreover, the urgency to remove the gearbox from service was a result of the HIDS team assessment that the presence of the oil dam (P/N 70351-38124-101), adjacent to the bearing was a barrier to chip migration. This (1) prevented the chip detector from indicating the true severity of the failure development and (2) created a reservoir of chips which may act to increase the failure progression rate. Action was taken to comply with the recommendation. Subsequent teardown and inspection confirmed that 13 of the 23 rollers in the bearing were severely spalled as shown in Figure 35. Inspection revealed a large amount of debris harbored by the oil dam, confirming the HIDS team suspicion that the oil dam acted as a chip reservoir.

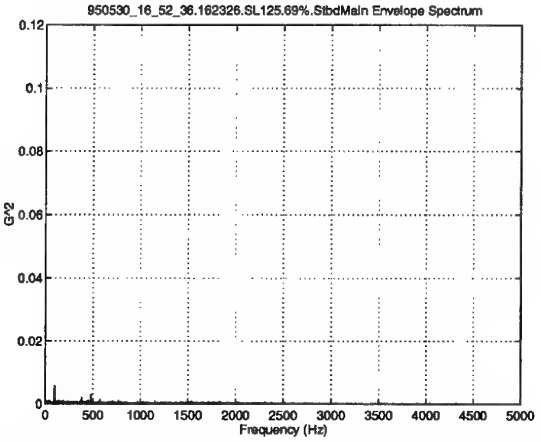

Fig. 31. Baseline Spectrum for Bearing SB 3313.

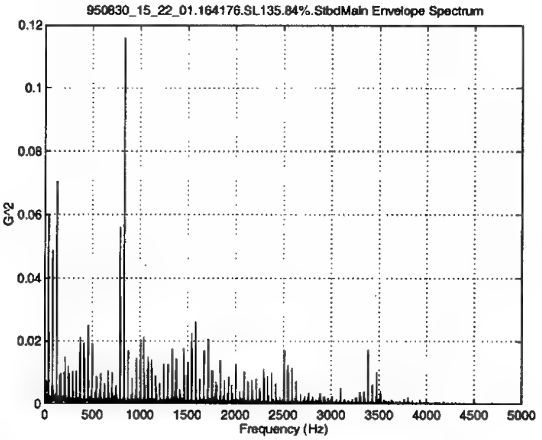

Fig. 32. Fault Spectrum for Bearing SB 3313.

12. Categorize diagnostic results with respect to aircraft flight regime to define optimized system acquisition and processing requirements. Review of Figures 33 and 34 reveals a great deal of scatter in the value of the faulted bearing indicator. This is due to the differences in flight regime and torque. A fault must be loaded to excite a discrete frequency, and a determination of what regimes produce satisfactory results is needed.

13. Demonstrate the diagnostics ability to reduce component "false removals" and trial and error maintenance practices. Several fleet removed components which were tested at Trenton were found to be fault free. Four hydraulic pumps removed for oil pressure problems were found to operate normally in the Trenton test cell. An input module removed for chip generation was tested. No debris was generated, and the diagnostics indicated a healthy component. Subsequent teardown inspection at Sikorsky revealed no dynamic component degradation.

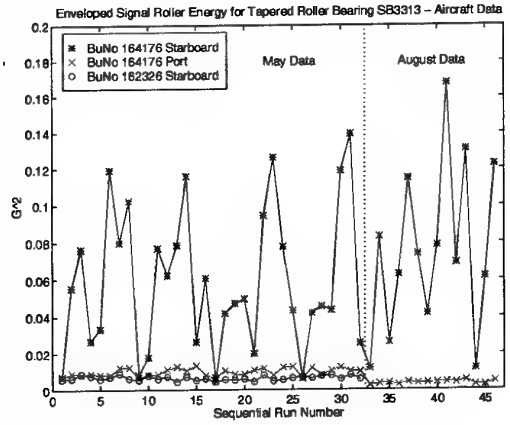

Fig. 33. Enveloped Signal Roller Energy for Bearing SB 3313, Aircraft Data.

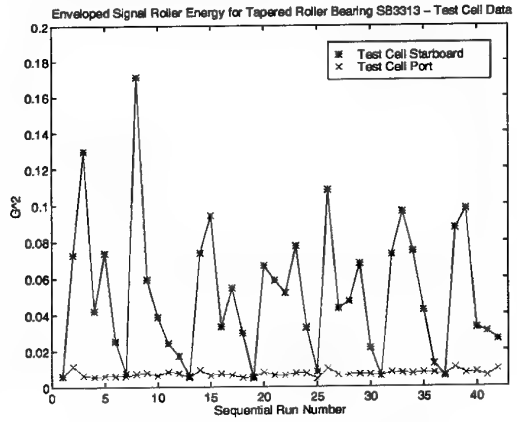

Fig. 34. Enveloped Signal Roller Energy for Bearing SB 3313, Test Cell Data.

14. Demonstrate methods that reduce false alarms and improve component condition assessments. Numerous indicators have been developed to quantify health of the drive train components. Rather than use each of these indicators in isolation, utilizing data fusion can derive additional benefit. Previous multiple sensor data fusion techniques have had great success in fault detection and classification. An automated data fusion technique currently under investigation is Hotelling's T^2 Multivariate Analysis. This technique combines multiple indicators into one composite indicator. The composite indicator has been shown to increase the robustness of condition calls since the indicator changes by orders of magnitude in the presence of a fault. In addition, false alarm calls are reduced by establishing tighter control limits that take advantage of the underlying correlation among the indicators.

In order to select the indicators that produce a more robust response, a goodness of fit test is being employed to ensure that the assumption of normality is not being violated on baseline data. All indicators not falling within the multivariate normal distribution are dropped from consideration. A correlation study is performed to further select indicators with favorable relationships. The indicators showing the strongest change in correlation between fault and baseline data are used in the T^2 analysis.

The advanced statistical quality control technique has been applied to the HTTF crack propagation data and compared to current component condition call indicators. A preliminary study produced good results and will be reported under a future NAWCAD report. This technique has provided a more robust classification of the fault with a large reduction in false alarm calls. Alternative methods exist which yield a more robust estimate of the in-control parameters, which would further decrease false alarm rates while preserving the responsiveness of the T^2 analysis to faults.

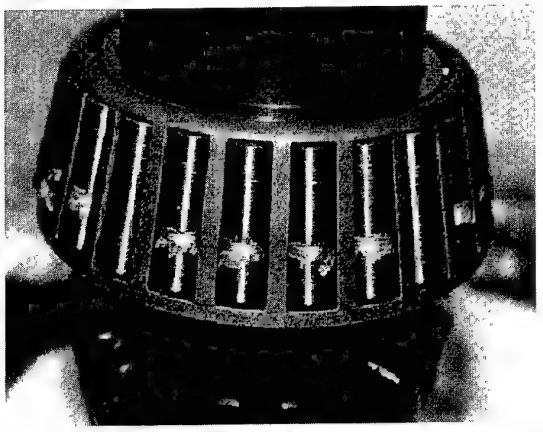

Fig. 35. SB 3313 Removed from PAX Aircraft.

Structural Usage Monitoring

Objectives

One primary HIDS program objectives was to introduce a family of structural usage data acquisition and

processing algorithms. Given this capability, parts life determination is now individualized and based upon the actual helicopter usage. The usage monitoring subsystem determines the percentage of flight time the helicopter has spent in each flight mode (regime) as well as the specific regime sequence. The regime data is then used to calculate the rate that various structural components are being used up and when they need to be removed from service to maintain the required reliability rate. This capability is particularly important for aging aircraft because it enables life usage history tracking for an aircraft and its parts.

Methodologies

HIDS aircraft usage was quantified using a basic building block, or regime. Regimes are generally defined by a particular operational phase, such as takeoff, hovering, level flight, various turns and landing. Time histories of flight parameters are analyzed to determine the instantaneous phase of flight. Normal acceleration (Nz), power and yaw rate are parameters that define subsets of regimes. The time spent within each regime (or subset), during a given flight is measured and tabulated as part of a usage spectrum. Although it is almost impossible for an aircraft to be flown into every regime on a single flight, the aircraft can be expected to fly into all basic regimes over time. The continuing summation of this multi-flight experience defines the usage spectrum for the aircraft and its components.

As mentioned previously, regime recognition algorithms map recorded aircraft parameter data to a set of ground/flight regimes. The process output includes several summary reports as well as calculated adjustments to the useful life of specific components. The first report, called the regime sequence report (flight profile), represents the time history of the aircraft operation. It lists the sequence of regimes encountered. The flight spectrum report summarizes the distribution of time spent in each regime and how often the regime is repeated. Computed component usage is then aggregated to the sum of the usage already carried by the system for that specific component.

In addition to providing an accurate determination of parts usage, the algorithms introduce improved data collection accuracy via automation. Usage data are collected for each flight of each aircraft - a process that produces a massive amount of usage information. Automated analysis converts this data into manageable information that is then archived. It is automatically distributed and archived to enhance the logistics decision-making process. This automated data collection enables individualized parts life determination, addressing the actual usage of each aircraft in the fleet. Additionally, all fleet aircraft in the model are now treated to the same effective margins of safety by the improved system of algorithms. This approach retains the high confidence levels (6-9's reliability) historically embodied in the original safety regulations. By the same token, it is designed to reduce inappropriate and unwanted parts life penalties.

Applications

Since its introduction in 1995, the HIDS structural usage monitoring capability has been extended to other joint BFG/Navy/USCG/USMC programs. These include USCG HUMS, the CH-53E Early Operational Aircraft (EOA) program, and the Integrated Mechanical Diagnostics (IMD) Cost and Operational Support Savings Initiative (COSSI) program, as well as to the commercial S-92/S-76 HUMS program. It is expected to provide a significant reduction in maintenance cost and improved flight safety in each of these applications.

Operational Description

The HIDS system includes all of the hardware and software to acquire data in flight. It provides on-aircraft warnings and maintenance advisories as well. The airborne portion includes interfaces to existing sensors, added production representative sensors, interfaces for all added production representative sensors as well as signal conditioning and data acquisition capability for all sensors. It executes the algorithms required to complete all of the in-flight functions and data transfer functions to the ground station. The HIDS system also includes a separate ground station that performs post-flight analysis, data report processing, maintenance diagnostics, and data archiving. The ground station hardware and software are designed to be operable in the current U.S. Navy, Coast Guard and Marine Corps maintenance environment. It provides maintenance data output products that can be readily integrated with the Navy's maintenance concept and daily operation.

Various signals are collected during the HIDS program by the on-board system. The system is comprised of two processors, a KT-1 (low frequency parameter capture, 1 Hz) and KT-3 (higher frequency parameter capture, 10Hz). The KT-1 captures aircraft state parameter data and the KT-3, high frequency vibration and optical tracker data. The KT-1 software commands the on-board system to constantly capture aircraft state parameter data at 10 Hz. When the condition is nominal, the parameter data is averaged into 1 Hz data before storing on the PCMCIA flash memory card in the Data Transfer Unit (DTU). For each exceedance, the higher rate data of a set of selected parameters is recorded for the 15 seconds before and after the exceedance. This information is stored in conjunction with the 1 Hz data record. The pilot or an aircrew member could

manually initiate higher rate data recording by pushing a button on the CDU. The parameter data is downloaded to the HIDS ground station after each flight. Regimes are then "recognized" in sequence by analyzing the downloaded data. The sequence is then tabulated to produce a usage spectrum. Figures 36 and 37 show an example of the HIDS ground station flight profile outputs of flight profile (i.e., regime sequence report) and flight spectrum, respectively, for a single flight. The parameter data and regimes can be cross-checked with the ground station regime data viewer, as shown in figure 38. This capability provides users the ability to verify the data as well as the regime definitions and algorithms. Parts life tracking is performed with the cumulative flight spectrum that represents the usage history of all tracked parts installed on a given aircraft. Calculated total damage and retirement time for a given part-failure mode are presented in the usage report shown in figure 39. Other mechanical conditions also contribute to a part's fatigue damage. For example, a properly balanced and smoothed helicopter that produces little or no vibration could prolong the structural usage of some aircraft parts. One of the HIDS (and other Navy program) goals is to establish a link between these areas so that structural usage, rotor track and balance, engine performance, and drive train diagnostics can be fully integrated and jointly performed on aging aircraft.

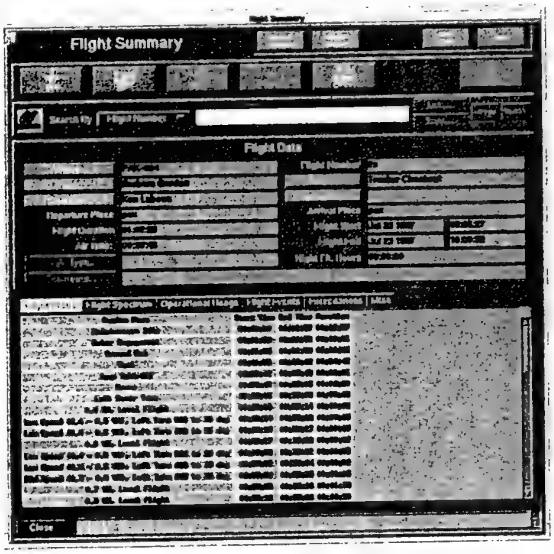

Fig.36. Regime Sequence Report for a single flight.

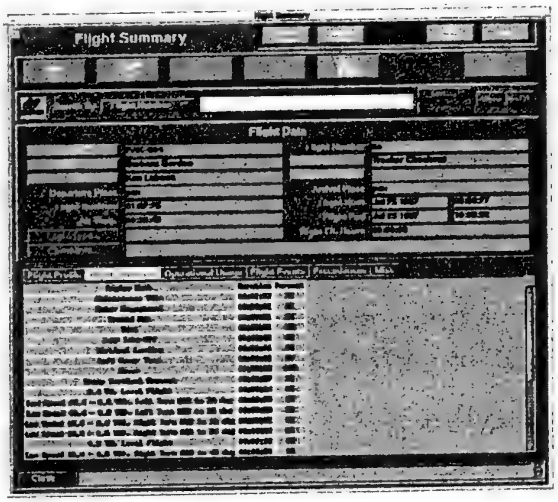

Fig.37.Regime Spectrum Report based on a single flight.

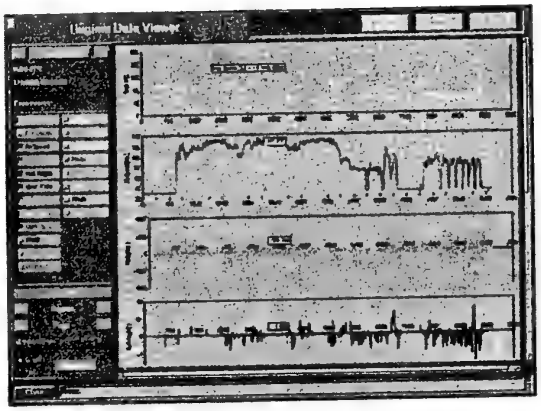

Fig.38. Regime data viewer for regime validation.

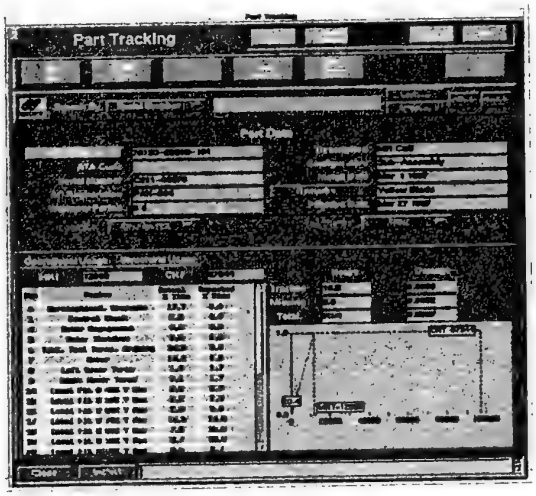

Fig.39. Parts life tracking based on actual aircraft usage.

Conclusions and Recommendations

1. This collaborative effort has provided significant benefit to the US, Australia, UK, government, commercial and university organizations in the form of a rich vibration database, diagnostic reports and integrated HIDS lessons learned.

2. Raw digital time series data files are a valuable asset for evaluating the performance of diagnostic and prognostic algorithms, and are necessary to identify system problems that result in false alarms. The data allows for development of additional system analysis and test capabilities to negate potential false alarms, and provides for system maintenance direction.

3. Technology to monitor and diagnose aircraft systems exists today, but reliable vibration diagnostics and prognostics requires the capability to record raw data for baseline development of various aircraft and component types to establish production system algorithms and thresholds.

4. Testing will continue in the HTTF to expand the database and refine the correlation of defect size to algorithm output level for alarm threshold settings on the SH-60 and H-53E. Continue refinement of vibration diagnostic algorithms and QA/QC routines and implement into aircraft system. Expanded testing to include the following:

(a). Continued testing of fleet gearboxes rejected for vibrations or chips. Support from the Class Desk and Depot has been coordinated for identification and testing of components.

(b). Continue testing of EDM notched gears and bearings for fault propagation testing at HTTF.

(c). Continued testing of additional planetary system seeded faults.

5. NAWCADPAX needs to continue flying to continue evaluation of functional capabilities while developing recommendations and requirements for a fleet system.

(a) Ongoing work is required to improve correlation of engineering diagnostic outputs with component conditioning to effect meaningful fleet information and recommended actions.

(b) Expand diagnostic system database for regime recognition and structural usage monitoring algorithms for the SH-60.

6. Testing for vibration analysis evaluation and validation in the HTTF has provided a tremendous foundation for a thorough understanding of the vibration characteristics and transmissibility between dynamic components of the SH-60 drive system. Future HTTF test efforts should require vibration databases to be established using the raw vibration data acquisition system. Upgrade the HTTF to allow for testing of the CH-53E at full power. Provide vibration test facilities at overhaul as a quality assurance check and initial aircraft baseline for when the component is installed. These data records will provide component level baseline prior to installation on the aircraft.

7. Both the potential and actual application of various diagnostic and prognostic techniques were successfully demonstrated during this program.

8. Further development and validation of advanced model based analysis, data fusion, and additional techniques for reducing and/or eliminating false alarms is needed to completely implement a fully comprehensive prognostic capability.

9. For engines, gearbox and drive trains, rotor head assemblies, and other structural components; diagnostic and life usage monitoring capabilities are invaluable for managing damage tolerance concerns on aging helicopter fleets.

10. There is a great benefit and need to conduct significant "seeded fault" tests in order to establish an experience base for realistic alarm threshold setting and to understand fault progression rates. An adequate understanding of various component fault progression rates taken to failure is needed to fully enable prognostics.

References

[1]Mission Need Statement for Integrated Diagnostic System, 3501 Ser 723/9197 of 25 Oct 93 and 3501 Ser NO2X/03100 of 18 Aug 93.

[3]Hardman, W., Hess, A., and Neubert, C. "SH-60 Helicopter Integrated Diagnostic System (HIDS) Program Experience and Results of Seeded Fault Testing", American Helicopter Society 54th Annual Forum, Washington, DC, May 20-22, 1998.

[4]Emmerling, W. C., "Helicopter Drive System Seeded Fault Test Program", AHS Rotary Wing Technical Specialists' Meeting, 26 Oct 93.

[5]Hardman, W. and Frith, P., "Analysis of a Severe IGB Tooth Fault Implanted in the 8W SH-60 Drive Train Rig", NAVAIRWARCENACDIVTRENTON-LR-PPE-95-7, Aug 95.

[6]Neubert, C., and Mimnagh, M., "Results of H-60 Helicopter Engine High Speed Shaft Assembly Imbalance Testing", NAVAIRWARCENACDIV-TRENTON-LR-PPE-96-4, Jun 96.

[7]Neubert, C., "Performance of QDM and IDM Oil Debris Monitors in a Full Scale Helicopter Transmission Test", NAVAIRWARCENACDIVTRENTON-LR-PPE-96-3, Mar 96.

Flaw Tolerant Safe-Life Methodology

D.O. Adams
MS S346A4
Sikorsky Aircraft Corporation
6900 Main Street, P.O. Box 9729
Stratford, CT 06497-9129, USA

ABSTRACT

Conventional safe-life methodology has been in general use in the helicopter industry for more than 40 years to substantiate fatigue-loaded dynamic components. However, it is seen to need improvement. One improvement is to reduce its sensitivity to the strength-reducing effects of flaws and defects that may occur in manufacturing and service use. Damage Tolerance methodology provides a means to accomplish this improvement but it is currently difficult to economically apply it to every fatigue mode on every component. Flaw Tolerant methodology is an available equal-choice option to Damage Tolerance for Transport Category civil rotorcraft, and it is offered here as a practical improvement to conventional safe life for military applications as well. Flaw Tolerance, which is based on the characteristics of initiation of cracks from flaws, is described and illustrated by means of examples of successful applications to helicopter components.

INTRODUCTION

This paper provides a description and examples of successful applications of Flaw Tolerance. The method is currently available for Transport Category civil rotorcraft via FAR 29.571, References 1 and 2. Although the method is applicable to composites, this discussion will be limited to metals applications. Also, the discussion focuses on fatigue-substantiated components in the rotor, drivetrain, and control systems, although there may be opportunities to apply Flaw Tolerance to airframe structure as well.

Definition of terms is an immediate difficulty in this field. Different sources may use conflicting definitions of common terms. This is due to the simultaneous evolution of fatigue substantiation methodologies in related but independent endeavors over the last 40 years. For example, the term "Damage Tolerance" is deliberately avoided in the FAR 29.571 advisory material, Reference 2, even though most readers think that this is precisely what is being discussed. This paper will use the definitions proposed as a joint position of the AIA/AECMA helicopter companies in Reference 3. The term Damage Tolerance will be used to describe the evaluation of crack growth characteristics, including the conclusion of no growth of cracks. The term Flaw Tolerance (also called Flaw Tolerant Safe Life or Enhanced Safe Life) will be used to describe the evaluation of crack initiation characteristics from flaws. Using these definitions for the methodology described in FAR 29.571 would result in saying that the FAA's "Fatigue Tolerance" requirement can be met equally by either a Damage Tolerance or a Flaw Tolerance approach.

Flaw Tolerance is being presented here because it is a method that is not well known and has not been widely used, or at least was not called Flaw Tolerance when it was used. However, it can provide the same benefits in helicopter fatigue applications as Damage Tolerance, while avoiding some of the issues which can make Damage Tolerance very difficult to apply in practice to every helicopter dynamic component. Flaw Tolerance could also be regarded as a useful and positive interim approach to improving helicopter fatigue substantiations while the Damage Tolerance Methodology matures and develops to a point where it can be used in practice more universally.

Finally, it is noted here that Flaw Tolerance is not used by all manufacturers, nor is it the first choice of all certifying agencies, however, all of the AIA/AECMA helicopter manufacturers have agreed that it should be retained as an available equal-choice alternate method for civil applications (Reference 3).

BACKGROUND

A conventional safe-life approach has been the most frequent choice of all helicopter manufacturers since the 1950's to substantiate fatigue-loaded flight-critical dynamic components in both civil and military applications. This approach requires knowledge of three elements for each substantiated component: 1) S-N curves representing the crack initiation fatigue strength for each mode of failure; 2) Loads for each flight regime in the mission spectrum; and 3) Rate of occurrence in service (usage) for each of these regimes. The strength, loads, and usage elements are combined, by a linear cumulative damage rule (Miner's Rule), to calculate a safe retirement time. The conservative margins included in each of the three elements produce a very high level of reliability in the result. However, in spite of its overall success in helicopter applications, this method does not account for any component strength that deviates from the strength distribution assumption made during the fatigue substantiation process. Historically, many of these strength-reducing problems derive from flaws and defects generated as a result of manufacturing, maintenance, and service use.

The need to improve civil helicopter structural tolerance to flaws and defects was recognized by the Federal Aviation

Presented at The NATO Research and Technology Organization Applied Vehicle Technology Panel Meeting on Aging Systems, Corfu, Greece, April 22, 1999

Paper presented at the RTO AVT Specialists' Meeting on "Application of Damage Tolerance Principles for Improved Airworthiness of Rotorcraft", held in Corfu, Greece, 21-22 April 1999, and published in RTO MP-24.

Administration in the U.S. in the 1980's. Damage Tolerance methodology was also being applied at that time with considerable success to fixed wing aircraft in both military and civil applications. These ideas represented a significant and important change in direction for the civil helicopter community. The requirements were promulgated in Amendment 28 to Paragraph 29.571 of the Federal Aviation Regulations, Reference 1, and Advisory Circular 29-2A Amendment 1, Reference 2, applicable to Transport Category helicopters (over 2700 kg gross weight). These requirements use the words "fatigue evaluation of structure including flaw tolerance" and permit either a "Fail-Safe Evaluation" (residual strength after flaw growth) or a "Flaw Tolerant Safe-Life Evaluation".

Although confusing in terms, the new rule required the application of either Damage Tolerance or Flaw Tolerance to all Primary Structural Elements unless it was shown to be impractical, in which case a conventional safe-life approach could be used. Flaw Tolerance was included to provide the manufacturers a means of accounting for flaws and defects using basic safe-life methodology that was highly developed and whose shortcomings were very well understood. Damage Tolerance had already achieved a high level of success in transport aircraft, and had seen some successful applications in the helicopter world as well. However, it was seen as a major risk to commit to applying it to all new helicopter dynamic components, given the high cycle rate of fatigue loading and the possibility of frequent difficult inspections.

There has also been some direct experience with Flaw Tolerance, although it may have been called something else when we used it. Sikorsky conducted a fatigue program for the U.S. Navy in 1986 where the effects of known strength-reducing conditions on CH-53A/D dynamic components were evaluated with a coupon program and safe-life methods. In addition, Sikorsky has employed a Flaw Tolerant approach in the resolution of several field problems, and in the original substantiation of some military components. Examples of all of these are found later in this paper. A technical paper, Reference 4, with authors from 3 U.S. helicopter companies, promoted consideration of "degraded modes" in safe-life substantiations in 1988.

Only one completely new civil helicopter project has applied for certification under the new rule - the Sikorsky S-92 "Helibus", Figure 1. All options permitted by the rule were evaluated and used. Flaw Tolerance was the method most frequently chosen for the initial substantiation of the dynamic components. As the substantiation progresses and strength and loads data are obtained, this choice will be reevaluated. The S-92 is currently in the early stages of its flight test development, and its application of Flaw Tolerance methodology can be examined, as described in an example later in this paper.

Figure 1. Sikorsky S-92 "Helibus".

THE FLAW TOLERANCE METHOD

The following description of the Flaw Tolerant method is extracted from Reference 3. It meets the requirements of FAR 29.571, and includes provisions to derive inspection intervals for flaws, which is not required by some interpretations of FAR 29.571 and its advisory material.

Just as with Damage Tolerance, Flaw Tolerance is intended to assure that should serious corrosion, accidental damage, or manufacturing/maintenance flaws occur within the specified retirement time and/or inspection intervals of the component, the structure will not fail.

Basics of the Flaw Tolerant Method

The Flaw Tolerant method provides component management requirements based on the assumption of the existence of flaws in the component's critical areas. Two sizes of flaws are considered:

1) "Barely Detectable Flaws" are used to conservatively represent the largest probable undetectable manufacturing or service-related flaws.

2) "Clearly Detectable Flaws" are the largest probable manufacturing or service-related flaws that would not normally be detected in a routine visual inspection such as a pre-flight or weekly.

The approach to Flaw Tolerant design of Principal Structural Elements depends on the type of structure. The approach for single load path structure has two requirements:

1) A barely detectable flaw will not initiate a propagating crack within the retirement time of the component; and

2) A clearly detectable flaw will not initiate a propagating crack within an inspection interval, inspecting for the presence of the flaw.

The approach for multiple load path or fail-safe structure also has two requirements:

1) A barely detectable flaw will not initiate a propagating crack within the retirement time of the component; and

2) A barely detectable flaw in a second load path, after the first load path failure, will not initiate a propagating crack within an inspection interval, inspecting for first load path failure.

Determining Flaw Types and Sizes

Flaw types and sizes to be imposed on each component being substantiated by Flaw Tolerance are defined, and are submitted with accompanying rationale to the certifying agency for approval. The first element of this process is a systematic evaluation of the types and sizes of flaws to be considered for each component. The types of flaws considered should include nicks, dents, scratches, inclusions, corrosion, fretting, wear, and loss of mechanical joint preload or bolt torque.

The systematic evaluation should include a compilation of historical experience with similar parts and materials, including field service reports, overhaul and repair reports, metallurgical evaluations, manufacturing records, and accident/incident investigations. The design, manufacturing, maintenance, and overhaul practices and processes that could result in errors or defects should also be evaluated. Planned inspection methods and practices also define what size and locations of flaws are likely to be detectable. A coupon program is valuable in indicating the strength-reducing effects of various types of flaws, S-N curve shape and statistical scatter for flawed parts, and, if needed, determination of "equivalent" flaw types and sizes that may be used on full-scale test specimens. This is illustrated in Figure 2.

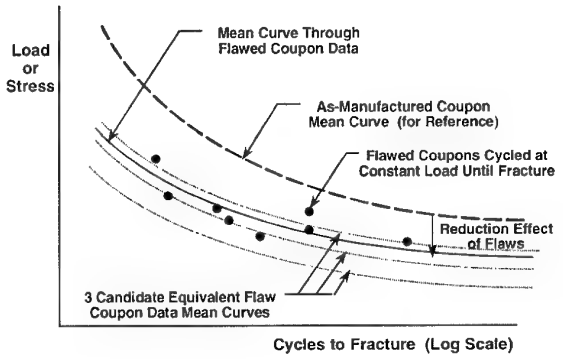

Figure 2. Coupon Evaluation of Flaws.

Consideration should also be given to factors that reduce the chance of error, such as "frozen processes", Flight Critical Parts programs, material selection to avoid inclusions and defects, and procedures to reduce manufacturing errors. Another possibility is to limit the flaws considered if the design includes surface treatments that protect against environmental and/or accidental mechanical damage. In addition, it may be appropriate to show by means of a joint probability analysis that some flaws may be eliminated from consideration because they have an extremely remote chance of a critical occurrence. This analysis combines the distribution of likely flaw sizes, the criticality of location and orientation, and the likelihood of being missed in an inspection.

If this evaluation determines that a possible flaw is a true crack, the Flaw Tolerance method may not be valid. Cracks of this sort could be related to manufacturing errors in plating or surface treatments, heat treatment, or cold working. For these specific defects, an analytical evaluation should be conducted, using fracture mechanics methods, to verify that these cracks will not grow under the expected spectrum of flight/ground loads.

Determination of Life Limits and Inspection Intervals

A Flaw Tolerant fatigue test program should include three types of specimens. At least one "as-manufactured" specimen is needed to establish a baseline of strength and to correlate with design analysis. Multiple specimens with barely detectable flaws in critical areas are then tested to determine an overall retirement time. At least one specimen with clearly detectable flaws in critical areas is used to determine inspection intervals. It should not be necessary to provide new specimens for each phase of this program, since runouts (non-fractures) is a likely result from the as-manufactured specimen, and possibly from the barely detectable flaw specimens. Flaws can be added to these runout specimens and used in the next phase of the program. The testing itself is conventional accelerated load S-N testing with crack detection by the best laboratory means available. Multiple load path specimens can have the first load path failed "naturally" as a consequence of the S-N testing, or "artificially" by sawcutting, removing fasteners, or otherwise disabling a load path.

For both single load path and multiple load path structure, the retirement time is based on the assumption that barely detectable flaws are present in the structure at all critical locations. The inspection interval for single load path structure is based on the assumption that clearly detectable flaws are present in the structure at all critical locations. The inspection interval for multiple load path structure is based on the life of the second load path, with barely detectable flaws in all critical locations, following complete fracture or disabling of the first load path. No assumption needs to be made as to the cause of failure of the first load path, however, limit load capability should be verified with the one load path failed or disabled.

Determination of retirement times and inspection intervals is done by conventional safe-life calculations using the flawed mean strengths demonstrated by test and/or analysis. Working curve reductions may be smaller than for the conventional calculation, typically "2-sigma" instead of the conventional "3-sigma". Using the conventional reductions would essentially be an assumption that every component in service had the maximum flaw in every critical location for its entire lifetime - an excessively conservative assumption. The flight loads, usage spectrum, cycle counts, prorates, and damage calculation methodology used should be the same for each calculation. Multiple load path inspection interval calculations should include a correction for damage that may occur in the second load path in the time before the first load path is completely severed.

A retirement time should also be calculated using the strength of the as-manufactured specimen and conventional working curve reductions. This should be compared with the retirement time for the barely detectable flaw specimens with the reduced working curve reductions. The lower of the two results is used to retire the part.

Inspections on Flaw Tolerant parts are for the presence of the flaw, not a crack. If the flaw is not found, the part may be returned to service for another inspection interval, up to the overall retirement time of the part. If the flaw is found, the part is retired, or, if a repair procedure has been qualified and approved, repaired and returned to service for another inspection interval, up to the overall retirement time of the part.

EXAMPLES OF FLAW TOLERANT SUBSTANTIATIONS

CH-53A/D Horizontal Hinge Pin

An out-of-production U.S. Navy helicopter was evaluated to determine what actions were required to extend its service life considering the effects of known degrading conditions occurring on the dynamic components. The method selected was: first, an engineering evaluation of each component's sensitivity to known degrading conditions; second, coupon testing to determine potential strength reductions from the various types of selected degrading conditions; and third, application of these reductions to existing full-scale fatigue data from conforming parts. Actions were formulated using conventional damage calculations based on the reduced full-scale strength.

One of the evaluated components was the main rotor head horizontal hinge pin, a 4340 steel component that was subject to corrosion in service. Coupon testing with various degrees of corrosion indicated a significant reduction in strength - up to 63% for "worst case" corrosion pitting. Figure 3 illustrates the penalty for this effect considered as a further-reduced working curve. A "life" of 1500 flight hours results from using this curve and the standard damage calculation for this model helicopter. The action recommended for this component was to inspect for corrosion at the scheduled overhaul every 1200 hours. Corroded parts are rejected, clean parts are returned to service for another overhaul interval, up to their normal 8300-hour retirement time.

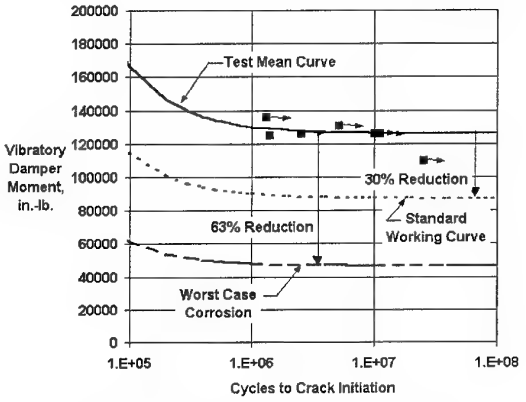

Figure 3. Effect of Corrosion on Hinge Pin

This example is very nearly the Flaw Tolerant methodology recommended above, except that full-scale tests with flaws are not conducted. The working curve is set at the maximum reduction for corrosion, rather than reducing the mean by the average effect of the flaw and then taking a further 2-sigma reduction. The two approaches would produce similar results.

The inspection for corrosion is easy, and may be conducted at the time of overhaul when the component is disassembled.

S-76 Tail Rotor Pitch Horn

Corrosion was discovered on some in-service tail rotor pitch horns at in the critical fatigue site for the safe-life substantiation. These horns are aluminum and have a conventional safe life of 22,000 hours. A full-scale fatigue test program was conducted which included horns with the worst service-related corrosion, and horns subjected to a severe salt fog chamber exposure.

Results of the full-scale program are shown in figure 4. The effect of corrosion is much smaller in this case, although there is a high scatter when the conservative salt fog chamber results are included. A standard working curve is used in this case, in order to capture the lowest corroded data point. The life calculation for this working curve produces a 12,000 hour result. The retirement time for all S-76 tail rotor horns was changed to this value.

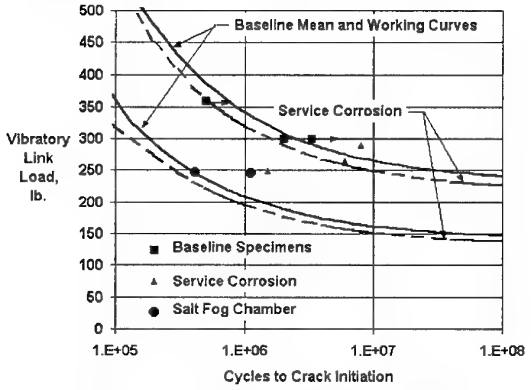

Figure 4. Effect of Corrosion on Pitch Horn.

As a Flaw Tolerant substantiation, this example contains the elements of full-scale test with flaws, and worst case flaws imposed by a conservative but somewhat artificial means. Imposing a retirement time instead of an inspection option is due to the fact that almost every horn will have some degree of corrosion at 12,000 hours anyway, and a rework procedure was not substantiated.

SH-60B Horizontal Stabilizer

This component was substantiated in fatigue as if it were a dynamic component, in spite of its "airframe" design features. Full-scale fatigue testing of the prototype configuration revealed two cracking modes - in the web of the forward spar of the right-hand wing panel, and in the aft attachment fitting of the center box structure. These cracks were several inches long and stopped by reaching a joint or edge. The conventional safe lives for these modes were low and a redesign was initiated. However, an interim position was needed to allow the program to continue until the redesign was available. The method chosen was to conduct "crack re-initiation" testing of the unit it its cracked condition. 250 hours of testing was accomplished on the wing panel and 160 hours on the center box at conservative loads without the initiation of any additional cracks. A visual inspection for the original cracks was added to the daily walkaround inspection. The cracks were easy to find visually and the inspection did not require any disassembly.

This is an example of a multiple load path Flaw Tolerant substantiation. The first load path failures are the initial cracks, which were not propagating further. A good crack re-initiation interval was demonstrated for the remaining load paths, albeit without an S-N curve and rigorous methodology, allowing an easy inspection to be conducted at a short interval (daily). If the initial cracks were found, the part would be removed from service.

SH-60B Servo Beam Rails

These four components provide the mounting hardpoints for the three horizontally mounted main rotor servocylinders on the SH-60B, each one mounted to two rails, two feet on each. Barrel nuts in each rail lug receive the servo mounting bolts. The conventional S-N testing on the rails showed fretting fatigue origins in the barrel nut holes, yielding calculated safe-lives of 4000 to 5000 hours. An evaluation of fail-safety was then conducted by continuing the testing until an additional crack initiation was noted, usually at a different location in the same barrel nut hole. The two crack re-initiation results for one of the rail types are shown in Figure 5. The "life" calculation, conservatively using a conventional "3-sigma" working curve, produced a 2900-hour result. This result was proposed to be used to justify a phase inspection for the initial cracks at 300 hours. No disassembly is required, and the initial cracks are easily seen in a visual inspection.

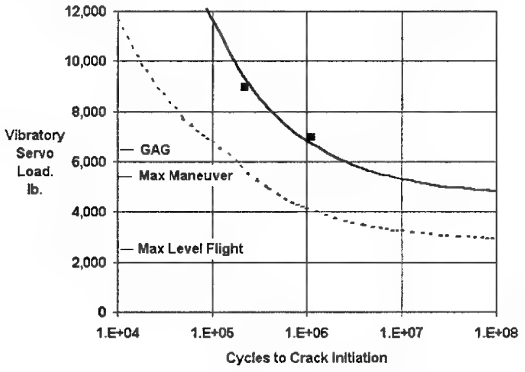

Figure 5. Crack Re-Initiation on Servo Beam Rail

S-92 Main Rotor Hub

Most of the S-92 dynamic components have been initially selected for a Flaw Tolerant substantiation. The main rotor hub is the largest and most complex of these - a titanium forging, machined all over, and designed for easy inspections, Figure 6. At the time of this writing the first, as-manufactured,

full-scale fatigue specimen testing has been completed, but none of the flawed specimens have been tested. The result for the first hub specimen was a runout (non-fracture), because of the inability to increase the test load beyond the hub's geometric flapping limits. Strain surveys indicated that the hub was operating in the test at about half the conservative design fatigue allowable for the material.

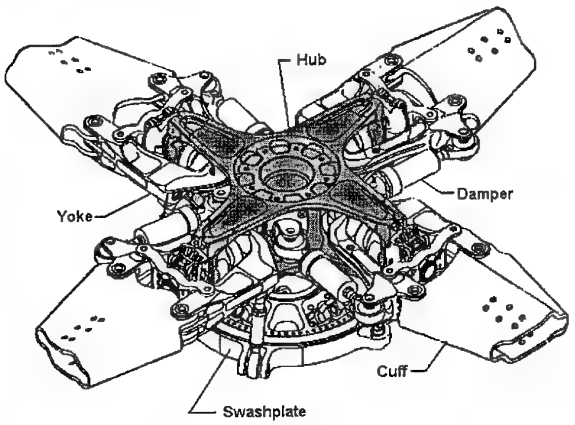

Figure 6. S-92 Main Rotor Head

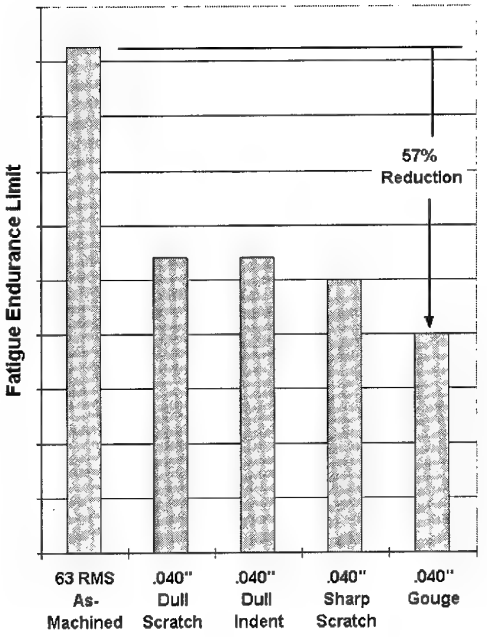

Figure 7. Coupon Evaluation of Flaws on Titanium

Even though the strength of the flawed full-scale hub is not available, the results of a Flaw Tolerant substantiation can be estimated. A coupon program evaluating the effects of various types of flaws indicates which type is most critical and provides a conservative estimate of the strength-reducing effect. A study of fielded Sikorsky components indicated that an .040" deep flaw was possible on titanium, and this was selected as the Clearly Detectable Flaw size. The Barely Detectable Flaw was selected as .005" deep based on the easily-seen appearance of a flaw of this depth on the titanium coupons with the as-manufactured surface finish. The coupon results showed little or no effect of the Barely Detectable Flaws - scratches, indents, or gouges. However, the Clearly Detectable Flaw study showed a fatigue strength reduction of up to 57%, the worst being an .040" deep gouge, Figure 7.

Figure 8 illustrates how the Flaw Tolerance substantiation should look. The runout full-scale test result is doubled in strength based on the strain survey, providing an estimate of the actual as-manufactured hub strength. This curve is then reduced by 57% to account for the potential effect of .040" gouges in critical sections. A further reduction of 20% (2-sigma) is added to produce a working curve for the flawed strength. A "life" calculation with this working curve, predicted flight loads, and the commercial usage spectrum produces a 15,000-hour result. This figure could be used as an inspection interval, inspecting for the presence of the flaws. In practice, the inspection would likely be done at the time of a major inspection interval, such as 1250 hours.

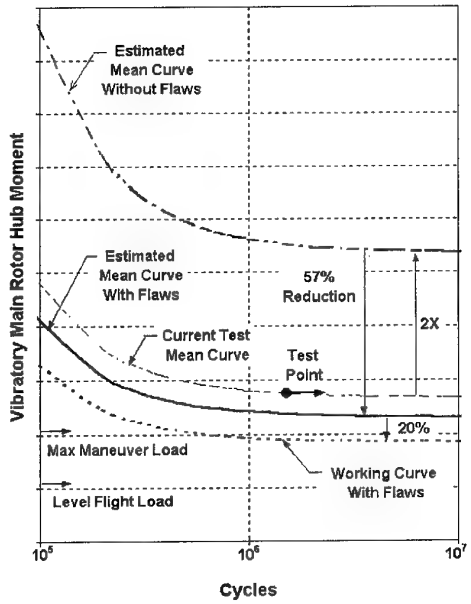

Figure 8. Flaw Tolerance Evaluation of S-92 Hub.

COMPARISON OF METHODS

Having the Flaw Tolerant method available provides an additional capability to successfully achieve the design goals of a helicopter project. Table 1 illustrates the pros and cons of the choice of method for single load path metal structure. The Damage Tolerance approach for helicopters has been shown as both the "No/Benign Crack Growth" method and the "Slow Crack Growth" method. These methods are also described as "Damage Tolerance Without Inspection", and "Damage Tolerance With Inspection", respectively.

The Slow Crack Growth method of Damage Tolerance provides the significant advantage that it does not matter what the original source or cause of the cracking is (up to the point where the initial crack size is bigger than the minimum inspectable size). So flaws and defects of different character, size, or location than anticipated would still be accommodated by the substantiation. However, as discussed in Reference 5, every inspection method and interval must be compatible with the missions, limitations, and economics of helicopter operations worldwide. This is the critical difficulty in applying Slow Growth Damage Tolerance to helicopter dynamic components. Improvements in analytical methods, design concepts, materials, and NDI methods are needed to make it practical to confidently apply this method more frequently than we can today.

Both the No/Benign Crack Growth method and the Flaw Tolerant method require some degree of a priori research and decisioning on the types and severities of flaws and defects that will be considered in the substantiation. However, currently these methods offer the telling advantage of being practical to the operator - the No/Benign Crack Growth method requiring no inspections, the Flaw Tolerant method only requiring inspections for significant flaws, at reasonably long intervals. All three methods (Flaw Tolerance, Slow Crack Growth, No/Benign Growth) provide retirement times much higher than frequently achieved today by conventional safe life.

Change in the original substantiation assumptions of a new model helicopter are inevitable, and have differing effects on the structural substantiation methods. In the case of the No/Benign Growth method and the Flaw Tolerant method, initial assumptions must be made with respect to the initial level and location of damage. If these assumptions are not well-founded and sufficiently conservative, new levels, types, or locations of damage which occur during the service life of the component may require a resubstantiation involving new tests and/or analysis. In the case of the Slow Growth Damage Tolerance method, this event is much less likely.

The most likely change to occur is an increase in loads. "Mission creep", configuration changes, higher gross weights,

Table 1.
Pros and Cons of Method Choice
Single Load Path Metal Components

Method	Recurring Inspection Required	Initial Damage Assumption	Consequence of Increased Initial Damage Assumption	Consequence of Increased Load or Spectrum	Principal Design/Application Issue
No/Benign Crack Growth Dam. Tol.	None	Evaluation of Manufacturing and Service Defects	New Analysis/Test, New Life Limit	New Analysis/Test, New Life Limit	Defining/Using Initial Crack Size
Slow Crack Growth Dam. Tol.	Inspect for Cracks	None Required	No Change	New Analysis/Test, New Insp. Interval	Achieving Practical Insp. Method and Interval
Flaw Tolerance	Inspect for Flaws	Evaluation of Manufacturing and Service Defects	New Analysis/Test, New Life Limit or Insp. Interval	New (Simple) Analysis, New Life Limit or Insp. Interval	Defining and Applying Flaws

and more powerful engines are all part of the growth and evolution of a helicopter model, and all contribute to higher loads in the dynamic components. All three of the methods can accommodate these changes, by reducing life limits and/or inspection intervals as needed. The basis for the change in the Damage Tolerance methods is a new fracture mechanics analysis and/or test program incorporating the higher loads. Flaw Tolerance on the other hand, can accommodate higher loads by a simple modification to the existing damage calculation.

The above discussion is appropriate only if all of the methods are valid and well founded. The critics of the Flaw Tolerant method argue that it is entirely empirical and not based in any scientific principal of damage accumulation. Advocates argue that Flaw Tolerance is a proven methodology and does offer a significant improvement over conventional safe life, even if it is empirical. Then, given that it is currently impractical to apply Damage Tolerance to every possible fatigue mode on every helicopter component, we need to be able to continue to take advantage of the benefits of the Flaw Tolerant methodology.

CONCLUSIONS

1. Helicopter fatigue substantiations can be and should be significantly improved by the consideration of flaws and defects.

2. Damage Tolerance offers promise to provide this improvement but currently cannot be economically applied to every fatigue mode on every helicopter dynamic component.

3. Flaw Tolerance can achieve the desired improvement using methods that are available and proven effective, and can do so within reasonable cost, weight, and maintainability constraints.

4. Flaw Tolerance should continue to be an equal-choice method for civil helicopter fatigue substantiations, and considered as a practical alternate to Damage Tolerance in military substantiations.

ACKNOWLEDGMENTS

The author wishes to thank Sikorsky Engineers Bob Holt, Stan Magda, Bill Boyce, Dave Hunter, and Paul Inguanti for their important contributions to this paper. Additionally recognized are the many significant contributions made by the AIA/AECMA "fatigue specialists" who created Reference 3.

REFERENCES

1. Regulation - Federal Aviation Administration Airworthiness Standards: Transport Category Rotorcraft, Paragraph FAR 29.571, "Fatigue Evaluation of Structure".
2. Advisory Circular - Federal Aviation Administration Advisory Circular AC 29-2A, Appendix 1, "Fatigue Evaluation of Transport Category Rotorcraft Structure (Including Flaw Tolerance)".
3. Technical Paper - "Rotorcraft Fatigue and Damage Tolerance", W. Dickson, J. Roesch, D.O. Adams, B. Krasnowski, Prepared for the Technical Oversight Group on Aging Aircraft (TOGAA), January 1999 (unpublished at the time of this meeting, copies available from D.O. Adams).
4. Technical Paper - "Methodology for Fatigue Substantiation of Alternate Sources and Degraded Modes on Helicopter Dynamic Components", D.O. Adams, C. Albrecht, W.D. Harris, 44th Annual Forum of the American Helicopter Society, Washington DC, June 1988.
5. Technical Paper - "Damage Tolerance Applied on Metallic Components", T. Marquet, A. Struzik, 24th European Rotorcraft Forum, Marseilles, France, September 1998.

DAMAGE TOLERANCE APPLIED ON METALLIC COMPONENTS

AUTHORS :
Thierry MARQUET / Alain STRUZIK

EUROCOPTER
Etablissement de Marignane
E/TM.C
13725 Marignane Cedex – France

thierry.marquet@eurocopter.fr
alain.struzik@eurocopter.fr

SUMMARY :

New requirements including damage tolerance were inserted in FAR 29.571, amendment 28 in 1989 to increase the safety level of helicopters.

" Flaw tolerance safe life " and " fail safe " - or a combination thereof, were proposed to fulfil the damage tolerance requirements. If unpractical, " safe life " evaluation was acceptable.

A working group called TOGAA was mandated by the US Senate to propose modifications to the FAA rules. Harmonised recommendations from rotorcraft manufacturers (RCWG) had been gathered in a " White Paper ". The TOGAA commented this methodology and concluded in mid 1998, that the " flaw tolerant safe life " concept should be purged in FAR 29, and advocated the exclusive use of crack propagation for single and multiple load paths.

This paper presents EUROCOPTER's statistical analyses of the root causes of accident in flight. EUROCOPTER's philosophy in reply to FAR & JAR 29-571 is detailed, showing a significant and measurable improvement over conventional " safe-life " methodology. This philosophy has already been applied to several current projects (EC 155, NH 90), and the RCWG simply wanted it to be left in the current rules.

The main technical arguments presented to the TOGAA are set out.

1. BACKGROUND

Fatigue[1] evaluation of metallic parts, the failure of which could have catastrophic effects on the rotorcraft was based till now on the " safe-life " concept. Parts are retired from service at specified times, regardless of their condition.

This service life was determined from analysis or/and fatigue testing performed on full scale as-manufactured[2] components with a high load safety factor (typical 1.4 for gears, 1.8 to 3 for other components as shown in figure 1).

In addition, safety was largely improved by:

- routine visual inspection or preventive scheduled maintenance actions (defined in the Recommended Maintenance Program); these were based either on flight hour intervals to check fretting, wear, loss of tightening torque, impact, scratch, etc. or on calendar intervals to check for corrosion (atmospheric, galvanic or stress).
  These inspection intervals were generally based on previous experience acquired with similar designs and updated according to the behaviour noted during overhauls.

- specific maintenance actions (reported directly to operators or/and approved repair shops).

  These actions (recommended or mandatory) were drawn from the analysis of damages found during overhauls, accidents[3] or major incidents[4] that occurred on the fleet.

- detection of abnormal helicopter behaviour.

Paper presented at the RTO AVT Specialists' Meeting on "Application of Damage Tolerance Principles for Improved Airworthiness of Rotorcraft", held in Corfu, Greece, 21-22 April 1999, and published in RTO MP-24.

Several potentially major accidents or accidents were avoided further to the detection of abnormal helicopter behaviour by an operator (poor blade tracking, leaks, vibrations, noise, etc.) or by the use of a Health Monitoring System equipped with accelerometers and load gages.

New civil regulations FAR 29-571 (Federal Aviation Regulation, Part 29 applicable to rotorcraft over 6,000 lbs = 2,700 kg, structural fatigue evaluation) were introduced to increase the helicopter safety level mandating proof of damage tolerance in amendment 28 date 27 November 1989. Furthermore, an associated Advisory Circular (AC 29-571) was issued in 1995.

No helicopter in the world has yet been fully substantiated according to these requirements.

2. FAR & JAR REQUIREMENTS (including damage tolerance)

The damage tolerance philosophy was developed to eliminate- or at least reduce, fatigue failures affecting components with pre-existing manufacturing quality deficiencies (e.g. inclusion, scratch, flaw, burr, crack, etc.) or service induced damage (impact, scratch, loss of bolt torque, wear, corrosion, fretting corrosion, etc.) that were the root causes of cracking.

The damage tolerance approach is based on the assumption that a damage or a crack in a component can be safely detected before the failure of this component.

In these new requirements, it is now required to consider the effects of environment, intrinsic / discrete flaws and accidental damage in the fatigue evaluation, unless it is established that this cannot be achieved within the limitations of geometry, inspectability or good design practice for a particular structure. (A " safe life " approach should be used in that case).

Two different concepts were proposed to fulfil the damage tolerance requirements :

- FLAW TOLERANT SAFE LIFE
- FAIL SAFE

or a combination thereof.

These concepts are detailed hereafter.

2.1 Flaw Tolerant Safe Life Concert

This is understood as the capability of a flawed structure to sustain, without measurable flaw growth, the spectrum of operating loads expected during the service life of the rotorcraft or during an established replacement time.

2.2 Fail Safe Concept

This is understood as the capability of a structure with a standard crack (Initial Quality Crack) or a detectable crack (using a prescribed inspection plan) to sustain the spectrum of operating loads expected during the inspection interval.

Fail safe design can be provided through different concepts (figure 2).

Figures 3 (single load path) and 4 (2 active multiple load paths) (extracted from AC 29-571) explain how the inspection intervals are set (difference between the time when the damage becomes detectable and the time when the extent of the damage reaches the critical value for residual static strength).

3. EUROCOPTER'S PHILOSOPHY

Some specific tasks were performed by EUROCOPTER to identify the type of damages encountered in service throughout the literature [ref. 1] and the analyses of the root causes of accidents in flight.

The prime results of the survey are roughly summarised below:

- Rate of accident : 37 per million of flight hours (16 of which were fatal).
  (EUROCOPTER average rate of accidents for the last five years on a " world-wide/all mission " basis)

- Reasons for accident :

  - **77%** were due to **operational conditions and environment** (poor estimation of distance with fixed or moving obstacle, poor piloting (weather condition, fuel shortage, non observance of flight manual limitations), wrong behaviour upon non catastrophic events or failures, non qualified pilots (rotorcraft type, weather conditions), pilot's physical inability to performed the required tasks).

  - **17%** were due to **incorrectly performed maintenance** (misassembly, omitting components, non performance of a mandatory modification, assembling of components not-approved by manufacturer, polluted fuel, non detection of a detectable damage, ground personnel errors during movements or rotations).
  - **3.1%** were due to **engine malfunction**.

- **2%** were **pending cause**

- **0.6%** were **non-identified cause**.

- **0.3%** were due to poor design, non conformity of components, poor substantiation, more severe load spectrum usage than expected, non-identified cause of fatigue cracks (cracks generally appearing in high stress concentration areas or otherwise from minor defects which are not the cause but the catalyst of fatigue cracks).

EUROCOPTER estimates that some accidents (less than 20 over 43 millions of flight hours) and major incidents could have been avoided by using the damage tolerance approach.

The causes of these cracks were distributed as follows :

- 30% corrosion (galvanic, atmospheric, stress)
- 25% fretting, wear
- 20% bearing
- 15% flaws (manufacturing or maintenance)
- 10% loss of bolt tightening torque.

Although this survey does not claim to be comprehensive, it can be concluded that wherever conventional " safe life " helicopter methodology is applicable (full-scale fatigue test on as-manufactured parts, in flight load measurement, conservative load spectrum and high load safety factors), it is successful in providing a high reliability.

Important Research & Development programs are in progress to reduce significantly accidents (94%) due to operational conditions and environment (all weather helicopters, improvement of Man Machine Interface, Fly-By-Wire, etc.) and due to incorrectly performed maintenance (Health and Usage Monitoring System, etc.).

Moreover, EUROCOPTER proposes to improve the substantiation of inspection intervals based on :

- flaw tolerant inspection interval
- slow crack propagation
- multiple load paths

Although the wording is similar to the one used in the FAR 29.571 (report to chapters 2.1 and 2.2), EUROCOPTER's philosophy is slightly different and detailed below.

3.1 Flaw Tolerant Inspection Interval

This is understood as the capability of flawed[5] structures to sustain, without measurable flaw growth or fatigue crack initiation, the spectrum of operating loads expected during the established inspection interval.

At the time of the periodic interval, the part may be :

- retired without inspection
- returned to service if no flaw is found
- retired or repaired if a flaw is detected.

The inspection generally is a detailed visual inspection and more (Non Destructive Examination) if a doubt exists.

3.2 Slow Crack Propagation

This is understood as the capability of a single load structure with a detectable (using a prescribed inspection plan) fatigue crack to sustain the spectrum of operating loads expected during the established inspection interval.

At the time of periodic interval, the part may be :

- retired without inspection
- returned to service if no crack is found
- retired or repaired if a crack is detected.

The inspection will generally involve a Non Destructive Examination.

3.3 Multiple Load Paths

This is understood as the capability of a multiple load structure (N load paths) with detectable (using a prescribed inspection plan) failed load path (n) to sustain the spectrum of operating loads expected during the established inspection interval.

At the time of periodic interval:

- if a failed load path is found, all the components of the load path will be retired
- if no failed load path is found, parts may be returned to service

- if some parts are found with flaws, these parts may be retired or repaired individually.

The inspection will generally involve a visual inspection to detect the failure of one load path.

In this concept, full-scale fatigue tests are performed with the remaining load paths (N-n) with as-manufactured parts, and the inspection interval is based on the initiation of a fatigue crack in the remaining overloaded load paths.

As far as new designs are concerned, the damage tolerance aspects have to be considered at a very early design stage.

This is why EUROCOPTER undertook with its own and European funds under the BRITE/EURAM program [ref. 2] a significant research program to fill the knowledge gap in crack propagation theory and in material data base (see figure 5 - crack growth rate versus stress intensity factor range curves).

Although know-how was significantly advanced, the main conclusion was that an industrial methodology fully applicable to helicopters was not available (and probably will not be available in at least 10 years) because data are missing regarding:

- propagation near the threshold region
- effects of load spectrum (retardation, acceleration effect)
- short crack propagation (crack size less than 0.5 to 1 mm in depth)
- mixed mode propagation (tensile, bending and shear stresses)
- fatigue crack path in complex 3D components
- calculation of stress intensity factor by Finite Element Method
- effect of compressive loading
- material data base (near the threshold region)
- reliable safety factors (lack of experience of in-service components designed with crack propagation methodology)

Moreover, the difficulties in practically achieving a slow crack growth design in metallic components of helicopter with a reasonable interval/method are listed hereafter:

- small component size
- high number of cycles per hour (typical 15,000 for main rotor components , 60,000 for anti-vibration system components, 75,000 for tail rotor components, 300,000 for tail rotor control components, 60,000 to 1,300,000 for rotating shaft components)
- highly stressed with alternative loads
- large crack size surely detectable in the field (table 1) often induces to a short propagation time
- Once the fatigue crack propagates, the stiffness of the component changes, and the dynamic loading of the part on the rotorcraft may be changed (but will never be measured in flight).

In conclusion, a slow crack growth could be achieved for a few components only:

- components which are mainly loaded by Ground-Air-Ground cycles (1 to 10 cycles per hour)
- components already oversized (minimum technological thickness, stiffness requirements, ...)
- component the features of which (pressurised chamber, vibration sensor, etc.) surely could detect cracks, with a low false alarm rate.

Meanwhile, EUROCOPTER undertook with its own and French government funds a significant test program to deal with flaw tolerant inspection interval methodology.

Three of the most critical damages (corrosion, scratch and impact) were selected. For each of them, a statistical analysis of sizes found during overhauls was performed. The results are dependent on the type of material used (figure 6).

A standard damage per material had been defined for each type covering 90% of the damage encountered during the service life.

Fatigue tests were performed on specimens with these standard damages on different kinds of material (steel, stainless steel, titanium, aluminium alloy, magnesium alloy).

Figure 7 shows the influence of 0.15 mm deep scratch on steel parts.

Moreover, in the " flaw tolerant inspection interval " concept, the protection of structures against flaws (via characteristics of the material, protective coating, anti-damage shield, etc.) may be used to determine the initial flaw types and sizes to be considered.

Design efforts were made to prevent flaws in the NH 90 helicopters (figure 8) in particular:

- critical components usually made of steel (rotor hub, sleeve, screws,...) are now made of titanium, or stainless steel to prevent corrosion.

- deposits resistant to fretting or wear have been applied on most critical interfaces.

- the number of bearings has been limited to a minimum by using super-critical tail rotor drive shafts or spherical elastomeric thrust bearings.

Finally the authorities approved for NH 90 (figure 8) and EC 155 (figure 9) the damage tolerance qualification program based on both conventional safe life (initiation of fatigue crack using as-manufactured component) and repetitive inspection intervals based on one of the 3 equal concepts (flaw tolerant inspection interval, slow crack propagation and multiple load paths).

4. TOGAA/RCWG

Meanwhile in the USA, a working group called TOGAA[6] was required by the US Senate to give some thoughts to the general tolerance to damage of fixed wing aircraft problem, with the possibility to propose some modifications to the FAA rules. Following discussions with fixed-wing aircraft manufacturers and FAA/JAA, this group proposed a new FAR 25-571 paragraph related to fatigue evaluation.

From 1993 onwards, the TOGAA discussed with the helicopter manufacturers and requested in 1997 that the RCWG[7] provide the TOGAA with a " White Paper " on fatigue and damage tolerance that would form the basis for a revision of Advisory Circular AC 29-571, and possibly FAR 29-571, if warranted.

After a very constructive co-operation with the US and European manufacturers, a harmonised methodology for fatigue and damage tolerance focusing on metals was found and a " White Paper " was prepared and submitted to the TOGAA for comments.

The following technical arguments were developed to cope with potential questions or concerns:

1. How undetectable or barely detectable flaws are covered by manufacturer methodology ?

Intrinsic material defects and manufacturing defects should be covered as follows:

- Intrinsic material defects (inclusions)

  Intrinsic material defects which are undetectable or barely detectable by reasonable industrial means could be substantiated by a combination of statistical approaches based on the probability of occurrence of the damage, severity of the damage demonstrated by tests, analysis or in-service experience and stress level applied on the part in service.

  EUROCOPTER experience of cracks initiated from intrinsic material defects (table 2) shows that type of material, inclusion class for steel and load safety factors are of prime importance.

- Manufacturing defects

  Potential manufacturing defects can occur upon every step of elaboration (semi-finished products, blanks, machining, heat treatment, anti-corrosion process, inspection, welding, etc.).

  As far as critical components are concerned, EUROCOPTER past experience of elaboration involved freezing the essential manufacturing parameters (i.e. cutting or grinding conditions, type of tools, cutting speed, part clamping, etc.), high quality controls and traceability.

  Moreover, process and inspection methods are continually improved. Examples of improvement are listed below :

  - elimination of sensitive processes such as black oxidising, chemical etching,
  - use of nitriding, shot-peening for compression near the surface of the component,
  - degassing treatment to avoid hydrogen embrittlement,
  - nital etching to detect grinding cracks,
  - microfocus to inspect welded joints

  In addition, destructive inspections are performed after full-scale fatigue tests on as-manufactured components to check for any defect originating the crack.

  This expensive procedure helps ensure that the serial parts shall be produced with the same process used for fatigue evaluation, including eventual pre-

existing cracks resulting from the process itself, if any.

A conventional safe life with conservative working curves accommodates the occasionally very small flaws.
Our experience regarding flaws of this size is that they had little or no effect and could be detected once they were big enough to have an effect.

In conclusion, EUROCOPTER considers that the use of material with better inclusion cleanliness related to in-flight stress level, the freezing and traceability of elaboration and inspections (continually improved by experience) of critical components, on the one hand, and the use of conservative working curves, on the other hand, should accommodate the occasionally very small flaws much better than in the past.

2. How flaw types and sizes are selected?

The flaw types and sizes imposed to each component are submitted with a rationale to the authorities for approval.

The types of flaw that are systematically considered should include scratch, corrosion, fretting, wear and loss of bolt torque.

These flaws should have the maximum size that can be reasonably expected during the service life.

A Consensus between the industry and the authorities should be easily found for selecting standard flaw type, size and geometry as done in the past for accelerated ageing and definition of impacts on composite components.

3. Can the successful experience from fixed-wing aircraft using crack propagation methodology be transposed to helicopter ?

Regarding the success of fixed-wing aircraft certification exclusively based on crack propagation, a synopsis of some differences between helicopter and fixed-wing aircraft is presented in table 3.

The main reason for this success is mainly load frequency and the detectable crack size large enough to be reliably detected.

This success is all the more emphasised as cracks in service occur on a very large fraction of aircraft components.

This poor experience may be due to poor choice of allowable (load safety factor equals to 1.15 for fixed wing compared to typical 1.8 to 3 for helicopter) and inadequate control of component quality related to fatigue.

In conclusion, the success of fixed-wing aircraft certification based on crack propagation can be explained but cannot be transposed to helicopter due to its specificity (high load frequency and detectable crack size).

4. Can the past manufacturer experience of crack propagation methodology be generalised to all the components of helicopter ?

Manufacturers already used crack growth analyses and tests to solve service cracking problems.

However inspection intervals, deduced from microscopic observations of the failure of the component, are often short. These constraints and overcosts are generally accepted by the operators because the action is temporary and the manufacturers are looking for a final solution at fleet level.

Moreover, the method of inspection is particularly suitable to the problem and the operators specially careful.

Finding a known crack in a precise location on a particular part is one thing, but finding an improbable small crack somewhere in every critical component of a helicopter is another.

In addition to the unavailability of a full and reliable methodology for crack growth applicable to helicopters, and to the difficulties inherent to obtaining a reasonable interval/method, the manufacturers feel uncomfortable with having the reliability (and liability) of a part depends on the success of individual helicopter operators finding small cracks.

In fact, the detection of cracks larger than the detectable size is not a certainty, as it is affected by many factors, namely the geometry of the component, material, skill of the operator, specificity of the task, accessibility, Non Destruction Examination process (i.e. X-ray, Eddy Current, Ultrasonics, dye penetrant, etc.) and environmental factors (corrosion, painting...).

Finally, manufacturers are very pessimistic regarding the issue of a lawsuit between an operator and a manufacturer, if detectable cracks were not detected and an accident resulted.

The " White Paper " was presented by the RCWG to the TOGAA during a meeting held in Monterey, California in March 1998,then, during a final meeting held in Lake Oswego, Oregon in January 1999 [ref. 4].

The TOGAA commented the harmonised manufacturer philosophy (ref. [3]) as follows:

- The use of " fatigue flaw tolerant inspection interval " as a repetitive inspection interval was discussed.

- The use of as-manufactured components for the establishment of a safe life or repetitive inspection for multiple load paths was commented.

- The exclusive use of crack propagation for single and multiple load paths was advocated.

- The recently revised AC & FAR 25-571 for large transport fixed wing aircraft was proposed to be the convenient starting point for the future revised rotorcraft AC & FAR 29-571.

5. CONCLUSION

A survey was performed by EUROCOPTER to identify types of damages encountered in service and root causes of accidents in flight.

For the last five years on a « world-wide/all mission » basis , EUROCOPTER average rate of accidents is 37 per million of flight hours.

Important Research & Development programs are in progress to reduce significantly accidents due to operational conditions and environment (77%) (all weather helicopters, improvement of Man Machine Interface, Fly-By-Wire, etc.) and due to incorrectly performed maintenance (17%) (Health and Usage Monitoring System, etc.).

EUROCOPTER estimates that less than 20 over 43 millions of flight hours could have been avoided by using the damage tolerance approach.

The RCWG prepared at the TOGAA request a « White Paper » on fatigue and damage tolerance based on both safe life (initiation of fatigue cracks using as-manufactured components) and repetitive inspection intervals demonstrated with one of the three equal concepts (flaw tolerant inspection interval, slow crack propagation and multiple load paths).

The advantage of this pragmatic approach, already approved by the authorities for EC 155 and NH 90, is to improve what exists today, i.e. the substantiation of inspection intervals with tests and/or an analysis formerly based on experience.

This philosophy was discussed with the TOGAA which advocated the exclusive use of crack propagation for single and multiple load paths.

To date (end of February 1999), final agreement of « White Paper » is pending.

ACKNOWLEDGEMENT

Special thanks to D. ADAMS (SIKORSKY), J.M. BESSON, J.J. CASSAGNE, J.L. DESBUIS, R. FRANCOIS , R. GARCIN, J.C. GASQUY, M. LAFARGUE, J.L. LEMAN, B. PLISSONNEAU, J.M POURADIER (EUROCOPTER).

GLOSSARY

(1) **Fatigue** : fatigue is the progressive process of crack initiation of a part due to the repeated application of varying amplitude loads, any one of which will not produce failure.

(2) **As-manufactured** : As-manufactured condition of a component which is produced by the nominal performance of manufacturing processes specified for that component

(3) **Accident** : accident with loss of life, hull damage, full or partial destruction of the rotorcraft

(4) **Major incident** : Every malfunction which could interrupt, cancel or delay significantly the mission or endanger the crew (loss, failure or damage of critical safety components, use of emergency procedures (engine failure, abnormal heating that might start a fire)).

(5) **Flaw** : A localised defect or anomaly related to manufacturing or service use.
In metals this includes corrosion, fretting, nicks, dents, scratches and gouges, ...
In assemblies, this includes loss of bolt torque, ...

(6) **TOGAA** : Technical Oversight Group for Ageing Aircraft

This group, composed of high level figures from the US aerospace community, was created in 1989 following ALOTA AIRLINES BOEING 737 accident as a result of ageing problems.
Beginning with fixed wing aircraft, the TOGAA expanded to include engines and rotorcraft. The TOGAA mission is to review every age related safety issues and make recommendations to implement corrective actions.
As part of this mission, the TOGAA has expressed concerns regarding the current FAR 29-571 (Rotorcraft fatigue evaluation) and the associated Advisory Circular.

(7) **RCWG** : Rotorcraft Community Working Group.

This group, composed of representatives from the major helicopter manufacturers in the United States and Europe, from the US (FAA) and European (JAA) airworthiness authorities and operators, was appointed to facilitate communication with the TOGAA.

REFERENCES

[1] A survey of serious aircraft accidents involving fatigue fracture
Aeronautical note NAE-AN-8-
NRC NO.21277

[2] BRITE/EURAM " DAMTOL "
Contract n° BREU-0123
DAMAGE TOLERANCE OF HELICOPTER METAL PARTS (1990-1993)
EUROCOPTER DEUTSCHLAND (prime contractor)
EUROCOPTER, AGUSTA, WESTLAND

[3] TOGAA comments on the " white paper " dated April 13, 1998

[4] " white paper " – final issue
prepared for the TOGAA in January 1999
available from Thierry Marquet
thierry.marquet@eurocopter.fr

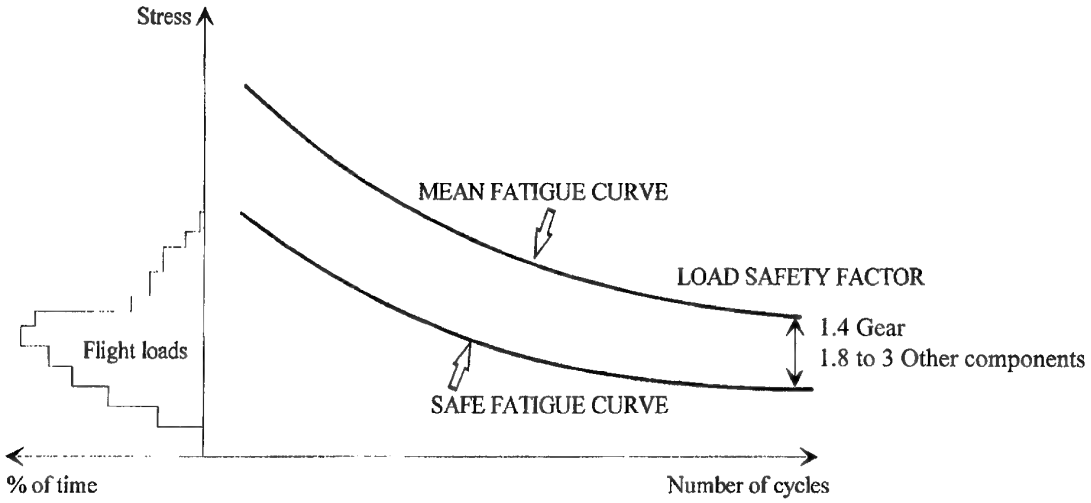

Figure 1 : Eurocopter Safe Life Substantiation Philosophy

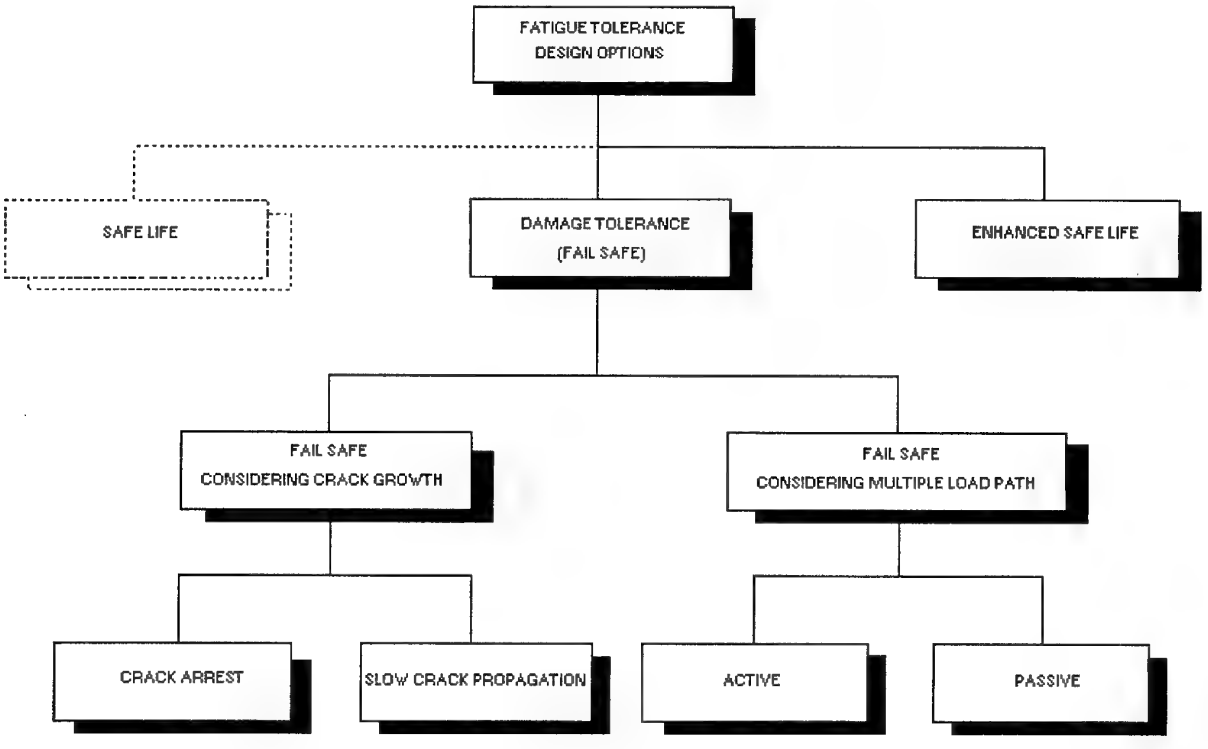

Figure 2 : Fatigue Tolerance Design Options

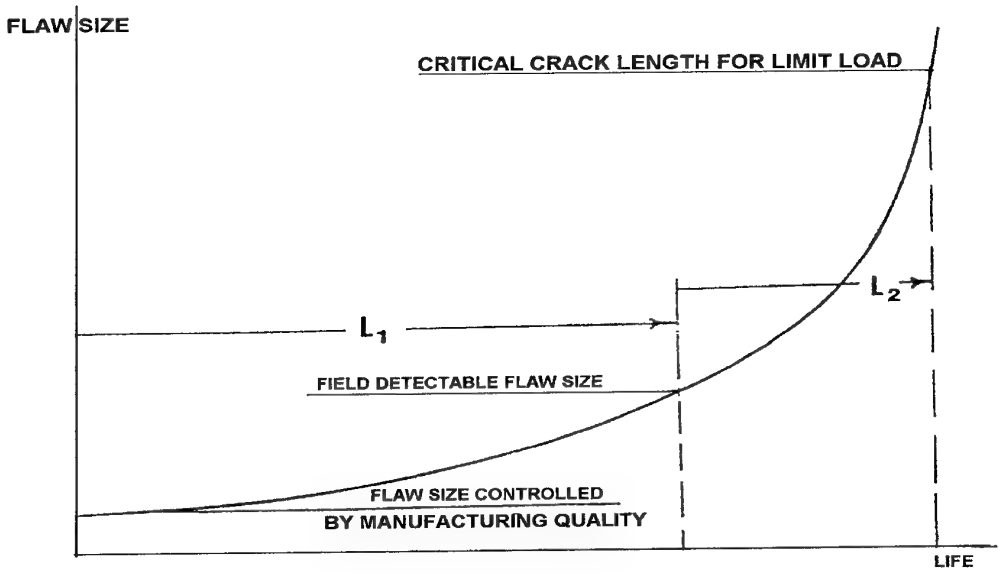

Figure 3 : Crack Growth for Single Element Structure

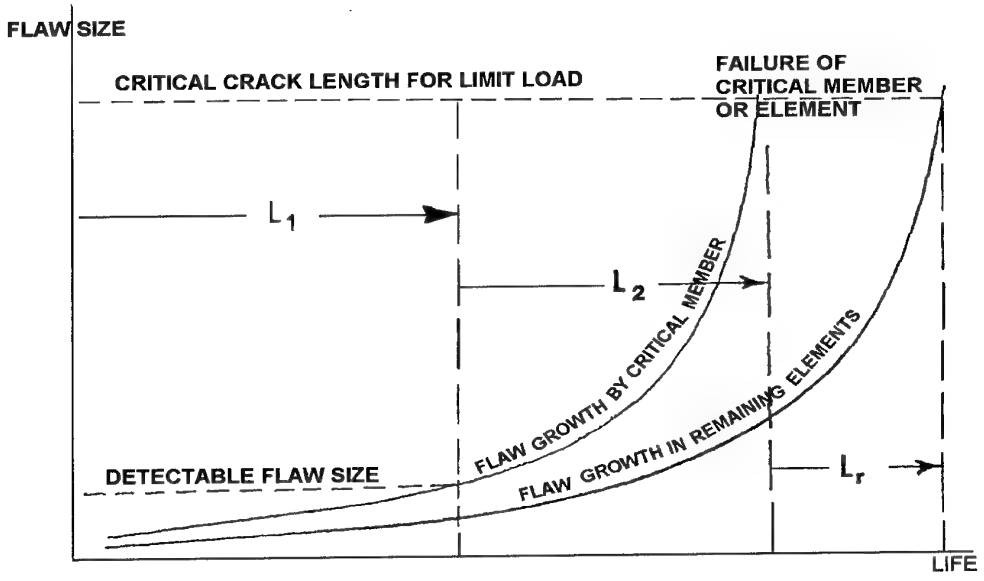

Figure 4 : Crack Growth for Remaining Elements of Multiple Element Structure

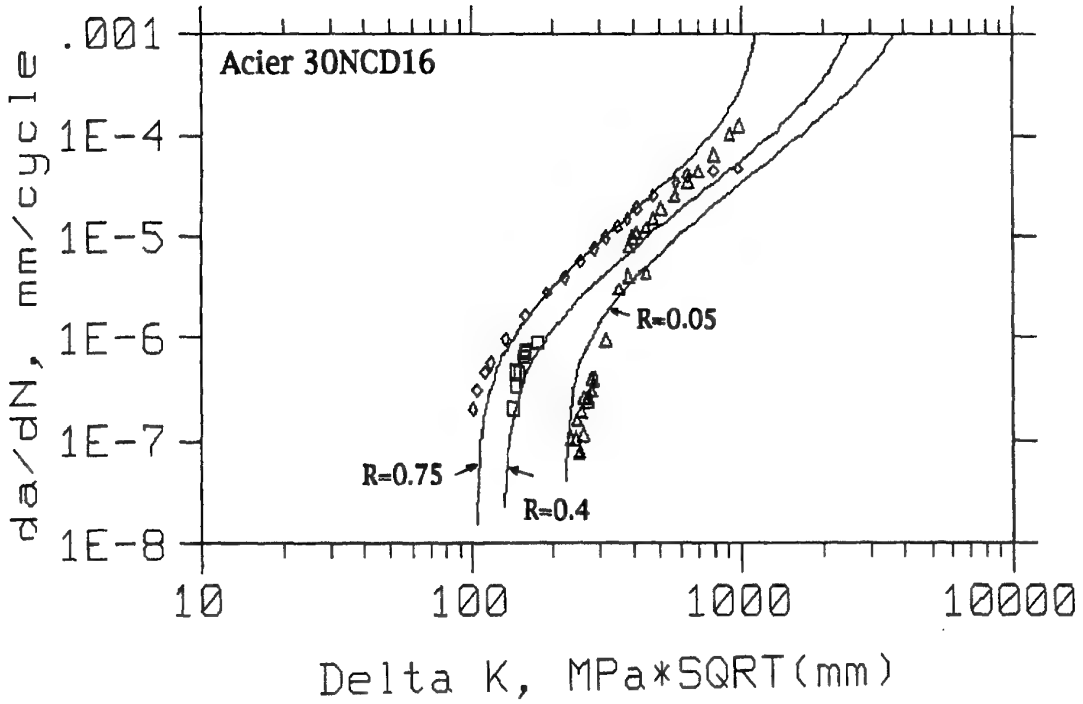

Figure 5 : Crack Growth Rate Versus Stress Intensity Factor Range for 30NCD16 (High Strength Steel)

FIELD DETECTABLE CRACK SIZE DETERMINED BY EC QUALITY DEPARTMENT, WITH A SAFETY LEVEL OF 95 % :

MAGNETIC PARTICLE	**3.6 MM**	**0.14 INCH**
DYE PENETRANT	**4 MM**	**0.16 INCH**
ULTRASONIC	**6 MM**	**0.24 INCH**
EDDY CURRENT	**6 MM**	**0.24 INCH**
VISUAL INSPECTION ON BRIGHT PAINTING	**15 MM**	**0.60 INCH**
VISUAL INSPECTION ON DARK PAINTING	**30 MM**	**1.20 INCH**

Table 1 : Reliable Field Detectable Crack Size

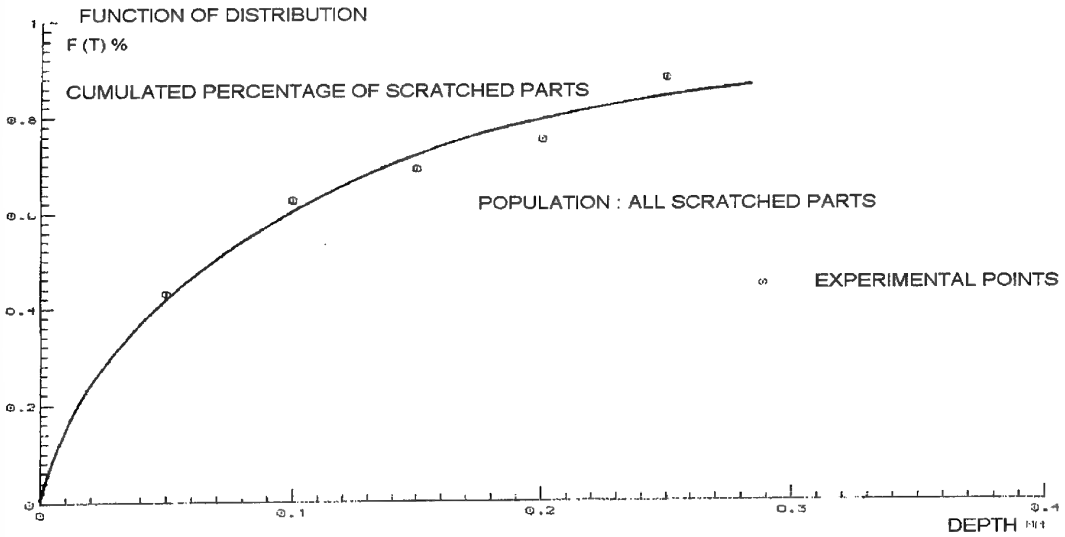

Figure 6 : Statistical Distribution of Scratch Depths Over Steel Parts

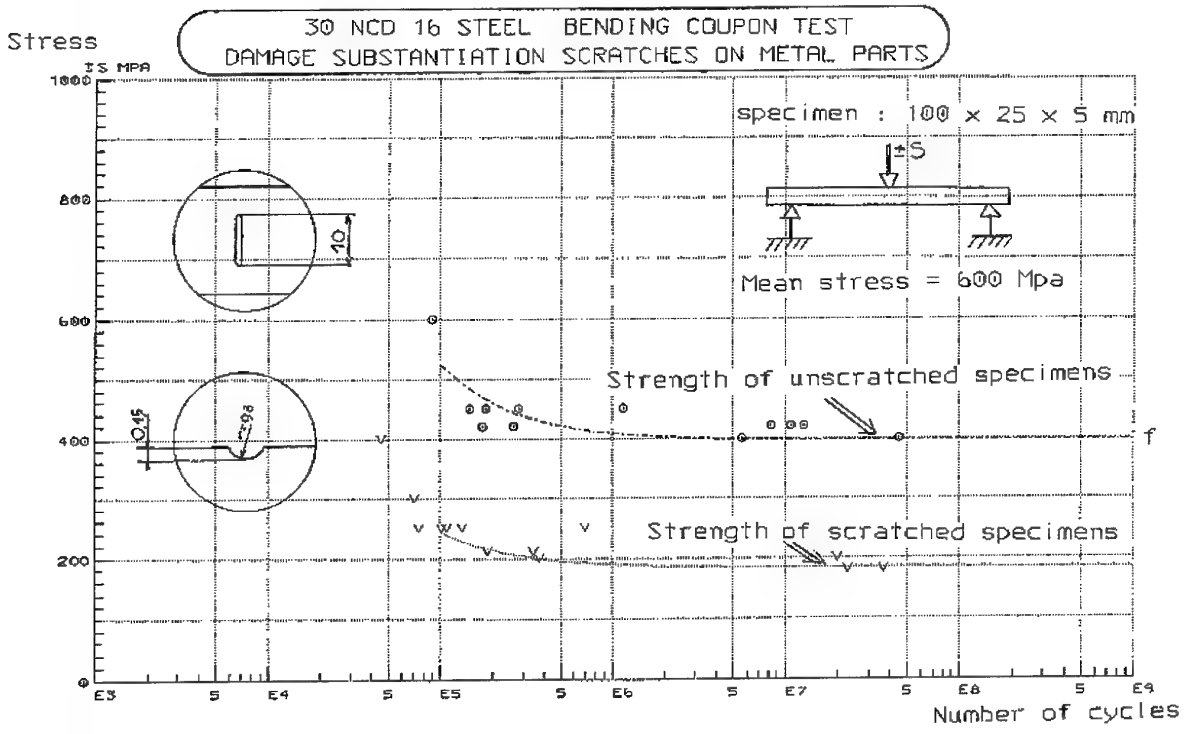

Figure 7 : Fatigue Curve on Flawed Specimens

Figure 8 : NH 90 (Medium Heavy Helicopter)
(EUROCOPTER, AGUSTA, FOKKER)

Figure 9:- EC 155 (Medium Helicopter)

(EUROCOPTER)

		STEEL		ALUMINIUM ALLOYS	TITANIUM
		Class 2	Class 3 or 4		
STRESS LEVEL	Gear teeth of pinions substantiated with load safety factor of 1.4	Several	None	/	/
	Other components substantiated with load safety factor of 1.8 to 3	None	None	None	None

Table 2 : Eurocopter in Service Experience of Material Defects
Representative of 43 Millions of Flight Hours (12/97)

Type	Load Cycle Rate	Fatigue Origins	Structure	Loading	Number of cracking structures	Typical Minimum Crack Length Considered
Large Transport Aircraft	1 to 200 cycles per hour	Frequently Multiple cracks on one component or one crack on multiple identical components	Multiple Identical components	Large Areas Identically Loaded	Large Fraction of the Fleet	15 mm (≈ 0.6 inch) to more than 100 mm (≈ 4 inches)
Helicopter	10,000 to 1,500,000 cycles per hour	Single crack on single component	single or a few components	Significant Load Variation Over Small Areas	Extremely Remote	4 mm (≈ 0.15 inch)

Table 3 : Fixed Wing / Helicopter Comparison

STRATEGIES FOR ENSURING ROTORCRAFT STRUCTURAL INTEGRITY

Robert G. Eastin
Federal Aviation Administration
Los Angeles Aircraft Certification Office
3960 Paramount Blvd.
Lakewood, CA 90623-4137
USA

OVERVIEW

The views presented in this paper are those of the author and should not be construed as representing official Federal Aviation Administration rules interpretation or policy.

Part 29.571 of reference [1] contains several strategies that, with certain qualification, applicants are allowed to adopt to ensure adequate structural integrity throughout the operational life of a rotorcraft. There has been a continuing debate concerning the merits of the various strategies. Much of the discussion has centered on the damage tolerance versus the flaw tolerance philosophies and the pros and cons of each. Additionally, the appropriate role of the traditional safe-life philosophy has been debated at length.

This paper begins by considering what the objective of Part 29.571 is and then examines each of the strategies and their strengths and weaknesses. Following this a recommended strategy is proposed which is believed to offer the most rational path at the present time to achieving the stated objective.

INTRODUCTION

The primary objective of Part 29.571 is to mitigate catastrophic failures due to fatigue by maintaining a minimum level of structural integrity throughout a structure's operating life. The level of structural integrity that a newly delivered rotorcraft must be shown to have is defined in Part 29.305 of reference [1]. In short the structure must be able to support limit loads without detrimental or permanent deformation and ultimate loads without failure where ultimate loads are 1.5 times limit. Compliance is generally shown by a combination of analysis and testing of structure that is as representative as possible of the production design and free from any known defects. This level of structural integrity will be referred to as the "baseline integrity" that each structure is required to begin life with. It is also one of the basic type design requirements. Additionally, Part 21.183 of reference [1] implies that for an aircraft to be considered airworthy it must always conform to type design.

Based on the above it is believed that maintenance of baseline integrity must always be considered when evaluating philosophies aimed at precluding catastrophic failures due to fatigue. Consistent with this has been the FAA's "flyable cracks" policy which has always included a requirement to show ultimate load capability, with a known crack, as a fundamental prerequisite before considering continued operation without repair. Also consistent with this line of thinking is the requirement to apply the basic type design requirements of Part 29.305 of reference [1] to any repairs or modifications to operational aircraft regardless of age. There are, in short, no provisions for relaxing structural integrity requirements as a structure ages.

THREATS TO STRUCTURAL INTEGRITY

For a new structure whose design is certified and which possesses an airworthiness certificate the probability of catastrophic failure due to fatigue should be zero. This follows from the fact that the probability of meeting the strength and deformation requirements of Part 29.305 of reference [1] should be 1.0 and that it has not experienced any cyclic loading. However, once it is put into service there are many mechanisms that can give rise to fatigue cracks and eventually lead to catastrophic failure. For the following discussion these mechanisms, or threats to structural integrity, are divided into two categories. The first category will contain those mechanisms which will lead to "normal" fatigue. The second category will contain those mechanisms which could lead to "anomalous" fatigue.

Normal Fatigue

Normal fatigue is the expected, inevitable (if we are operating above the endurance limit) fatigue that will occur if a structure was designed without error, manufactured as planned and operated and serviced as expected. Normal fatigue is predictable and the probability of it occurring is steadily increasing with time. Traditional fatigue testing is performed to characterize normal fatigue at the detail, component and aircraft level. If one defines a discrete endpoint to life, such as the appearance of a 1mm crack, the time to reach that endpoint typically follows a statistical distribution. Normal, Log Normal and Weibul distributions are typically used to characterize the behavior. Given a statistical distribution of life to a defined endpoint the degradation of failure strength capability with time can be conceptually depicted as shown in figure 1. This assumes the structure had some small margin of strength above the basic requirement. The cumulative probability of reaching a fatigue state such that the structure will fail at ultimate load is shown by a solid curve and the limit critical cumulative probability is given by the dashed curve. It follows that point A represents the average time to degrade to ultimate capability and point B is the average time to degrade to limit. This also illustrates that there is some period of time during which a structure can be considered to be virtually crack free and

Paper prepared for the RTO AVT Specialists' Meeting on "Application of Damage Tolerance Principles for Improved Airworthiness of Rotorcraft", held in Corfu, Greece, 21-22 April 1999, and published in RTO MP-24.

therefore expected to meet the baseline integrity requirements with high probably.

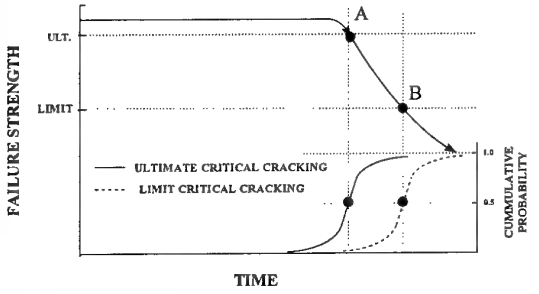

Figure 1 Degradation of strength with time due to normal fatigue (50% probability)

Anomalous Fatigue

Anomalous fatigue occurs due to unexpected and unpredictable events. Sources of anomalous fatigue include but are not limited to:

- Design oversights/errors
  - underestimating external loads
  - underestimating internal loads
  - underestimating peak stresses
- Manufacturing errors/mistakes
  - omission of critical processes
  - introduction of defects
- Operational and service anomalies
  - severe usage (relative to expected)
  - service induced defects

Considerable effort is made during design and manufacture to mitigate the risk of anomalous fatigue. Likewise, controls are typically put into place once an aircraft enters service to minimize the risk of operational and service related anomalies. However, in spite of our best intentions, anomalous fatigue does occur and can result in increased maintenance costs at best and loss of aircraft and life at worst.

The degradation of failure strength capability due to anomalous fatigue can be conceptually depicted as shown in figure 2. Curve 1 is the degradation of strength due to normal fatigue and is included for reference. Curves 2 - 6 depict degradation due to anomalous fatigue. Since the time of occurrence of the anomaly and its severity are unpredictable by definition any reliable statistical modeling is questionable. The flat dashed curve is meant to depict the cumulative probability of anomalous fatigue occurring. As was discussed above concerted efforts are typically made to drive this to as near zero as possible. While it may be argued that there is some increase in cumulative probability with time (e.g. due to increased exposure to anomalous sources) it might be considered to be relatively low and virtually constant.

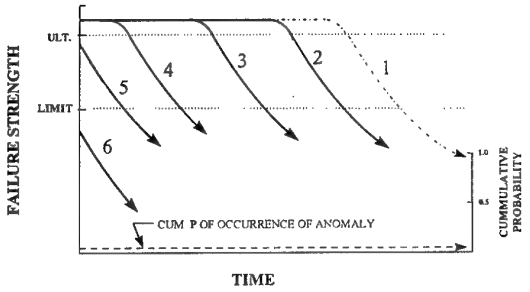

Figure 2 Degradation of strength with time due to anomalous fatigue

THREAT STRATEGIES

Strategies employed to deal with the threat of normal and anomalous fatigue are discussed below. It is argued that the traditional safe-life philosophy and damage tolerance philosophy can be used to effectively deal with normal and anomalous fatigue respectively. The flaw tolerance philosophy is also discussed since it is currently included as an acceptable strategy in Part 29.571 of reference [1]. However, it is suggested that the flaw tolerance philosophy is unduly pessimistic relative to the normal fatigue threat and inadequate with respect to the anomalous fatigue threat.

Safe-Life Philosophy

Before going further with this discussion it is considered necessary to clarify the author's definition of "safe-life" within the context of this paper. Two existing definitions are referenced for purposes of discussion. The first definition is given in reference [2] and is as follows:

> "Safe-Life means that the structure has been evaluated to be able to withstand the repeated loads of variable magnitude expected during service without detectable cracks."

The second definition is given in reference [3] and is as follows:

> "Safe-Life of a structure is that number of events such as flights, landings, or flight hours, during which there is a low probability that the strength will degrade below its ultimate value due to fatigue cracking."

The first definition correlates best with the words that currently exist in the safe-life rules of reference [1]. Here the focus is on the absence of detectable cracks. It is suggested that this focus can result in some ambiguity since what is detectable is a function of the inspection method. With inspection methods improving with time this definition is somewhat of a moving target and therefore less than adequate.

The second definition focuses on the baseline integrity discussed in the beginning of the paper. This focus is unambiguous and follows directly from the requirements of reference [1] for type design and airworthiness certification. Because of this it is suggested that it is the most appropriate and will be the definition used in the context of this discussion.

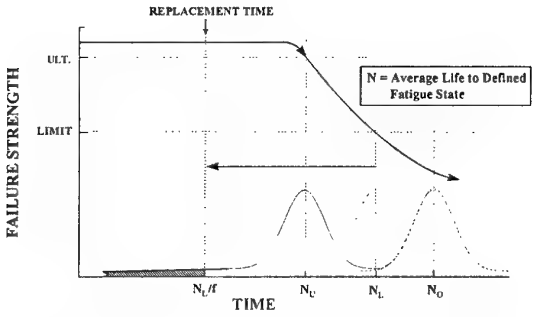

Figure 3 Application of traditional safe-life philosophy

Based on the second definition of safe-life discussed above and the nature of normal fatigue as depicted in figure 1 it is concluded that the traditional safe-life philosophy is adequate for dealing with the normal fatigue threat. This is conceptually depicted in figure 3. An average fatigue life is established based on analysis and test for a nominal part free from known defects. A factor is then applied to this life to establish a replacement time when the part is to be removed from service. Figure 3 illustrates the case of the replacement time being based on some fraction of the average time to develop cracking which would cause the structure to fail at limit load. Distributions of life to ultimate critical and sub limit critical are also depicted. It is believed that, in the past, average lives associated with fatigue states, that did not degrade the failure strength below ultimate, have often been used. In this case a replacement time based on N_U/f would certainly result in "low probability that the strength will degrade below its design ultimate value due to fatigue cracking." For the scenarios where the average fatigue life corresponds to fatigue states where the failure strength is below ultimate the probability of having a fielded part's failure strength degrade below ultimate may be higher but still may be acceptably low depending on the value of f used. This is also illustrated in figure 3 for the case where N_L is used. The retirement life is given by N_L/f and the cumulative probability of failing below ultimate is small and represented by the fractional shaded area under the life to ultimate critical distribution curve.

A frequent deficiency of the safe-life philosophy as currently applied is the failure to quantify the fatigue state being addressed and its impact on failure strength. It is suggested that this should be corrected in the future so that there is no ambiguity relative to meeting the stated objective. Beyond this it may be desirable to quantify the cumulative probability of the strength degrading below ultimate at the replacement time.

Damage Tolerance Philosophy

Reference [4] discusses the adoption of a damage tolerance philosophy by the USAF. As discussed in the reference the primary motivation was the recognition that anomalous fatigue was a significant threat that had to be dealt with and that it wasn't being adequately taken care of by the safe-life philosophy which had been previously employed. The USAF requirements, which derive from their philosophy, were originally specified in reference [5]. It has been noted on numerous occasions, (e.g. see reference [6]), that anomalous fatigue due to manufacturing and in-service damage has been successfully controlled in the USAF fleet through the adoption of the damage tolerance approach in 1975. The common ground between the USAF damage tolerance philosophy and the one promoted herein is the requirement to assume a fatigue crack(s), perform a damage tolerance evaluation using fracture mechanics principles and establish inspection requirements consistent with the damage tolerance characteristics of the structure. Additionally, the USAF requirements specify crack sizes to be assumed and set minimum acceptable standards for crack growth life and inspection intervals. The key difference between the USAF philosophy and the one in reference [1] is that the USAF requirements result not only in a damage tolerance based inspection program but also a minimum acceptable level of tolerance to damage. In comparison, a design which is not inherently damage tolerant can still be found in compliance with reference [1] provided the inspection requirements match its damage tolerance characteristics (however good or marginal the characteristics might be).

The damage tolerance philosophy as advocated herein is based on (1) the assumption of a crack(s), (2) characterization of the growth and impact on strength of the crack(s), (3) assurance of a minimum strength equal to the highest loading that could be expected within the design operating envelop (e.g. limit load), (4) establishment of inspection requirements consistent with the damage tolerance characteristics of the structure and (5) implementation of inspections. It should be noted here that the setting of inspection requirements based on the assumption of anomalous defects, and insuring no failure at "limit" load, is only applicable to the period of time during which normal fatigue cracking is not expected to occur (i.e. low cumulative probability). Beyond this point additional action must be taken to deal with the constantly increasing probability of normal fatigue. As discussed above, replacement based on the traditional safe-life philosophy would be one way to deal with this.

It is believed that while no philosophy can be expected to precluded catastrophic failures due to fatigue with 100% certainty the damage tolerance philosophy provides the best protection against anomalous fatigue due to the kind of mechanisms previously noted. One of its strongest assets is that it deals directly with cracks which are, in the end, what cause the failure. The damage tolerance philosophy forces one to consider how a structure behaves with cracks and this insight can be used to modify the design such that there is at

least a minimum level of tolerance to cracks. It also generates inspections that are geared to detect what actually causes a structure to fail (i.e. cracks). A damage tolerance philosophy can even be of benefit for anomalous fatigue due to design errors and severe usage that results in unexpected cracking. Even if the inspection intervals and inspections methods are not optimum for the subject cracking there will be some probability of precluding a failure because one is inspecting in the right location for the right thing.

Another ancillary benefit of a damage tolerance based inspection program is the additional protection from the normal fatigue threat that it provides. Since inspections are typically defined to detect cracks in fatigue critical areas premature "normal" cracking will have a measurable probability of being detected if it should occur before the replacement time is reached. In this case the replacement time could be reassessed to mitigate any potential risk to the fleet. Consistent with this it might be feasible to depart from tradition and be less conservative with the factor, f, used to determine the replacement time, provided that a damage tolerance inspection program is in place. This notion is discussed in more detail below.

Flaw Tolerance Philosophy

The flaw tolerance philosophy is included as an alternative to the damage tolerance philosophy in showing compliance with Part 29.571 of reference [1]. This philosophy focuses on crack initiation from defects that might be envisioned to occur during manufacture or in the service life of the structure. Traditional safe-life methodology is employed using fatigue data for intentionally flawed test specimens. Replacement times are derived from test data for "barely detectable" flawed specimens and in-service inspection requirements are derived from test data for "clearly detectable" flawed specimens.

In general, the flaws to be considered are not cracks but instead include nicks, dents, scratches, fretting or corrosion that may occur during manufacture or during the service life of the structure. Application of the flaw tolerance philosophy requires the determination of the maximum probable undetectable and clearly detectable flaw sizes and critical locations based on a review of historical data and manufacturing processes. It is implicitly assumed that the impact on baseline integrity of these threats is conceptually the same as depicted for normal fatigue as shown in figure 1. That is, there is some quantifiable crack initiation phase followed by a crack growth phase and that the time to initiate a crack follows a statistical distribution which can be established based on fatigue testing of flawed specimens and/or flawed production components. The degradation of strength with time trend is conceptually illustrated in figure 4 for a production part without flaws, with barely detectable flaws and with clearly detectable flaws.

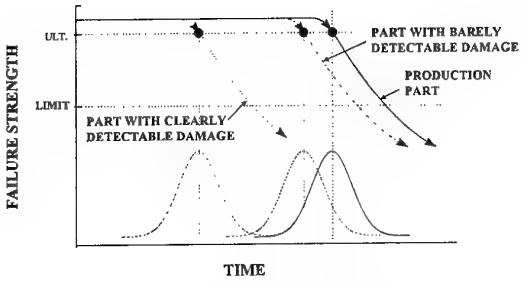

Figure 4 Impact of flaw tolerant flaws (50% probability)

It is the author's opinion that while the flaw tolerance philosophy could be considered an acceptable, but pessimistic, alternative to the traditional safe-life philosophy it should not be considered an acceptable alternative to the damage tolerance philosophy.

The flaw tolerance philosophy sets replacement times based on flawed part crack initiation life. The flaws considered are those that could go undetected during the manufacturing process and reduce the life below that of a "properly" manufactured part. This approach could easily yield replacement times that are less that those that would be set based on the traditional safe-life philosophy. This would appear to unduly penalize the majority of the population, make part replacement more of an economic burden than it is now and not significantly help mitigate the anomalous fatigue threat.

The flaw tolerance approach establishes inspection requirements based on precluding crack initiation from an in-service detectable flaw. The resulting inspections are aimed at detecting dings, bangs, scratches, corrosion, etc. and the intervals are based on the time to initiate cracks from these kinds of defects. While in-service inspections should be performed to look for these kinds of flaws this in itself falls short of what is required. It is difficult to imagine that potential flaw sources can be anticipated, flaw types characterized and severity quantified to a degree that is sufficient to bound all significant anomalous threats of this nature. It is also believed that the adequacy of the bounding will present a major dilemma for the regulators. The flaw tolerance philosophy does not produce inspections that have crack detection as their primary objective. This is a major deficiency since cracking is what ultimately results in failure The bottom line is that an inspector who is looking for cracks has a chance of finding them if they are there and will also detect and report any dents, scratches, corrosion, etc., if present. The converse is not necessarily true. Additionally, there are anomalous threats such as design oversights/errors and severe usage that can result in premature cracking without any tell tale "clearly detectable" flaws being present. The flaw tolerance philosophy does little to help mitigate failures due to these threats.

A Proposed Strategy

It is suggested that an appropriate and effective strategy for meeting the objective of Part 29.571 of reference [1] would be to use a traditional safe-life philosophy to deal with the threat of normal fatigue and a damage tolerance philosophy to deal with the threat of anomalous fatigue. This strategy would have two primary elements which are summarized as follows:

1. Establish replacement times for all principle structural elements based on the traditional safe-life approach and remove them from service before there is any significant probability of developing cracks due to normal fatigue. Inherent with this would be a high probability that the baseline integrity would be maintained up to the time of replacement.

2. Establish in-service inspection requirements for all principle structural elements based on their damage tolerance characteristics determined from a damage tolerance evaluation (supported by analysis and test) unless it could be shown that this was impractical. If inspections tied rigidly to the damage tolerance characteristics of the structure were shown to be impractical detail inspections of critical areas for cracking would still be required using mutually agreed to NDI methods and intervals based on good engineering judgment. Additionally, extra precautions (e.g. more rigorous detail analysis, testing, loads monitoring, etc.) would be required for these parts to help mitigate potential sources of anomalies.

The proposed strategy is based on the concept of not allowing parts to operate beyond a point when there is a significant probability that the baseline integrity is compromised due to normal fatigue and rigorously inspecting the parts for potential cracking caused by anomalous fatigue up to that point. A rigorous inspection program must be derived from the results of a damage tolerance evaluation. Ideally the inspection location, method, threshold and interval would all correlate with the evaluation results. In some cases this might prove to be impractical however inspections for cracks in the appropriate areas should be imposed as a minimum. When a completely rigorous inspection program is practical, implementing it will also provide an additional safeguard against the normal fatigue threat. Because of this, traditional "safety factors" on life and/or fatigue strength might be reduced without reducing the level of safety achieved with traditional factors but without damage tolerance based inspections.

SUMMARY

Part 29.571 of reference [1] contains requirements aimed at mitigating the risk of catastrophic failure due to fatigue. Structural evaluations must be performed and "inspections, replacement times, combinations thereof, or other procedures" must be defined to achieve the desired result. Three different philosophies are recognized in the rule. Either the flaw tolerant or damage tolerance philosophies must be used unless the applicant establishes that these philosophies cannot be practically applied. In that case it is acceptable to use the safe-life philosophy.

For new structure we can divide all potential fatigue cracking into two categories. One is "normal" fatigue which is unavoidable, inevitable and predictable. The second is "anomalous" fatigue which we try to avoid and whose potential occurrence is unpredictable. Given the different nature of each it is natural that two different strategies must be used to deal with each.

Part 29.305 of reference [1] contains basic structural integrity requirements for strength and deformation. These are basic type design requirements and per Part 21.183 of reference [1] they must be met if an aircraft is to be considered airworthy. These fundamental type design requirements must always be kept in mind when considering appropriate strategies to be used against the threat to structural integrity that fatigue presents.

The flaw tolerance philosophy should be dismissed as an inappropriate strategy for dealing with both normal and anomalous fatigue. It unduly penalizes the majority of a part population relative to the normal fatigue threat and does little to help mitigate the risks associated with the anomalous fatigue threat. The fact that it does not result in inspections that are devised to detect cracks is also a major deficiency.

An effective strategy for meeting the objective of part 29.571 of reference [1] and maintaining airworthiness per part 21.183 of reference [1] is to use both the safe-life and damage tolerance philosophies. Replacement times are specified based on the safe-life philosophy and parts are removed from service before the probability of normal fatigue and not meeting type design requirements becomes significant. Inspection programs are established, for the period of time during which normal fatigue is not expected to occur, based on the damage tolerance characteristics of the part. Implementation of these inspections would adequately mitigate risks associated with anomalous fatigue. A caveat to this strategy might be a reduction in the magnitude of traditional "safety-factors" used to define replacement times. This could result in significant economic benefits without reducing safety levels below those achieved with higher factors but without damage tolerance based inspections.

REFERENCES

1. Code of Federal Regulations, Title 14, Chapter 1 - Federal Aviation Administration Department of Transportation.

2. FAA Advisory Circular No. 25.571-1B.

3. FAA Advisory Circular No. 25.571-1C.

4. Wood, H.A., "Application of Fracture Mechanics to Aircraft Structural Safety", Engineering Fracture Mechanics, 1975, Vol. 7, pp.557-564, Pergamon Press.

5. MIL-A-83444 (USAF), "Airplane Damage Tolerance Requirements".

6. Lincoln, J.W., "Life Management Approach for USAF Aircraft", AGARD Conference Proceedings 506.

TREATMENT OF HIGH-CYCLE VIBRATORY STRESS IN ROTORCRAFT DAMAGE TOLERANCE DESIGN

John W. Lincoln and Hsing C. Yeh
Technical Advisor
Aeronautical Systems Center
Engineering Directorate, USAF
2530 Loop Road West
Wright-Patterson Air Force Base, OH 4533-7101
United States

SUMMARY

Fixed wing aircraft manufacturers have adopted the damage tolerance design philosophy with great success for both military and commercial aircraft. However, rotorcraft manufacturers currently still primarily use the classical safe life approach or a modification thereof. One reason for this is that, at this time, no clearly defined damage tolerance design criteria exist for rotorcraft structures because of the analysis and test problems associated with the high cycle loading environment.

This paper describes a study performed by the United States Air Force (USAF) to assess the impact of the damage tolerance approach on the design of a rotorcraft component affected by high-cycle vibratory stresses. The assessment consisted of developing the stress spectrum for a critical rotor system location and performing fracture analyses to determine the potential for establishing inspection intervals based on the damage tolerance approach. They performed sensitivity studies to determine the maximum range truncation that would yield results with acceptable accuracy. They considered the influence of the small-crack effect in all fracture mechanics calculations. The resulting crack growth functions provided the basis for establishing whether an inspection program was viable for the component. They examined the effect of stress reduction measures such as shot peening to enhance the damage tolerance capability of highly stressed components. Therefore, the paper identifies the main issues related to the use of damage tolerance for rotorcraft, and additionally makes recommendations for rotorcraft design criteria.

INTRODUCTION

The USAF made the decision to adopt damage tolerance in the early seventies. They did this when it became apparent that the safe life approach adopted through the Aircraft Structural Integrity Program (ASIP) in 1958 in response to fatigue failures in operational aircraft (1) did not achieve the desired results. These service failures resulted in costly redesign and modification programs on many aircraft. The USAF, in part, attributes the failure of the safe life approach to the fact that it did not properly account for the possibility of a large remotely occurring or "rogue" defect in the structure. The manufacturing process or in-service maintenance of the aircraft may induce this type of defect. Now, all of the major weapons in the USAF have had their Force Structural Maintenance Plans (i.e. the how, when and where to inspect or modify an aircraft to maintain safe and economical operations) updated by the damage tolerance approach.

The USAF believed that the damage tolerance approach they developed for fixed wing aircraft (2) could apply to engine structures. They have done this with considerable success. Initially they applied the damage tolerance approach to the TF-41. Subsequently, in 1978, they applied it to the F-100 engine used in the F-15 and F-16. This assessment proved to the USAF that if they had incorporated damage tolerance methods in the initial design of this engine, the damage tolerance requirements would have precluded the use of the low toughness materials. In addition, the manufacturer would have been able to better balance the design for durability. Retirement for cause (i.e. the damage tolerance approach) has demonstrated a substantial reduction in the maintenance burden and improved safety of the parts that the USAF previously managed under the safe life concept. Later, damage tolerance applications to other engines also demonstrated that this approach was technically sound.

Based on success with fixed wing aircraft and engines the United States Air Force (USAF) in 1983 sponsored a damage tolerance assessment (DTA) of the HH-53 helicopter (3). Sikorsky performed this pioneering assessment based on the approach that had proved to be successful in the earlier DTAs. The HH-53 DTA posed a considerable challenge to Sikorsky. Their approach to the design of rotor components had been a modification of the safe life approach used by the USAF. They used fatigue methodology based on Miner's rule of linear cumulative damage. They tested component parts with a constant amplitude spectrum to determine the fatigue strength. They assumed a normal distribution for the fatigue strength and used a "working" S-N function that is approximately three standard deviations from the mean. This process is similar to that used by the engine manufacturers to determine low cycle fatigue (LCF) lives for their production parts. This process did not require Sikorsky to perform a detailed stress analysis of the components tested. It did incorporate, however, conservatively derived data from flight tests to determine the LCF lives. The damage tolerance approach, however, does require that the analyst accurately know the stress spectrum. The stress analysis and the determination of the usage were major

Paper presented at the RTO AVT Specialists' Meeting on "Application of Damage Tolerance Principles for Improved Airworthiness of Rotorcraft", held in Corfu, Greece, 21-22 April 1999, and published in RTO MP-24.

efforts in the DTA. Sikorsky, however, could not remove all of the conservatism in the applied loads for the DTA because of time and budget constraints.

In recent years, researchers have found a connection between the results of a classical safe life testing and fracture mechanics. R. Everett, in his comparison of fatigue life prediction methodologies for rotorcraft (4), found that constant amplitude testing of polished coupons and the crack growth method based on "small-crack" crack growth data and a crack-closure model yielded comparative results. He performed this study on AISI 4340 steel. This is a material of choice for many rotor components. Based on earlier work he used an initial flaw size of 15 microns. This size defect is approximately an order of magnitude smaller than could be found by currently available inspection methods.

At the time of the initiation of the HH-53 DTA the USAF had accumulated approximately one million man-hours of experience with fixed wing aircraft DTAs and approximately 200,000 man-hours of experience with the engine assessments. Therefore, it was logical to use this background as a pattern for the helicopter effort. The process (5) included the following five tasks:

(1) Identification of critical areas

(2) Development of the stress spectrum

(3) Establishment of the initial flaw criterion

(4) Establishment of the operational limits

(5) Development of the Force Structural Maintenance Plan

The critical areas are those where an inspection or modification is required during the life of the structure. As was found for fixed wing aircraft, the analyst augments the identification of critical areas from knowledge of the service problems, laboratory fatigue testing, stress analyses, and surveys for strain. There are, however, some major differences between the fixed and rotary wing aircraft. The laboratory fatigue testing is concentrated on the rotor systems and in many cases, there is no full-scale fatigue test on the helicopter airframe. In addition, the manufacturer performs most of the laboratory testing of rotors on a component basis to support the safe life analysis and consequently there is a question whether they have identified all areas of structural concern. Lack of comprehensive full-scale fatigue testing in combination with a lack of a detailed stress analysis and strain survey data compounds this problem. These problems force the analyst to initially identify the critical areas in somewhat conservative fashion and then reduce the number for a detailed examination by a preliminary screening process. Typically, this initial identification would include, as a minimum, all of the components in the main and auxiliary rotor systems and all of the airframe components influenced by the rotor system dynamics. This preliminary screening activity usually involves finite element analyses of some components followed by a simplified evaluation of the stress spectra and a fracture analysis.

The stress spectrum development was typically the most difficult to perform of all the tasks for the fixed wing DTAs. Much of the difficulty arises because of the need for accuracy. This need for accuracy is also vital for the helicopter. As stated in (2) there are three phases in the development of the stress spectrum for a fixed wing aircraft. For a helicopter, the procedure is similar for the airframe and rotor systems. For both the airframe and rotor systems, the desirable first phase is to derive operational loads and stress data from service usage. However, helicopter usage tracking data is essentially nonexistent. Therefore, to develop an estimate of the usage the analyst will need to conduct interviews with pilots. This, in combination with knowledge of the basic mission of the vehicle and a general knowledge of how helicopters are used will provide a usable basis until the operators initiate an individual aircraft-tracking program. The second phase in the development of the stress spectrum for the airframe is to determine the external loads on the structure for a given maneuver or gust condition. This process is generally tractable with analytical procedures for the external loads on the airframe. The exception is the loads derived from the dynamics of the rotor systems. For rotor locations and airframe locations that have dynamic loads from the rotor system imposed on them, the manufacturer generally obtains the external loads by direct strain measurements from these locations during flight test. The third phase of the stress spectra development is to determine the detail stresses in the critical areas resulting from the external loads. The USAF found in the entire fixed wing DTAs that knowledge of the detail stresses was lacking. This was due, at least in part, to lack of computer capability at the time of the acquisition process and use of the safe life method for qualification. Consequently, the DTA needed to have a significant number of man-hours expended to correct this deficiency. This situation also exists for helicopters.

The desired product of the stress spectra development is a flight-by-flight spectrum of stresses for each of the critical areas. In the DTAs of fixed wing aircraft, the USAF found that a change in the ordering of the flights in the spectrum does not have a significant effect if they used a random ordering. They found this true also for the helicopter stress spectra. In addition to the development of the baseline spectra, which they intended to represent average usage, they found it necessary to generate variations of these spectra that represent the expected range of usage of the vehicle. The successful completion of the fracture analyses and

tests with these spectra provides confidence that there is a sound basis for the tracking program.

The third task of the DTA is for the analyst to determine the initial flaw size for the subsequent fracture analysis. The USAF experience, derived from the fixed wing DTAs, has shown that for fastener holes in airframe structure an initial flaw of 1.27 mm is adequate to provide safety of flight. They derived this initial flaw size from the observation that they have never experienced an aircraft failure in the flight time required for this size flaw to grow to critical. They have also found that for airframe structure that a semicircular surface flaw with a radius of 3.175 mm is similarly adequate. Although the initial flaw basis for helicopter airframe structure is limited, the flaw sizes above should be adequate since the manufacturing processes are similar to fixed wing aircraft. The USAF does not believe, however, that these flaw sizes are the minimum for the rotor structure components since the quality control of these components is better than for airframe components. The USAF believes that the rotor DTA should use the engine DTA approach for establishing the initial flaw size. For DTAs performed on engines, the USAF approach is quite different than for those performed on airframe structure. For engines, they perform a deterministic DTA for surface flaws with initial flaw sizes based on inspection capability. For imbedded defects, the approach is probabilistic based on perceived distribution of initial internal defects. Experience with engine components has shown that smaller initial flaw sizes than used for airframe are adequate to provide safety. For engines, the USAF established the surface flaw size for initial design (5) as 0.762 mm, and they established the corner flaw the initial flaw size as 0.381 mm. The USAF recommends that manufacturers use these flaw sizes as the initial defects of helicopter rotor components. As was found for the engine assessments, the inspection capability for helicopter rotor components is extremely important. The USAF found that inspection capability was the essential ingredient that made retirement for cause for engines a viable concept. The Engine Structural Integrity Program (ENSIP) Military Standard (5) released in 1984 states that the detectable flaw size using eddy current or ultrasonic surface wave techniques is 0.381 mm (uncovered length). This capability is adequate for many of the helicopter rotor components. It is a practical limit since smaller cracks introduce problems in testing for crack growth and the "short crack" phenomenon emerges to complicate the fracture process. Further, and possibly a more important consideration, is that when a structure is sensitive to flaws smaller than this, the manufacturer should modify the structure rather than inspect it to maintain its safety for service operations.

The analyst derives the operational limits for the helicopter from the fracture analyses and tests based on the stress spectrum for each critical area in combination with the initial flaw associated with that area. As reported in (2), the predominant problem with fixed wing aircraft is fastener holes. This is, in general, not the case with the rotor system critical areas. In many cases, such as threaded parts and lugs, the stress intensity solution is more difficult to determine. However, in rotor systems it is rare to find that the critical crack size is large enough to change the stress distribution from that found when the structure is in its pristine condition. As with airframe structures, testing is essential for verification of crack growth for rotor system structure. These tests are difficult because of the large number of cycles in the stress spectrum for some parts.

The Force Structural Maintenance Plan (FSMP), as indicated above, is the plan that describes inspection and modification program for the helicopter during its anticipated operational life. The analyst determines the inspection intervals from the operational or safety limits (i.e. the crack growth life from an initial or detectable flaw to critical crack size). The USAF recommends dividing the safety limit by a factor of two to determine the inspection interval. This procedure is identical to that used for aircraft with fixed wings.

The results of the HH-53 DTA showed that many of the rotor component areas are damage tolerant. That is, an inspection program could be developed that would permit economically viable inspection periods. There are other areas, however, that are subjected to such a severe environment that the time to critical size was unacceptably short even from an initial flaw of 0.127 mm. These locations would be candidates for modification. These large differences would probably not have been found if the manufacturer had applied the damage tolerance approach during the initial design. It is noted that the component replacement time for the spindle threads in the tail rotor, which has a 10 hour crack propagation time from a 0.127 mm deep flaw, has a recommended component replacement time of 11,000 hours. There are cases where the recommended component replacement time is less than the crack propagation time from a flaw of 0.127 mm. Thus, the DTA revealed a lack of consistency between the recommended component replacement times and the crack propagation times. This paper discusses some possible reasons for these problems and suggests some strategies for solution.

DISCUSSION

There has been considerable progress made since the HH-53 DTA in the development of technologies that would enhance helicopter structural integrity. One of these is a better understanding of the "small-crack' effect. This has increased the confidence in calculations that involve crack growth in the ΔK threshold region. It has permitted the analyst to perform fracture mechanics calculations that correlate with the growth of intrinsic defects in materials such as aluminum and titanium. Figure 1 shows derived

intrinsic flaw distribution for Ti-6Al-4V developed from constant amplitude testing (6) during the F-15 development program. Another development is computer controlled shot peening. The USAF believes this process significantly enhances the reliability of shot peened parts that the manufacturer uses in safety of flight critical locations. This development is important since the integrity of many helicopter parts relies on shot peening. Another development is the technology for usage tracking of helicopter components. It has the potential for reducing the economic burden of inspection or part replacement without compromising flight safety.

There have been important developments in the certification requirements for helicopters. The Federal Aviation Administration (FAA) has made important changes through Amendment 28 to FAR Part 29. The FAA asserts in this document that the manufacturer will design a new helicopter using damage tolerance or flaw tolerance methods. They will not accept the classical safe life approach except for areas where damage tolerance or flaw tolerance is not feasible. The damage tolerance approach in these requirements is essentially the same as outlined above for the HH-53. The flaw tolerance approach is new. This method is a modification of the classical safe life method. The modification is that the parts prior to testing are subjected to an array of damages including nicks, scratches, gouges, and corrosion damage that would be representative of in-service operation experience. If the analyst maintains all of the other elements of the safe life method then this approach appears to add more conservatism to the determination of the component lives. One difficulty with this approach is convincing the authorities that the damage inflicted is representative of actual in-service damage. Another problem is that it has the potential for the same errors that are inherent with the classical safe life method. In addition, the added conservatism adds to the already significant economic burden of the usual safe life approach. The Technical Oversight Group for Aging Aircraft (TOGAA), an advisory group to the FAA, has campaigned vigorously in opposition to the flaw tolerance approach. The helicopter industry in the United States, however, does not speak with a single voice on the certification issue. Some believe that the FAA should retain flaw tolerance as acceptable approach until the damage tolerance approach has matured further. Others believe that flaw tolerance should be the only acceptable approach. These certification issues will likely not be resolved soon.

The U.S. Army and U.S. Navy develop all of the military helicopters in the United States. At this time, the certification base used by both of these services for helicopters is the classical safe life method.

EXAMPLE PROBLEM

The USAF developed a sample problem to reveal many of the difficulties associated with analyses involving high cycle fatigue. The selected sample problem is typical of helicopter component. The more obvious difficulties with an analysis such as this are as follows:

The large number of cycles increases the computer run time significantly.

Many cycles occur at relatively high mean stress.

Lack of data around the crack growth threshold.

Another problem is the modification of the stress intensity solution to account for the effect of life enhancement measures such as shot peening. For this paper, the USAF used the expected change in the stress distribution as the basis for the modification. Since the high-cycle vibratory stresses accounted for a large percentage of the total cycles, the USAF investigated the effects of high-cycle stress range truncation. In the block spectrum consisting of 1000 hours of usage, the truncation greatly affected the total number of cycles. The following results clearly illustrate this for the Ti-6Al-4V material.

The analyst based the cycle-by-cycle, flight-by-flight stress spectra on a nominal block time of 1000 hours, which represents 10 percent of one service life. From the given utilization, the analyst determined the number of flights for each mission types. He then ordered the flights randomly. However, he maintained the order of the segments within each mission type.

Since each segment in each mission type consisted of particular flight or ground operation conditions, the analyst associated the appropriate low-cycle exceedances with each segment. For each segment in each mission type, he adjusted the low-cycle occurrences to account for segment time and total missions for the mission type. He then distributed these occurrences randomly across the same segments in all the flights of each mission type. Finally, he constructed a low-cycle flight-by-flight stress spectrum by randomly ordering the occurrences in each segment in each random flight.

To construct the high-cycle spectrum, the analyst superimposed the oscillatory stress cycles on each peak and valley of the low-cycle spectrum. He determined the number of high-cycles for each peak and valley from the rotor rotational frequency and maneuver time. Figure 2 shows the method of superimposing the oscillatory stresses. The addition of these oscillatory stresses vastly increased the number of cycles imposed on the structure since he superimposed up to 200 oscillatory cycles on each low-cycle peak and valley.

The damage tolerance analysis procedure is based on Forman's crack growth rate equation and requires

appropriate input data such as stress intensity factor equation, retardation factor, and ΔK threshold. The sensitivity studies indicate the effect of ΔK threshold on damage tolerance life can be significant.

Figures 3 shows the geometric configuration and Figure 4 show the stress exceedance functions. As shown in Figure 5, the high-cycle stresses reduce the life from 4500 hours to 100 hours for an initial flaw of .254mm. For an initial flaw of 1.27mm, the reduction is from 1000 hours to 50 hours. This demonstrates the oscillatory stresses have a major influence on the damage tolerance derived inspection intervals. Figure 6 shows the affect of the ΔK threshold for the high cycle spectrum. The initial flaw for the crack growth functions in Figure 6 is 0.254 mm.

To develop a practical analysis spectrum, the analyst performed a study to determine the best compromise for stress range truncation. Figure 7 shows the effect of high-cycle range truncation for an initial flaw of 1.27 mm. Below 34.48MPa, they found no noticeable difference in the crack growth function. Truncation to 51.72MPa resulted in the best balance between analysis run time and accuracy for this material. This type of study needs to be performed for each material and spectrum associated with the critical components of the helicopter rotor system. The analyses must be supported by tests with initial cracks approximately the inspectable crack size.

Truncation MPa	Cycles per 1000 hours
Low-Cycle Only	144,682
86.19	388,849
68.95	1,725,650
51.72	14,530,800
34.48	40,791,800
0.00	41,404,000

The remaining analyses for the example problem investigated the effects of shot peening and the influence of changing the stress spectrum. The analyst approximated the shot peening effect by superposition of the stress intensities for the basic geometry and stresses and the stress distribution derived from shot peening. He found the effect on life from shot peening to be very significant. For an initial defect on the high side of the intrinsic defect distribution in the material (0.127 mm), the increase in life from shot peening is of the order of 10 as shown in Figure 8. One observes for the stress used in this analysis the crack growth life from a detectable flaw is too short for a damage tolerance derived inspection program. The analyst needs to reduce the stress by a factor of 1.6 to attain an inspection interval that would be consistent with rotors with normal maintenance periods.

CONCLUSIONS

The results derived from the HH-53 DTA indicate that many of the parts in its rotor systems are critical and will require either inspections, modifications or replacement during their operational lives. Based on experience with DTAs on fixed wing aircraft and engines the USAF expected this result. In most of the DTAs on these systems, they identified many extremely critical parts. In many cases, these critical areas identified themselves through in-service failures or full-scale fatigue test failures. As indicated in (2), the USAF addressed these problems individually and the USAF determined an approach that preserved safety at minimum cost.

The indication of part criticality from the HH-53 DTA may be overly conservative since Sikorsky did not include the beneficial effects of shot peening in the calculations. The results shown in the example problem indicate that shot peening can significantly extend the inspection intervals for components with flaws that the USAF could detect with confidence. The effect of shot peening is even more dramatic for flaw growth from the intrinsic defects found in aluminum and titanium. The example problem illustrates the results that a manufacturer would derive from testing smooth fatigue specimens with and without shot peening. From this illustration, it becomes clear why there could be a large difference between the safe life calculated for a shot peened component and the inspection interval derived from a fracture analysis of the same component without shot peening. The omission of the effects of shot peening in the determination of the inspection intervals of the components of the HH-53 led to results that made the maintenance of this rotor system unmanageable through damage tolerance principles.

One observes another significant feature from the example problem. Many components in operational rotor systems have stresses so high they must rely on some life enhancement procedure such as shot peening, laser peening, or cold expansion. Although these processes enhance the life of the part, it may still be in category of damage tolerant non-inspectable. As indicated above it appears justified to use engine inspection procedures and associated inspectable flaw sizes for DTA of helicopter rotor components. In addition, as indicated above, there was some conservatism in the stress spectra used for the HH-53 assessment. The results of the DTA, however, clearly show that there is a requirement for a high reliability nondestructive inspections for small flaw sizes if the operator uses the damage tolerance approach for operational helicopters. A reasonable goal for inspection capability is a flaw size of 0.254 mm for a disassembled rotor system. The USAF believes that this capability is attainable if they inspect the parts with the techniques developed for the engine community. Further, this defect size is compatible with current methods for fracture mechanics testing for analysis

verification. This test verification of the analytical crack growth predictions is an essential ingredient of the damage tolerance process. Components that exhibit crack growth periods from this size defect less than a factor of two times a reasonable rotor disassembly time should be candidates for redesign and replacement. For the HH-53, there were several members of the structure in this category.

The damage tolerance approach generally demands that the manufacturer reduces the stresses from that required for a safe life design. The manufacturer can mitigate some of the weight impact associated with this stress reduction by the balanced design they would achieve with damage tolerance. There have been a few studies of the weight impact associated with the incorporation of a damage tolerant design. R. Boorla (7) accomplished one of these. He performed an analysis of parts (including steel, titanium, and aluminum) from the prototype of the V-22 aircraft, which was designated the XV-15. He found that the weight impact was not significant in this particular case.

The results of the sample problem study indicate that many influences impact the damage tolerance life. These include high-cycle vibratory stresses, high-cycle stress range truncation, ΔK threshold, and initial flaw size. Using the generally recommended initial flaw sizes for fixed wing airframe structures may be too severe for many rotary wing high-cycle vibratory stress components. However, use of reduced flaw sizes for analysis would require the substantiation of production and maintenance inspection methods. This study concludes that one can use the damage tolerance design approach for high cycle components if the designer considers high cycle vibratory stresses, ΔK thresholds, and appropriate initial flaw sizes in the design processes.

Finally, there is a need to generate usage data through tail number tracking systems. The use of tracking data will enable the designer to quantify the range of aircraft usage as represented by the total pilot population rather than the experienced flight test pilot. Further, it will permit the maintenance organization to recognize when the helicopters have undergone a usage change and modify their maintenance actions accordingly. The technology is currently available to perform the tracking function.

ACKNOWLEDGEMENT

The authors express their gratitude to Mr. Robert Gerami and Mr. Doug Cornog of USAF Aeronautical Systems Center for their development work on the high cycle spectrum.

REFERENCES

1. Negaard, G. R., 1980 "The History of the Aircraft Structural Integrity Program," Aerospace Structures Information and Analysis Center (ASIAC) Report No. 680.1B.

2. Lincoln, J. W., 1985 "Damage Tolerance - USAF Experience," Proceeding of the 13th Symposium of the International Committee on Aeronautical Fatigue, Pisa, Italy.

3. Lincoln, J. W., 1987 "Damage Tolerance for Helicopters," Proceeding of the 14th Symposium of the International Committee on Aeronautical Fatigue, Jerusalem, Israel.

4. Everett, R. A. Jr., 1992" A Comparison of Fatigue Life Prediction Methodologies for Rotorcraft" Journal of the American Helicopter Society

5. Department of the Air Force, 1984 "Engine Structural Integrity Program (ENSIP)," Military Standard MIL-STD 1783.

6. Lincoln, J.W. and Melliere, R.A., 1998 "Economic Life Determination for a Military Aircraft," AIAA/ASME/ASCE/AHS/ASC Structures, Dynamics, and Materials Conference, Long Beach, CA.

7. Boorla, R., 1984 "Damage Tolerance Trade-Off Study," Bell Boeing Report No. 901-910-001.

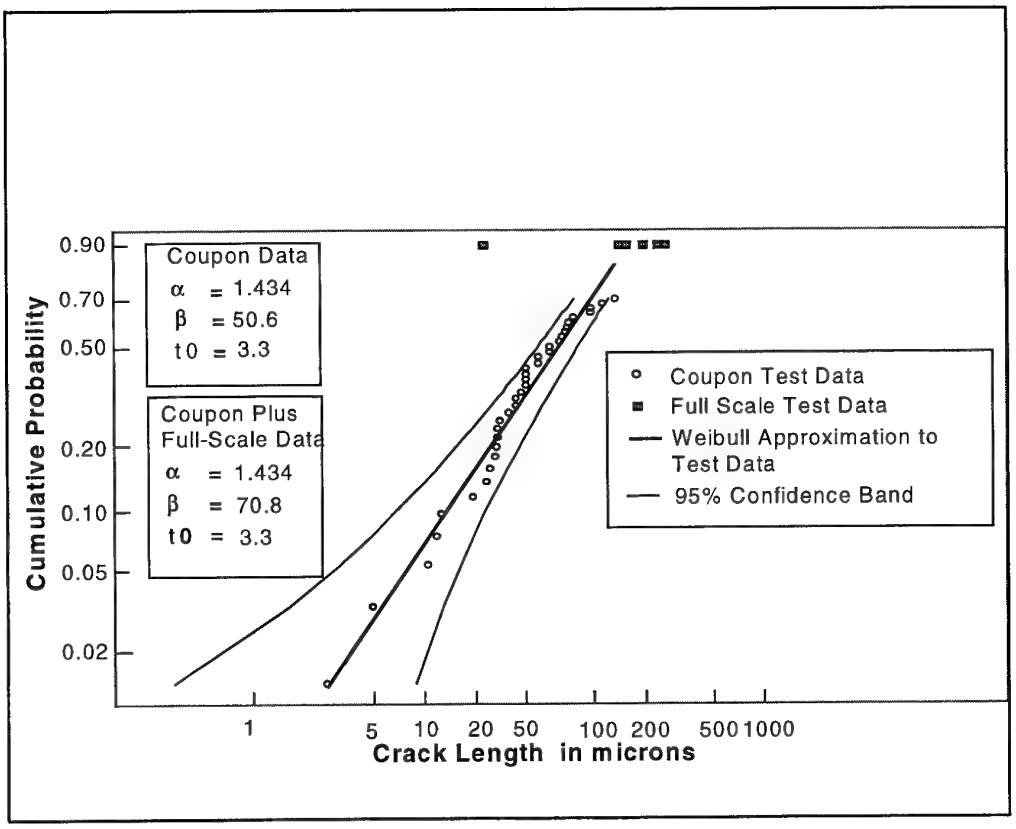

Figure 1 Intrinsic Flaw Distribution

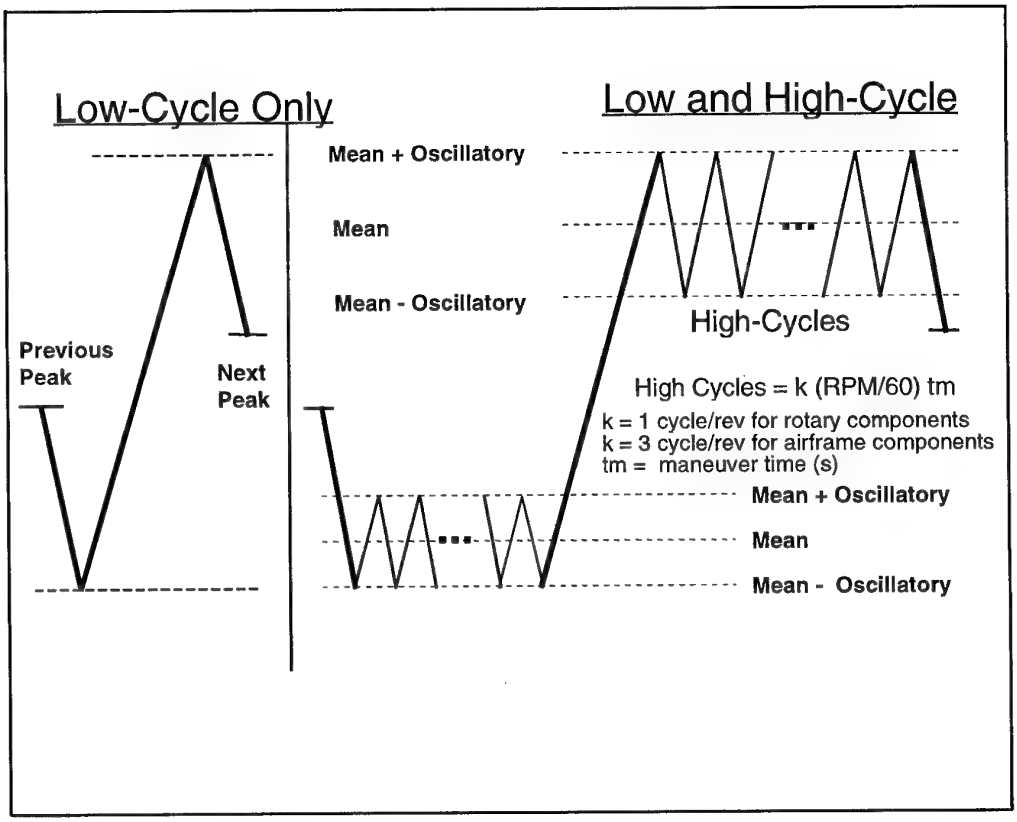

Figure 2 Addition Of High-cycle Stresses

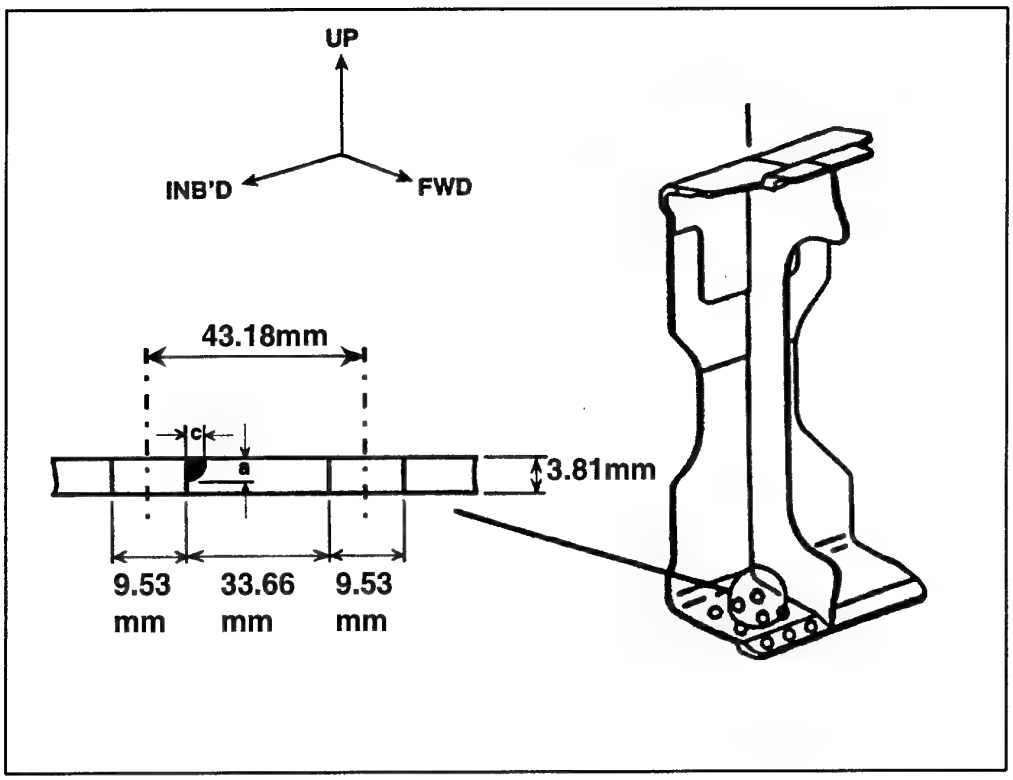

Figure 3 Splice Fitting Fastener Hole

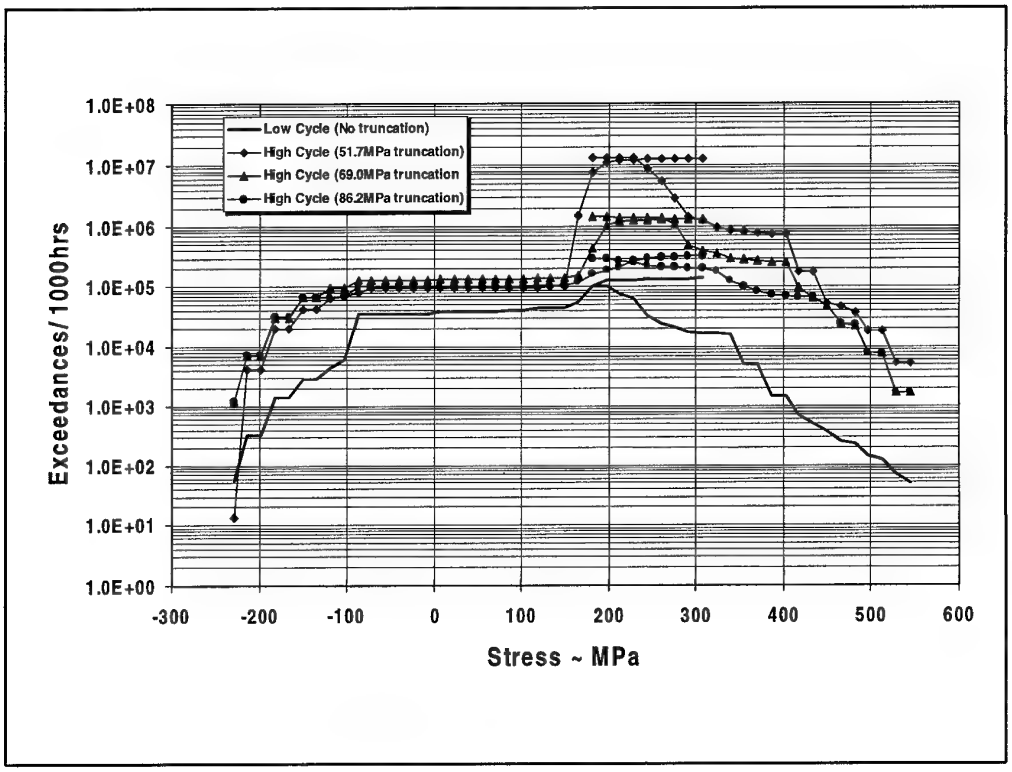

Figure 4 Stress Exceedance Functions

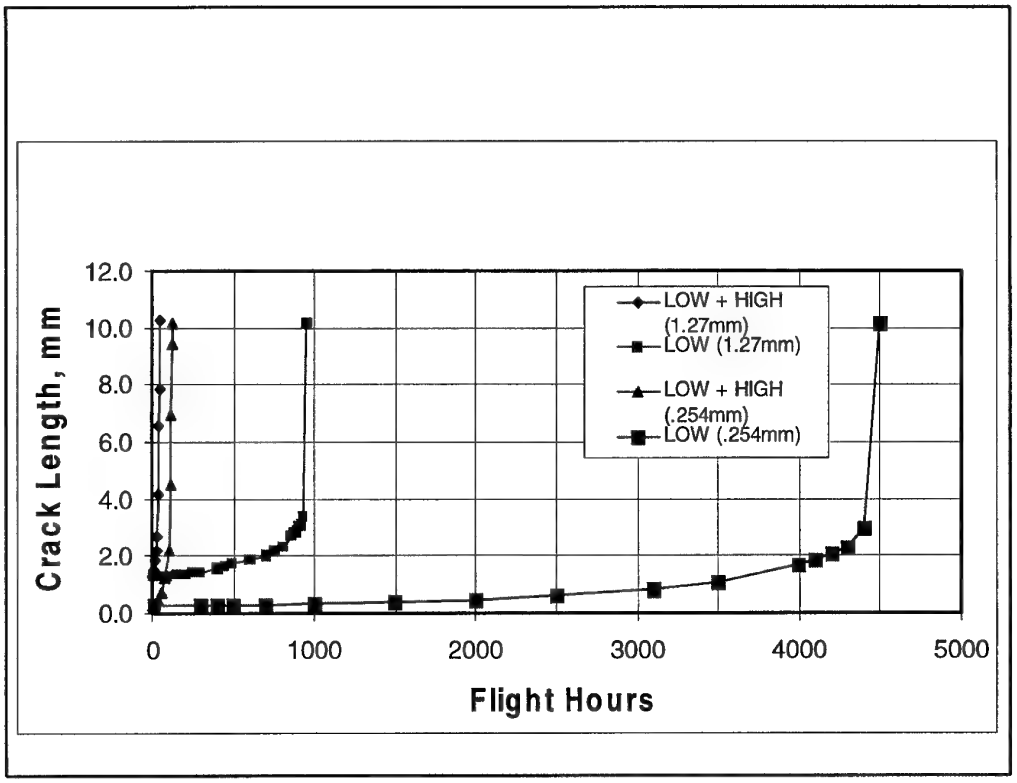

Figure 5 Structure Damage Tolerance Life

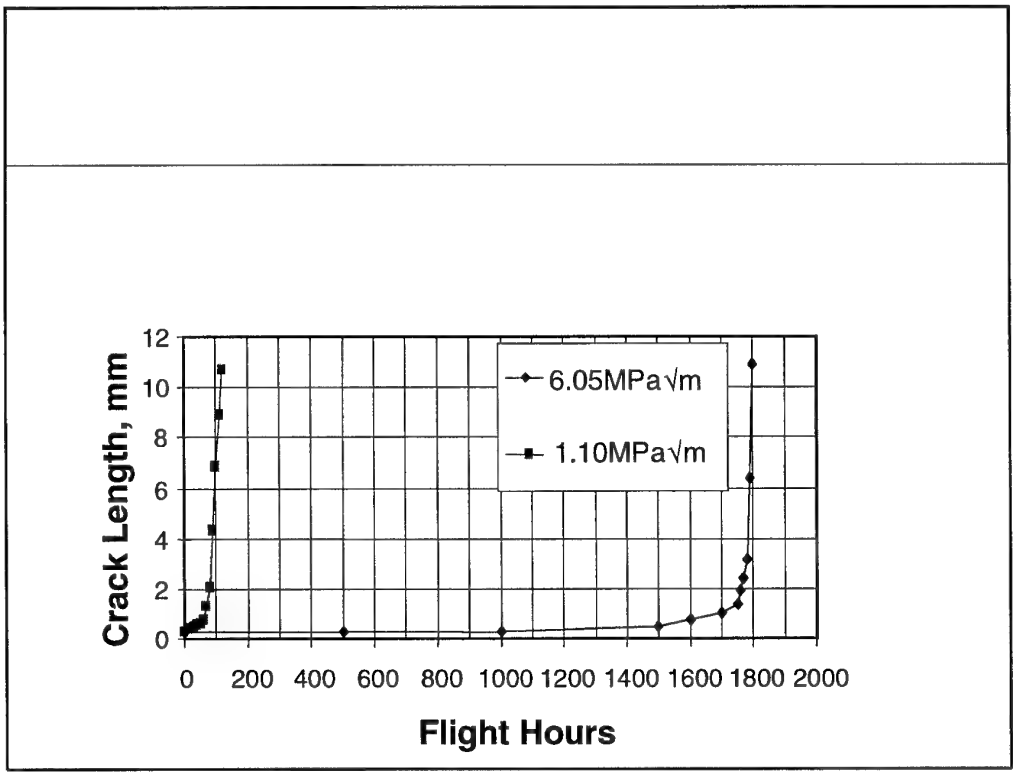

Figure 6 Effect Of ΔK Threshold On Structural Life

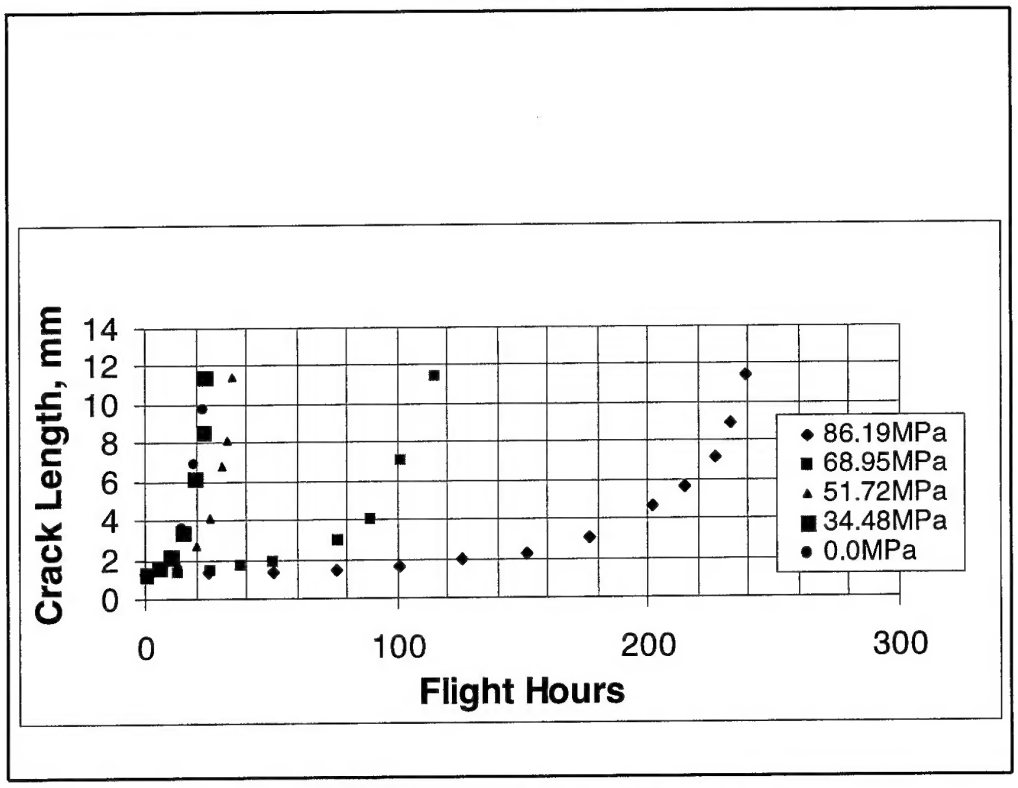

Figure 7 Effects Of Stress Range Truncation

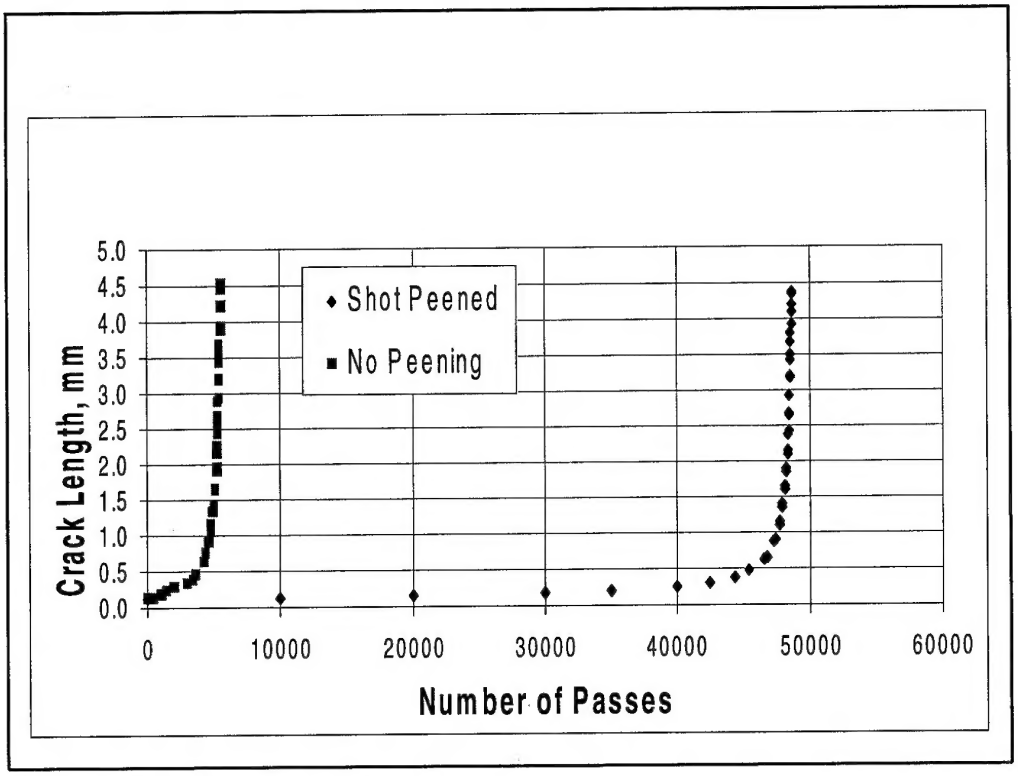

Figure 8 Shot Peening Study

REPORT DOCUMENTATION PAGE

1. Recipient's Reference	2. Originator's References	3. Further Reference	4. Security Classification of Document
	RTO-MP-24 AC/323(AVT)TP/12	ISBN 92-837-1024-X	UNCLASSIFIED/ UNLIMITED

5. Originator Research and Technology Organization
North Atlantic Treaty Organization
BP 25, 7 rue Ancelle, F-92201 Neuilly-sur-Seine Cedex, France

6. Title
Application of Damage Tolerance Principles for Improved Airworthiness of Rotorcraft

7. Presented at/sponsored by
the Applied Vehicle Technology Panel (AVT) Specialists' Meeting held in Corfu, Greece, 21-22 April 1999.

8. Author(s)/Editor(s)	9. Date
Multiple	February 2000
10. Author's/Editor's Address	**11. Pages**
Multiple	202

12. Distribution Statement There are no restrictions on the distribution of this document. Information about the availability of this and other RTO unclassified publications is given on the back cover.

13. Keywords/Descriptors

Rotary wing aircraft
Helicopters
Airworthiness
Damage
Tolerances (mechanics)
Service life
Safety
Fatigue (materials)
Design
Flight control
Systems engineering
Crack propagation
Loads (forces)
Delaminating
Equipment health monitoring
Structures
Metals
Composite structures
Composite materials

14. Abstract

The Specialists' Meeting dealt with Aging Systems and more specifically Application of Damage Tolerance Principles for Improved Airworthiness of Rotorcraft. These proceedings include a Keynote Address and fifteen papers having the objective of discussing and presenting the applicability of the new design approach to major rotorcraft components such as the dynamic system, primary load carrying structures and flight control systems. Both metal and composite structures including special material related topics such as crack growth models and delamination modelling were examined.

There were three sessions covering the following topics:
— Material Data and Crack Growth Models for DT-Approaches of Helicopter Structures
— Design Application of DT-Principles
— Operator Experience and Certification Issues

A Technical Evaluation Report of this meeting is also included.

NORTH ATLANTIC TREATY ORGANIZATION

RESEARCH AND TECHNOLOGY ORGANIZATION
BP 25 • 7 RUE ANCELLE
F-92201 NEUILLY-SUR-SEINE CEDEX • FRANCE
Télécopie 0(1)55.61.22.99 • E-mail mailbox@rta.nato.int

DIFFUSION DES PUBLICATIONS
RTO NON CLASSIFIEES

L'Organisation pour la recherche et la technologie de l'OTAN (RTO), détient un stock limité de certaines de ses publications récentes, ainsi que de celles de l'ancien AGARD (Groupe consultatif pour la recherche et les réalisations aérospatiales de l'OTAN). Celles-ci pourront éventuellement être obtenues sous forme de copie papier. Pour de plus amples renseignements concernant l'achat de ces ouvrages, adressez-vous par lettre ou par télécopie à l'adresse indiquée ci-dessus. Veuillez ne pas téléphoner.

Des exemplaires supplémentaires peuvent parfois être obtenus auprès des centres nationaux de distribution indiqués ci-dessous. Si vous souhaitez recevoir toutes les publications de la RTO, ou simplement celles qui concernent certains Panels, vous pouvez demander d'être inclus sur la liste d'envoi de l'un de ces centres.

Les publications de la RTO et de l'AGARD sont en vente auprès des agences de vente indiquées ci-dessous, sous forme de photocopie ou de microfiche. Certains originaux peuvent également être obtenus auprès de CASI.

CENTRES DE DIFFUSION NATIONAUX

ALLEMAGNE
Streitkräfteamt / Abteilung III
Fachinformationszentrum der Bunderswehr, (FIZBw)
Friedrich-Ebert-Allee 34
D-53113 Bonn

BELGIQUE
Coordinateur RTO - VSL/RTO
Etat-Major de la Force Aérienne
Quartier Reine Elisabeth
Rue d'Evère, B-1140 Bruxelles

CANADA
Directeur - Recherche et développement - Communications et gestion de l'information - DRDCGI 3
Ministère de la Défense nationale
Ottawa, Ontario K1A 0K2

DANEMARK
Danish Defence Research Establishment
Ryvangs Allé 1, P.O. Box 2715
DK-2100 Copenhagen Ø

ESPAGNE
INTA (RTO/AGARD Publications)
Carretera de Torrejón a Ajalvir, Pk.4
28850 Torrejón de Ardoz - Madrid

ETATS-UNIS
NASA Center for AeroSpace Information (CASI)
Parkway Center
7121 Standard Drive
Hanover, MD 21076-1320

FRANCE
O.N.E.R.A. (ISP)
29, Avenue de la Division Leclerc
BP 72, 92322 Châtillon Cedex

GRECE (Correspondant)
Defence Industry Research & Technology General Directorate/ Technological Research & Technology Directorate
Dim. Soutsou 40 str.
GR-11521, Athens

HONGRIE
Department for Scientific Analysis
Institute of Military Technology
Ministry of Defence
H-1525 Budapest P O Box 26

ISLANDE
Director of Aviation
c/o Flugrad
Reykjavik

ITALIE
Centro documentazione tecnico-scientifica della Difesa
Via Marsala 104
00185 Roma

LUXEMBOURG
Voir Belgique

NORVEGE
Norwegian Defence Research Establishment
Attn: Biblioteket
P.O. Box 25, NO-2007 Kjeller

PAYS-BAS
NDRCC
DGM/DWOO
P.O. Box 20701
2500 ES Den Haag

POLOGNE
Chief of International Cooperation Division
Research & Development Department
218 Niepodleglosci Av.
00-911 Warsaw

PORTUGAL
Estado Maior da Força Aérea
SDFA - Centro de Documentação
Alfragide
P-2720 Amadora

REPUBLIQUE TCHEQUE
VTÚL a PVO Praha /
Air Force Research Institute Prague
Národní informační středisko obranného výzkumu (NISČR)
Mladoboleslavská ul., 197 06 Praha 9

ROYAUME-UNI
Defence Research Information Centre
Kentigern House
65 Brown Street
Glasgow G2 8EX

TURQUIE
Millî Savunma Başkanliği (MSB)
ARGE Dairesi Başkanliği (MSB)
06650 Bakanliklar - Ankara

AGENCES DE VENTE

NASA Center for AeroSpace Information (CASI)
Parkway Center
7121 Standard Drive
Hanover, MD 21076-1320
Etats-Unis

The British Library Document Supply Centre
Boston Spa, Wetherby
West Yorkshire LS23 7BQ
Royaume-Uni

Canada Institute for Scientific and Technical Information (CISTI)
National Research Council
Document Delivery
Montreal Road, Building M-55
Ottawa K1A 0S2, Canada

Les demandes de documents RTO ou AGARD doivent comporter la dénomination "RTO" ou "AGARD" selon le cas, suivie du numéro de série (par exemple AGARD-AG-315). Des informations analogues, telles que le titre et la date de publication sont souhaitables. Des références bibliographiques complètes ainsi que des résumés des publications RTO et AGARD figurent dans les journaux suivants:

Scientific and Technical Aerospace Reports (STAR)
STAR peut être consulté en ligne au localisateur de ressources uniformes (URL) suivant:
http://www.sti.nasa.gov/Pubs/star/Star.html
STAR est édité par CASI dans le cadre du programme NASA d'information scientifique et technique (STI)
STI Program Office, MS 157A
NASA Langley Research Center
Hampton, Virginia 23681-0001
Etats-Unis

Government Reports Announcements & Index (GRA&I)
publié par le National Technical Information Service
Springfield
Virginia 2216
Etats-Unis
(accessible également en mode interactif dans la base de données bibliographiques en ligne du NTIS, et sur CD-ROM)

Imprimé par le Groupe Communication Canada Inc.
(membre de la Corporation St-Joseph)
45, boul. Sacré-Cœur, Hull (Québec), Canada K1A 0S7

NORTH ATLANTIC TREATY ORGANIZATION

RESEARCH AND TECHNOLOGY ORGANIZATION
BP 25 • 7 RUE ANCELLE
F-92201 NEUILLY-SUR-SEINE CEDEX • FRANCE
Telefax 0(1)55.61.22.99 • E-mail mailbox@rta.nato.int

DISTRIBUTION OF UNCLASSIFIED
RTO PUBLICATIONS

NATO's Research and Technology Organization (RTO) holds limited quantities of some of its recent publications and those of the former AGARD (Advisory Group for Aerospace Research & Development of NATO), and these may be available for purchase in hard copy form. For more information, write or send a telefax to the address given above. **Please do not telephone.**

Further copies are sometimes available from the National Distribution Centres listed below. If you wish to receive all RTO publications, or just those relating to one or more specific RTO Panels, they may be willing to include you (or your organisation) in their distribution.

RTO and AGARD publications may be purchased from the Sales Agencies listed below, in photocopy or microfiche form. Original copies of some publications may be available from CASI.

NATIONAL DISTRIBUTION CENTRES

BELGIUM
Coordinateur RTO - VSL/RTO
Etat-Major de la Force Aérienne
Quartier Reine Elisabeth
Rue d'Evère, B-1140 Bruxelles

CANADA
Director Research & Development
Communications & Information
Management - DRDCIM 3
Dept of National Defence
Ottawa, Ontario K1A 0K2

CZECH REPUBLIC
VTÚL a PVO Praha /
Air Force Research Institute Prague
Národní informační středisko
obranného výzkumu (NISČR)
Mladoboleslavská ul., 197 06 Praha 9

DENMARK
Danish Defence Research
Establishment
Ryvangs Allé 1, P.O. Box 2715
DK-2100 Copenhagen Ø

FRANCE
O.N.E.R.A. (ISP)
29 Avenue de la Division Leclerc
BP 72, 92322 Châtillon Cedex

GERMANY
Streitkräfteamt / Abteilung III
Fachinformationszentrum der
Bunderswehr, (FIZBw)
Friedrich-Ebert-Allee 34
D-53113 Bonn

GREECE (Point of Contact)
Defence Industry Research &
Technology General Directorate/
Technological Research &
Technology Directorate
Dim. Soutsou 40 str.
GR-11521, Athens

HUNGARY
Department for Scientific
Analysis
Institute of Military Technology
Ministry of Defence
H-1525 Budapest P O Box 26

ICELAND
Director of Aviation
c/o Flugrad
Reykjavik

ITALY
Centro documentazione
tecnico-scientifica della Difesa
Via Marsala 104
00185 Roma

LUXEMBOURG
See Belgium

NETHERLANDS
NDRCC
DGM/DWOO
P.O. Box 20701
2500 ES Den Haag

NORWAY
Norwegian Defence Research
Establishment
Attn: Biblioteket
P.O. Box 25, NO-2007 Kjeller

POLAND
Chief of International Cooperation
Division
Research & Development
Department
218 Niepodleglosci Av.
00-911 Warsaw

PORTUGAL
Estado Maior da Força Aérea
SDFA - Centro de Documentação
Alfragide
P-2720 Amadora

SPAIN
INTA (RTO/AGARD Publications)
Carretera de Torrejón a Ajalvir, Pk.4
28850 Torrejón de Ardoz - Madrid

TURKEY
Millî Savunma Başkanliği (MSB)
ARGE Dairesi Başkanliği (MSB)
06650 Bakanliklar - Ankara

UNITED KINGDOM
Defence Research Information
Centre
Kentigern House
65 Brown Street
Glasgow G2 8EX

UNITED STATES
NASA Center for AeroSpace
Information (CASI)
Parkway Center
7121 Standard Drive
Hanover, MD 21076-1320

SALES AGENCIES

NASA Center for AeroSpace Information (CASI)
Parkway Center
7121 Standard Drive
Hanover, MD 21076-1320
United States

The British Library Document Supply Centre
Boston Spa, Wetherby
West Yorkshire LS23 7BQ
United Kingdom

Canada Institute for Scientific and Technical Information (CISTI)
National Research Council
Document Delivery
Montreal Road, Building M-55
Ottawa K1A 0S2, Canada

Requests for RTO or AGARD documents should include the word 'RTO' or 'AGARD', as appropriate, followed by the serial number (for example AGARD-AG-315). Collateral information such as title and publication date is desirable. Full bibliographical references and abstracts of RTO and AGARD publications are given in the following journals:

Scientific and Technical Aerospace Reports (STAR)
STAR is available on-line at the following uniform resource locator:
http://www.sti.nasa.gov/Pubs/star/Star.html
STAR is published by CASI for the NASA Scientific and Technical Information (STI) Program
STI Program Office, MS 157A
NASA Langley Research Center
Hampton, Virginia 23681-0001
United States

Government Reports Announcements & Index (GRA&I)
published by the National Technical Information Service
Springfield
Virginia 22161
United States
(also available online in the NTIS Bibliographic Database or on CD-ROM)

Printed by Canada Communication Group Inc.
(A St. Joseph Corporation Company)
45 Sacré-Cœur Blvd., Hull (Québec), Canada K1A 0S7

ISBN 92-837-1024-X